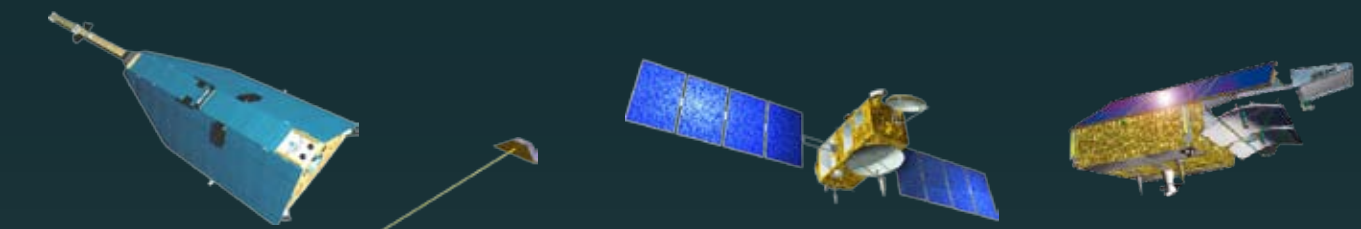

Mass Transport and Mass Distribution in the Earth System

Contribution of the New Generation of Satellite Gravity and Altimetry Missions to Geosciences

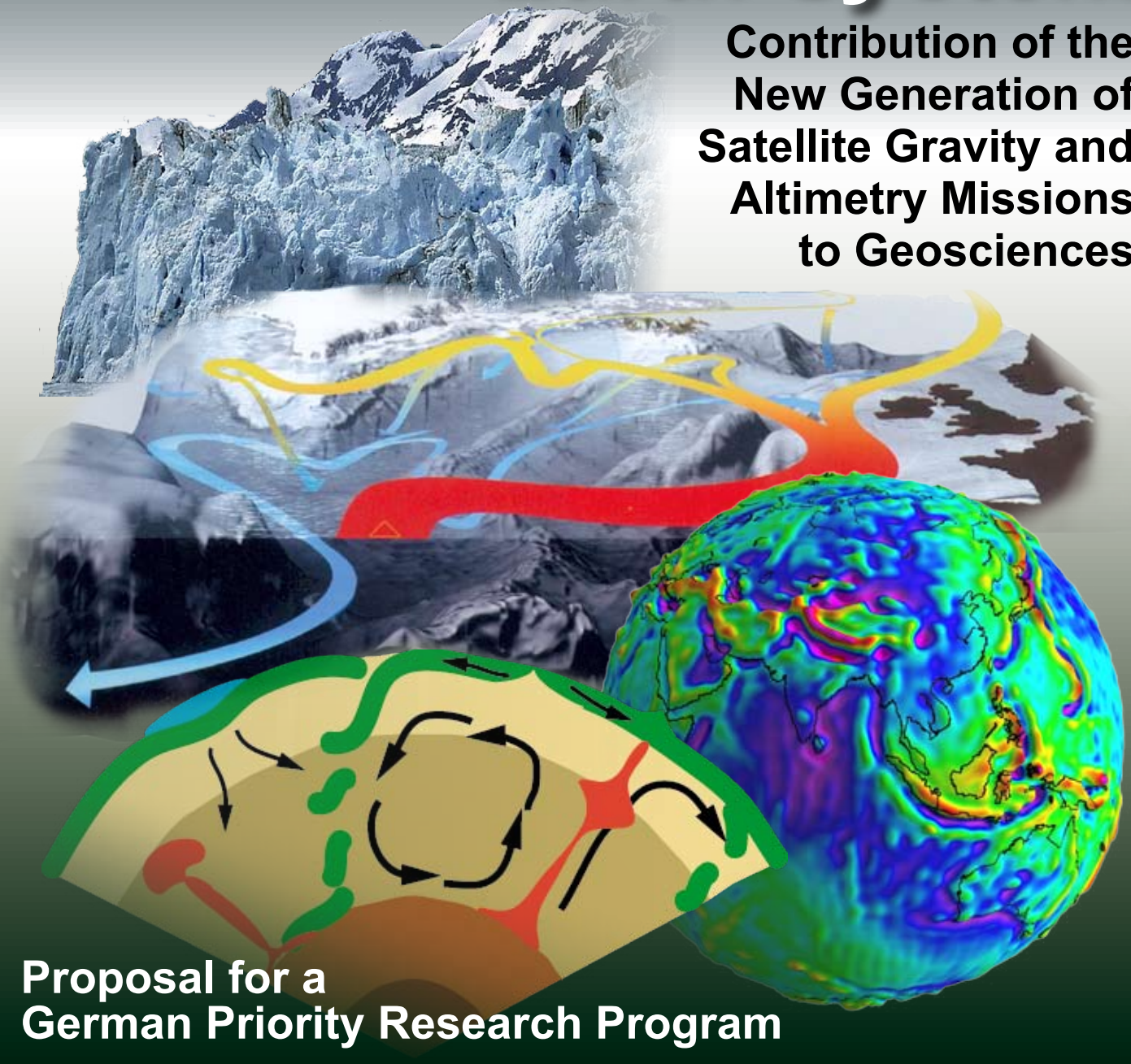

Proposal for a German Priority Research Program

Contact:

GOCE-Projektbüro Deutschland
Institut für Astronomische und Physikalische Geodäsie
Technische Universität München
Arcisstraße 21
D-80290 München
Germany
Telephone: +49 89 289 23190
flury@bv.tum.de
http://www.goce-projektbuero.de
http://step.iapg.verm.tu-muenchen.de/iapg/

GeoForschungsZentrum Potsdam
Telegrafenberg
D-14471 Potsdam
Germany
Telephone: +49 331 288 1130
psch@gfz-potsdam.de
http://www.gfz-potsdam.de

Layout: W. Bosch

printed by GeoForschungsZentrum Potsdam
2nd Edition, January 2005

Mass Transport and Mass Distribution in the Earth System

Contribution of the New Generation of Satellite Gravity and Altimetry Missions to Geosciences

Proposal for a German Priority Research Program

K.H. Ilk[1)], J. Flury[2)], R. Rummel[2)], P. Schwintzer[3)], W. Bosch[4)], C. Haas[5)], J. Schröter[5)], D. Stammer[6)], W. Zahel[6)], H. Miller[5)], R. Dietrich[7)], P. Huybrechts[5)], H. Schmeling[8)], D. Wolf[3)], H.J. Götze[9)], J. Riegger[10)], A. Bardossy[10)], A. Güntner[3)], Th. Gruber[2)]

[1)] Institut für Theoretische Geodäsie, Bonn
[2)] Institut für Astronomische und Physikalische Geodäsie, München
[3)] GeoForschungsZentrum, Potsdam
[4)] Deutsches Geodätisches Forschungsinstitut, München
[5)] Alfred Wegener Institut für Polar- und Meeresforschung, Bremerhaven
[6)] Institut für Meereskunde, Hamburg
[7)] Institut für Planetare Geodäsie, Dresden
[8)] Institut für Meteorologie und Geophysik, Frankfurt am Main
[9)] Institut für Geowissenschaften, Kiel
[10)] Institut für Wasserbau, Stuttgart

GOCE-Projektbüro Deutschland, Technische Universität München
GeoForschungsZentrum Potsdam

Januar 2005

In memory of

Peter Schwintzer

who passed away
during the final preparation
of this program document.

Table of Contents

Table of Contents (continued)

Introduction

The exceptional situation of getting simultaneous and complementary observations from a multiple of geo-scientific and environmental near-Earth orbiting satellites opens the unique opportunity to contribute significantly to the understanding of global Earth dynamics. This will enable to quantify processes in the geosphere and the interactions with the atmosphere and the hydrosphere and to predict future developments. A consequence of this research is, on the one hand, to contribute to a deeper knowledge of the Earth system, and on the other hand, the possibility to contribute to the development of sustainable strategies to safeguard the human habitat for future generations.

The key parameters that are provided globally are of physical and geometric nature and allow, when combined, an enhanced modelling of the mass distribution and mass transport within the Earth, at the Earth's surface and its envelope. The knowledge of the Earth's mass distribution and redistribution is of crucial importance for the exploration of geodynamic convective and climatologically driven processes within Earth system. The temporal scales addressed by these processes range from sub-seasonal and interannual to decadal and secular variations on a global to regional spatial scale according to the satellites' data resolution capability.

The overall goal of the multi-disciplinary effort outlined in this document is a breakthrough in the understanding and modelling of geodynamics, ocean circulation and sea level, ice mass balance, and the global hydrologic water cycle as well as the mutual coupling of these processes constitutive to the highly dynamic Earth system. The challenges will be the identification and separation of the relevant signals in the satellite and complementary data products, signal analyses and model assimilation, and interdisciplinary model integration to achieve a consistent representation of the changing Earth.

The present document emphasizes the need for **a coordinated national research program on mass transport and mass distribution in the Earth system** in view of the considerable German scientific and financial support during promotion, preparation and realization of the satellite missions. Such a program is an adequate way to fully exploit satellite missions' products in order to harvest the scientific return and to keep the leading role of German scientists within the international scientific and application community as far as kinematical, dynamic and climatologic Earth system processes are concerned.

The document

- lays down the scientific framework, the conceptual ideas, the strategy and prospects for the urgently needed coordinated activity (Chapter 1),
- describes the relevant actual and coming satellite missions, the state-of-the-art in product generation and expected improvements, and the missions' role within the fields addressed by this document (Chapter 2),
- gives detailed information about the individual transport processes in the Earth system, its present knowledge, modelling deficits and the expected benefits from joint analyses of the newly available Earth observations (Chapter 3): ocean transport processes (Chapter 3.1), ice mass balance and sea level change (Chapter 3.2), solid Earth dynamics and structure (Chapter 3.3), the continental hydrological cycle (Chapter 3.4), and – finally – about the role of atmosphere, tides and Earth core motion (Chapter 3.5),
- defines the interrelations, interfaces and requirements for a multi-parameter and multi-disciplinary product exploitation and a coupled modelling using the satellite missions' and complementary remote sensing signal analysis and balancing results iteratively as the common basis and an information system and data centre as the focal point (Chapter 4),
- reports the theoretical and mathematical background of the satellites' data processing and of the tools for modelling the various Earth system processes, complemented by satellite missions' fact sheets (Annex).

1 Framework of a coordinated research program

The goal of a coordinated research program is a breakthrough in the understanding and modelling of important processes in the highly dynamic Earth system. The exceptional situation of getting simultaneous and complementary observations from a multiple of geo-scientific and environmental near-Earth orbiting satellites opens the unique opportunity to contribute significantly to the understanding of global Earth dynamics. The key quantities derived from these satellite missions are measured changes of surface geometry and mass distribution and mass transport in and among the Earth components. A deep understanding of our complex Earth system is the basis to develop sustainable strategies to protect our planet, its climate and environment and preserve it for future generations.

1.1 Space research and Earth system: mass transport, mass distribution, and mass exchange

Circulation in the oceans and in the atmosphere, water fluxes between various terrestrial water storages, melting ice, river discharge, changing sea level, and convective flow in the Earth's mantle – these and other processes cause a permanent transport of mass and a redistribution of mass on the Globe. *How much mass* is transported and redistributed? This is a fundamental question for the understanding of these processes and their dynamics. In the past, changes of the mass distribution in the Earth system were difficult to observe directly and, consequently, interpretations of sparse data or predictions of individual processes were incomplete or wrong. This situation has changed dramatically through a unique constellation of simultaneously operating *satellite gravity and altimetry missions*, equipped with very precise and novel sensors.

The gravity field and its variations – measured by satellites with unprecedented accuracy – are closely interrelated with mass transport and mass distribution. Fig. 1.1 gives an overview of gravity related phenomena, associated with anomalous signals in the geoid, in gravity or with temporal changes of geoid or gravity. The atmosphere, hydrosphere, ice covers, biosphere, land surface and solid Earth interact in various ways, ranging from subseasonal and interannual to decadal and secular variations on a global to regional spatial scale. This makes it difficult to develop realistic models that are capable to yield realistic predictions. Rather sophisticated partial models exist, for example, for weather predictions, the coupled atmospheric and ocean circulation, of local hydrological scales, of glacial isostatic mass adjustment, but we are still far from a comprehensive description and understanding of the dynamics of Earth system. An important, and so far missing, segment of Earth system models is the determination of mass anomalies, mass transport and

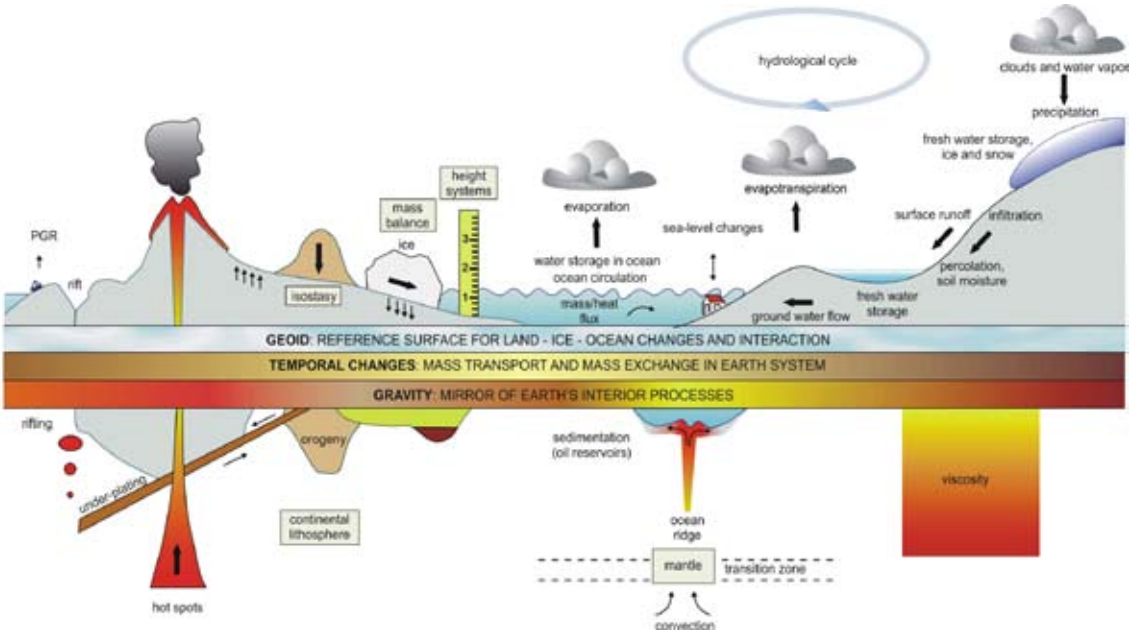

Figure 1.1: *The interrelation of gravity, gravity variations, mass transport and distribution.*

mass exchange between Earth system components and, ultimately, the establishment of global mass balance.

With the new quality in observing the Earth's gravity field, and the sea and ice surface and their temporal variability, the tools are for the first time available to recover globally mass transports in the Earth system through their effects on the gravity field and the sea and ice surface geometry. This will allow us to investigate the physical causes and, furthermore, to establish a firm basis for predictions of future changes and their effects. Those insights are essential for future climate scenario predictions, and in particular for our understanding and the prediction of the global water cycle. It is expected that the integrated research proposed in this report will contribute to revolutionize our understanding of the dynamical processes on the Earth's surface and in its interior, enabling a new view of geodynamics in a broader sense to evolve.

We distinguish three kinds of mass signals to be discussed in this report, and three ways to use satellite observations to recover these mass signals. The first kind is *time variation of mass distribution* in oceans, in continental water storages (such as ground water), in ice sheets, in the atmosphere and in the Earth's interior, with seasonal, annual and inter-annual contributions as well as secular trends. Our goal is a monitoring and understanding of mass transport within these Earth system components, of mass balances (for ice sheets, ocean basins, river catchments and ground water) and of mass exchange across the borders between atmosphere, ice, land and oceans. The mass changes and redistributions are reflected in small amplitude, but large scale changes of gravity and the geoid, which are now for the first time observable by the satellite gravity missions CHAMP and GRACE, with a resolution from global scales down to a few hundred kilometers. Simultaneously, satellite altimetry missions observe the shape of ocean and ice surfaces as well as tiny changes in their geometry with centimeter accuracy. This extraordinary favorable data situation will enable for the first time reliable estimates for the Antarctic ice mass balance, for deep ocean currents variability and for the contributions to sea level change by all involved processes. For large scale mass variations in continental hydrology, which have been unobservable up to present, first impressive results based on GRACE data are already available. Thus, observed changes of water mass in the global hydrological cycle represent a new quantity for the improvement of understanding, modelling and forecasting processes of the Earth's climate.

For the oceans, another type of mass signal gets involved. The combination of precise altimetry

and gravity (geoid) information leads to the determination of the absolute surface current including its time mean and time varying part. Combined with in-situ data the absolute flow field can be determined - a long-standing problem of physical oceanography that finally seems in reach given the modern satellite technology. Those absolute currents can then be used to determine *transports of water masses and heat* by the oceanic current systems. That transport of mass and energy in the oceans is a major mechanism for the stabilization of the Earth's climate. Only the combination of satellite altimetry, in-situ data and geoid information from the GRACE and GOCE satellite missions can provide the new information required to model and understand the ocean flow field, its changes and the role of the ocean in the climate system.

The third type of mass signals is the *stationary mass and density structure* of the Earth's mantle and crust. Observations of the stationary geoid and gravity anomalies reflect the internal structure and can be used to constrain dynamical models of processes in the Earth's interior such as convection flow, sinking plate slabs and rising mantle plumes, as well as to infer the structure of the crust, for instance, in plate collision zones. For these goals, the gravity field, seismic information and laboratory experiments complement each other. Gravity field methods will gain in importance, as the gravity field model obtained from GRACE and GOCE will – in particular for large and medium spatial scales – be more accurate by orders of magnitude than the information available before, with a globally homogeneous coverage.

There is growing public concern about the future of our planet, its climate, its environment and about an expected shortage of our natural resources, even of such an elementary one as water. Any consistent and efficient strategy of protection against these threats depends on a profound understanding of Earth system, including mass related processes. In modern times these processes are influenced, as well, by man-made effects; to what extent is still unknown. Certain, however, is that they affect our life and the life of future generations. Major decisions facing human societies will depend on a much deeper understanding of this complex system, and international efforts on governmental and scientific levels are currently underway towards this goal. The research proposed in this report will support in particular the understanding of stability and variability of climate and of the various elements of the global water cycle, which is within the scope of large international scientific programs, such as the World Climate Research Programme (WCRP) or the International Geosphere-Biosphere Programme (IGBP).

1.2 Interdisciplinary cooperation within a coordinated research program

Quantification and understanding of mass transport and mass distribution based on the new satellite data requires a close cooperation of many Earth system research areas: oceanic transport, continental hydrology, ice mass balance and sea level, dynamics of mantle and crust, and geodetic signal analysis of the satellite missions, see Fig. 1.2. Such an inter-disciplinary approach is necessary due to two reasons. The first reason is the importance of water mass exchange across the boundaries of the system components oceans, land, ice and atmosphere. The goal is a consistent modelling, where mass output from one model (e.g. for an ice sheet) is used as mass input for another model (e.g. for the neighboring ocean). The other reason is the integral character of the satellite observations. The satellite gravity data as well as surface geometry changes observed by satellite altimetry contain a complex superposition of various mass signals. For instance, in Antarctica gravity and height changes due to ice mass changes are superimposed by similar signals from mass change in the Earth's mantle due to glacial isostatic adjustment, from tectonics, and from mass changes in the adjacent oceans and in the atmosphere. To enable a reliable separation of such effects, an intensive exchange of results is required. The role of the atmosphere requires a special remark: it is not a core research area in this program, as atmosphere research will prob-

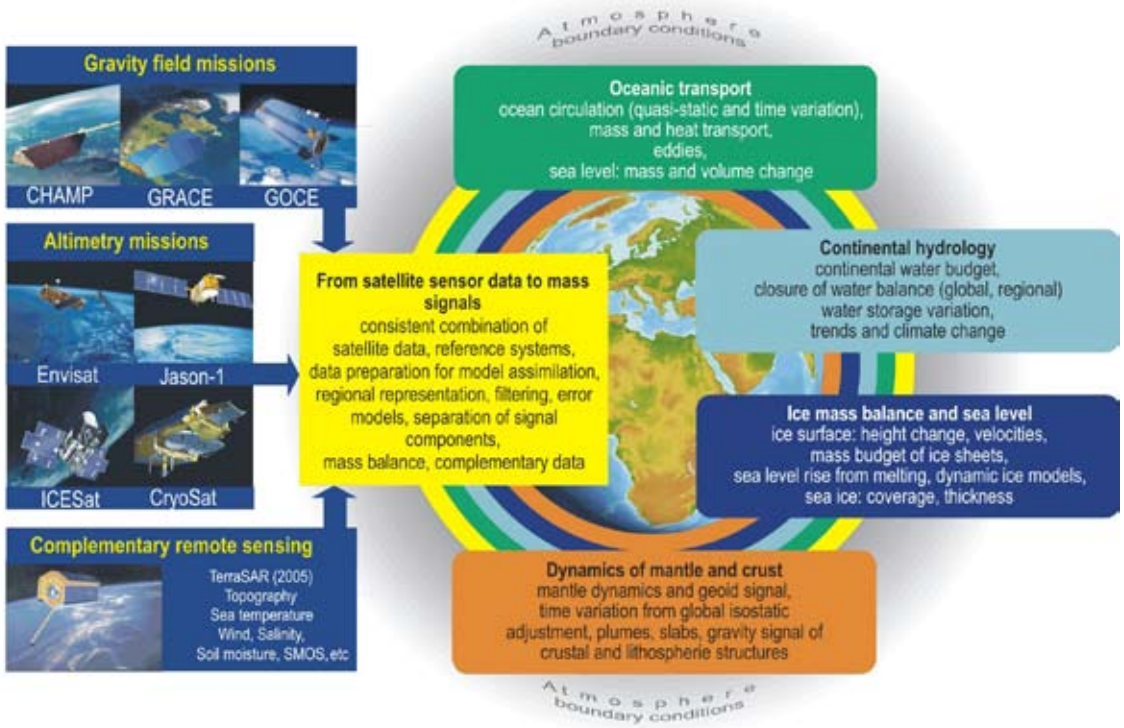

Figure 1.2: *Exploitation of satellite gravity and altimeter mission products to determine mass transport and mass distribution in a multi-disciplinary environment.*

ably not directly benefit from this kind of satellite data. However, the contribution of atmospheric mass variations to the satellite data has to be modelled very carefully. In addition, atmospheric forcing and mass exchange with the atmosphere are research themes in various components of the proposed program.

The authors of this document propose to establish a national research program to quantify mass distribution, transport and exchange by adding novel observables, in particular gravity and gravity variations as well as surface geometry and changes in the geometry of oceans and ice covers. These observables can be provided by dedicated satellite gravity field missions based on the principle of satellite-to-satellite tracking such as CHAMP and GRACE and of satellite gravity gradiometry such as GOCE. They will be combined with precise tracking by the satellites of any of the global positioning systems GPS, GLONASS and in future GALILEO. A new generation of remote sensing satellites, the altimetric ice missions CryoSat and ICESat will allow to measure surface geometry of land and sea ice and variations thereof with unprecedented accuracy. Ocean surfaces have been and will be measured with cm-precision by the altimetric ocean missions JASON and ENVISAT and their predecessors. Also the height and height variations of water surfaces on land – lakes, rivers, wetlands – are observed by the altimetric satellites (Fig. 1.3). The satellite missions provide gravimetric and geometric data with globally homogeneous coverage and data quality, and with a good sampling in space and time. In contrary to terrestrial data, they are not contaminated by local effects. Thanks to these advantages, the satellite data allow the detection of many mass signals which have been unobservable before. The joint use of geometry and gravity, in addition, will allow in many cases a separation of physical causes, such as thermal expansion and mass sur-plus in the oceans.

Prerequisite for a consistent use of the satellite data is a precise geodetic-geodynamic reference frame for all numerical analysis procedures, the application of new computation standards and a user oriented processing of the mission products. Traditionally, geodesy is capable of measuring

Figure 1.3: *Geo-scientific and environmental near-Earth orbiting satellites providing simultaneous and complementary observations.*

1) changes in surface geometry of ocean and ice surfaces as well as horizontal and vertical deformations of land surface (geokinematic component),
2) changes in Earth rotation, traditionally subdivided into nutation, polar motion and variations in spin rate and associated with all processes of angular momentum in Earth system (Earth rotation component), and
3) the spatial and temporal variations of gravity and of the geoid (gravity/geoid component).

The constituents of an integrated geodetic-geodynamic monitoring system are shown in Fig. 1.4.

The satellite configuration currently in orbit or approved to be in orbit soon will improve each of these three components significantly in capability and precision. We will have a new generation of satellites monitoring land deformation, ocean and ice surfaces, determining the gravity field and geoid with unprecedented accuracy and, in addition, enhance atmospheric sounding due to the growing number of low orbiting and navigation satellites. If we succeed to integrate this unique system of satellites into one common reference system at a precision level of one-part-per-billion (mm to cm precision) and stable and consistent in time and space these sensors can

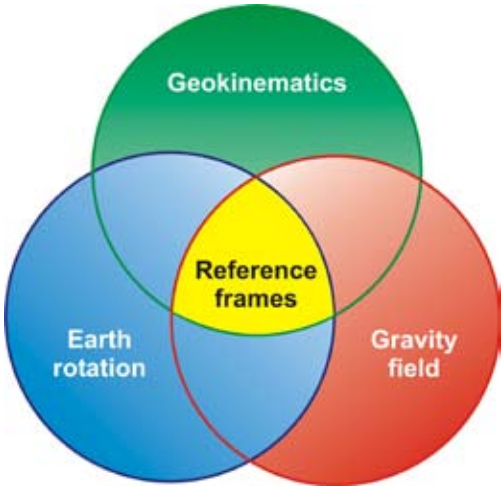

Figure 1.4: *Constituents of an integrated geodetic-geodynamic monitoring system.*

operate so-to-say as one Earth encompassing global observatory. The combination will be achieved by means of the global geodetic space techniques VLBI, SLR, GPS and DORIS in the framework of the International Earth Rotation and Reference System Service (IERS).

From the combination of the three fundamental components geometry, gravity/geoid, Earth rotation and, in addition, atmospheric sounding, mass anomalies, mass transport and mass exchange emerges. The quantities to be delivered are small and therefore difficult to determine. In order to be useful for global change studies they have to be derived free of bias and consistently in space and time. In general they are derived from the combination of complementary sensor and observation systems. For example, dynamic ocean topography is to be derived from the accurate measurement of the ocean surface by radar altimetry in combination with a geoid surface provided by gravity satellite missions. It shows that a variety of sensor systems, mission characteristics, and tracking systems have to be com-bined with utmost precision. The interconnections between mass transport processes, and the relations between observable parameters of gravity and geometry and the different processes are sketched in Fig. 1.5.

In the past, geophysical research concerned with the three geodetic components, geometry, Earth rotation and gravity/geoid, as well as with the sounding of the atmosphere, concentrated on individual processes and not so much on the added-value that can be drawn from their integration. The new satellite data are time series – along orbit tracks – related to a variety of geometric and gravimetric quantities that will be combined to provide global time series of geophysical parameters related to mass phenomena. These represent a new generation of input data for Earth models in the fields of oceanography, glaciology, hydrology and geophysics (Fig. 1.2). Since each of these Earth system components interacts with all others a thorough analysis of their interfaces is required, too. A link has to be established between the global time series of geodetic parameters (related to deformation processes, mass changes and exchange of angular momentum) and all relevant geophysical models. This is a highly interdisciplinary task and asks for a close cooperation of geodesists, geophysicists/geologists, glaciologists, oceanographers, hydrologists and atmospheric physicists. The ultimate goal should be the development of comprehensive numerical Earth models that are able to assimilate time series of global surface, mass transport and mass exchange processes. They are expected to enable a deeper understanding for solid Earth processes such as glacial isostatic adjustment, tectonic motion, volcano activity or Earthquakes, as well as for near-surface processes such as ice mass dynamics and balance, heat transport in the oceans, the various components of sea level change, the global water cycle and atmospheric dynamics.

The measured temporal variations of gravity/geoid and the Earth rotation represent the total, integral effect of all mass changes in the Earth system. Thus, methods have to be conceived for their separation into the individual contributions. This is a difficult but important task and requires the development of a sophisticated over-all strategy. The use of complementary satellite techniques, tailored sampling strategies, satellite formation flights, terrestrial calibration sites, permanent recordings, dedicated campaigns and geophysical models will prove important for this. Of similar character is the problem of aliasing due to the limited resolution in time and space, in general, of satellite missions.

The proposed research program is certainly intended not to cover all components of the Earth system, at least not in a first step; for example, the electro-magnetic constituent as well as atmosphere and ionosphere and the source structure of core and inner mantle as well as the various relations

between these sub-systems are not taken into account. The same holds for exogene influences of the solar system and the translational and rotational motion of the Earth with respect to an Inertial Reference System. Even important mass transport phenomena are not included as long as alternative observables than gravity field quantities and geometric observables are better suited to improve the respective models. For example, at present one does not expect that gravity field observations can improve the atmospheric and climatological models. But to avoid contamination and aliasing effects available models have to be considered properly, as the water mass exchange between the atmosphere on the one hand, and oceans, ice and the continental water cycle on the other hand – just to mention one important example.

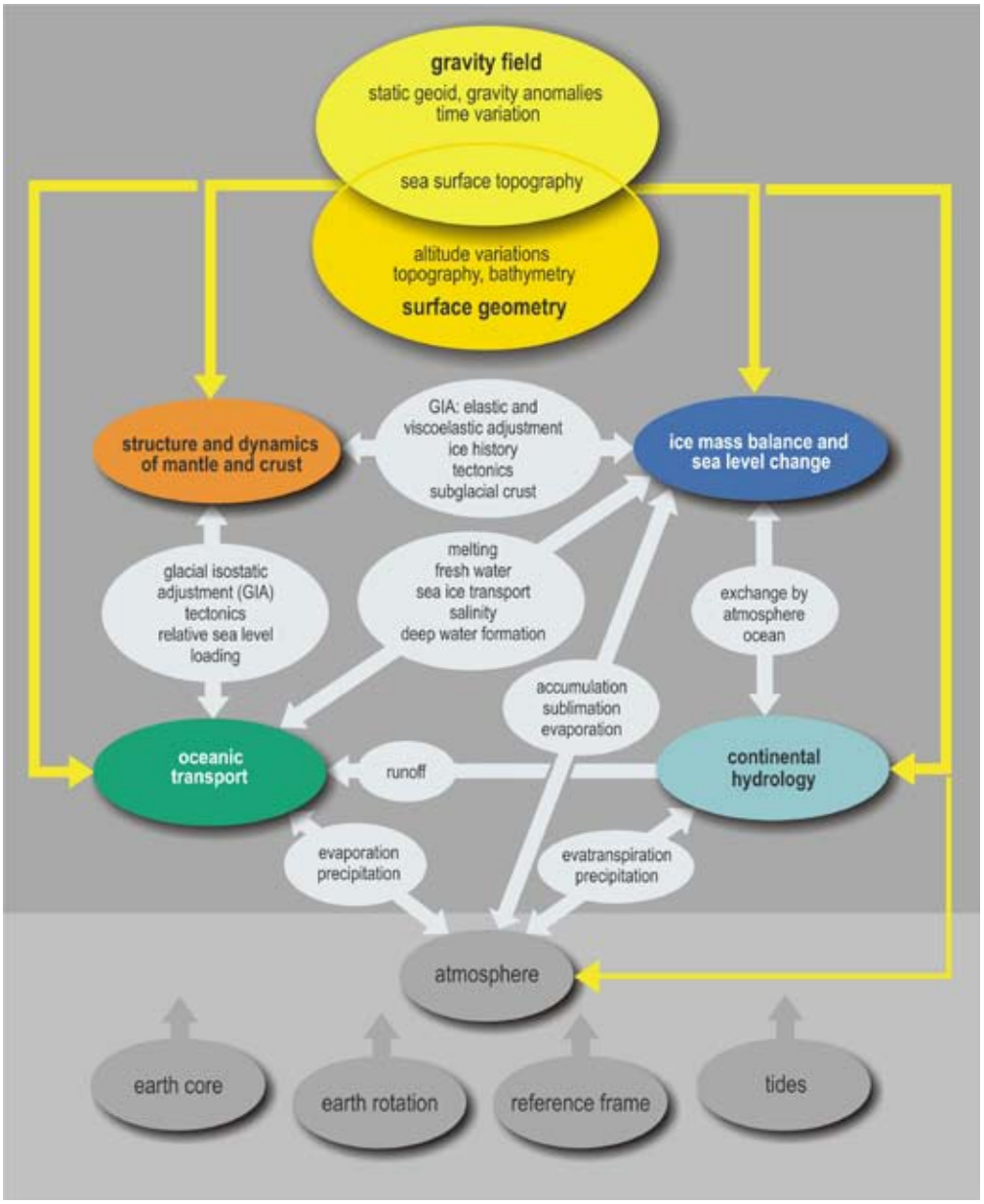

Figure 1.5: *Interconnections between mass transport processes, and their relation to gravity and geometry. Mass exchange and dynamic feedback are indicated by light grey arrows. Yellow arrows show the relations between observable parameters and the different processes.*

1.3 Research topics and establishment of a national research program

A unique research opportunity emerges from the fact that a multiple of geodesy related missions, the gravity missions CHAMP, GRACE and GOCE, the altimetric ice missions CryoSat and ICESat, the ocean altimeter missions TOPEX/Poseidon and JASON and the environmental satellite mission ENVISAT but also the envisaged satellite navigation system GALILEO are simultaneously in orbit. It will allow the coherent global study of mass balance and transport processes for the first time. Germany has invested considerably in all of the above missions (except in JASON and ICESAT) and German scientists played a leading role in the promotion and study of these mission concepts. It is of interest that the German scientific community can adequately harvest scientific return and play a significant role in this important segment of Earth system research. Precondition is a coherent priority research program in this area that combines all necessary elements of solid Earth physics, oceanography, geodesy, glaciology, sea level research and hydrology.

The joint research program will focus on the determination of processes that are associated with mass distribution, transport, exchange and balance. Earthquakes, volcano eruptions, tectonic deformations, land slides, glacial isostatic adjustment, deglaciation, sea level rise, ocean mass and heat transport, deep ocean circulation, the water cycle, atmospheric and ocean loading and many more are typical and well known phenomena of this kind. Mass anomalies, the transport and exchange of masses and mass balances are not measurable by any other means and add significantly to the understanding of global Earth dynamics. In the following, potential research topics as part of a national research program are specified.

Mass transport: signal analysis and signal balancing - Precise simultaneous measurement of gravity field variations and surface deformation lead to the possibility to investigate mass distribution, mass transport and mass exchange in the Earth system for the first time. Separation of the individual signal contribution and a process oriented balancing becomes possible by combining this new generation of measured mass signals with the models and techniques of all related disciplines. Prerequisite is a precise geodetic-geodynamic reference frame for all numerical analysis procedures, the application of new computation standards and a user oriented processing of the mission products. Topics of research are: integration of reference systems and computation standards, harmonization and development of a precise consistent reference frame in space and time; development and application of solution procedures and space-time filtering methods for the mission products with the task to separate the signal in its contributions and combination with scales of geophysical models involved; validation, separation and balancing of measured temporal changes of the gravity field and the ice and ocean surfaces respectively by model results and complementary data sets.

Ocean circulation and transport – The combination of geoid and altimetry allows for the first time the direct determination of the global dynamic ocean topography. The geostrophic balanced surface currents can be deduced from the inclinations of the dynamic topography. From these, complete profiles of the ocean circulation can be derived by combination with traditional hydrographic measurements. New insights in global and basin related heat and mass transport can be expected. Temporal variations of the dynamic ocean surface are caused mainly by temperature related volume changes where the mass column remains unchanged. Mass changes by fluid dynamics causes more problems and can be detected only by changes of the gravity field as expected by the GRACE mission. This will lead to a clear progress in the understanding of ocean circulation. Topics of research are: determination of large-scale heat and mass transport; investigation of circulation systems as the Antarctic circum polar current, Weddell- and Ross eddies; separation of steric and eustatic changes of the global sea surface and of the dynamics of currents; interaction of temporal

and quasi-static circulations (eddies, fronts).

Hydrological cycle – The determination of the continental water storage in space and time is not possible nowadays with sufficient accuracy. The time dependent gravity field as expected from the GRACE mission enables for the first time to detect continental mass changes with a resolution of 1cm water column in monthly snapshots. This allows to close the hydrological cycle at different scales in time and space. Topics of research are: global water balance and water transfer between atmosphere, continents, oceans and ice shield; large-scale variations of terrestrial water storage under characteristic conditions; large scale temporal variations of evapotranspiration; evaluation and development of large-scale hydrological models; water balances in difficult accessible regions; long term trends of continental water storage as a consequence of environmental changes; identification of hydrological problem zones with respect to water management and the availabilty of water resources.

Ice mass balance and sea surface – The polar ice caps play a key role in Earth system because imbalanced masses and resulting changes of the sea surface are global. Of central relevance is the precise determination of the mass balance of the complete ice shields by the actual gravity field missions CHAMP, GRACE and GOCE. Altimetry enables the precise measurement of the topography and of ice height changes, with the missions CryoSat and ICESat also in the climate sensitive ice shield regions. Interferometric SAR (ENVISAT) enables the area wise determination of ice motions which can be compared to balance velocity models. The precise measurement of the thickness of the sea ice (CryoSat) provides new insight in the actual climate development. Topics of research are: registration of mass changes of the polar ice caps and the consequences for sea level rise; investigation of the changes in the border areas of ice masses; validation and improvement of glaciological models as important component in coupled climate models; determination of ice mass induced recent crust deformations (glacial isostasy); additional data sets for validation, densification and interpretation of satellite data; modelling of sea ice dynamics based on new remote sensing data.

Crust and mantle – The new gravity field missions open new dimensions in the research for geodynamic mass transport within the Earth: GOCE will improve the resolution of the static gravity potential and its gradients in the medium and short wavelength range by more than one magnitude; GRACE will provide for the first time the temporal variation of the potential down to a resolution of 400km; it can be expected that mass distribution and mass transport will become directly observable. Topics of research are: glacial-isostatic adjustment processes and lateral variations of mantle viscosity; global mass transport in the mantle and dynamic topography based on new seismic tomography data and 3D-distributions of mantle viscosity; sub-lithosphere mantle convection and deviations of seismic discontinuities in 410 and 600 km depth; models of active and passive continental margins based on high-resolution gravity data, decoupling processes at active subduction zones; episodic mass redistributions at plate margins; improvement of global and regional crust and lithosphere models.

Atmosphere and Tides – Mass transports by the atmospheric circulation and by tides make up an integral part of mass variations and transports in the Earth system. For the purpose of the proposed program, both components are regarded as known from observations and models. They are treated as correction terms during gravity field analysis. However, the contribution of their uncertainty to the total error budget of mass variation estimates has to be assessed. Furthermore, the atmospheric conditions are required as input for models of the oceans, the continental hydrosphere and the cryosphere to drive mass transport and mass exchange processes.

2 The satellite missions: observing the Earth system from space

There is a unique situation for the next years: Based on innovative sensor technologies such as accelerometers, satellite-to-satellite tracking, and gradiometry, the gravity field missions CHAMP, GRACE and GOCE will lead to dramatic improvements in Earth gravity field recovery. At the same time multi-mission altimetry continues to observe the ocean surface and ice sheets by ENVISAT, Jason-1, GFO, ICESat and CryoSat with a space-time sampling enabling to monitor the temporal variability with high resolution. The synergy of all these missions will help to improve the understanding of environmental and deep Earth processes.

2.1 Gravity field mapping

Tracking the orbits of some tens of satellites at different altitudes and orbit inclinations has over the last three decades gradually improved the knowledge of the Earth's gravity field. While these conventional methods have provided accurate information for the very large scale structures of the gravity field, they have insufficient accuracy and time resolution to support a wide range of applications. The limitations are due to the attenuation of the gravitational signal with altitude, the sparse tracking data coverage and the difficulties in modelling the non-gravitational forces acting on the satellites. The pre-CHAMP status in global gravity field recovery from space is represented by the model GRIM5-S1 (Biancale et al., 2000). With the **CHAllenging Minisatellite Payload (CHAMP) mission** (Figure 2.1), launched in 2000, the first dedicated gravity field mission has been realized: a low (initial altitude 454 km, now 370 km) and near-polar orbit, an on-board accelerometer for the measurement of non-gravitational forces such as air drag and solar radiation pressure, and a continuous precise tracking simultaneously by up to 10 high-orbiting GPS satellites. These characteristics led to a break-through in the determination of the long-wavelength gravitational field (Reigber et al., 2003) already from a limited amount of mission data and, for the first time, from the analysis of observed orbit perturbations of only one satellite (Figure 2.2).

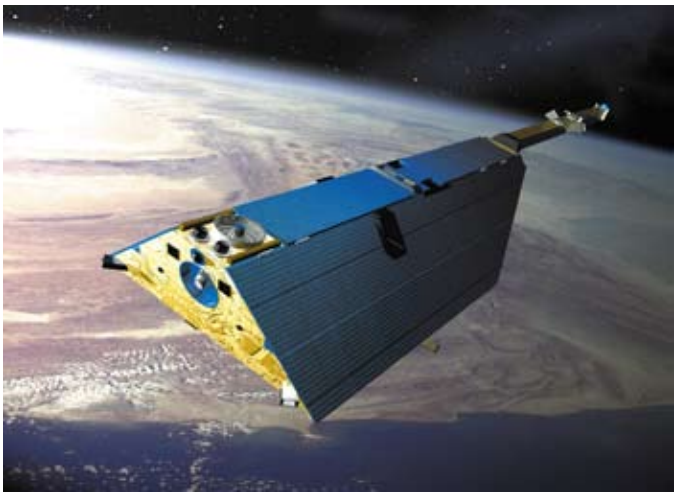

Figure 2.1: *The CHAMPsatellite*

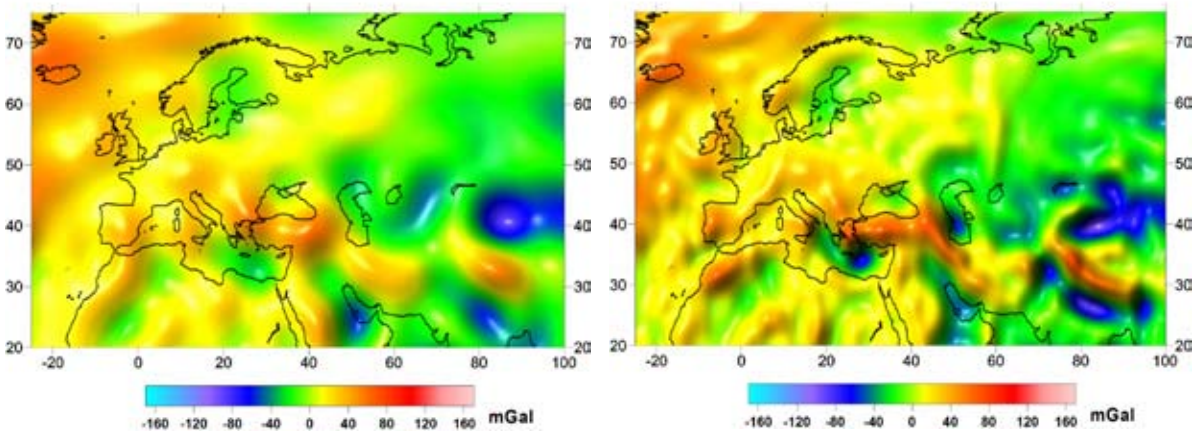

Figure 2.2: *Gravity anomalies over Europe derived from the pre-CHAMP multi-satellite global gravity field model GRIM5-S1 (left) and a CHAMP-only model derived from 33 months of mission data (right).*

The CHAMP mission (Reigber et al., 1999) is conducted since the beginning under full responsibility of GeoForschungsZentrum Potsdam (GFZ) with participation of the German Centre for Aerospace (DLR). The mission is funded by the German Ministry of Education and Research, GFZ and DLR. The mission lifetime will end around the year 2008.

It was noted already decades ago by Wolff (1969) that the intersatellite signal between a pair of satellites orbiting the Earth in the same orbit plane has significant information on the medium to shorter wavelength components of the Earth's gravitational field and, if this relative motion can be measured with sufficient accuracy, this approach will provide significant improvement in the gravity field modelling. This mission concept was proposed for the early GRAVSAT experiment by US scientists (Fischell and Pisacane, 1978) and the SLALOM mission in Europe (Reigber, 1978). Both of these as well as later similar mission proposals were not successful in being accepted for funding. The break-through came with the acceptance of the **Gravity Recovery and Climate Experiment (GRACE) mission** (Figure 2.3), proposed by Tapley and others in 1997 as a joint US-German partnership mission (Tapley et al., 2004a) within NASA's Earth System Science Pathfinder (ESSP) program. The science processing system is chaired by the Center for Space Research (CSR) of Texas University in Austin with a distribution of work between CSR, NASA's Jet Propulsion Laboratories (JPL) and GFZ (see also the CHAMP mission fact sheet in Annex A7).

The Gravity Recovery and Climate Experiment (GRACE) is a dedicated satellite mission whose objective is to map the global gravity field with unprecedented accuracy over a spatial range from 400 km to 40,000 km every thirty days. Meanwhile it has been proven (cf. Chapter 2.2) that the measurement precision provides a gravity field model whose accuracy for these length scales is about 20 times better than what was known before.

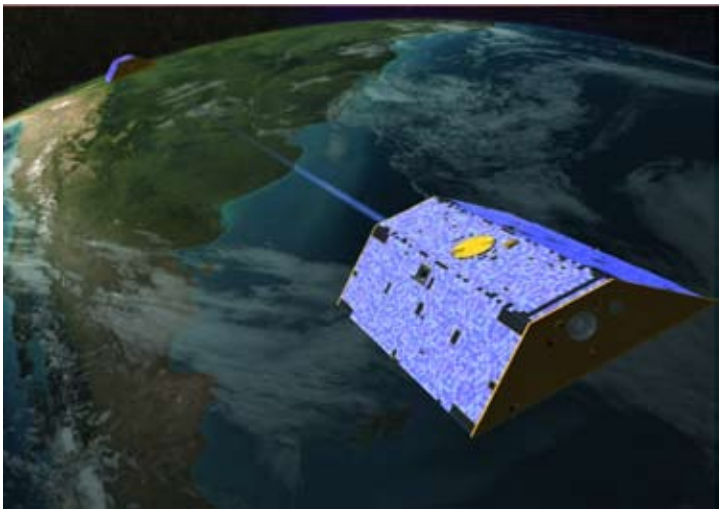

Figure 2.3: *The twin GRACE satellites.*

The twin GRACE satellites, based on CHAMP heritage, were launched on March 17, 2002 into an almost circular, near-polar orbit (inclination 89.0°) with an initial altitude of 500 km, for an at least 5 years mission. The natural decay of the orbital altitude since launch is about

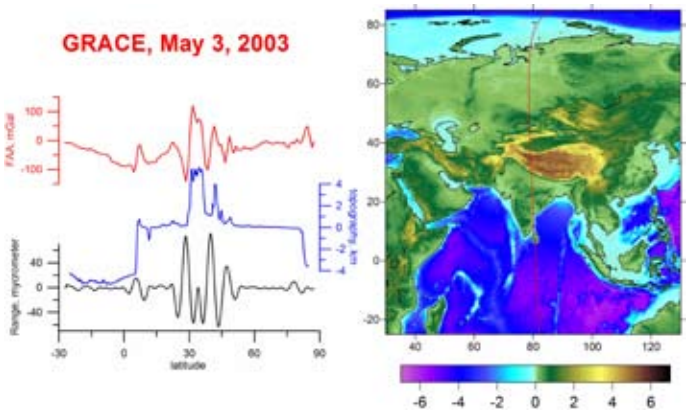

Figure 2.4: *High-pass filtered variations in GRACE satellites' separation (graph at the bottom of the left panel) during an over-flight of the Himalayas from South to North (right panel). The other two graphs show the topographic heights and free-air gravity anomalies along the profile.*

1.1 km/month. The GRACE configuration consists of two identical satellites that follow each other on the same orbital path and are interconnected by a K-band microwave link to measure the exact separation distance and its rate of change with an accuracy of better than 10 mm and 1 µm/s, respectively. Figure 2.4 gives an example of measured range variations when crossing the Himalayas. Both satellites are equipped with the highly advanced BlackJack GPS flight receiver instrument for high-low satellite-to-satellite tracking, a three-axis SuperSTAR accelerometer to observe the non-gravitational forces, and two star-cameras to measure the inertial orientation of the satellites. The instrumentation and on-board instrument processing units are described in detail in Dunn et al. (2003), see also the GRACE mission fact sheet in Annex A7.

Figure 2.5 demonstrates the progress in spatial detail resolution of a GRACE derived gravity field model and proves the enhanced capabilities of the GRACE mission concept compared to a single satellite mission like CHAMP.

The primary objective of the GRACE mission is the observation of non-tidal temporal gravitational field variations. These are mainly due to seasonal, interannual and long-term mass redistributions in and among the Earth's atmosphere, hydrosphere, cryosphere and solid Earth. The observation of these climatologic and environmental phenomena becomes possible thanks to uninterrupted GPS and KBR space-based tracking allowing accurate gravity field solutions at monthly intervals. As a novel result, from the analysis of the sequence of gravity field solutions, seasonal global scale continental water storage variations (Figure 2.6) could successfully be recovered from space (Schmidt et al., 2004, Tapley et al., 2004b, Wahr et al., 2004). At present, the GRACE data analysis is being extended to address ocean and ice sheet mass variability.

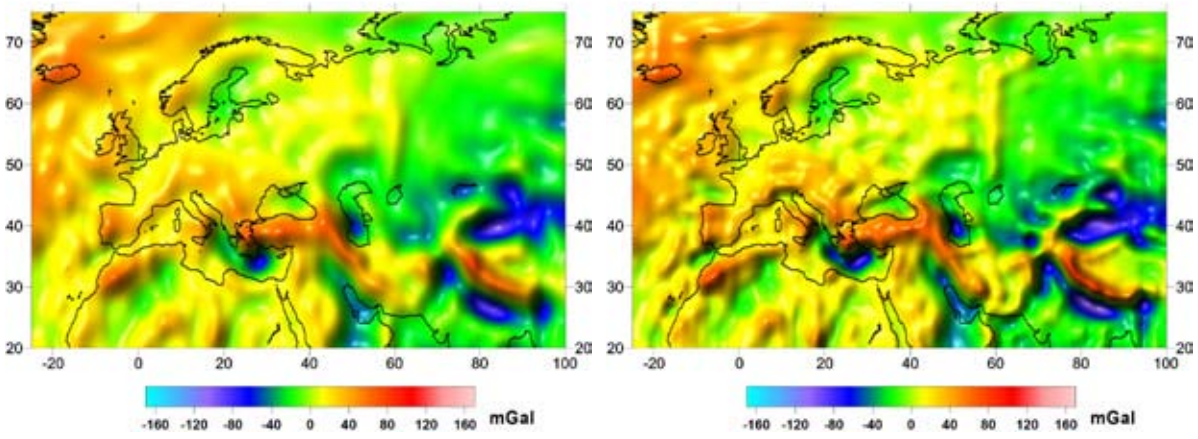

Figure 2.5: *Gravity anomalies over Europe derived from 33 months of CHAMP data (left) and 110 days of GRACE data (right).*

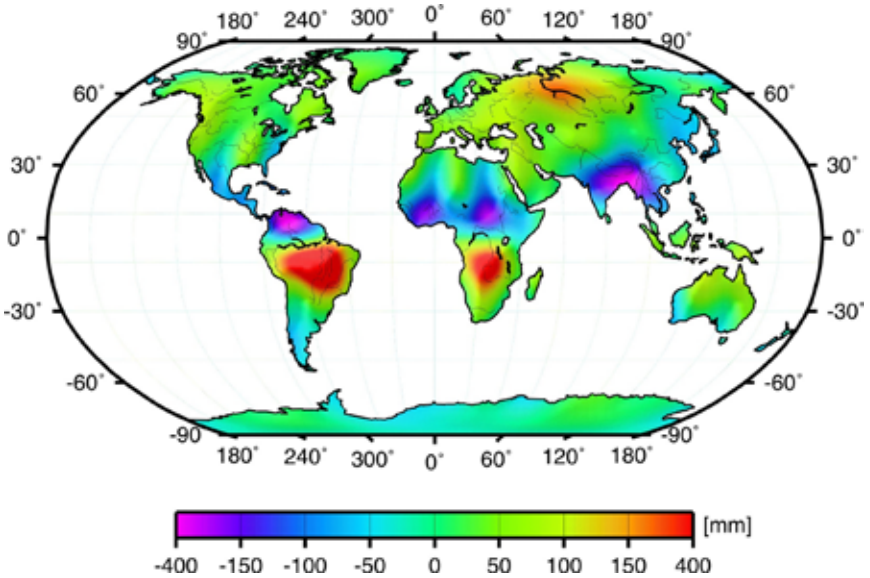

Figure 2.6: *Spring minus summer 2003 difference in continental water storage as observed with GRACE (in units of equivalent water column).*

During the anticipated five to eight years' duration of the CHAMP and GRACE missions, the orbits of the satellites will come closer to the Earth's surface enhancing the sensitivity with respect to spatial and temporal gravity field variations. From this, the increasing observation periods and from the combination of both CHAMP and GRACE data, further improvements in gravity field recovery with respect to accuracy, resolution and reliability are expected to come.

The third satellite in the sequence of dedicated gravity satellite missions will be **GOCE (Gravity field and steady-state Ocean Circulation Explorer)** (Figure 2.7). GOCE is planned to be launched in 2006 and was selected as the first Core Mission within the Living Planet Earth Observation Programme of the European Space Agency (ESA 1999). The payload of GOCE will consist of a GPS receiver, again for orbit determination and resolving the large spatial scales of the gravity field, and a gravity gradiometer consisting of six three-axes accelerometers to measure in-orbit

Figure 2.7: *The GOCE satellite. The orbit will be sun-synchroneous, the same side facing to the sun over all the mission duration, to ensure thermal stability and power supply.*

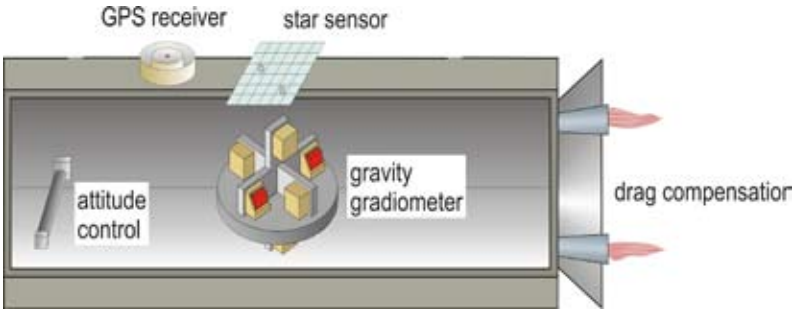

Figure 2.8: *Sensors and actuators on board of GOCE.*

gravity gradients in three spatial directions (Figure 2.8). For the first time gravity field recovery from space will not be based purely on the analysis of orbit perturbations. The sensitivity of the GOCE accelerometers will be further increased. The satellite will fly in a near polar, extremely low orbit (250 km altitude) which is permanently maintained by ion-thrusters compensating for air-drag (drag-free concept). The mission duration will only be 20 months.

The low orbit height and the measurement of gradients (2nd derivatives of the gravity potential) help to counteract the attenuation of the gravity signal in space and allow GOCE to achieve a very high spatial resolution for the gravity field down to half wavelengths below 100 km. By this, the requirement of the oceanographers for a high-resolution precise geoid shall be fulfilled. The geoid is needed as a physical reference surface for the determination of the global ocean circulation pattern in combination with satellite altimetry. The GOCE resolution will also open new possibilities for modelling of the structure of the Earth's crust and mantle, and it will bring a big step forward for regional combined geoid modelling with terrestrial gravity data, to get a globally consistent height reference in 1cm accuracy for geodesy (see also the GOCE mission fact sheet in Annex A7).

The combination of GPS high-low satellite-to-satellite tracking with accelerometry, a low-low intersatellite link and/or a gradiometer on low Earth orbiting platforms provides an excellent tool for mapping the Earth's gravity field homogeneously from space with ever increased accuracy and resolution over the globe and in time. The three missions, although competitors in certain respects, perfectly complement each other. CHAMP as the first low Earth orbiter collecting continuously precise orbit data already brought a new level of gravity accuracy as well as important experience for the succeeding missions. GRACE will achieve an extremely high precision for the long and medium wavelengths and will thus allow to observe temporal variations, while GOCE, being less accurate for the lower part of the signal spectrum, will reach a very high spatial resolution for the static gravity field.

For the new data types delivered by the three missions (continuous time series of observations), currently new techniques for gravity field analysis are developed and implemented. To assess the expected high quality of the results, new strategies for validation using independent data are required.

From observables to gravity field coefficients

The signal of the Earth's irregular gravity field at satellite's altitude is visible in gravitational orbit perturbations (deviations from the Kepler ellipse) of a free-flying Earth orbiting satellite. Superimposed to the gravitational orbit perturbations are surface force induced non-gravitational orbit perturbations arising from air drag (for low flying satellites) and direct and indirect solar radiation pressure.

Precise tracking of the satellite's orbit is a prerequisite to allow a precise restitution of the satellite's orbit for getting access to the orbit perturbations. By subtracting the non-gravitational orbit perturbations, either applying air density and radiation models or more accurately taking directly the on-board accelerometer measurements (CHAMP and GRACE), the purely gravitational orbit signal is available for gravity field recovery. On GOCE, the non-gravitational orbit perturbations are automatically balanced out during flight by the drag-free control system that operates within the gradiometer measurement bandwidth.

The resolution in global gravity field recovery, when applying orbit perturbation analysis from a single satellite is restricted to half wavelengths approximately corresponding to the flight altitude. The increase in resolution comes in case of GRACE through the additional measurement of along track distance variations between the two co-orbiting satellites, yielding relative orbit perturbations over a 220 km long basis, and in the case of GOCE, different from orbit perturbation analysis, through the on-board gravity gradient component measurements.

The traditional approach to exploit gravitational orbit perturbations for gravity field recovery uses a numerically integrated orbit (arc length of e.g. 1 day) based on an initial gravity field and other force models. The difference between the tracking observations (GPS ranges) and corresponding quantities computed with the integrated orbit then are used in a least squares adjustment to solve simultaneously for orbit (state vector) and measurement configuration dependent parameters, and after accumulation of a sufficient amount of single arc normal equation systems, for the looked-for spherical harmonic coefficients (cf. Annex A1) describing the global gravity field model (e.g. Reigber et al., 2003).

The known temporal gravity field variations have to be accounted for when integrating the orbit and adjusting the gravity field parameters in order to avoid aliasing from higher (1 rev per 2 months) into lower temporal frequencies and thus degrading e.g. monthly gravity field solutions. Also the orbital fit between the integrated and observed orbit is improved. The temporal gravitational field variations presently being considered within the adjustment process are Earth and ocean tides, and non-tidal atmospheric and oceanic mass redistributions. A series of monthly gravity field models does therefore not include the effects from these sources that are based on tidal and ocean circulation models, and global air pressure data with a resolution of six hours. Averages of these ‚de-aliasing products' over the individual months have then to be computed and added back to the monthly gravity field solutions in order to get the full ‚real' gravity field model representing the average of a particular month (or any other time interval). Hydrologic models and data over land are not yet complete and reliable enough to be included within the process, i.e. the hydrologic signal should be present in the solutions anyway.

The fact, that the orbits of the new generation of satellite gravity missions are continuously observed by multi-directional GPS tracking allows for the first time to restitute the orbit in a geometric or kinematic approach that is completely independent of any gravitational and non-gravitational force modelling. Based on these kinematic orbits, new evaluation approaches became possible: direct determination of the gravitational potential at satellite's altitude (e.g. Gerlach et al., 2003) applying the energy conservation law (the sum of kinematic and potential energy is constant, after having subtracted the dissipating non-gravitational contribution), or a spectral analysis of the kinematic orbits (Mayer-Gürr, et al., 2004), or conversion of positions into gravitational accelerations (e.g. Reubelt et al., 2003). The values of the gravitational potential or accelerations along the orbit then are converted to the looked-for spherical harmonic gravitational coefficients in a subsequent least squares adjustment. Other approaches use a localizing parameterization (e.g. wavelets) of the gravity field for a regional recovery of the gravity field in areas of interest (e.g. Fengler et al., 2003).

Also, the completely new type of measurements becoming available with GOCE, the gravity gradients, will stimulate completely new methods of global and regional gravity field recovery.

2.2 Gravity field results from CHAMP and GRACE

Since the launch of CHAMP in 2000 and GRACE in 2002 numerous gravity field models have been generated from the mission data each time refining the processing methods and enlarging the data base. The efforts are concentrating on producing a **mean field model**, i.e. representing the part of the Earth gravity field that is constant in time, and a time series of monthly gravity field models from GRACE representing the **gravity field variations with time**. Only GRACE has the capability to resolve temporal gravity field variations due to mass redistributions in the Earth system with a meaningful temporal and spatial resolution.

Mean field models

The purpose of the mean field models is twofold: (1) satellite-only models, i.e. derived solely from CHAMP and GRACE data, shall provide the best available geoid for use as a reference surface in altimetric mapping of the sea surface topography for oceanographic modelling, and (2) combined models, i.e. a joint gravity field solution from satellite tracking and surface data compiled from satellite altimetry over the oceans and gravimetry over the continents, shall provide a

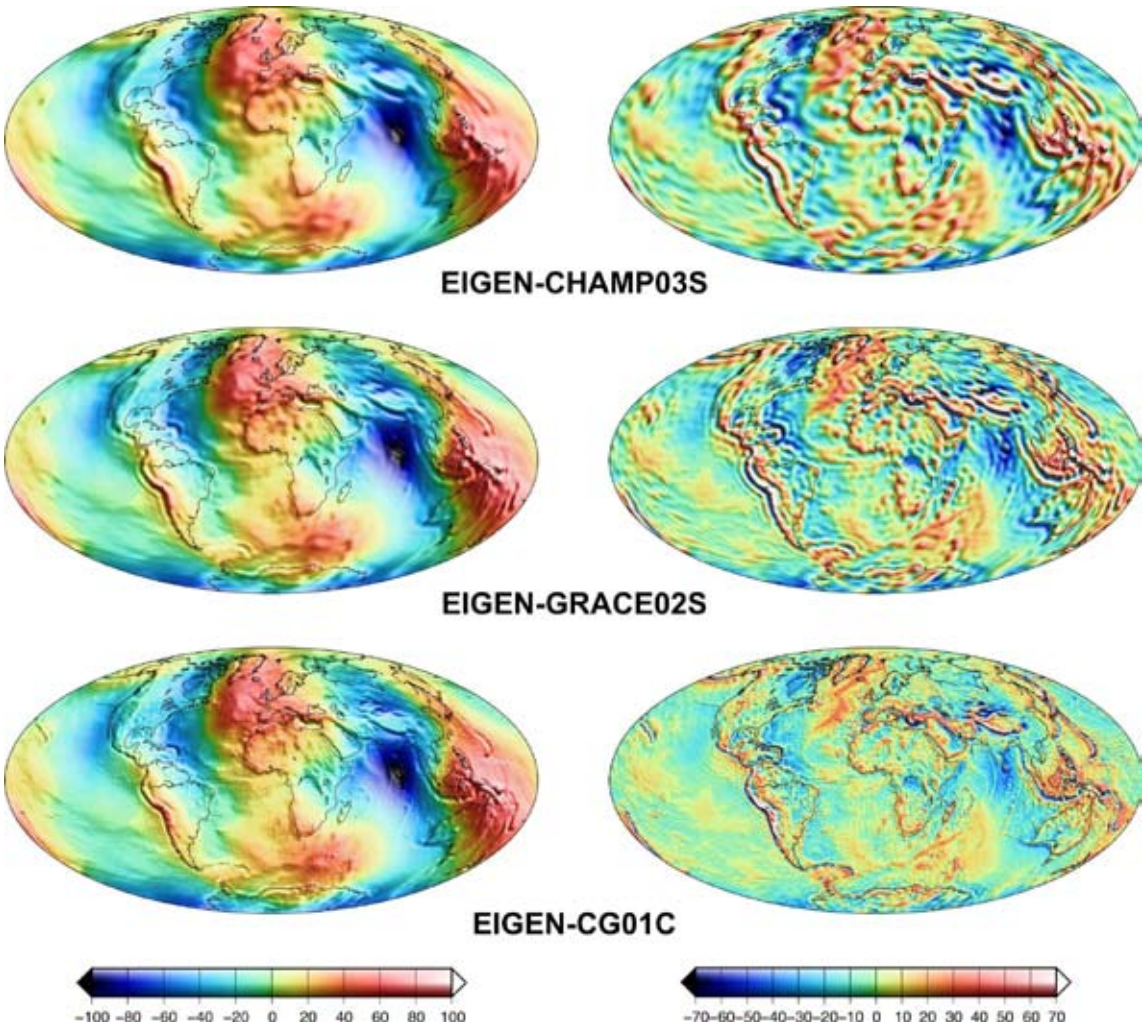

Figure 2.9: *Geographical distribution of geoid heights (left panel in meter) and gravity anomalies (right panel in mgal) derived from the CHAMP and GRACE satellite-only models, and the satellite/surface data combined high-resolution model (from top to bottom).*

high-resolution model for use in geodesy (regional geoid and gravity modelling) and geophysics (geotectonic/geodynamic interpretation and modelling).

Figure 2.9 shows the geoid and gravity anomaly maps of the latest CHAMP-only, GRACE-only and combined global gravity field solutions, as generated by the CHAMP and GRACE processing centres at GFZ Potsdam. The third generation CHAMP-only solution is based on 33 months of CHAMP data and is called EIGEN-CHAMP03S (Reigber et al., 2005). The second generation GRACE-only solution is based on 110 days of GRACE data and is called EIGEN-GRACE02S (Reigber et al., 2004a). The combined solution incorporates the CHAMP and GRACE mission data from the two satellite-only solutions as well as a global compilation of 0.5°x0.5° gridded surface data from altimetry (oceanic geoid and gravity anomalies), and air-borne and terrestrial gravimetry (gravity anomalies). The combined high-resolution global gravity field model is called EIGEN-CG01C (Reigber et al., 2004b).

Due to the characteristics of the data sources, the three models have a different spatial resolution and accuracy, as will be discussed below. Roughly speaking, the CHAMP solutions resolves features in the gravity field exceeding 333 km (half-wavelength or pixel-size) at the Earth's surface, GRACE those exceeding 200 km, and the combined solution those exceeding 55 km corresponding to the input data grid resolution.

Each computed global gravity field model undergoes various tests in order to evaluate the accuracy of the obtained solution. Comparisons of a satellite-only gravity field model in the spatial domain against independent gravity anomalies or geoid height data are capable to test the model accuracy homogeneously over all spherical harmonic coefficients up to the considered resolution. For this purpose, gravity anomalies and geoid heights were computed from the spherical harmonic coefficients of the gravity field models on an equal angular global grid at two different resolutions (5° and 2.5° spacing). These are compared against appropriately filtered geoid heights derived from altimetry over the oceans (sea surface heights minus sea surface topography) and altimeter derived gravity anomalies. The root mean squares of the differences (after bias elimination) as given in Table 2.1 show the striking gain in accuracy and resolution from the pre-CHAMP over the CHAMP-only to the GRACE-only model. At the accuracy level meanwhile reached with GRACE, these comparisons are more or less plausibility checks as the rms values mainly reflect the large scale errors in the surface data used for comparison.

Another method to test the quality of global gravity field model is the comparison against geoid heights determined point-wise by GPS positioning and leveling (GPS-leveling). Table 2.2 shows

Table 2.1: *Comparison of geopotential models with altimeter derived geoid heights (N, 'CLS01 minus ECCO' oceanic geoid) and gravity anomalies (Δg, NIMA marine gravity anomalies) for a grid spacing of 5° x 5° (degree/order 36) and 2.5° x 2.5° (degree/order 72).*

Model	rms(dN)		rms (dΔg)	
	5°×5°	2.5°×2.5°	5°×5°	2.5°×2.5°
GRIM5-S1 (pre-CHAMP)	44 cm	76 cm	2.00 mGal	5.40 mGal
EIGEN-CHAMP03S	15 cm	30 cm	0.48 mGal	3.23 mGal
EIGEN-GRACE02S	14 cm	16 cm	0.28 mGal	1.25 mGal
EIGEN-CG01C	14 cm	15 cm	0.28 mGal	0.97 mGal

rms – root mean square of difference about mean

Model	rms(dN)
GRIM5-S1 (pre-CHAMP)	51 cm (37 ... 360 CGO1C)
EIGEN-CHAMP03S	42 cm (37 ... 360 CGO1C)
EIGEN-GRACE02S	39 cm (72 ... 360 CGO1C)
EIGEN-CG01C	38 cm

rms – root mass mean square of differences
(bias per data set removed)

Table 2.2: *Comparison of geopotential models with GPS-leveling derived geoid heights over USA, Canada and Europe, models filled with EIGEN-CG01C coefficients.*

the results for the models under consideration using GPS-leveling points from USA (6169 benchmarks), Canada (1930 benchmarks) and Europe (186 benchmarks). The resulting rms-values are relatively large due to the omission error in the global models when comparing with point values. Nevertheless the improvement from the earlier to the most recent models is obvious. The satellite-only fields were filled up starting at a reasonable degree of truncation with the coefficients of the combined model in order to make the rms values comparable.

There is almost no possibility to evaluate the accuracy of the combined solution EIGEN-CG01C by external data comparison because except GPS-leveling data nearly all available data have been incorporated to create the high-resolution model. From the knowledge of the input data quality it is estimated that the EIGEN-CG01C solution has an average accuracy of 20 cm in terms of geoid heights and 5 mgal in terms of gravity anomalies at maximum resolution of 50 km half-wavelength. The accuracy is of course varying between oceans, polar areas and continents, as well as among different countries depending on the quality of the available surface gravity data. For the long- to medium-wavelength part of the model, i.e. for wavelength larger than 200 km, the model is almost completely determined by the GRACE satellite normal equations, i.e. of the same quality as the GRACE-only model (cf. Tables 2.1 and 2.2).

As the above given tests fail to give realistic accuracy numbers for the long- to medium-wavelength part of the gravitational spectrum, the accuracy of the most recent global gravity field models is estimated based on the difference of sub-set solutions generated from data out of different observation periods. The scattering of the spherical harmonic coefficients among the sub-set solutions yields the information to calibrate the formal error estimates that result from the adjustment. The calibration factors are determined as a function of the spherical harmonic degree of the solved-for gravitational coefficients. The error curves presented in Figure 2.10 over the gravitational spectrum are the calibrated ones and are considered to give a realistic impression of the models' accuracy.

Figure 2.10 depicts the signal degree amplitudes (cf. Annex A1.3) of the CHAMP, GRACE and combined gravity field solutions and the corresponding estimated error degree amplitudes in terms of geoid heights and gravity anomalies. The drastically improved performance in both accuracy and resolution with GRACE compared to CHAMP is clearly visible. The spectrum of the predicted GOCE accuracy (baseline mission assumption) is also given in Figure 2.10.

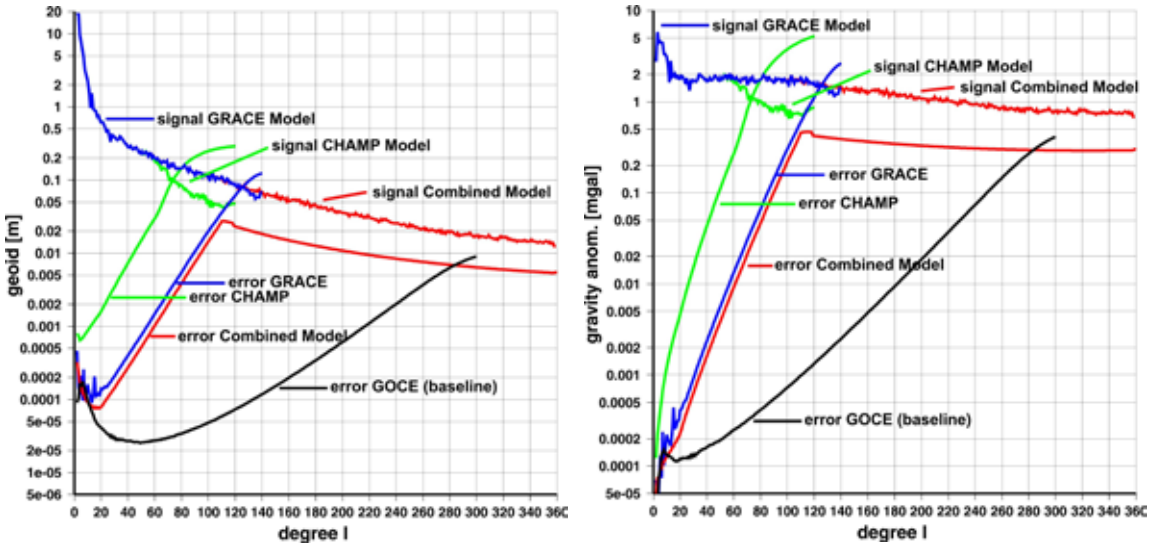

Figure 2.10: *Signal and error degree amplitudes in terms of geoid heights (left) and gravity anomalies (right).*

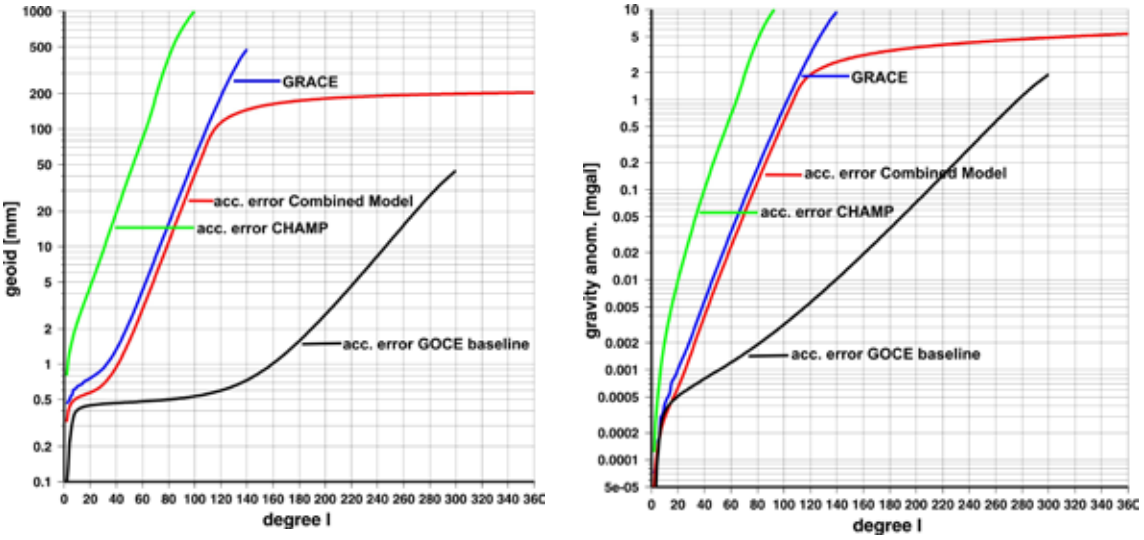

Figure 2.11: *Error amplitudes (accumulated) as a function of maximum degree l in terms of geoid heights (left) and gravity anomalies (right).*

Figure 2.11 gives degree-wise accumulated (degree 2 to *l*, cf. Annex A1.3) error degree amplitudes of the curves in Figure 2.10. The Figure reveals the overall geoid and gravity anomaly accuracy up to the selected maximum degree *l* of the spherical harmonic expansion (spatial resolution of λ=40000 km/*l*).

The threshold for geodetic, oceanographic and geophysical use of the static or mean gravity field as a dynamic reference surface and for density studies is on the 20 cm and 0.1 to 5 mGal level, respectively, whereby the requirements from oceanography are the most stringent ones.

Table 2.3 summarizes in view of these requirements the present stage in CHAMP, GRACE and combined global gravity field recovery for the mean field (cf. Figure 2.11) as well as the goal for the GOCE mission. The expected improvements in CHAMP and GRACE results are due to advances in data processing and the decreasing orbit altitude.

Table 2.3: *Mean gravity field recovery: geoid (cm) and gravity anomaly (mGal) accuracy vs. resolution (λ/2 pixel side length).*

CHAMP (33 months) *achieved*	**GRACE (110 days)** *achieved*	**Combined *)** *achieved*	**GOCE**
10 cm, 1 mGal@350km; 1 cm, 0.02 mGal@650km	10 cm, 1 mGal@200km; 1cm, 0.02 mGal@330km	20 cm, 5 mGal@50km	
expected	expected	expected	expected
factor 1.5 improvement	factor 5 improvement	6 cm, 3 mGal@50km with GOCE	2 cm, 1 mGal@100km

*) CHAMP + GRACE + Surface Gravity Data

Temporal Gravity Field Variations

A first generation of monthly GRACE global gravity field solutions has been computed from more than two years of data available. In case of longer data gaps, two subsequent months have been combined into one solution. From these solutions, the differences between pairs of later on recovered gravity fields being 6 and 3 months apart were investigated for seasonal temporal gravity field variations: April/May 2003 minus August 2003, April/May 2002 minus November 2002, and November 2002 minus April/May 2003. As mass variations due to atmosphere, tidal and non-tidal ocean variability were considered during processing, the differences should mainly reflect

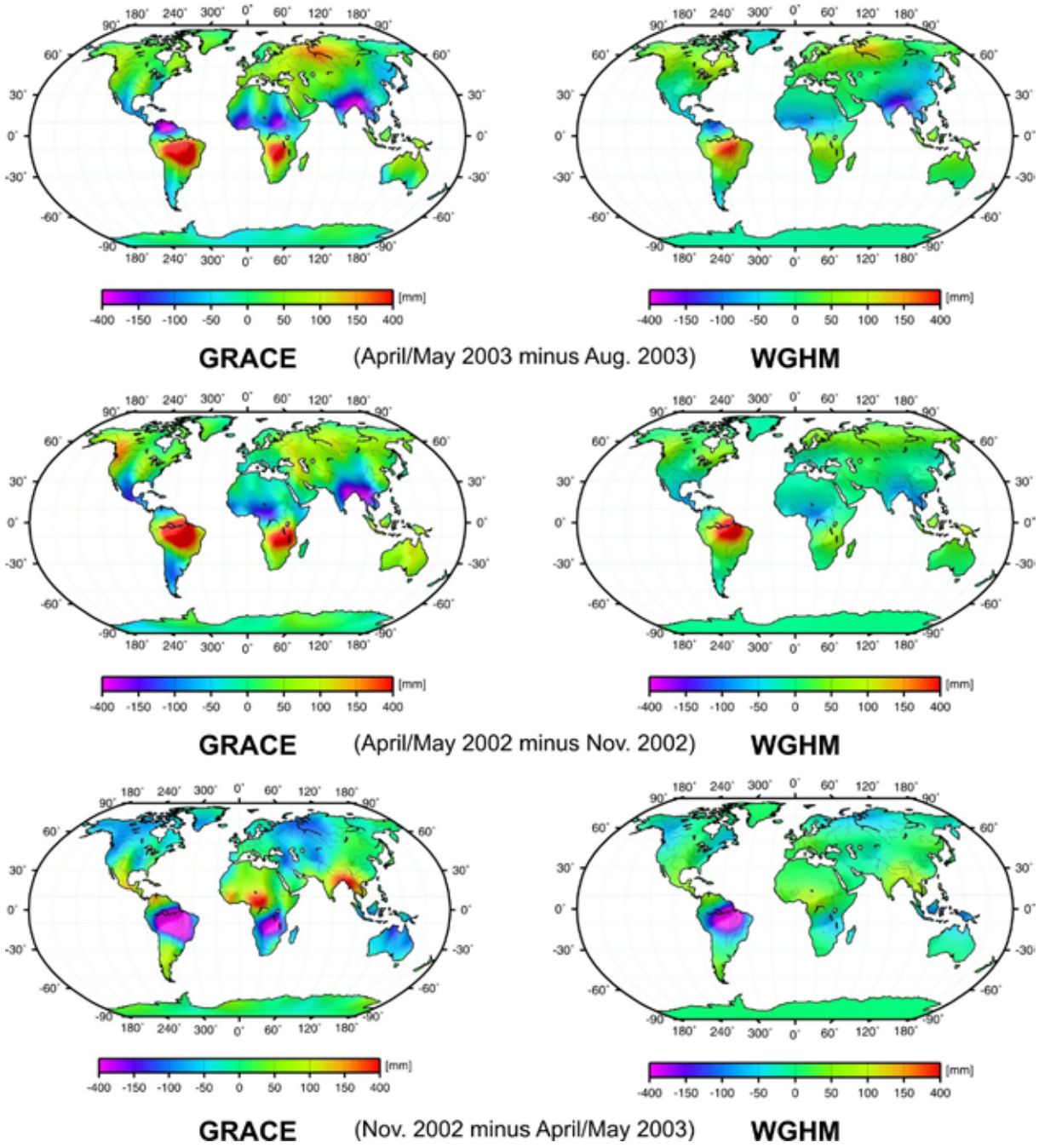

Figure 2.12: *Geographical distribution of differences over continents between (left hand side) GRACE gravity field solutions and (right hand side) those predicted by the WGHM continental hydrology model (in mm of equivalent water column); averaging radius 750 km.*

continental water storage variations. For evaluation, the GRACE results were then compared with the predictions from a global continental hydrological model: the Water GAP Global Hydrology Model (WGHM) (Döll et al., 2003), representing water storage in snow packs, rooted soil zone, groundwater, on vegetation surfaces, and as surface storage in rivers, lakes and wetlands for 50 % of the global land area (excluding Greenland and Antarctica).

Prior to the comparison, the GRACE and WGHM model results were filtered applying a Gaussian-type filter, as proposed by Jekeli (1981) and used in Wahr et al. (1998). Here an averaging radius of 750 km in the spatial domain was chosen, corresponding to a spherical harmonic degree of $l = 27$ in the spectral domain. There is almost no higher frequency signal left in the filtered, i.e. averaged, grid values and the filtered spherical harmonic coefficients. Moreover the coefficients of degree 15 to 27 (half wavelengths 1333 to 750 km) are considerably damped. These filter parameters account for the GRACE models error curve which grows up with increasing degree, which is typical for a space-based gravitational observation system.

Figure 2.12 gives the direct comparisons of the GRACE derived and WGHM model predicted fields in estimated continental water storage difference between the time periods introduced above. The results are expressed in terms of equivalent water column height (cf. Annex A 1.3, A 1.4). It is found that, when filtering with an averaging radius of 750 km, the hydrological signals generated by the world's major river basins are clearly recovered by GRACE: tropical river basins (Amazon in South America, Congo and Niger in Africa, Ganges and Brahmaputra in North India) and the Russian basins (Ob and Yenisei). A background uncertainty of some 25 mm in equivalent water column height from a monthly solution is estimated to be inherent in the present GRACE solutions at the selected filter length. The GRACE differences over three and six months (Figure 2.12) reveal a signal of some 75 mm scattering with peak values of 400 mm in equivalent water column height changes over the continents, which is about 50 % larger than predicted by the WGHM and other global hydrological models. This reflects, apart from residual systematic modelling errors in the GRACE solution, as a first important result the current limitations in the hydrological models to represent total continental water storage change in particular for the major river basins. Global hydrology modelling will clearly benefit from the continuation of GRACE gravitational monitoring and the expected advancements in GRACE data processing aiming at error reduction and improved temporal signal separation. The early GRACE results, presented here in brief, are discussed in detail in Schmidt et al. (2004).

To give an indication for the signal to noise ratio, Figure 2.13 depicts for the long-wavelength spatial constituents GRACE's error degree amplitudes (monthly solution) vs. the (unfiltered) signal degree amplitudes of seasonal mass redistributions from models/data of land hydrology (WGHM model as above), atmosphere (ECMWF data) and non-tidal ocean variation (adopted from Wahr, personal communication), and in the Antarctic ice sheet (Sasgen 2004, Vaughan 1999). For illustration, the degree amplitudes are given in terms of geoid heights, gravity anomalies and equivalent water column (cf. Annex A 1.3, A 1.4). The GOCE error curve is omitted here because GOCE shall not contribute to the recovery of temporal field variations. The GRACE error curves in Figure 2.13 are the formal ones, i.e. as resulting from the actual adjustment of monthly gravity field solutions without applying an a posteriori calibration. The formal errors represent the potential of the GRACE mission in large scale temporal field recovery once the modelling and processing procedures are more advanced than what has been used in the early solutions.

The signal degree amplitudes in Figure 2.13 are derived from spherical harmonic expansions of the load distribution, i.e. these are averages over the whole Earth's surface. For loads that are of limited extension, an investigation in the spatial domain (like for hydrology above) is more appropriate as the gravitational signal over a specific region is of larger amplitude than the global average. The reliability of the oceanic, hydrologic and ice models is to a large extent unknown and shall be investigated within the project.

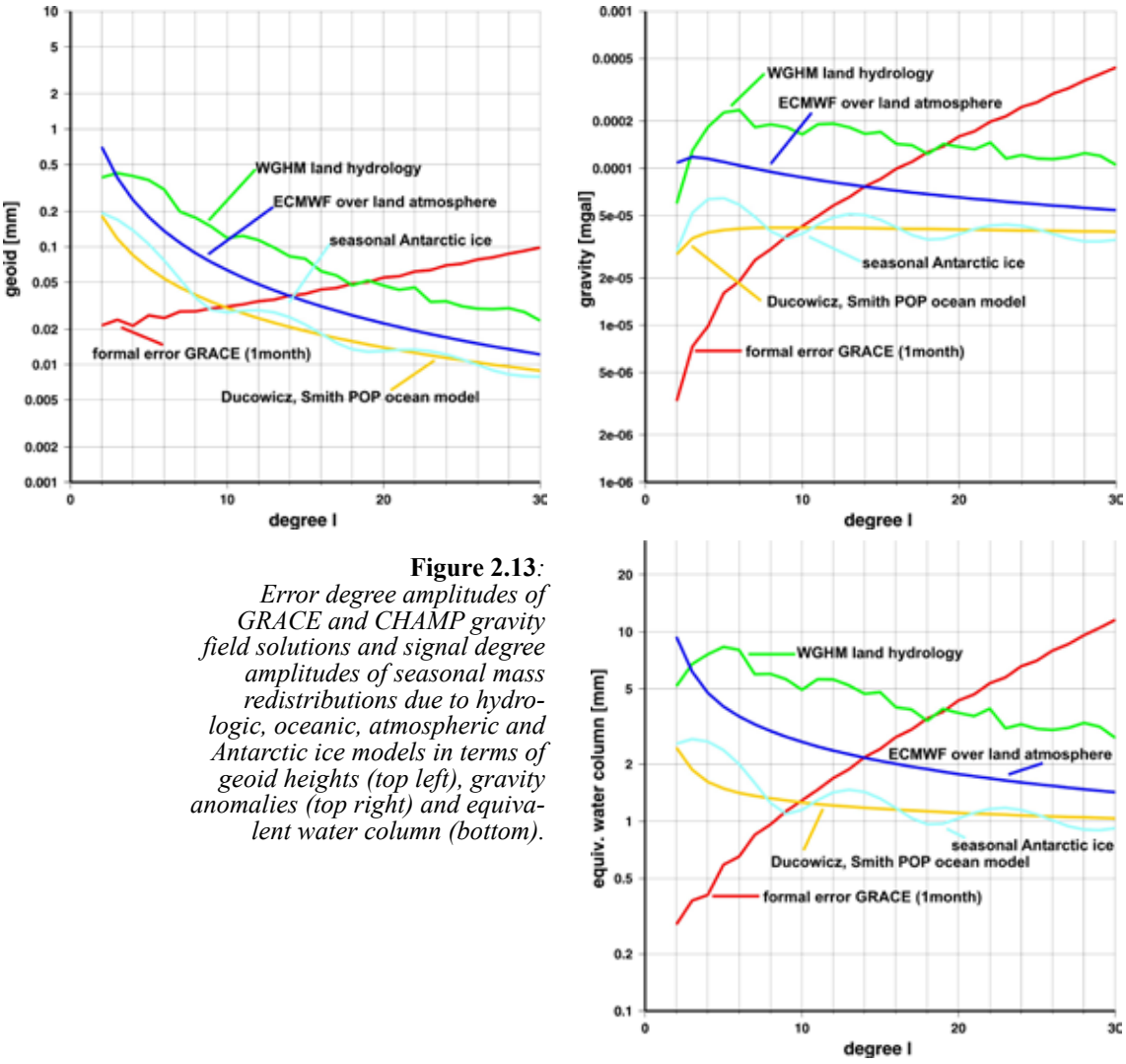

Figure 2.13: *Error degree amplitudes of GRACE and CHAMP gravity field solutions and signal degree amplitudes of seasonal mass redistributions due to hydrologic, oceanic, atmospheric and Antarctic ice models in terms of geoid heights (top left), gravity anomalies (top right) and equivalent water column (bottom).*

Table 2.4 summarizes the present state and the realistic expectation of the accuracy in GRACE monthly gravity field solutions for analyzing temporal field variations either in terms of geoid heights, gravity anomalies or equivalent water column. Efforts to combine GRACE and CHAMP data to increase the reliability of the monthly solutions are initiated.

Table 2.4: *GRACE (+CHAMP) temporal gravity field recovery: accuracy at 1000 km resolution (λ/2 pixel side length.)*

monthly solution	geoid height	gravity anomaly	equivalent water column
achieved expected	1 mm 0.15 mm	1 μgal 0.3 μgal	25 mm 10 mm

References

Biancale, R., G. Balmino, J.-M. Lemoine, J.-C. Marty, B. Moynot, F. Barlier, P. Exertier, O. Laurain, P. Gegout, P. Schwintzer, Ch. Reigber, A. Bode, R. König, F.-H. Massmann, J.-C. Raimondo, R. Schmidt, and S.Y. Zhu, 2000. A New global Earth's Gravity Field Model from Satellite Orbit Perturbations: GRIM5-S1, Geophys. Res. Lett., 27:3611-3614.

Döll, P., Kaspar, F. and B. Lehner, 2003. A global hydrological model for deriving water availability indicators: model tuning and validation, J. Hydrol. 270, 105-134.

Dunn, Ch., W. Bertiger, Y. Bar-Sever, S. Desai, B. Haines, D. Kuang, G. Franklin, I. Harris, G. Kruizinga, T. Meehan, S. Nandi, D. Nguyen, T. Rogstad, J. Brooks Thomas, J. Tien, L. Romans, M. Watkins, S.-Ch. Wu, S. Bettadpur and J. Kim, 2003. Instrument of GRACE - GPS Augments Gravity Measurements, GPS World, Feb. 1.

European Space Agency, 1999. Gravity Field and Steady-State Ocean Circulation Mission (GOCE), Report for mission selection, in The four candidate Earth explorer core missions, SP-1233 (1), Noordwijk, The Netherlands.

Fengler, M.J., W. Freeden, V. Michel, 2003. The Kaiserlautern Multiscale Geopotential Model SWITCH-03 from Orbit Perturbations of the Satellite CHAMP and its Comparison to the Models EGM96, UCPH2002_02_0.5, EIGEN-1S and EIGEN-2. Geophys. J. Intern., accepted 2003.

Fischell, R.E. and V.L. Pisacane, 1978. A drag-free lo-lo satellite system for improved gravity field measurements, In: Proc. of the 9th GEOP Conference, Dept. of Geod. Sci. Rep. 280, Ohio State Univ., Columbus, 213-220.

Gerlach, Ch., L. Földvary, D. Svehla, Th. Gruber, M. Wermuth, N. Sneeuw, B. Frommknecht, H. Oberndorfer, Th. Peters, M. Rothacher, R. Rummel, P. Steigenberger, 2003. A CHAMP-only Gravity Field Model from Kinematic Orbits Using the Energy Integral. Geophys. Res. Lett., 30 (20), 2037, doi: 10.1029/2003GL018025.

Mayer-Gürr, T., K.H. Ilk, A. Eicker and M. Feuchtinger, 2004. ITG-CHAMP01: A CHAMP Gravity Field Model from Short Kinematical Arcs of a One-Year Observation Period, submitted to Journal of Geodesy.

Jekeli, C., 1981. Alternative methods to smooth the Earth's gravity field, Rep. 327, Dep. of Geod. and Sci. and Surv., Ohio State Univ., Columbus.

Kuang, D., Y. Bar-Server, W. Bertiger, S. Desai, B. Haines, B. Iijima, G. Kruizinga, Th. Meehan, and L. Romans, 2001. Precise Orbit Determination for CHAMP using GPS Data from BlackJack Receiver, in 2001 ION National Technical Meeting Proceedings, Session E1: Scientific Applications, Timing, and Frequency, Long Beach, California.

Reigber, Ch., 1978. Improvements of the gravity field from satellite techniques as proposed to the European Space Agency, In: Proc. of the 9th GEOP Conference, Dept. of Geod. Sci. Rep. 280, Ohio State Univ., Columbus, 221-232.

Reigber, Ch., P. Schwintzer, and H. Lühr, 1999. The CHAMP geopotential mission, Boll. Geof. Teor. Appl., 40:285-289.

Reigber, Ch., P. Schwintzer, K.-H. Neumayer, F. Barthelmes, R. König, Ch. Förste, G. Balmino, R. Biancale, J.-M. Lemoine, S. Loyer, S. Bruinsma, F. Perosanz, and T. Fayard, 2003. The CHAMP-only EIGEN-2 Earth Gravity Field Model, Adv. Space Res., 31 (8):1883-1888.

Reigber, Ch., R. Schmidt, F. Flechtner, R. König, U. Meyer, K.-H. Neumayer, P. Schwintzer and S.Y. Zhu, 2004a. An Earth gravity model complete to degree and order 150 from GRACE: EIGEN-GRACE02S, J. Geodynamics, in press.

Reigber, Ch., P. Schwintzer, R. Stubenvoll, R. Schmidt, F. Flechtner, U. Meyer, R. König, H. Neumayer, Ch. Förste, F. Barthelmes, S.Y. Shu, G. Balmino, R. Biancale, J.-M. Lemoine,

H. Meixner and J.C. Raimondo, 2004b. A High Resolution Global Gravity Field Model Combining CHAMP and GRACE Satellite Mission and Surface Data: EIGEN-CG01C, Journal of Geodesy, subm.

Reigber, Ch., H. Jochmann, J. Wünsch, S. Petrovic, P. Schwintzer, F. Barthelmes, K.-H. Neumayer, R. König, Ch. Förste, G. Balmino, R. Biancale, J.-M. Lemoine, S. Loyer and F. Perosanz, 2005. Earth Gravity Field and Seasonal Variability from CHAMP. In: Reigber, Ch., Lühr, H., Schwintzer, P., Wickert, J. (eds.), Earth Observation with CHAMP – Results from Three Years in Orbit, Springer, Berlin, 25-30.

Reubelt, T., G. Austen and E. Grafarend, 2003. Space Gravity Spectroscopy – Determination of the Earth's Gravitational Field by Means of Newton Interpolated LEO Ephemerides. Case Studies on Dynamic (CHAMP Rapid Science Orbit) and Kinematic Orbits. Advances in Geosciences 1, 127-135.

Sasgen, I, 2004. Geodetic signatures of glacial changes in Antarctica: rates of geoid-height change and radial displacement due to present and past ice-mass variations. Diplom thesis, Department of Geophysics, Ludwigs-Maximillians-University of Munich.

Schmidt, R., P. Schwintzer, F. Flechtner, Ch. Reigber, A. Güntner, P. Döll, G. Ramillien, A. Cazenave and S. Petrovic, 2004. GRACE Observations of Changes in Continental Water Storage, Global and Planetary Changes, subm.

Tapley, B.D., S. Bettadpur, M. Watkins and Ch. Reigber, 2004a. The gravity recovery and climate experiment: Mission overview and early results, Geophys. Res. Lett., 31, L09607, doi: 10.1029/2004GL019920.

Tapley, B.D., S.V. Bettadpur, J.C. Ries, P.F. Thompson and M.M. Watkins, 2004b. GRACE measurements of mass variability in the Earth system, Science, 305, 503-505.

Vaughan, D.G., J.K. Bamber, M. Giovinetto, J. Russel and P.R. Cooper, 1999. Reassessment of net surface mass balance in Antarctica. J. Clim., 12, 933-946.

Wahr, J., Molenaar, M., and F. Bryan, 1998. Time variability of the Earth's gravity field: Hydrological and oceanic efffects and their possible detection using GRACE, J. Geophys. Res., 103(12), 30205-30229.

Wahr, J., S. Swenson, V. Zlotnicki and I. Velicogna, 2004. Time-variable gravity from GRACE: First results, Geophysical Research Letters, 31, L11501, doi:11501.11029/12004GL019779.

Wolff, M., 1969. Direct Measurements of the Earth's Gravitational Potential Using a Satellite Pair, Journal of Geophysical Research, 74 (22), 5295-5300.

2.3 Satellite altimetry

Within a few decades satellite altimetry has become an operational remote sensing technique with important application in oceanography, geodesy and geophysics. Today, the ocean surface is by far better known than the Figure of the Earth over large areas of the continents (see Figure 2.14). Altimetry has essentially contributed to the improved knowledge of the Earth gravity field. It allows to deduce features of the sea floor topography, to control continental ice and to observe sea ice and its moving margin. Above all altimetry is able to monitor the sea level and its variability in a fast, global and precise way. It thus contributes essentially to a better knowledge of the ocean dynamics, the ocean mass redistribution and its impact to the Earth gravity field, the question of sea level rise and its possible acceleration, one of the most prominent indicators of global change.

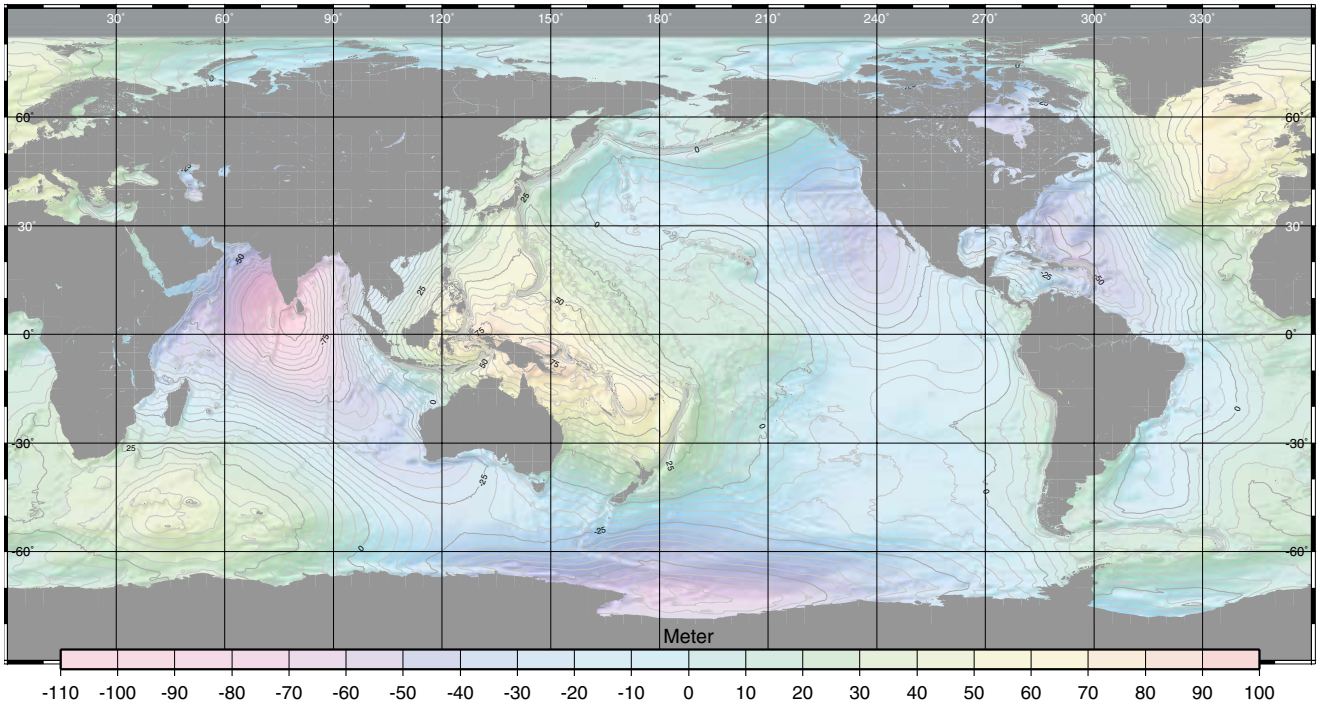

Figure 2.14: *The CLS01 mean sea surface height model (Hernandez and Schaeffer, 2002), computed from harmonized altimeter data of TOPEX/Poseidon, ERS-1 and ERS-2. The high spatial resolution is based on the geodetic phase of ERS-1.*

Pulse-width limited altimeter systems

The measurement principle of satellite altimetry is straightforward: With a carrier frequency at about 13.6 GHz (Ku-band) frequency-modulated impulses of a few nano seconds duration and a repetition rate of about 1 KHz are emitted from the altimeter antenna into nadir direction. The pulse-width limited radar signals propagate with a beamwidth of a few degree and are reflected at the ocean surface with a backscatter depending on the wind speed and the sea state (see Figure 2.15). After the round-trip travel time of a few milliseconds the echo of the radar signals is received again by the altimeter antenna and sampled into 64 or 128 bins. The analysis of the sampled echo, in particular the fit of a theoretical echo model to the bin values, allows to estimate three basic parameters, namely

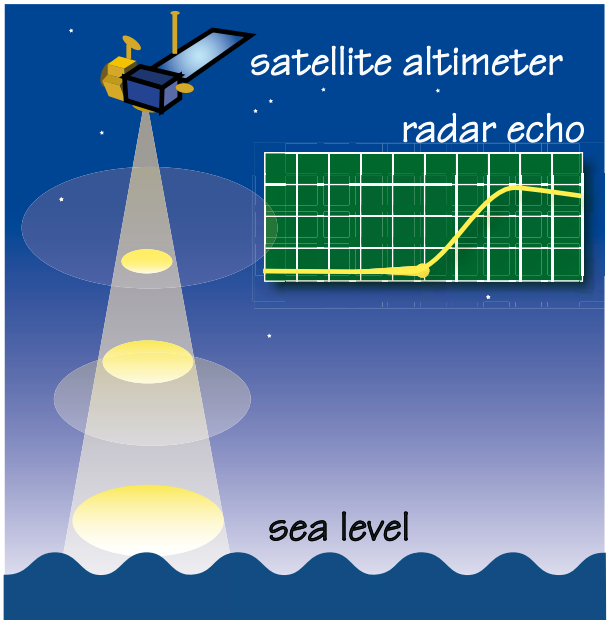

Figure 2.15: *The measurement principle of pulse limited radar altimeter systems*

- the travel time of the signal,
- the slope of the leading edge of the echo, and
- the total energy of the radar echo.

The travel time of the signal is converted to length and gives the instantaneous height of the antenna above the sea surface. The slope is proportional to the significant wave height and the energy budget gives the backscatter coefficient allowing to estimate the surface wind speed.

In order to derive sea surface heights the altimeter ranges have to be subtracted from the radial component of the position of the spacecraft which is obtained from precise orbit determination. However, to maintain the measurement precision and to compare sea surface heights taken at different epochs a number of corrections is required:

Instrumental errors, offsets from the antenna phase centre to the satellites centre of gravity, range biases and drifts are crucial for a precise geocentric reference of the sea level.

Media corrections are required because the radar signal travels twice through the atmosphere. For the troposphere two effects are distinguished: the delay of the radar echo caused by the presence of dry air and the wet component, related to the presence of water vapour. Dual frequency altimeters like TOPEX/Poseidon, Jason and ENVISAT allow the in-situ estimation of the ionospheric delay through the dispersive nature of the ionosphere. Single frequency altimeters must rely on ionospheric prediction models like Bent or IRI2001 or on global ionospheric maps (GIMs), since 2002 generated from GPS/GLONASS sites of the IGS network. However, these models are not able to account for the turbulent character of the ionosphere.

Other corrections have to be applied for the radar target, the sea surface: The instantaneous water level is affected by ocean and solid Earth tides, the loading through the deformation of the solid Earth and the pole tide, a small effect due to the variation of the Earth rotation axis. The inverse barometer correction assumes that sea level is depressed by 1 cm if air pressure increases by 1 hPa. Finally, the sea state bias is due to the fact that wave crests reflect the radar signal less than wave troughs, causing the altimeter to measure too long.

The first altimeter experiments on Skylab (1973) and with the Geos-3 (1975-1978) satellite can be considered as proof-of-concept phase. In 1985 the U.S. Navy launched Geosat, an altimeter largely based on the design of Seasat (which failed in 1978 after a few month of operation). Geosat was first applied for a high resolution mapping of the marine geoid (the GM military mission phase with data declassified later on) and then, from September 1986 to October 1989 manoeuvered into a Seasat exact repeat orbit (the ERM mission phase).

In the past decade, satellite altimetry was characterized by the simultaneous operation of the extremely successful TOPEX/Poseidon mission (Fu et al.1994) with ERS-1 and its follow-on, ERS-2. With the launch of Jason-1 in December 2001 and ENVISAT in March 2002 a period began with five altimeter systems operating simultaneously (see Figure 2.16). The transitional phase between „old" missions (TOPEX/Poseidon and ERS-2), and the new, follow-on missions Jason-1 and ENVISAT, lastet several years and was used for an intensive cross-calibration, in particular during a few months tandem configurations (see below). In addition, Geosat Follow-On (GFO), launched in February 1998, is still successfully operating. New missions with alternative missions design, dedicated for ice application complement the mission scenario: ICESat, launched in 2003, carries

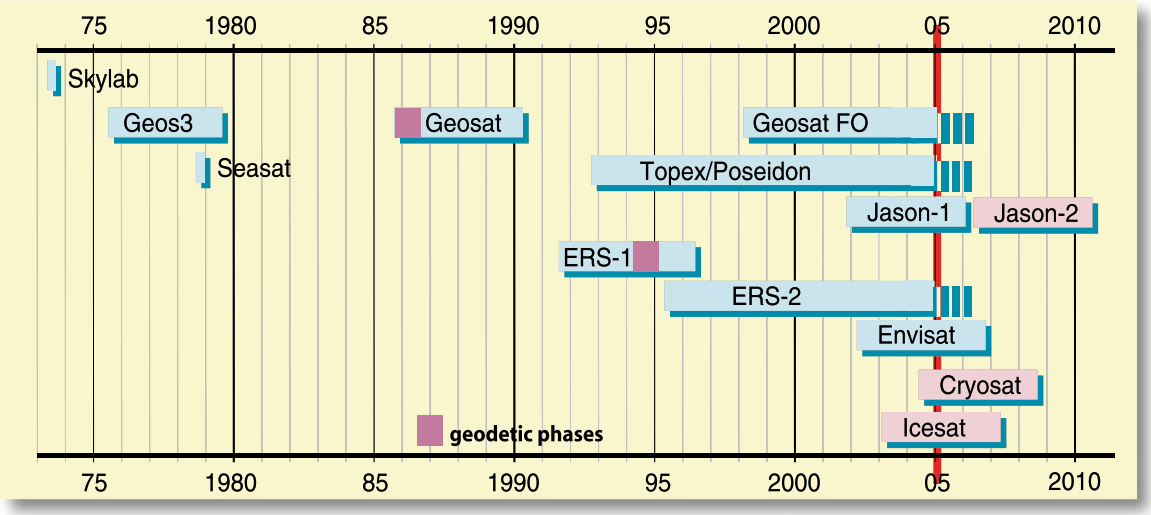

Figure 2.16: *Satellite altimeter mission history and perspective*

a Geoscience Laser Altimeter System (GLAS) and shall provide multi-year elevation data over Greenland and Antarctica. Cryosat is planned for a launch in 2005. More details to these missions are given below. Appendix A7 summarizes the altimeter mission characteristics.

In general, the multi-mission situation offers a unique chance to cross-calibrate all altimeter systems and to continue the long-term monitoring of the ocean surface and to fully exploit the synergies of missions with different sampling characteristics.

TOPEX/Poseidon, dedicated to the measurement of the ocean surface topography, provided high altitude and high precision orbits, a repeat period of 9.9156 days with the ability to de-alias the major tidal constituents, and the two frequency TOPEX altimeter sensor, that allows the in-situ estimation of the range delay due to ionospheric refraction. The low overall error budget of TOPEX/Poseidon has never been achieved before and may be characterized by ± 6 cm rms for crossover differences with short time delay (AVISO 1999). This includes not only radial orbit errors but also all errors of the environmental corrections. Jason-1 continues this time series over the same ground track while the orbit of TOPEX/Poseidon was shifted by half the ground track spacing in order to double the spatial resolution. TOPEX/Poseidon was operating until the end of 2004.

On the other hand, orbit and sampling characteristics for ESA‘s Remote Sensing Satellites ERS-1 and ERS-2 were governed by the multi-disciplinary mission objectives. The high inclination implies a latitude coverage up to ± 81.5° such that even polar areas with continental and ocean ice like Greenland and the Ross ice shelf can be monitored. The sun-synchronous ERS-1 repeat cycle was set to 3, 35 and 168 days in order to fulfill specific requirements for ice, ocean and geodetic application respectively. The follow-on ERS-2 was kept in a 35 day repeat cycle, the best compromise for multidisciplinary requirements. ENVISAT is now measuring over the same subsatellite ground track. The operation of ERS-2 is more and more degraded - a failure of the tape recorder allows to transmit altimeter data only over parts of the North Atlantic.

Due to orbit dynamics, high spatial and high temporal resolution exclude each other. The 10 day repeat cycle of TOPEX/Poseidon and Jason-1 imply an equatorial track spacing of about 315 km. The lower temporal resolution of the 35 day repeat for ERS-1, ERS-2 and ENVISAT provide an improved spatial resolution with an equatorial track separation of only 80 km. The „geodetic“ phase of ERS-1 brought the track separation even down to 16 km! Thus, the NASA/CNES and the ESA-missions complement each other in an optimal way, as for example elaborated by Le Traon et al. (1999). Figure 2.17 shows the track pattern of the repeat missions and the density of measurements achieved by the geodetic mission phases.

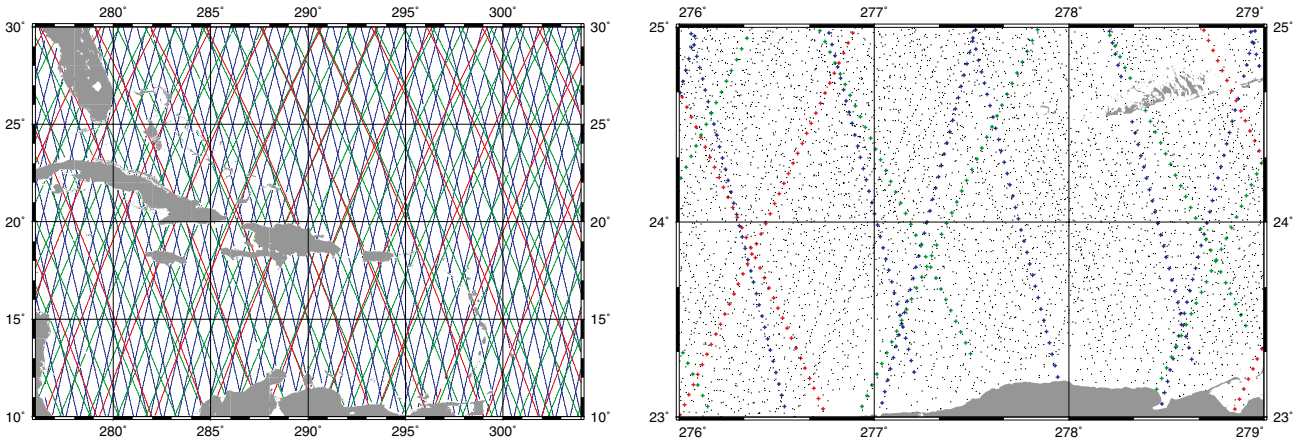

Figure 2.17: *Spatial resolution of the repeat missions Jason-1, ENVISAT and GFO (left hand) and (right hand) the repeat tracks with additional spatial resolution achieved by the geodetic mission phases of Geosat and ERS-1. The right panel is a 2°x3° sub area of the Caribbean Sea and Gulf of Mexico region shown left*

In order to take advantage of the simultaneous operation of altimeter systems with different temporal and spatial sampling characteristic two general requirements are to be fulfilled, namely

- the harmonization of mission data and
- the (cross-) calibration of the vertical component

Harmonization of altimeter mission data is possible only to a certain extend. Of course, tidal corrections can be based on the same ocean tide model and orbits can be re-computed with an improved gravity field model. But the effect of the so called „geographically correlated“ orbit errors and of different tracking systems (Laser, DORIS, PRARE, or GPS) is difficult to assess. Missions without a dual frequency altimeter must rely on global prediction model for the total electron content (like the Bent model or the International Reference Ionosphere, IRI). Also, a missing onboard radiometer degrades the error budget (as for Geosat). The sea state bias is sensor specific and can not be harmonized at all. Because of the computational burden and missing resources, a re-processing of the complete mission data can be performed – if at all – by a few expert groups only and in general does not keep track with the development of improved algorithms and the availability of new models.

AVISO (1996) improved the ERS-1 and ERS-2 orbits by a global minimization of dual satellite crossover with TOPEX/Poseidon (Le Traon et al., 1995) and provides user friendly along-track data in terms of corrected sea surface heights and sea level anomalies. The NASA/JPL Pathfinder Project performed a harmonization and unification of the vertical reference for TOPEX/Poseidon, ERS-1, ERS-2 and the Geosat mission.

The second requirement concerns the (range) calibration and the long-term stability of altimeter systems. Concatenation of data of different missions may, for example, generate an apparent sea level rise if the altimeter range measurements are not properly (cross-) calibrated. The same effect may result from an undetected drift of the altimeter sensor or auxilary sensors (like the radiometer) used to correct the range measurements. ENVISAT and Jason-1 are cross-calibrated with their predecessors by so called tandem configurations, an approach first applied for the transition from ERS-1 to ERS-2: For a few month the orbit of both satellites are configured such that they observed the same subsatellite track with a short time delay (one day, 30 minutes or even shorter). The relative range bias of both satellites can then be estimated with millimetre precision from the dual observation of a repeated global ocean surface profiles. Common multi-mission crossover analysis of nearly simultaneous crossover events are under investigation (Bosch 2004) and promise to identify small but systematic geographically correlated errors.

Although the cross-calibration by the tandem approach is extremely precise it is not able to detect long-term changes of the altimeter systems. Oscillator drifts of TOPEX/Poseidon, for example, were detected through the relative comparison of altimetric sea level time series and recordings of carefully selected island tide gauges (Mitchum, 1998). In the same way drifts of ancillary on board sensors like the radiometer could be identified by comparison with wet tropospheric path delays estimated from GPS observations. The oscillator drift of ERS-1/2 is monitored internally and amounts to a non-neglecting rate of about 8 mm/year. The long-term stability of altimetry crucially depends on the knowledge about such drift rates.

Cross-calibration by tandem configuration and drift estimation by relative comparison with external observation series are important, but cannot substitute the absolute calibration, performed by scenarios at a single calibration site where a closure between the position of the satellite, the corrected altimeter range observation and the instantaneous sea surface is established by means of independent measurements. It should be emphasized that the absolute calibration is the only approach that determines the scale of satellite altimetry. An error of only 1 cm in the range bias estimate may translate within a decade to an apparent 1 mm/year sea level rise. The calibration of TOPEX/Poseidon at the Harvest Platform (Christensen et al., 1994), performed quasi continuously over the whole missions lifetime, is therefore mandatory. For ERS-2 there was no absolute calibration at all! The scale of ERS-2 was carried over from ERS-1 by the tandem phase and ERS-1 got its scale from the rather short calibration campaign at the Venice tower (Francis et al. 1992).

The impact of the new gravity field missions (CHAMP, GRACE and GOCE) on satellite altimetry is twofold: First, the orbits of altimeter satellites can be computed more precise than today - even for low orbiting satellites like ENVISAT (the modelling of non-gravitational surface forces remains problematic). Second, the improved knowledge of the marine geoid will allow a more significant estimation of the absolute ocean dynamic topography. With known density profiles, it appears feasible to derive a three-dimensional view of the ocean currents. These synergies are discussed below in more detail.

In order to overcome the limitations of the pulse-width limited altimetry new mission concepts with alternative or modified system design are already realized, are approved or are under investigation.

CryoSat and ICESat altimeter missions

The CryoSat mission is the first mission of ESA´s Earth Explorer Opportunity Mission planned for launch in September 2004. The mission has been defined in order to determine fluctuations in the mass of the Earth's major land and marine ice fields. Predicting future climate and sea level depends on knowledge of these fluctuations. Satellite observations are the unique source of these measurements at large space and time-scales. The goals of CryoSat are to measure variations in the thickness of perennial sea and land ice fields to the limit allowed by natural variability, on spatial scales varying over three orders-of-magnitude. The natural variability of sea and land ice depends on fluctuations in the supply of mass by the atmosphere and ocean, and snow and ice density. CryoSat measurement requirements are determined from estimates of these fluctuations.

The measurement requirements and averaging areas of the CryoSat system are:

- Over sea ice the averaging area of interest is 100,000 km^2 with a required accuracy of resolving temporal changes of 1.6 cm per year.
- Over ice-sheet margins an averaging area of 10,000 km^2 is assumed with a measurement accuracy of 3.3 cm of ice thickness change per year.
- Over the interiors of the ice-sheets the averaging area is 13,800,000 km^2 (the surface area of Antarctica) with a measurement accuracy of 0.7 cm of ice thickness change per year.

Figure 2.18: *Artist view: CryoSat in operation (courtesy ESA)*

CryoSat will perform measurements over three full years in order to detect the interannual variability and possible trends. It will have a 92° high inclination orbit to cover polar regions, i.e. extending observations up to 88° latitudes, and a repeat cycle of 369 days with 30day sub-cycle.

With pulse-limited radar-altimeter data from ERS-1 and ERS-2 first successful case studies of the determination of ice mass fluxes (Wingham et al., 1998; Shepherd et al., 2003) and sea ice thickness changes (Laxon et al., 2003) have been made. In order to extend these results to regions covered by sea-ice and to the margins of the ice sheets, respectively, it was necessary to improve the spatial resolution of the altimeter measurement system. CryoSat (see Figure 2.18) will thus carry a unique high spatial resolution radar altimeter, the Synthetic Aperture Interferometric Radar Altimeter SIRAL as the primary payload. It will operate in the Ku-band at a frequency of 13.8 GHz. The radar is capable of operating in a number of different modes, optimised for measurements over different surfaces. A conventional, pulse-width limited, low-resolution mode will provide the measurements over the central regions of the ice sheets, to continue the ERS and ENVISAT measurement series. This mode will also be used over most of the oceans. The SAR mode will enable an enhancement of the spatial resolution to 250 m along-track (Figure 2.19). This mode will be used over sea-ice to enable measurements over relatively narrow leads of open water which would be indistinguishable in low-resolution mode. Over the topographic surfaces of the ice-sheet margins this SAR mode will be enhanced by interferometric operation across-track so that the arrival angle of the echoes can be measured.

Similarly to CryoSat, NASA's ICESat (Ice, Cloud, and land Elevation Satellite) mission has the goal to provide three to five year elevation data over Greenland and Antarctica needed to determine ice sheet mass balance. Additionally it will measure cloud and aerosol heights, as well as land topography and vegetation characteristics. Sea ice is not an explicit goal of the mission, but some ice freeboard retrievals will also be possible. ICESat has been launched in January 2003 and extends to 86° latitudes.

ICESats primary payload is GLAS, the Geoscience Laser Altimeter System. GLAS is designed to detect changes in ice sheet surface elevation as small as 1.5 cm per year over areas of 100 km by 100 km. It is a laser altimeter operating at 1064 (infrared) and 532 (visible green) nanometers wavelengths. Thus, ICESat can only perform measurements of the Earth surface if there are no clouds. This is a severe limitation for polar applications, in particular for sea ice investigations. The laser altimeter has a footprint of 70 m, and a spatial sampling interval of 170 m along the ground track. Orbit and attitude will be controlled by means of GPS and star trackers.

First ICESat data are already available from the polar ice covers. Figure 2.19 shows an example of an ICESat track across Dronning Maud Land, Antarctica. The figure shows the high quality and spatial resolution of the data, which significantly improves currently available topographic information. Figure 2.20 demonstrates application of ICESat for sea ice thickness measurements (Kwok et al., 2004). With this data, it is for the first time possible to obtain regional spaceborne ice thickness information.

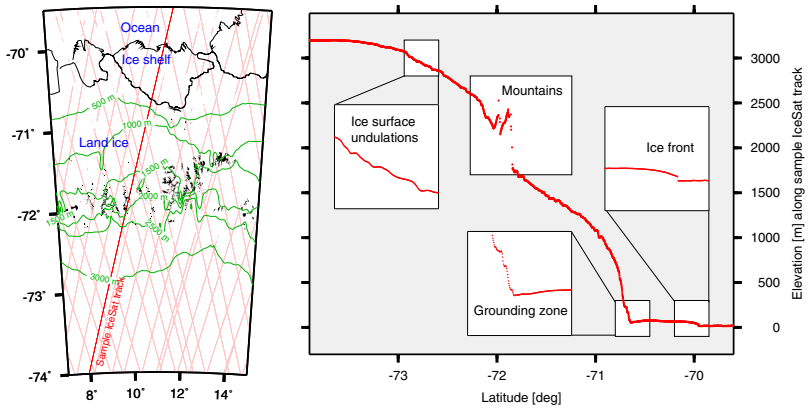

Figure 2.19: *Illustration of IceSat Laser altimeter measurements over Antarctica. The shown sample track crosses the region of the Schirmacher Oasis / Central Dronning Maud Land / East Antarctica (left map). The elevation profile observed by IceSat (subfigure right) reveals topographic details such as ice surface undulations, mountains, the grounding zone and the ice front. (Figure by M. Wiehl, M. Scheinert, TU Dresden; IceSat data are distributed by the US National Snow and Ice Data Center (NSIDC)).*

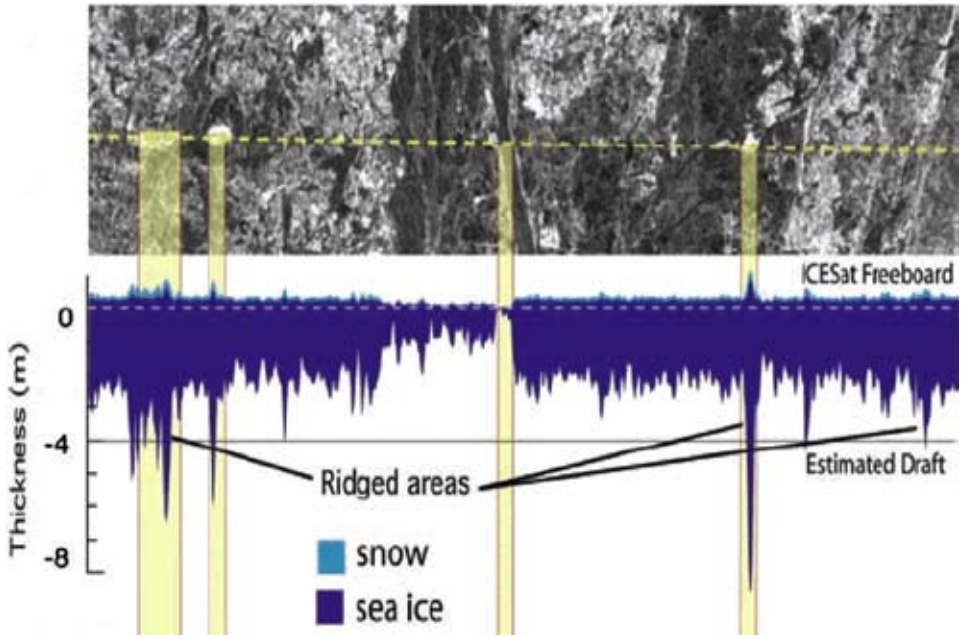

Figure 2.20*: Ice thickness profile obtained from ICESat over Arctic multiyear sea ice. The top panel shows the satellite ground track superimposed on a coincident SAR image of the same area. The lower panel presents the corresponding ice thickness profile, where freboad has been converted to snow thickness and ice draft based on assumptions of snow and ice density. Shaded bars indicate the location of ridges and refrozen leads visible in both data sets. From Kwok et al., 2004.*

Both missions, CryoSat and ICESat, are using new, unique technology, and are setting new benchmarks in the achieved accuracy of the measurements. However, this also requires careful validation of the height and thickness retrievals before the data can be widely and confidently used.

References

AVISO, 1996. Aviso User Handbook: Merged Topex/Poseidon Products. AVI-NT-02-101-CN, Edition 3.0.

AVISO, 1999. Aviso CalVal yearly report: 6 years of TOPEX/Poseidon data. AVI-NT-011-316-CN, Edition 1.0.

Bent R.B., K. Llewellyn, G. Nesterczuk, and P.E. Schmid, 1976. The development of a highly successful worldwide empirical ionospheric model. In: Goodman J. (Ed.) Effect of the ionosphere on Space System and Communications. Natl.Tech. Inf. Serv., Springfield, VA, pp.13-28.

Bosch, W. 2004: Simultaneous crossover analysis for contemporary altimeter missions. ESA Scientific Publication of the ENVISAT Symposium, Salzburg, 2004, in press.

Chelton D.B. (Ed.), 2001. Report of the High-Resolution Ocean Topography Science Working Group Meeting. College of Oceanic and Atmospheric Sciences, Oregon State University, Corvallis, Oregon.

Christensen E.J., B.J. Haines, S.J. Keihm, C.S. Morris, R.A. Norman, G.H. Purcell, B.G. Williams, B.D. Wilson, G.H. Born, M.E. Parke, S.K. Gill, C.K. Shum, B.D. Tapley, R. Kolenkiewicz, and R.S. Nerem, 1994. Calibration of TOPEX/Poseidon at Platform Harvest. J. Geophys. Res., 99 (C12), 24465-24486.

Francis C.R. (Ed.), 1992. The calibration of the ERS-1 radar altimeter. ESA Report ER-RP-ESA-RA-0257, ESA/ESTEC Noordwijk, The Netherlands.

Francis, C.R., 2001. Cryosat, Mission and Data Description, ESA ESTEC, CS-RP-ESA-SY-0059

Fu, L., E. Christensen, C. Yamarone, M. Lefebvre, Y. Menard, M. Dorrer, and P. Escudier, 1994, TOPEX/Poseidon mission overview. J. Geophys. Res., 99 (C12), 24369-24381

Hernandez F. and P. Schaeffer, 2002. The CLS01 Mean Sea Surface: A validation with the GSFC00 surface. In press, CLS, Ramonville St. Agne, France

Kwok, R., H.J. Zwally, and D. Yi. 2004. ICESat observations of arctic sea ice: a first look. Geophysical Research Letters 31: L16401, doi:10.1029/2004GL020309.

Laxon, S., N. Peacock, and D. Smith, 2003. High interannual variability of sea ice thickness in the Arctic region, *Nature*, 425, 947-950.

Le Traon,P.Y., P. Gaspar, F. Bouyssel, H. Makhmara, 1995. Using TOPEX/Poseidon data to enhance ERS-1 orbit. J. Atm. Ocean. Techn.,Vol.12, 161-170.

Le Traon P.Y., Dibarboure G., 1999. Mesoscale Mapping capabilities of Multiple-Satellite Altimeter Missions, J. Atmosphere, 16, 1208-1223.

Le Traon, P.Y., J.P. Dumont, J. Stum, O.Z. Zanife, J. Dorandeu, P. Gaspar, T. Engelis, C. Le Provost, F. Remy, B. Legresy and S. Barstow, 1996. Multi-mission altimeter inter-calibration study, ESA contract 11583/95/NL/CN.

Mitchum, G., 1998. Monitoring the Stability of Satellite Altimeters with Tide Gauges. J. Atmospheric and Oceanic Technology, Vol. 15, 721-730.

Shepherd, A., D. Wingham, T. Payne, and P. Skvarca, 2003. Larsen Ice Shelf has progressively thinned. Science, 302, 856-859.

Wingham, D. J., Ridout, A. J., Scharroo, R., Arthern, R. J., and Shum, C. K., 1998. Antarctic elevation change from 1992 to 1996. Science 282, 456-458.

2.4 Integrated observations to understand environmental and deep Earth´s processes

Besides the important application of gravity field observations for exploring the Earth interior, the knowledge of the Earth‘s gravity field and its variation with time is essential for the understanding of environmental processes.

The striking results in global gravity field recovery immediately obtained from the CHAMP and GRACE mission data have brought to evidence that data from a consistent long-term observation of the Earth‘s gravity field will open, when joined with satellite altimetry in multi-parameter data sets, new areas of multi-disciplinary research and application.

The multi-year data records, which will be collected with CHAMP and GRACE, and the high-resolution spatial gravity field recovery with GOCE, will demonstrate, that gravity is one of the key elements for an integrated geodetic-geophysical observing system, and that a permanent gravity mapping from space with advanced present-day satellite and sensor technology will become feasible. Such a permanent observation is urgently needed within the following fields of Earth system, environmental and global change diagnostics and prognostics:

a. ocean currents and heat flux
b. sea-level rise and Greenland/Antarctic ice sheets
c. water cycling (ground water storage and snow/ice pack)
d. solid Earth processes (mantel flow & plate tectonics, post glacial adjustment)

Whereas the first and fourth point also require a high spatial resolution (down to some 10 km) of the gravity field, all points address temporal field variations with periods from weeks to centuries. Although the three satellite gravity missions will not yet fulfil all stringent requirements concerning accuracy and resolution, these are to be considered as forerunners and concept missions for a long-term improved gravity field recovery from space.

Integrated Earth’s observation: benefits and objectives

The following paragraphs outline the importance of the combination of complementary data sets and its joint analysis to fully exploit the information content, to resolve ambiguities and to separate signal sources for a precise and reliable interpretation of the Earth‘s dynamics and the interactions between the various spheres.

- **Global Gravity and Altimetry**

  Over the oceans and ice caps, satellite altimetry is employed to derive the surface geometry and its changes with time. Several European, French and American altimeter missions are presently operating: TOPEX/Poseidon, GFO, Jason-1 and ENVISAT. Two missions are designed for altimetry over the marine and continental polar ice sheets: the American IceSat (in orbit since 2003) and ESA‘s Cryosat, which are to be launched in 2004, respectively.

  The altimetry records covering now continuously more than a decade can only be fully exploited for climatologic processes if combined with highly precise and high resolution global gravity data. The gravitational potential in terms of the geoid is needed as a reference surface to derive the major ocean currents which control the climate of the Earth by transporting heat and CO_2. The re-evaluation of the altimeter data being available back to the 1980ies would

also largely benefit from an improved global geoid to uncover precisely the evolution of ocean currents by assimilation in a global hydrostatic ocean circulation model.

Time varying gravity is needed to separate the mass effect due to changes in the ocean/continent/atmosphere water mass balance and in the water/ice mass balance from pure thermal water volume changes and ice volume changes due to compaction. This applies to short period (seasonal, interannual) ocean surface currents and ice mass variations as well as to the global trend in sea level rise and ice coverage. Thus, ongoing climate processes can only be currently interpreted if altimetry is combined with gravity.

- **Global Gravity and Land-based Hydrological Data and Models**

  Over land, it shall be for the first time demonstrated with GRACE, that satellites are able to globally probe the Earth for largely unknown soil moisture and aquifer changes on seasonal and interannual time scales. Being important for the understanding of the global water cycle, a satellite-based system shall continue to trace global hydrology after the five-years lifetime of GRACE.

  An assimilation of global gravity field changes into models from land-based measurements of groundwater levels, snowloads and point measurements of soil moisture will be the tool to connect the small hydrological length scales with longer scales in order to estimate the dynamics of the water cycle and its evolution with time on continent-wide and global spatial scales.

- **Global Gravity and Seismology**

  The worldwide seismic broadband station network enables the improvement of global models of the Earth‘s crust (density distribution and thickness) and of tomographic velocity models of the Earth‘s mantle. The observed spatial structure of the gravity field gives boundary values for an isostatic model of the Earth‘s lithosphere to investigate its static equilibrium (medium to short-scale) and, by this, to infer the dynamic topography due to mantle dynamics for the mantle‘s temperature and density distribution by forward computations and velocity-gravity inversions. For global solid Earth‘s physics studies, the knowledge of the Earth‘s crustal structure and the resolution and accuracy of tomographic models is compared to the knowledge of the gravity field, rather low. Therefore, for this application there is a need for improving the seismologic sounding and modelling rather than the gravity field recovery. This situation changes, when turning to regional tectonic modelling, where accurate gravity down to wavelengths of some kilometers is required, and satellite gravity field missions will provide the longer wavelengths frame for a reliable detailed geoid and gravity field modelling with a data coverage densified by terrestrial and ship- and airborne measurements.

  Seismic tomography, dynamic topography, surface deformations, gravity and the vertical and lateral viscosity structure of the mantle are the key observables and parameters for a three and four dimensional modelling of mantle dynamics as the engine for plate tectonics.

- **Global Gravity and Geodetic Networks**

  Continent-wide (ECGN) and global (GGOS) geodetic networks, including absolute and super-conducting gravimeters and GPS (Galileo) precise point positioning and height determination, will deliver a picture of secular crustal deformations, height and gravity changes for Earth system science. Those networks, like the IGS and SLR networks, also provide the geometric reference frame and its evolution with time (Earth rotation, plate motions) to tie together all observations and for precise satellite orbit determination needed in global gravity field recovery and altimetry.

Vertical coastal crustal movements have to be analysed together with sea level observations by altimetry and tide gauges for a complete risk estimation. The observation of temporal gravity changes on a global scale reflects the gravitational effects of post-glacial crustal uplift and subsidence and therefore is the tool, combined with kinematic and stationary gravity measurements, to infer the elastic behaviour and properties of the solid Earth.

A precise high-resolution gravity field defines everywhere the ‚Mean Sea Level' which is the reference for the topographic heights. These heights are presently determined by time consuming and man-power intensive geometric levelling. Once the ‚Mean Sea Level' is known with a precision compatible to levelling, the traditional surveying method can be replaced by modern satellite-based methods, called GPS-levelling and later on Galileo-levelling. The ground receivers using the American Global Positioning System (GPS) or the European Galileo navigation satellite system then could easily deliver heights above ‚Mean Sea Level', i.e. topographic heights.

On the other hand, continent-wide distributed points, which are observed by both GPS and geometric levelling deliver the geoid heights defined in the national height reference system. The comparison with the global geoid observed from space reveals the differences in the realization of the national height systems, thus leading to a unified global height reference system.

World wide web pages with further information on the satellite missions	
CHAMP	http://op.gfz-potsdam.de/champ/ http://www.dlr.de/champ
GRACE	http://op.gfz-potsdam.de/grace/ http://www.csr.utexas.edu/grace/
GOCE	http://www.esa.int/export/esaLP/goce.html http://www.goce-projektbuero.de
ICESat	http://icesat.gsfc.nasa.gov http://www.csr.utexas.edu/glas/
CryoSat	http://www.esa.int/export/esaLP/cryoSat.html http://www.cryosat.de
ENVISAT	http://envisat.esa.int/
Jason-1	http://topex-www.jpl.nasa.gov/mission/jason-1.html
ERS-2	http://earth.esa.int/ers/
TOPEX/Poseidon	http://topex-www.jpl.nasa.gov/mission/topex.html
Geosat FO	http://gfo.bmpcoe.org/Gfo/

3 Transport processes and mass anomalies in the Earth system

This chapter gives detailed information about the individual transport processes in the Earth system, its present knowledge, modelling deficits and the expected benefits from joint analyses of the newly available Earth observations: ocean transport processes (Chapter 3.1), ice mass balance and sea level change (Chapter 3.2), solid Earth dynamics and structure (Chapter 3.3), and the continental hydrological cycle (Chapter 3.4). Research on these processes has to take into account the effects of atmosphere and tides (Chapter 3.5).

3.1 Ocean dynamics

Satellite altimetry has revolutionized our understanding of the variability and dynamics of the ocean. A decade of measurements of the sea surface height has led to new insight about processes in the ocean interior, its density structure and associated velocity field. Until now mostly temporal anomalies have been exploited with only little references to a geoid model. With the anticipated precise geoid and absolute sea surface dynamical height surfaces we hope for a similarly successful advance in our understanding of absolute structure of and transport in the ocean.

Physical oceanography and marine geodesy

Recently the interest of oceanographers in satellite altimetry and space geodesy has increased dramatically, primarily through the enormous success of the TOPEX/POSEIDON altimetric mission in studying ocean phenomena. Until now this progress was mostly limited to time-varying currents and other transient phenomena. However, the combination of a highly accurate altimetric sea surface height field with improved geoid models anticipated from GRACE and GOCE will revolutionize our skill in observing the ocean dynamic sea surface topography and associated surface currents. This implies that for the first time in the history of oceanography there is the possibility to obtain the absolute oceanic current field with a sufficient precision that allows the investigation of many long standing oceanographic problems, including the investigation of strong and narrow boundary currents, the absolute eddy field and its interaction with the mean flow, with the topography and flow instability processes. In particular, the new knowledge will help to determine oceanic transports with an accuracy that is required to enhance our understanding of the oceans role in climate variability and in the global hydrologic cycle. Equal-

Ocean Dynamics

Benefits

- Direct observation of the dynamic sea surface topography with cm-precision is key to determine the ocean circulation.
- For the first time, oceanic mass variations become observable with global coverage.
- Measurements of sea ice thickness and changes in continental ice cover allow a better understanding of forces driving the ocean circulation.

Challenges

- Assimilation of satellite gravity and altimetry data together with oceanographic in-situ data into ocean circulation models.
- Recovery of time-varying top-to-bottom absolute ocean current fields.
- Separation of contributions to sea level rise due to thermal expansion, ice melting, oceanic mass redistribution, and vertical land motion and simulating those effects properly in climate models.

ly important, it will enable us to identify heat and mass variations in the ocean, regionally and globally, to identify long-term changes and to improve numerical simulations of climate change.

Physical oceanography and marine geodesy have had a long symbiotic history through the joint problem of determining the marine geoid: While for the geodesist, the geoid height is a fundamental description of the shape of the Earth, to the oceanographer it is a reference surface necessary for computing the oceanic circulation and ocean transports from altimetric and in situ ocean observations. Many other branches of both sciences overlap as well, including the study of tides, mean sea level, Earth rotation and polar motion, and global and regional sea level rise and fall. As a result there exists an intimate relation between both disciplines that brings the determination of the ocean circulation and of ocean transport of mass and heat to the forefront of studying and understanding the system „Earth". Since Wunsch and Gaposchkin (1980) initially laid out the framework for a combined estimation of the Earth's geoid and the ocean circulation, enormous progress has been made in observing the ocean using satellite altimetry and in determining the Earth's gravity field. To a large extent, this progress is due to the success of the TOPEX/Poseidon altimetric mission. At the same time, ocean modelling also improved substantially, mostly through improvements in forcing conditions and through increased model resolution, i.e., through advances in computer technology. Lastly, uncertainties in marine geoid estimates have been reduced over the last decades to well below one meter on the scales resolved by ocean models. This uncertainty will be further reduced by orders of magnitude during the next few years based on GRACE and GOCE data. Despite the recent exciting success, the elements of a modern geodetic/oceanographic symbiosis remain the same. Because the sea surface nearly, but not quite, coincides with the geoid, slopes of the sea surface relative to the geoid imply measurable oceanic velocities. As the sea surface slopes relative to the geoid are less than one meter in thousands of kilometres, small errors in estimates of the slopes imply large erroneous oceanic mass and property fluxes. Thus, comparatively crude oceanic circulation estimates can provide relatively accurate estimates of the geoid height slopes. New approaches to combine altimetric and geodetic observations with in situ ocean data and with ocean models can therefore lead to significant progress in oceanography and geodesy.

A measured dynamic sea surface topography is shown in Figure 3.1.1 as a combination of satellite altimetry and a geoid model from GRACE. Please notice the contour interval of only 10 centimetres. Until today the varying sea ice coverage makes it impossible to derive stable estimates of the mean topography at high latitudes.

Ocean models, despite being not perfect and error-prone in many aspects, began to show encouraging degree of realism in several aspects (Griffies, 2000). Ocean state estimation aims to further improve those models by bringing them into consistency with ocean data. The goal of those „ocean syntheses" is to obtain the best possible description of the changing ocean and to estimate the atmospheric forcing fields that are in agreement with the ocean observations. At the same time, the method identifies model components that need improvements, including ocean mixing parameters, and produces guidelines to improved oceanic observing systems (e.g., Schröter and Wunsch, 1986). See Stammer et al. (2002) and Stammer (2004) for a detailed discussion.

Increased attention to the problem of a simultaneous determination of the marine geoid and the ocean circulation arose with the preparation and launch of the high accuracy geodetic missions CHAMP, GRACE and GOCE. GRACE will provide gravity field information with an accumulated accuracy of 2 cm down to scales of approximately 150 km and on time scales from months to the duration of the mission (cf. Figure 2.8). The GOCE mission will resolve stationary gravity field structures down to scales of approximately 70 km.

Wunsch and Stammer (2003) provide a revised discussion of the critical requirement for improvements of the joint estimation problem. A successful combination of altimetric data with in situ observations and an ocean model will determine the oceanic flow field that is in agreement with

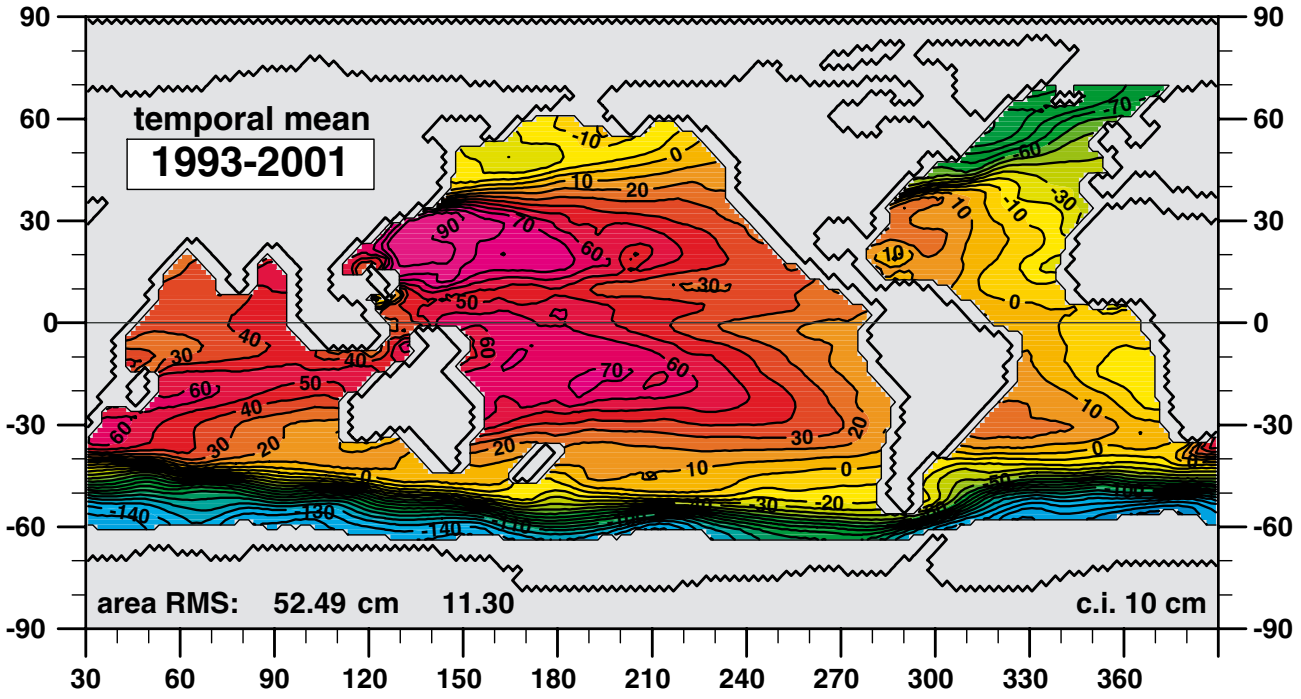

Figure 3.1.1: *Mean sea surface as the difference between the mean sea surface height from altimetry (CLS_SHOM98.2) and the geoid EIGEN_GRACE. The unprecedented accuracy of the GRACE mission allows for the first time the calculation of a realistic mean dynamic topography which is relevant for oceanography.*

observations of all types and will also provide an estimate of the marine geoid that is similarly in agreement with geodetic observations and known ocean dynamics. The estimates of the ocean flow field contain estimates of mass and heat transport and help to quantify interaction between stationary and time-dependent currents. This for the first time opens the possibility to obtain the absolute oceanic current field with a precision, necessary to approach long standing oceanographic and geodetic problems. Jointly with altimetry and ocean modelling, the new gravity data will enable us in particular to obtain a better understanding of the time-mean circulation.

The mutual connections involved in the process of jointly evaluating geodetic and oceanographic information will be outlined in the following. For that purpose, we will first discuss how improved GRACE and GOCE estimates of the geoid will advance estimates of the ocean circulation. Special emphasis is laid on oceanic transports and fluxes and related climate problems. The necessity of using oceanography to de-alias satellite gravity measurements is described. We will subsequently summarize how improved ocean estimates will feed back into the geoid estimation procedure. On global scale, the problem is complex and involves various different components of the Earth system. As an example, global sea level rise is associated with global ocean warming, but also with redistribution of mass from the cryosphere, the land or the atmosphere into the ocean. Understanding global sea level rise thus involves understanding global mass balances and glacial melting, among others (Chapter 3.2). At the same time, all those processes as well as the ocean circulation affect Earth angular momentum changes. It is obvious, therefore, that the ocean does play an important role as a link of otherwise isolated Earth components. Ocean modelling and data assimilation can thus help understanding all individual components in a mutually consistent way.

Impact of gravity field information on determining the ocean circulation

With the expected unprecedented accuracy of new geoid models from GRACE and GOCE the determination of global absolute ocean currents from measurements will become finally feasible. Then, for the first time altimetry, gravity field information and in situ data will yield a dynamically balanced description of temperature, salinity and tracer fields, sea level, currents and transports and their time evolution in almost all regions of the world ocean. Additionally we will obtain adjustments to changes of external forcing fields, such as wind stress, net heat flux or freshwater forcing. Glacial ice melting and the regional and global response in sea level is one of the most prominent examples with dramatic implications for society. Sequestering of heat and carbon dioxide in the ocean is another example of wide-ranging implications. The increasing knowledge of oceanic transports will help to obtain more realistic estimates of global change in the world oceans. A better analysis of ocean dynamics and mixing on shelf and adjacent sea regions will be very important to properly understand their role in setting global balances which are not well understood today.

Improved geoid models from GRACE and GOCE will significantly advance our skill in estimating ocean currents by using

- precise geocentric sea surface elevation obtained from global altimetric measurements, reprocessed according to a new geoid model,
- geoid models with the accuracy of the order of a centimetre on spatial scales down to the width of boundary currents,
- new information of precise bottom pressure change,
- corrections performed by powerful ocean models,
- additional oceanographic data sets required to constrain ocean circulation models with data assimilation.

With this improved knowledge it will become possible to efficiently study the interaction of stationary and time-dependent components of the absolute current field. It is through mean flows, as well as variabilities (e.g., eddies) that the ocean transports its heat, fresh water and dissolved and suspended matter. Eddies are being generated through instabilities of the time-mean flows. With a data constrained mean circulation, the role of variabilities in weakening or stimulating the mean flows as a result of non-linear interaction can properly be estimated and taken into account. We can expect to fundamentally improve the understanding of the features controlling the dynamical processes.

Hellmer et al., (2004) used an ocean model for deriving such a data-constrained mean circulation. Temporal altimeter anomalies as well as time varying sea surface temperatures, ice coverage and analysed atmospheric conditions are assimilated into a general ocean circulation model. In addition, oceanographic measurements about temperature, salinity and currents are used to derive a fully balanced model solution which is as close to observations as possible. The mean sea level of their model for the same period as the satellite dynamic topography is shown in Figure 3.1.2. Both surfaces have a remarkable similarity. The only major difference is in the Southern Ocean where the Antarctic Circumpolar Current of the ocean model is too weak and the associated drop in sea surface topography towards Antarctica is too small. Discrepancies of this kind allow us to gain more insight by improving ocean modelling as well as by estimating more realistic ocean transports and fluxes which cannot be obtained with conventional methods.

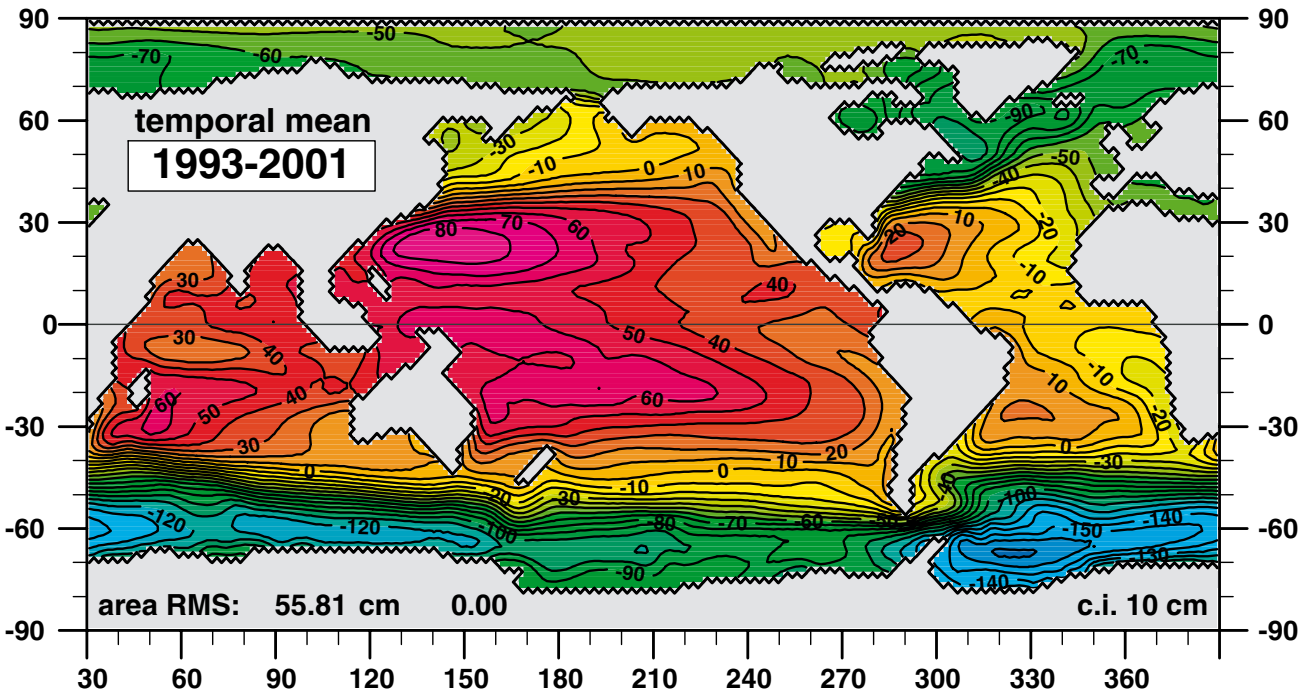

Figure 3.1.2: *Mean sea level as calculated from ocean modelling by averaging over the period 1993 to 2001. The ocean model reproduces all major topographic features that are measured. However, in the region of the Antarctic Circumpolar Current (ACC) the sea surface of the ocean model is not low enough which indicates underestimated velocities of the ACC. This discrepancy must be solved by data assimilation.*

Estimation of mass and heat transports in relevant oceanic regions

LeProvost et al. (1999) discuss the extent to which data from the GRACE and GOCE missions will help to enhance our understanding of oceanic transport processes. A suite of ocean models with and without assimilation are considered with different resolution and complexity. It is shown how modelled sea surface height differs substantially between ocean models and approaches and independent information will help resolve many relevant oceanographic problems. Schröter et al. (2002) point out that most of the expected improvement in our knowledge of oceanic transport will be due to the high resolution capabilities of GOCE.

Global numerical ocean modelling will play a central role in improving ocean circulation estimates and geoid estimates. For the oceanic transport it is necessary to better simulate where short spatial features interact with the mean current systems through momentum exchanges, or through transport of heat and mass. To date, ocean models are not capable of properly separating mean transport and eddy induced transport in a realistic manner (Griffies, 2000). Each model produces its own `climatological equilibrium‘ depending on resolution, details of the forcing fields, choice of model grid and other numerical implementations i.e. representation of advective and diffusive processes or vertical overturning. To date, only variability is exploited well from altimetric sea surface height. With the new gravimetric missions we can approach the same degree of knowledge and understanding also for the mean part of the circulation. Without that next step advancements in our understanding of the mean ocean circulation will be seriously hampered.

A region of great importance in this respect is the Southern Ocean where the Antarctic Circumpolar Current (ACC) plays a dominating role in exchanges between the ocean basins. The same applies to the deep ocean circulation, where the highly time-dependent formation of bottom water in the Weddell gyre represents an essential part. The ACC is characterized by sharp frontal areas, narrow jets and eddies exerting forces on zonal flows, where these forces vary within small ranges of latitudes across the ACC. The importance of the interaction of the flow field with the bottom topography in setting the dynamical balances over the ACC adds even more complexity in determining the correct ACC structures and transport variations.

To date ocean general circulation models have failed to appropriately simulate the ACC by itself. This is mostly due to uncertainties in the momentum balance which turns out to be the difference of large numbers. The ACC is accelerated by its internal (baroclinic) density structure with low density in front of a bottom ridge and high density behind it. This acceleration can be measured with some skill from research vessels probing the full water depth (Figure 3.1.3).

The counteracting force results from the gradient of the sea surface height which tends to slow down the ACC. It can only be measured by altimetry referenced to an accurate geoid model. Until now the measurements were insufficient to improve on purely oceanographic estimates. With novel gravity information it will be possible not only to better determine total transport and balances but increasingly the position, width and current speed of individual fronts.

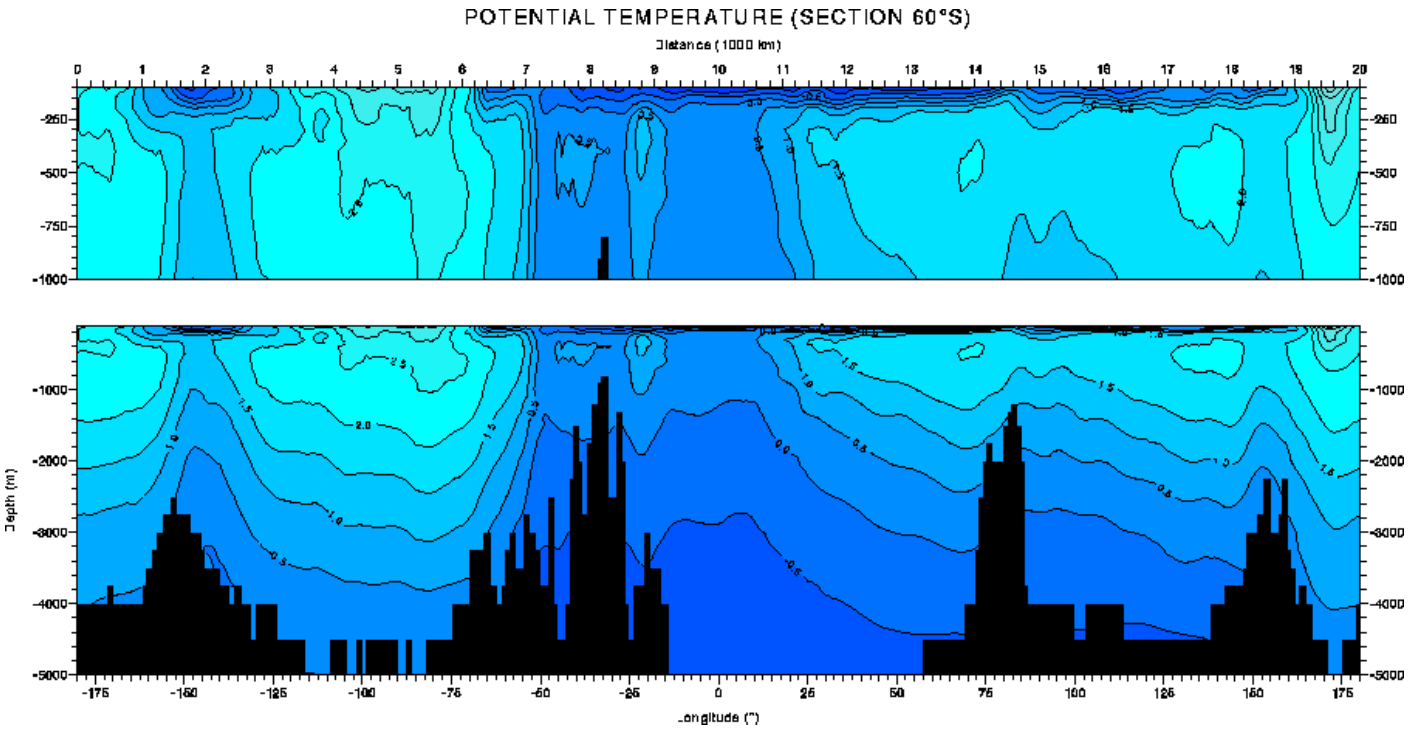

Figure 3.1.3: *The structure of potential density in the ocean along a section at 60^0 South. Density structure and bottom topography are clearly connected. West of each major ridge we find low densities while further to the east high densities are observed. This structure results in a force strongly accelerating the circumpolar current. It is almost fully compensated by the force excited by the gradient of the sea surface.*

Separating thermal expansion from mass increases in studies of global sea level rise

Global sea level rise is one of the major challenges of climate change (Church et al., 2001). Whether the sea level will be some centimetres or a few decimetres higher than now at the end of this century is of immediate concern for about half of the population of the Earth and has enormous economic consequences. The scientific community is asked for realistic prediction of sea level rise. Predictions vary widely, according to data sets used and principles applied (Church et al., 2001). Clearly it is not sufficient to measure sea level change at tide gauges and by altimetry but we must aim at understanding the underlying processes and quantify them. This holds especially for processes that will become more important in the future such as the response of the global ocean to local enhanced freshwater forcing from Greenland melting: Hypotheses suggest that Greenland might loose much of its ice volume over the next few decades. This situation could result in a substantial regional and global sea level rise that needs to be understood.

An example of the response of a quasi-global ocean circulation model with 1 degree spatial resolution to enhanced Greenland ice melting (on the order of 0.1 Sv freshwater input) is depicted in the Figure 3.1.4. It shows the differences of a control run and one that was perturbed by enhanced Greenland melting with otherwise similar model parameters as it occurs after 5 years (Stammer and Ueyoshi, 2004). The results demonstrate that the response is very dynamical leading to strong boundary wave activities that originate from the sub polar North Atlantic and that spread across the Atlantic in terms of boundary, Kelvin and Rossby waves with respective time scales. Clearly sea level increase is not uniform but leads instead to a dynamically caused depression in the central sub-polar North Atlantic by several centimetres. In contrast, coastal regions “feel” the enhanced freshwater much faster in terms of sea level rise. The figure clearly illustrates the threat of predominantly coastal sea level rise due to climate change.

With respect to sea level, we are primarily interested in monthly scales and periods up to a century. Local sea level change by surface waves and tides is fairly well understood and does not lead to substantial secular changes. The seasonal cycle of sea level rise and fall is dominated by redistribution of mass due to changes in ocean circulation and also by local warming and cooling.

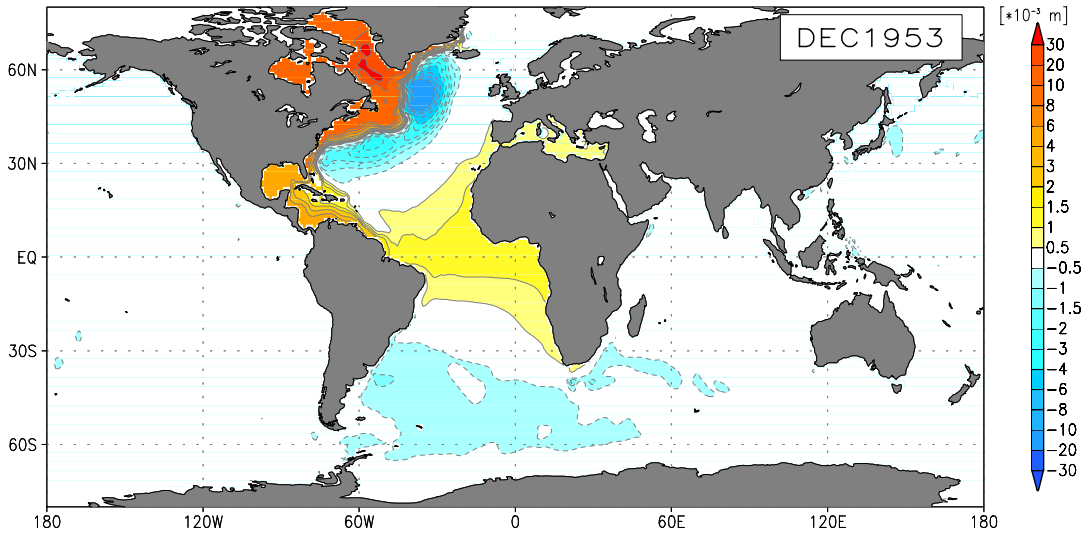

Figure 3.1.4: *The figure shows the response of a global ocean circulation model as it results to about 0.1 Sv increased runoff due to Greenland ice melting. The field shows the differences (in cm) of sea surface height as it results after 5 years of increased freshwater forcing due to ice melting. Colour range is +/-3cm. See Stammer and Ueyoshi (2004) for details.*

An additional global trend remains that results from an imbalance of the hydrological cycle which is thought to be mainly net inflow of melt water into the sea from glaciers, ice caps and polar ice sheets (Chapter 3.2). Superimposed on a regional basis are strong changes in the thermohaline (temperature and salinity) structure of the ocean. In principle, these can be measured. However, the vastness of the global ocean and the remoteness of large domains make such a task difficult. Even with novel techniques like thousands of autonomous drifting buoys from the ARGO project performing vertical probing the ocean remains undersampled in regions such as the arctic.

The magnitude of sea level rise due to ocean heating varies considerably. The specific volume of sea water (volume per unit mass) increases when the water is heated. This increase is known as thermosteric expansion. Its magnitude depends strongly on temperature and pressure: heating of warm water has a much bigger effect than that of water around the freezing point. Also water at high pressure in the deep ocean reacts much stronger than surface waters. The specific volume of sea water decreases when salt is added, denoted as halosteric contraction. Its magnitude is fairly constant over the whole ocean.

The stratification of the ocean interior is mostly stable. Heating from above has only local influence and does not reach deep into the water. Only when cooling or salinity increase result in an unstable water column the deep ocean is ventilated and its properties change. Both processes occur in high latitude where the primary ventilation regions of the world ocean reside. Areas with vertical overturning called convection are strongly linked to cooling, fresh water forcing and sea ice processes which will be discussed below.

Locally, sea level change varies strongly and may even change sign. It is difficult to derive stable estimates from tide gauges and even from altimetry (Church et al., 2001). In order to get closed budgets and to separate different contributions to the observed sea level changes it is possible to assimilate the observations in a global ice-ocean circulation model that conserves mass, heat, salt and momentum. Forcing is by the atmosphere only and by inflow of fresh water from land.

Volume change computed from the model results in dynamic topography change which must coincide with altimeter and tide gauge observations (Wenzel et al., 2001). When only surface data are assimilated there is an infinity of possible solutions. Only by using additional measurements from the deeper ocean the problem has a unique solution and the explanation found depends on the measurements in an unambiguous way. In Figures 3.1.5 to 3.1.7 results of such an assimilation experiment which exploits altimetry, geodesy and oceanographic data are depicted. Sea surface variability over the period 1993 to 2001 is modelled successfully. The analysis of linear trends reveals the dominance of local warming (cf. Figure 3.1.5) while changes in salinity have a much smaller effect as is shown in Figure 3.1.6. An interesting feature of ocean circulation is also found for the trend analysis performed here. Frequently, temperature and salinity variations are correlated in a way that leaves density unchanged. It is evident from the figures that strong temperature variations are not enough to change sea level. Associated variations in salinity must be considered simultaneously. The third mechanism to change the sea surface involves a change in mass. On the time scales of a decade considered here almost no variability remains (cf. Figure 3.1.7). Net inflow due to an imbalance of the hydrological cycle spreads approximately evenly over the whole globe. What is diagnosed in the assimilation experiment is a decrease in mass near Antarctica which is associated with an increase of transport of the ACC. The other remarkable change is a mass increase over the Arctic Ocean. For this no independent evidence is available at present.

The situation will change once the GRACE measurements can be fully exploited. Temporal anomalies of gravity field observations provided at periods from two months to the mission life time will yield information about the deep, time varying ocean mass distribution and circulation which otherwise is unobservable. This information, which is independent of steric contributions, can be used to distinguish steric from nonsteric contributions to altimeter measurements of sea surface

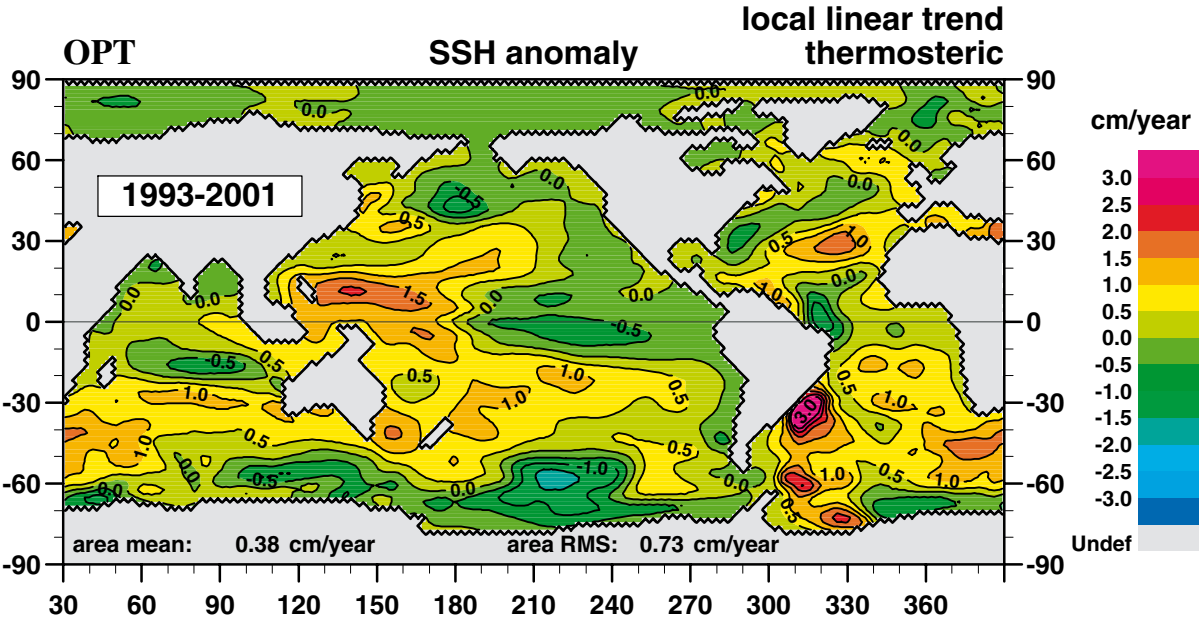

Figure 3.1.5: *Trends of sea level heights (SSH) due to thermal expansion. The effect is integrated over the full water column. Depicted here and in the following two figures are the results of assimilation of satellite altimetry and traditional oceanographic data into an ocean model. The solution is dynamically fully consistent and close to observations. Local trends exhibit a large variance due to strong interannual variability: For slightly different periods the patterns change significantly.*

height. Measured changes in mass distribution are useful for ocean model verification or falsification and can, in principle, also be assimilated.

The interpretation of the measurements is important. Knowing the steric contributions would make it feasible to approximate the changes in the vertically integrated heat and freshwater stor-

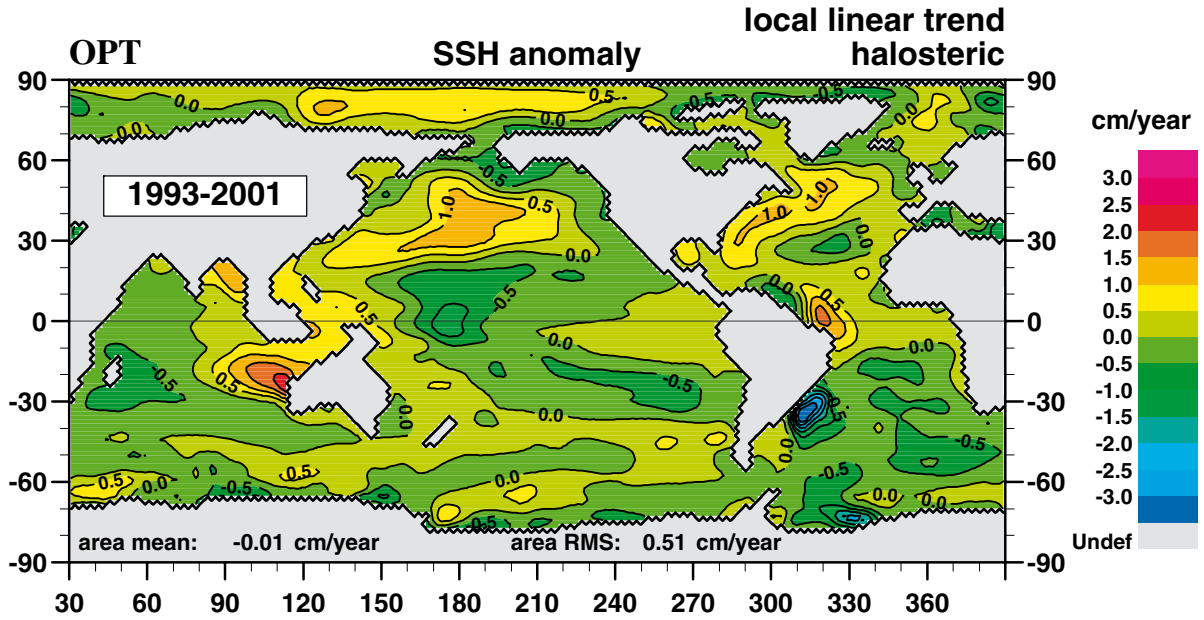

Figure 3.1.6: *Local sea level rise due to changes in salinity. In some areas the effect is as strong as that of warming, showing the importance of salinity. Note that for many strong signals an anticorrelation is found: although local warming is observed it has little impact on sea level as associated changes in salinity largely compensate thermal expansion keeping density fairly constant.*

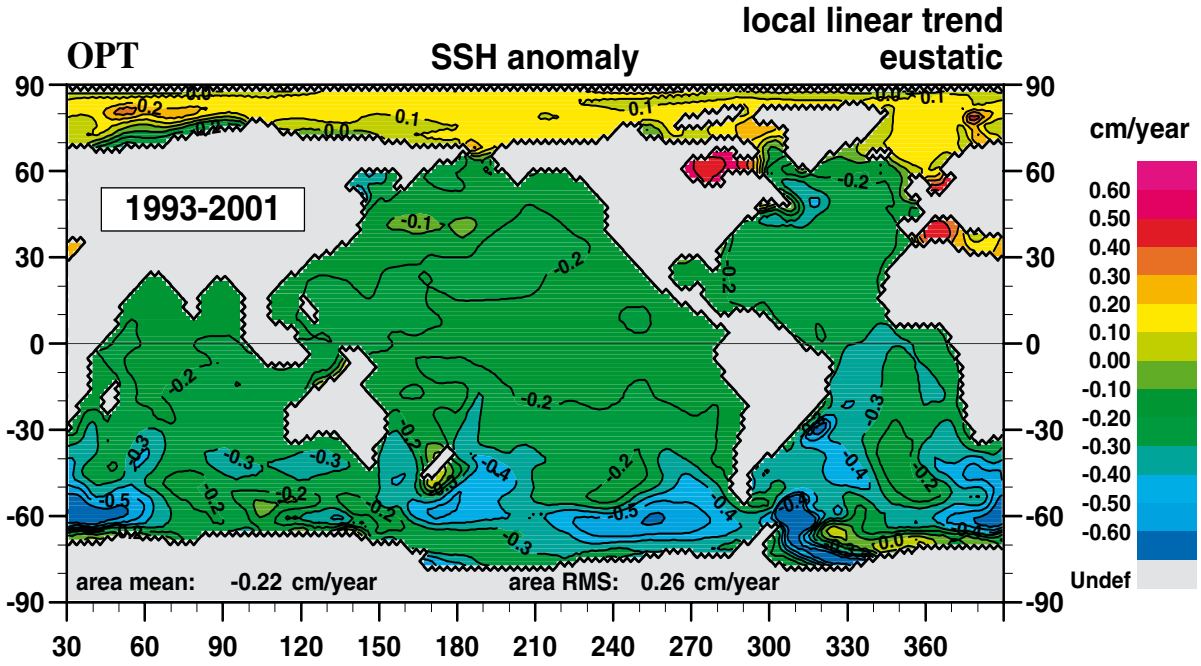

Figure 3.1.7: *Local sea level rise due to increases in total mass and regional redistribution. Over most over the globe there is practically no change. The clear sea level fall over the Southern Ocean is connected to an increase in the eastward velocity of the ACC. The mass change diagnosed here is large scale enough to be fully detectable by GRACE. Time varying gravity can be used for verification and ultimately for assimilation in dynamic ocean models.*

age over scales of a few hundred kilometres and larger and would thus contribute significantly to our understanding of global climate change in terms of buoyancy and mass variations. Regional fluctuations in ocean mass are directly linked to the wind field. Changes in mass on global scale are a measure of changes in the Earth freshwater cycle. Knowledge of both is urgently required and will lead to a better understanding of the relation between local and remote forcing in setting the mean and time-varying circulation

Sea ice thickness observations

Sea ice strongly modifies the global heat and energy balance due to its high albedo and latent heat. Therefore it plays an important role in the climate system. Sea ice is one of the main drivers for the global thermohaline ocean circulation by rejecting salt upon ice formation and releasing fresh water when melting. Its extent and thickness are sensitive indicators of climate change.

Sea ice floats in sea water, i.e. in the melt it has been growing from. It forms a source or sink of freshwater and latent heat . Sea ice related processes are therefore a major driving force of the ocean circulation. For instance, it is estimated (Olbers and Wübber, 1991) that about half of the Antarctic Circumpolar Current is a consequence of ice formation close to the coast and melting of the same ice more than one thousand kilometres further north. The possibility of measuring not only the sea ice distribution but also its thickness on a global scale is novel and exciting for the oceanographic community.

Deep water formation is strongly related to freezing of sea water. Sea ice is less saline than the surrounding water. When sea water freezes salt is rejected to the water below which becomes more saline and denser. If the water is dense enough it may convect down to the deep ocean tak-

ing oxygen and other gasses with it. This ventilation of the deep ocean is one of the major processes that determines the water mass characteristics and their distribution on a global scale and indirectly the global ocean circulation. Measurements of sea ice thickness and sea ice distribution allow the determination of sea ice volume, the fresh water cycle performed by sea ice processes and the associated changes in buoyancy at the ocean surface.

In recent decades passive microwave satellite data have revealed that the areal extent of sea ice in the Arctic has decreased by 3% per decade, with an accelerated trend of 8% per decade in the 1990s (Comiso et al., 2002). Sporadic observations on board of military nuclear submarines have shown that ice thickness in the central Arctic Ocean has decreased by 43% between 1958 to 1976 and 1993 to 1997. The interpretation of these changes is difficult due to the complex processes between atmosphere, ice, and ocean, in particular in the vicinity of the ice edge. Sea ice thickness measurements are particularly difficult to understand with respect to their relation to climate changes, because ice thickness shows a strong seasonal and interannual variability (Haas and Eicken, 2001), and because the regional thickness distribution strongly depends on the ice motion field, which is a function of atmospheric and oceanographic circulation regimes. With changing drift patterns, ice thickness might increase in one region whereas it decreases in another (Figure 3.1.8).

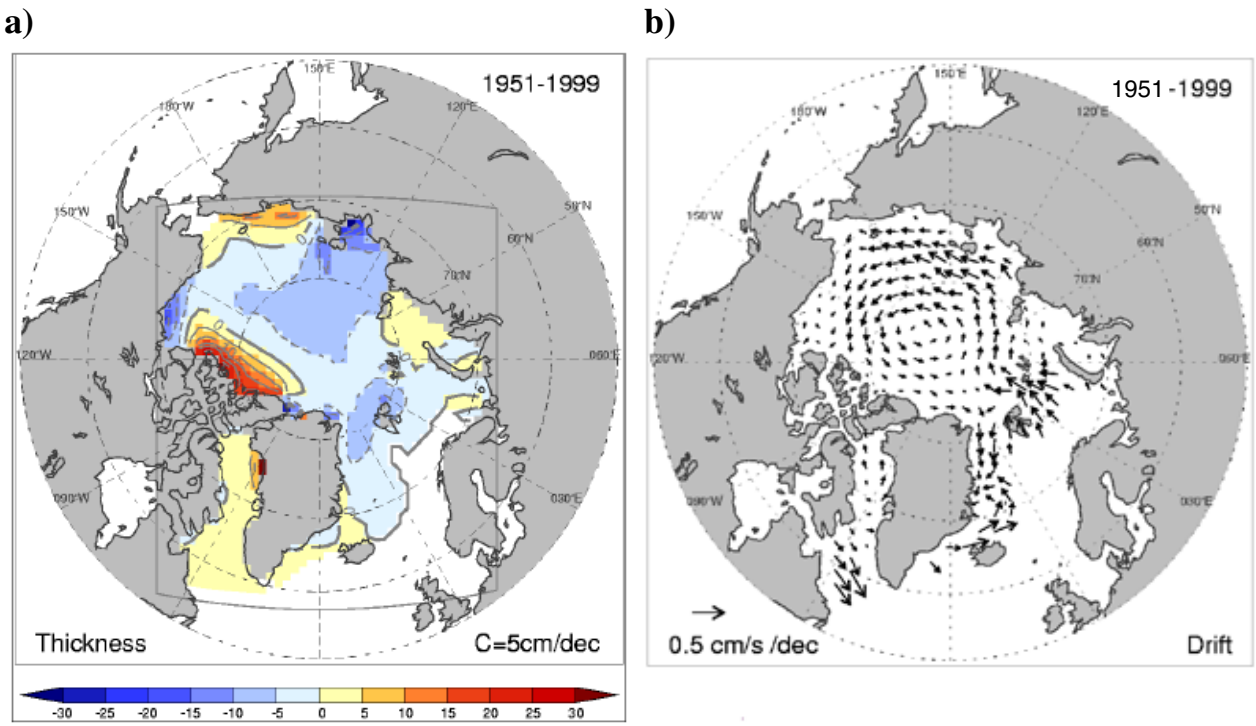

Figure 3.1.8: *Model simulation of Arctic ice thickness trends between 1951 and 1998, and the underlying ice drift anomaly. Thickness has increased in the marginal seas and decreased in the central Arctic Ocean. Ice motion has become more cyclonic, with decreasing sea level in the centre.*

Ocean modelling and its use for gravity field determination

Gravity field estimates obtained from GRACE and GOCE are restricted in their space-time sampling and will therefore alias unresolved high-frequency barotropic oceanic motions and diurnal and semidiurnal tides (Stammer et al., 2000). Using information about surface topography variations on daily to monthly periods from ocean circulation and variations in tidal bands from tide models, the recovery of the mean gravity field can be improved significantly by correcting them for high-frequency variations in mass distribution and thus reducing the aliasing effect (e.g. Stammer et al., 2000).

There is no a priori decision which signals should be used as corrections beyond the Nyquist frequency. In fact, this may differ according to the scientific goal. In an iterative procedure it should be determined which part of the oceanic mass movement is considered 'understood', such as tides, implying the signal can be dealiased from the gravity measurements. On the other extreme, signals have to be considered as 'true measurement' (e.g. interannual variations) which will be interpreted geophysically and can be used for data assimilation or verification of oceanic models.

GRACE data will provide information about bottom pressure changes on monthly and longer time scales with an accuracy of equivalent to 1 mm in sea surface height (cf. Figure 2.9). With this measurement precision, many traditional approximations in ocean models become questionable and secondary effects in ocean models have to be considered as well. Conventional approximations include the Boussinesq-approximation treating the fluid as essentially incompressible, simplifications of the equation of state of seawater and insufficient representations of the real bottom topography and bottom slopes in the models. Secondary effects include the interaction between ocean circulation and ocean tides, direct pressure forcing to improve the simulation of the ocean's response to atmospheric pressure loading (e.g., Thomas et al., 2001), and the loading and self-attraction effect due to ocean circulation induced mass redistributions (Condi and Wunsch, 2003). The latter effects are well known in the context of ocean tides. They are of measurable effect also for changes in ocean circulation (Condi and Wunsch, 2003). Mutual corrections of the gravity field and the mass redistribution in the ocean are necessary steps for improving our understanding of changes in the ocean circulation and the marine gravity field.

Frequently, oceanographers produce 'synthetic' geoids for assimilation of altimetric sea surface height. Such a synthetic geoid is calculated as the difference of altimetry and the dynamic sea surface of an ocean model. Evidently, the synthetic geoid varies from case to case and assimilation of altimetry has no influence on the mean state of the ocean model. In fact the procedure is equivalent to the well known collinear analysis where a reference data set is subtracted from each measurement and only temporal anomalies are considered further. Other 'oceanographic' geoids are hybrid and include geoid models as well as altimetry and the dynamic ocean surface. Least squares solutions which take into account the different error covariance structures are calculated e.g. by Seufer et al. (2003). Other possibilities make use of an ocean model into which altimetry referenced to a geoid model has been assimilated.

Studying the agreement with measurements having been assimilated with a priori error assumptions will lead to corrections of introduced in situ as well as of satellite data and in particular of gravity field data (see e.g. Kivman et al., 2005). Thus, investigating the characteristics of these corrections with respect to their physical plausibility is part of an iterative process of simultaneously improving ocean models and gravity field.

Testing gravity estimates through direct observations is not a trivial matter. Ocean data assimilation offers a unique opportunity to test the consistency of geoid estimates and associated error estimates with information available in form of ocean dynamics and ocean data. This can be done

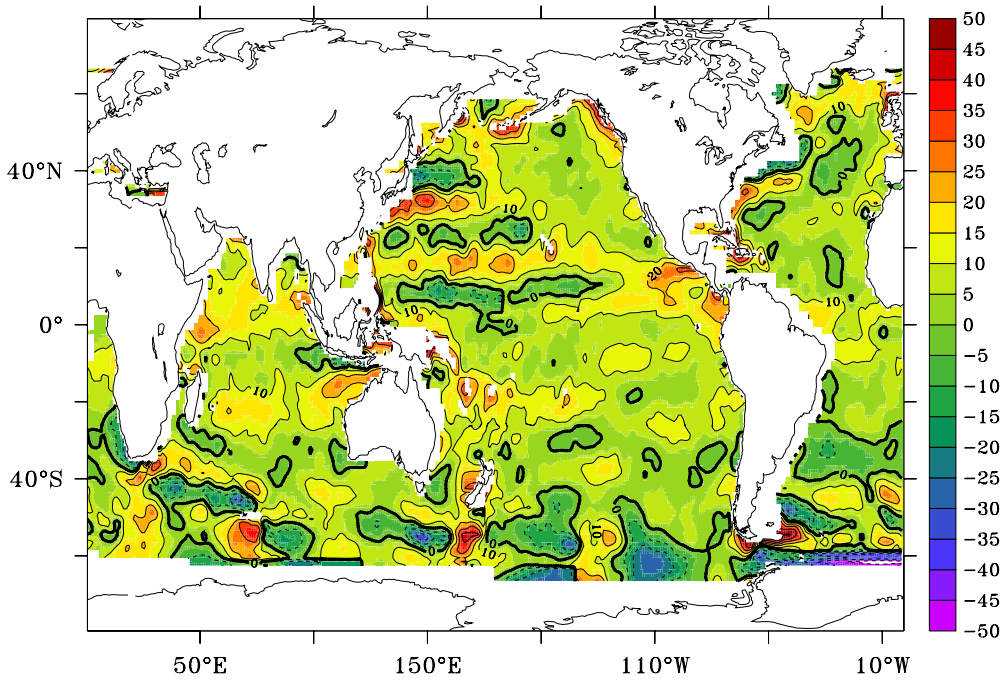

Figure 3.1.9*: Optimized ECCO SSH differences with respect to T/P-EGM96. Contour interval is 10cm. The field can be regarded as ECCO-computed adjustments to the EGM96 geoid to render it consistent with the model and the ocean data.*

by comparing estimated residuals in the mean surface topography with prior and a posterior error statistics and thus to test the consistency of all hypotheses involved, including geoid estimates and their error covariances. One such example is shown in Figure 3.1.9, showing discrepancies in EGM96 geoid error information with estimated sea surface height residuals. Stammer et al. (2004) investigated the consistency of ocean circulation estimates with existing geoid models. The differences are of the order of +/- 20 cm and reach +/- 50 cm near steep topography. Inconsistencies with the prescribed geoid errors are obvious. Those discrepancies have been identified subsequently as inconsistencies in the EGM96 error covariance based on new information available from GRACE.

The next figure (3.1.10) shows the corresponding residuals, in which now the SSH was imposed relative to GRACE. These residuals are much smaller, implying that the GRACE geoid is much closer to dynamical consistency with the GCM and other data than is EGM96. Using the respective time-mean TOPEX-GRACE dynamic topography in an assimilation effort did lead to measurable changes in the flow field especially in low latitudes (Stammer et al., 2004)

The last two figures illustrate the importance that ocean data assimilation can play in identifying consistencies or inconsistencies in the end-to-end geoid-altimeter ocean circulation estimation. It is obvious that in both cases large residuals remain especially in the southern oceans which are not understood. In particular it is unclear where the ocean model or the T/P data or the geoid are suboptimal. In the past, much emphasis was put on determining the time-varying error in the T/P data, which is being assumed here to be of the order of 2-3 cm (RMS). Recent comparison studies between T/P and JASON-1 data revealed that this number is most likely too optimistic: in some regions several large environmental corrections such as the EM-bias are poorly understood, and lead to RMS differences between the satellite data of order 5 cm over large regions. Equally important, little attention has been given to time-mean correction errors. To reach the goal of an optimal use of new geoid information for studying the ocean, the land hydrology or geophysics this involves a very detailed revisit of altimeter error corrections, especially their time-mean components.

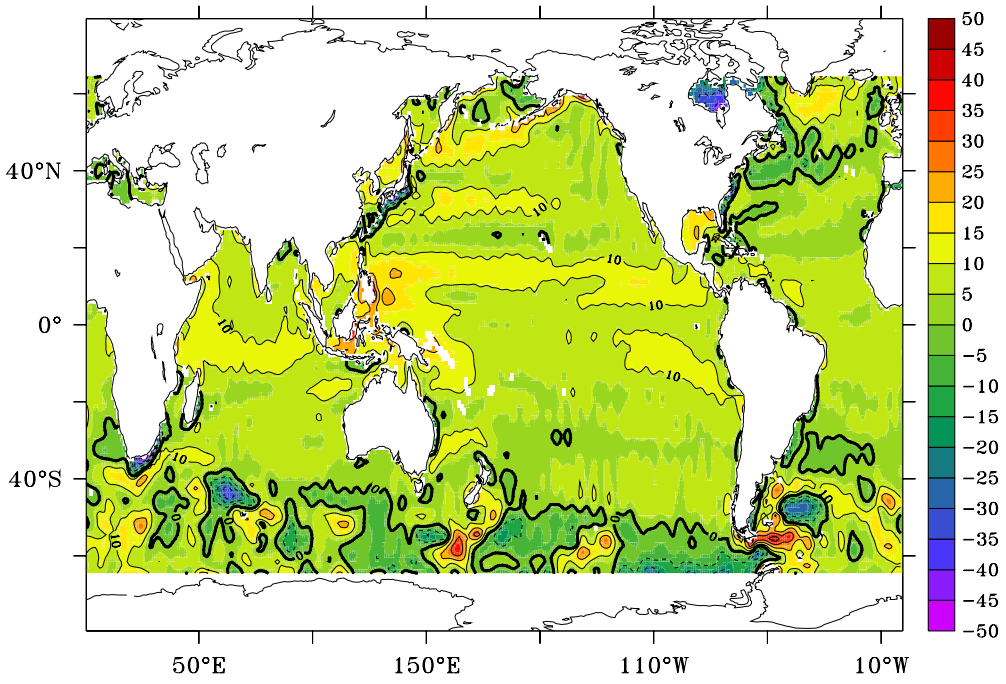

Figure 3.1.10: *Optimized ECCO SSH differences with respect to T/P-GRACE .Smaller values from GRACE as compared to EGM96 suggest greater dynamical consistency with the other data sets and the model.*

Towards a joint estimation of oceanographic and geodetic topographies

The novel accuracy of geoid height fields derived from GRACE and GOCE will be combined with highly accurate sea surface height from a combination of altimetric satellites to obtain measurements of the absolute dynamic height. For the first time we have the opportunity to obtain the absolute oceanic current field with a sufficient precision that allows the treatment of long standing oceanographic problems. The new knowledge will significantly advance our skill in determining oceanic transport with good accuracy and increase our understanding of ocean dynamics through the interaction of mean and time dependent flow.

Most processes that influence the mass distribution on the globe can be distinguished by their time and space scales. Fast motions in atmosphere and ocean are associated with strong signals in the GRACE and GOCE measurements. However, the aliasing associated with these mass changes must be successfully corrected using atmosphere and ocean models in conjunction with data assimilation. We don‘t understand the timescale of hydrological changes, especially over land. We therefore also don‘t understand their contribution to aliasing. On timescales of months and beyond variations in gravity and thus mass changes are adequately resolved by the sampling scheme of GRACE. Those observations will provide new information about mass changes in the atmosphere, the land system and cryosphere or the ocean and need to be investigated in adjoint analyses to attribute the measured changes to different geophysical processes.

Hydrological models are less mature than the other models involved in this context. A guiding principle in studies using GRACE and GOCE data could therefore be that ocean contributions should be corrected as best as possible from GRACE and GOCE results to allow studying the change in continental water storage, or the redistribution of mass in the solid Earth in more isolation (Chapters 3.2-3.4). Without a precise knowledge about the ocean contribution to GRACE

data not much improvement in hydrological models can be anticipated. On the other hand, information on the continental runoff and its variations are important information that will be required to properly simulate changes of the ocean over several years and longer.

Ultimately we must work on a joint analysis that takes into account all contributions from different processes simultaneously. However, first the measurements must be interpreted separately to assure maximum progress in understanding the individual components of the Earth system. A complicating aspect can be that underlying trends on longer time scales than the mission duration may be important. They cannot be understood from the new data sources and must be estimated from different measurements and models.

A joint analysis of ocean circulation and associated ocean mass distribution can be derived from the results of Hellmer et al. (2004). The global ocean bottom pressure anomaly and equivalent time series from GRACE monthly geoid solutions are compared in Figure 3.1.11. The closeness of model result and independent measurements is striking. However, at present only global comparisons are this favourable. Local changes agree less well.

This first attempt of a mass analysis is closely linked to the problem of sea level rise, ice melting and variations in the Earth angular momentum. Sea level rise involves many disciplines of the geosystems community, and need to address effects like glacial rebound (Chapter 3.2 and 3.3), changes in global water cycles, storage of water in man-made lakes (Chapter 3.4), as well as glacial melting (Chapter 3.2), and ocean warming. A detailed discussion of those effects is given in the recent IPCC report (Church et al., 2001).

Clearly, many aspects of sea level change have to be considered which requires a more extensive satellite data base than just altimetry and gravimetry. In particular the close link of sea level rise to polar ice melting requires data from ICESat and the upcoming CryoSat mission to be part of the analysis (Chapter 3.2). All those data sets will help to distinguish between local mass change and volume change in the ocean, or heat and freshwater/salt changes. Essentially the ocean estimation effort is the glue between those elements that would otherwise coexist as individual and somewhat isolated components. Estimates of the ocean circulation have to be in agreement with all individual contributions that involve heat or salt changes and thus mass changes.

After analysing all contributing signals individually it is possible to use ocean state estimation as a tool for combining the dynamics of ocean circulation models with measured data. The goal of such an 'ocean syntheses' is to obtain the best possible description of the changing ocean and to estimate the atmospheric forcing fields that are consistent with the ocean observations. As a by-product model components are identified which need improvements and we obtain guidelines where to improve oceanic and remote sensing observing systems.

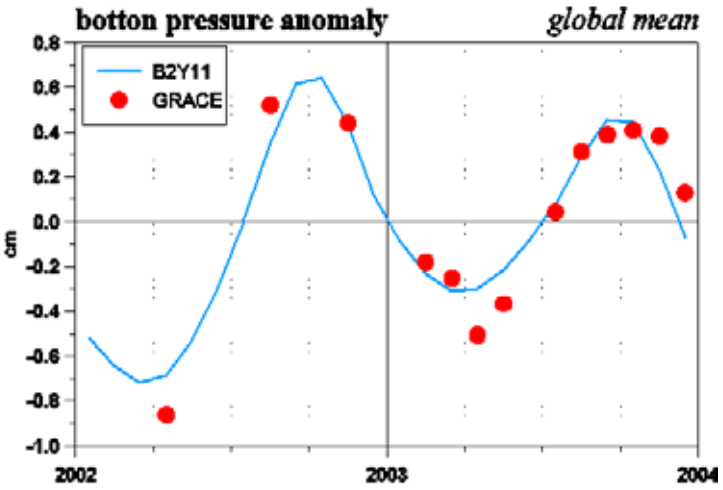

Figure 3.1.11: *Comparison of the global ocean bottom pressure from a 11 year data assimilation experiment (blue) to GRACE measurements (red). Monthly mean geoid solutions were inverted for equivalent mass variations. On a regional scale the assimilation model and data compare less well.*

References

Comiso, J.C., 2002. A rapidly declining perennial sea ice cover in the Arctic. Geophys. Res. Letters, 29 (20), 17 (1-4), doi 10.1029/2002GL015650.

Church, J.A., J.M. Gregory, Ph. Huybrechts, M. Kuhn, C. Lambeck, M.T. Nhuan, D. Qin, P.L. Woodworth, 2001. Changes in sea level. in: J.T Houghton, Y. Ding, D.J. Griggs, M. Noguer, P.J. Van der Linden, X. Dai, K. Maskell, and C.A. Johnson (eds.): Climate Change 2001: The Scientific Basis: Contribution of Working Group I to the Third Assessment Report of the Intergovernmental Panel on Climate Change, Cambridge University Press (Cambridge, New York), 639-694.

Condi, F. and C. Wunsch, 2003. Measuring gravity field variability, the geoid, ocean bottom field variations, and their dynamical implications, J. Geophys. Res., in press.

Greatbach, R.J. , 1994. A note on the representation of steric sea level in models that conserve volume rather than mass, J. Geophys. Res., 99 (C6), 12,767-12,771.

Griffies, S. M., C. Böning, F. O. Bryan, E. P. Chassignet, R. Gerdes, H. Hasumi, A. Hirst, A. M. Tréguier, and D. Webb, 2000. Developments in ocean climate modelling. Ocean Modelling, 2, 123-192.

Haas, C. and Eicken, H., 2001. Interannual variability of summer sea ice thickness in the Siberian and Central Arctic under different atmospheric circulation regimes. Journal of Geophysical Research, 106 (C3), 4449-4462.

Hellmer, H. H., Schodlok, M. P., Wenzel, M., Schröter, J. G. (2004). On a better representation of the Weddell Sea in a large-scale global ocean circulation model, Ocean Dynamics, submitted.

Kivman, G., S. Danilov, B. Fritzsch, S. Harig, C. Reick, J. Schröter, V. Seufer, D. Sidorenko, J. Staneva and M. Wenzel, 2005. Improved estimates of the oceanic circulation using the CHAMP geoid, In: Reigber, C., Lühr, H., Schwintzer, P. and Wickert, J.(Eds): Earth Observation with CHAMP, Results from Three Years in Orbit, Springer Berlin Heidelberg New York, 211-216.

LeProvost, C., E. Dombrowsky, P. LeGrand, P.-Y. LeTraon, M. Losch, F. Ponchaut, J. Schröter, B. Sloyan and N. Sneeuw, 1999. Impact of the GOCE mission for ocean circulation study, ESTEC 131 75/98/NL/GD.

Olbers, D., Wübber, C.(1991). The role of wind and buoyancy forcing of the Antarctic Circumpolar Current, In: Strategies for Future Climate Research, M. Latif (Ed.), MPI, Hamburg, 161-192

Schröter, J., and C. Wunsch, 1986. Solution of Nonlinear Finite Difference Ocean Models by Optimization Methods with Sensitivity and Observational Strategy Analysis, Journal of Physical Oceanography, 16, 1855-1874.

Schröter, J., M. Losch and B. Sloyan, 2002. Impact of the Gravity Field and Steady-State Ocean Circulation Explorer (GOCE) mission on ocean circulation estimates : Volume and heat transports across hydrographic sections of unequally spaced stations. Journal of Geophysical Research, 107 (C2), 4-1--4-20.

Seufer, V., J. Schröter, M. Wenzel and W. Keller, 2003. Assimilation of Altimeter and Geoid Data into a Global Ocean Model., In: Reigber, Ch., Lühr, H., Schwintzer, P. (Eds) First CHAMP Mission results for Gravity, Magnetic and Atmospheric Studies. Springer, Berlin, Heidelberg, New York, 187-192.

Stammer, D.C. and K. Ueyoshi, 2004. Response of the global ocean to Greenland and Antarctic ice melting. To be submitted

Stammer, D., C. Wunsch, R. Giering, C. Eckert, P. Heimbach, J. Marotzke, A. Adcroft, C.N. Hill, and J. Marshall, 2002. The global ocean circulation during 1992-1997, estimated from ocean observations and a general circulation model. J. Geophys. Res., DOI: 101029/ 2001JC000888.

Stammer, D., C. Wunsch and R. Ponte, 2000. De-Aliasing of Global High Frequency Barotropic Motions in Altimeter Observations. Geophys. Res. Letters, 27, 1175-1178.

Stammer, D., C. Wunsch, R. Giering, C. Eckert, P. Heimbach, J. Marotzke, A. Adcroft, C.N. Hill, and J. Marshall, 2003. Volume, Heat and Freshwater Transports of the Global Ocean Circulation 1993 --2000, Estimated from a General Circulation Model Constrained by WOCE Data. J. Geophys. Res., VOL. 108(C1), 3007, doi:10.1029/2001JC001115.

Stammer, D., A. Köhl, and C. Wunsch, 2004: The impact of the GRACE geoid on estimates of the ocean circulation. To be submitted for publications.

Stammer, D., 2004: Adjusting internal model errors through ocean state estimation, J. Phys Oceanogr., accepted.

Thomas, M., J. Sündermann and E. Maier-Reimer, 2001. Consideration of ocean tides in an OGCM and impacts on subseasonal to decadal polar motion excitation, Geophys. Res. Lett., 28, 12, 2457-2460.

Wenzel, M., J. Schröter and D. Olbers, 2001. The annual cycle of the global ocean circulation as determined by 4D VAR data assimilation. Prog. in Oceanog., 48, 73-119.

Wunsch, C. and E.M. Gaposchkin, 1980. On using satellite altimetry to determine the general circulation of the oceans with application to geoid improvement, Revs. Geophys. and space Phys., 18, 725-745, 1980.

Wunsch, C., and D. Stammer, 2003. Global Ocean Data Assimilation and Geoid Measurements, Space Science Reviews, 00:1-16; Kluwer Academic Publisher.

3.2 Ice mass balance and sea level

Changes in Antarctic and Greenland ice sheet mass balance have important consequences for global sea level. We still do not know whether the ice sheets are loosing or gaining mass. Before mass balance and sea level change can be better predicted in scenarios of global climate change, our current understanding and observational basis has to be further improved. The new altimetry and gravity missions will considerably contribute to reducing uncertainties in mass balance estimates and to improve our modelling and prediction capabilities of future sea level rise.

Sea level change is an important consequence of climate change, both for societies and for the environment. The level of the sea changes as a result of changes in water density and/or of the total mass of the ocean. Density is affected by the water's temperature and is reduced by thermal expansion as the ocean warms. Changes in the total mass of the ocean are primarily driven by exchanges with water stored on land. By far the most important land storage is frozen in continental ice masses, which contain more than 90% of the Earth's fresh water resources. It is estimated that total melting of the Antarctic ice sheet, the Greenland ice sheet, and all other mountain glaciers and small ice caps would raise global sea level by 60 m, 7 m, and 0.5 m respectively. Although it is very unlikely that this will happen any time soon, it is clear that even small fractional changes in ice volume would have large consequences. Other storages of continental water include surface lakes, wetlands, ground water reservoirs and permafrost, but water exchanges between these reservoirs and the ocean are not sufficiently quantifiable yet (cf. Chapter 3.4).

Ice Mass Balance and Sea Level

Benefits

- For the first time, complete and reliable estimates for the ice mass balance of the complete Antarctica and Greenland ice sheets will become possible.
- This will allow important conclusions on present climate state and sea level change.

Challenges

- Separation of gravity and surface height signals due to ice mass variations, bedrock isostatic uplift, and firn density changes.
- Satellite data must be supported and validated by a sufficient number of glaciological in-situ data, GPS vertical land movement observations and interferometric SAR data of ice flow velocities.

The level of the sea varies as a result of processes operating on a variety of time scales. The global ocean thermohaline circulation has a memory of centuries. The ice sheets react to climate change on the time scale of millennia, and could be gaining or losing mass as a result of climatic variations extending back to the last glacial period. Another long time scale is added by isostatic adjustment of the Earth's crust to changes in the ice loading and the corresponding mass transfer to the ocean (Chapter 3.3). Postglacial rebound from melting of the ice from the Last Ice

Age is still occurring and can have magnitudes comparable to observed sea level changes at the coast or to ice thickness changes on the residual ice sheets. Glaciers and small ice caps are more sensitive to climate change than ice sheets, and are capable to adjust more rapidly to changes in snow accumulation and ice melting, and may dominate the response on a century time scale.

In order to predict future sea level change with more confidence, it is necessary to better understand the current evolution of continental ice masses, and to quantify their present mass balance. The present and upcoming gravity missions CHAMP, GRACE, and GOCE are expected to lead to significant advances in our knowledge of ice mass balance and sea level. The new altimetry missions ICESat and CryoSat will provide a detailed picture of the spatial distribution of surface elevation and its temporal evolution, and will cover polar areas beyond latitudes currently accessed. Synthetic aperture radar interferometry provides the surface velocity field of ice sheets, including short-term variability in their flow and extent. The determination of the Earth's time-variant gravity field by the GRACE mission will provide additional constraints on mass redistributions, of which ice mass imbalances and isostatic rebound are crucial components. To properly interpret these satellite data in terms of ice volume changes, numerical models of the coupled ice-sheet/ice-shelf/lithosphere system are required. Ice sheet models assist to distinguish between the longer-term ice-dynamic evolution and short-term mass-balance changes, and are needed to extract the current ice mass evolution from gravity and altimetry trends contaminated by postglacial rebound. These models require the best possible input data derived from satellite remote sensing, and provide unique tools for predictions.

Sea ice does not contribute to sea level change, but is an important indicator of climate change. However, its thickness is closely related to atmosphere and ocean circulation. CryoSat and ICESat offer the opportunity for sea ice thickness measurements with unprecedented accuracy.

Ice mass balance and sources for sea level rise

Ice mass balance

Ice sheets and glaciers continuously exchange fresh water with the ocean. They gain mass by accumulation of snow, which is gradually transformed into ice, and lose mass by melting at the surface or base with subsequent runoff. Ice may also be removed by discharge into a floating ice shelf or glacier tongue, from which it is lost by basal melting and calving of icebergs. The difference between total mass input and total mass output is called the mass balance. Net accumulation occurs at higher altitude, net ablation at lower altitude. To compensate for net accumulation and ablation, ice flows downhill by internal deformation of the ice and sliding and bed deformation at the base. In ice sheets, the discharge at the margin mostly occurs concentrated in outlet glaciers and ice streams, which often lie in depressions and move much faster than the surrounding ice.

The average annual precipitation falling onto the Antarctic and Greenland ice sheets is equivalent to 6.5 mm of sea level (Church et al., 2001). For glaciers and small ice caps, the value is about 1.9 mm per year. This input is approximately balanced by loss from melting and iceberg calving. For the two polar ice sheets, the balance of these processes is not the same, on account of their different climatic regimes. Antarctic temperatures are so low that there is virtually no surface runoff; the ice sheet mainly loses mass by ice discharge into floating ice shelves, which experience melting at their underside and eventually break up to form icebergs. On the other hand, summer temperatures on the Greenland ice sheet are high enough to cause widespread melting, which accounts for about half of the ice loss, the remainder being discharged as icebergs or into small ice-shelves. If mass-balance terms do not balance, sea level will change and the mass and shape

of the ice sheets will adjust until a steady state is regained. This occurs over time scales of the order of 100 to 10000 years. Hence it is likely that the ice sheets are still dynamically adjusting to their past history (long-term background trend). This trend is separate from the direct response to mass-balance changes in the recent past (one or two centuries), and both components need to be accounted for when assessing their future contributions to sea level. Despite recent advances in the understanding of polar ice sheets, their current mass balance is still not known.

Mass budget estimates of polar ice sheets

The traditional method to obtain the state of balance of the polar ice sheets, or parts thereof, is to estimate individual mass balance terms and calculate the budget. With present-day measurement precision, the budget method is not able to constrain the total balance of both polar ice sheets to better than ± 20 % of their mass input (Church et al., 2001). The major error source is related to the mass loss terms, as recent accumulation estimates display a tendency for a convergence towards a common value with a remaining error of about 5%. For Antarctica, the ice discharge from the grounded ice sheet dominates the uncertainty because of the difficulty of determining the position and thickness of the ice at the grounding line, where grounded ice starts to float and transforms into an ice shelf. There, also assumptions about the vertical velocity have to be made. For Greenland, surface runoff of meltwater is an important term. However, net ablation has only at a few locations been measured directly and therefore has to be calculated from models, which have considerable sensitivity to the surface elevation and the parameters of the melt and refreezing methods used. An additional complication is the important role played by bottom melting below floating glaciers in northern Greenland, when considering calving fluxes. These terms are neglected in earlier analyses. In a nutshell, current mass budget results suggest, that the mass balance of both ice sheets lies between -35% and +5% of their annual mass input, or a combined imbalance equivalent to a sea-level contribution of between +2.4 and –0.2 mm/ year. This range is large compared to the central estimate of 1.5 mm/year of total sea level rise for the last century, but not significantly different from zero (Church et al., 2001).

Direct monitoring of surface elevation changes of ice sheets

Provided that changes in ice and snow density and bedrock elevation are small or can be determined otherwise, elevation changes can be used to estimate changes of mass of the ice sheets. In the past five years, important progress was achieved based on altimetric methods, both from satellites and from aircraft. Improvements of nearly two orders of magnitude have occurred in the accuracy of the localisation of satellite and aircraft platforms and the reduction of other error sources. Recent results from Greenland from 20 years of SEASAT/GEOSAT satellite radar altimetry data and 6 years of airborne laser altimetry data show a broad picture of a small thickening in the interior and a mixed pattern of a substantially larger thinning in the ablation area (Krabill et al., 2000; Thomas et al., 2001). ERS-1/ERS-2 satellite between 1992 and 1999 indicate that much of interior East Antarctica is close to balance, but with substantially more negative trends in West Antarctica, largely located in the Pine Island and Thwaites Glacier basins (Wingham et al., 1998; Shepherd et al., 2002)

Problems with current satellite data are missing data poleward of 72°N/S (SEASAT/ GEOSAT) or 82°N/S (ERS-1/ERS-2) as well as from the steeper parts at the margin, so that important areas with possibly large changes remain undetected. Another limitation is the short period over which satellite data are presently available. Altimetry records are at present too short to confidently distinguish between a short-term surface mass-balance variation and the longer-term ice-sheet dynamic imbalance.

Numerical modelling of ice sheets

Modelling of the past history of the ice sheets and their underlying beds over a glacial cycle is an independent way to obtain an estimate of the present ice evolution. Current large-scale, three-dimensional thermomechanic flow models simulate the flow and form of ice sheets on grids of 20-40 km horizontal spacing with 10-30 vertical layers. They include ice shelves, basal sliding and visco-elastic bedrock adjustment and need bedrock elevation and surface mass balance as main inputs. They calculate the three-dimensional velocity field, the distribution of ice thickness, the temperature distribution inside the ice, and the spatial extent of the ice. Glacial cycle simulations require time-dependent boundary conditions (surface mass balance, surface temperature, and sea level to model grounding-line changes) derived from sediment and ice core records. The results are constrained by geomorphological and glacial-geological data of past ice sheet stands. Recently, such ice sheet models are coupled to models of the other components of the climate system to investigate the interactions with oceans and atmospheres. 3-D ice-sheet models are presently applied to the Antarctic ice sheet (Figure 3.2.1), the Greenland ice sheet, and the Quaternary ice sheets of the northern hemisphere continents during the ice ages (Marshall et al., 2002; Charbit et al., 2002; Huybrechts, 2002).

Current ice-sheet simulations suggest, that the Greenland ice sheet is close to balance, while the Antarctic ice sheet is still losing mass, mainly due to incomplete grounding-line retreat of the West Antarctic ice sheet since the Last Glacial Maximum (LGM; Huybrechts and Le Meur, 1999). The long-term ice-dynamic response is estimated to be between –0.1 and 0.0 mm/year of sea-level equivalent from the Greenland ice sheet and between +0.1 and 0.5 mm/year from the Antarctic ice sheet. Model simulations forced by output from Atmosphere-Ocean General Circulation Model (AOGCM) simulations suggest that anthropogenic climate change could have produced an additional contribution of between –0.2 to 0.0 mm/year of sea-level from increased accumulation in Antarctica over the last 100 years, and between 0.0 and 0.1 mm/year from Greenland, from both increased accumulation and ablation.

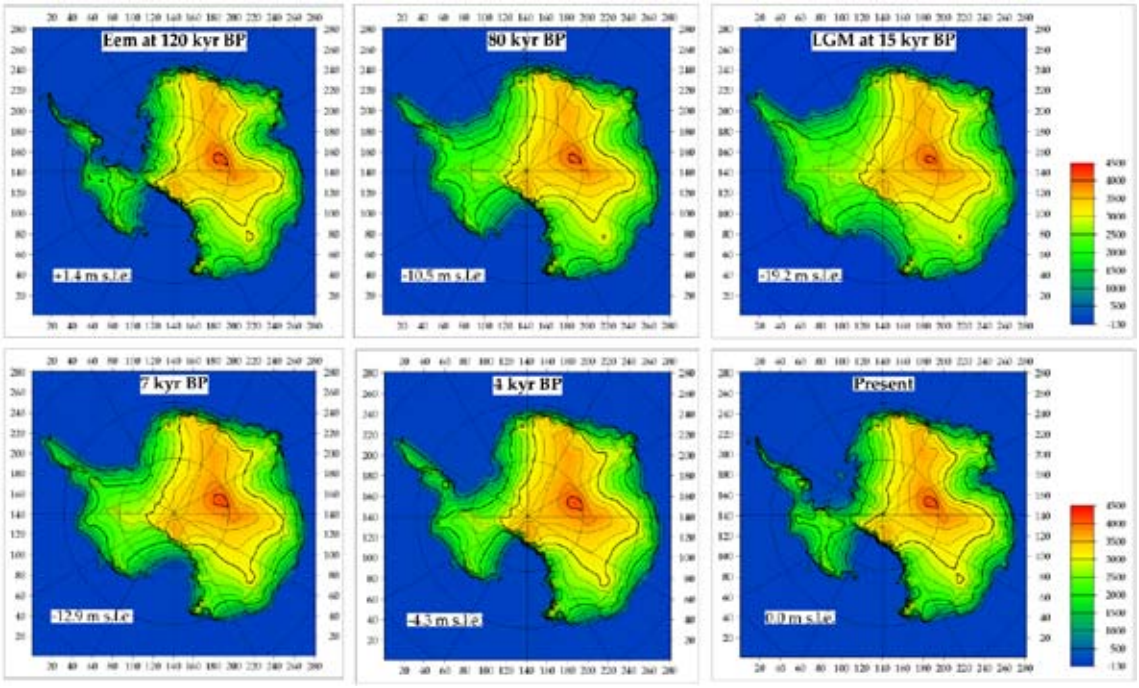

Figure 3.2.1: *Snapshots of Antarctica's ice-sheet evolution during the last glacial cycle obtained from a comprehensive 3-D ice-sheet model (s.l.e. = sea-level equivalent). The ice mass balance can be diagnosed from the ice-sheet response at the present time (Huybrechts, 2002).*

The quality of glacial cycle simulations depends on how good the past history of environmental conditions can be described and on how good the models deal with certain aspects of ice dynamics. Large uncertainties are associated with past patterns of climatic change beyond the information which can be derived from ice cores. Increased use of output from General Circulation Models is needed to improve the prescription of surface mass balance. A critical point in these models is the grounding line. At this transition zone, there is a fundamental change in the dynamic flow regime. This is of relevance for the Antarctic ice sheet and for parts of the Quaternary ice sheets bordering the Arctic Ocean. Another weakness is the incorporation of concentrated flow in outlet glaciers and ice streams, which are responsible for most of the discharge into the ocean. These features often have dimensions at the sub-grid scale and, therefore cannot be explicitly considered. Also, the approximations on which both grounded ice sheet and ice shelf models are based may break down in these areas because of the large stress gradients. One step ahead is to nest higher-order local models, which take into account the full stress balance equations, into large-scale ice sheet models, with the use of multi scale techniques.

Contribution from glaciers and ice caps

Because of their higher accumulation and ablation rates, glaciers and ice caps have shorter turnover times and are more sensitive to climate change than the polar ice sheets. To evaluate their contribution to global sea level change, we need to know the rate of change of total glacier mass. Unfortunately, sufficient measurements only exist for a small minority of the world's 100000 glaciers. Therefore global algorithms are developed (Gregory and Oerlemans, 1998), incorporating area-wise glacier distribution, mass-balance sensitivity, and dynamic response, but the database for such studies from glacier inventories is still incomplete in many of the main glaciated mountain areas (Alaska, Patagonia, Central Asia). There is consensus that the global glacier volume substantially decreased since the high stand of the middle 19th century. Current estimates place the average sea-level contribution from glaciers and ice caps during the 20th century to between 0.2 and 0.4 mm/year (Church et al., 2001).

Explaining mean sea level rise over the past century

The primary source of information on secular trends in global sea level during the past century are tide gauge observations. Tide gauges measure the level of the sea surface relative to that of the land, and therefore need to be corrected for vertical land displacements. The most important contributor to such changes is postglacial rebound, and its corrections are usually obtained from geophysical rebound modelling constrained by geological observations to estimate Earth response functions or ice-load parameters (Peltier and Jiang, 1997; Lambeck et al., 1998). Other corrections include the Earth's elastic and gravitational response to the changed water loading when mass is added into the oceans. This has the effect of reducing the observed rise at continental margin sites from ongoing mass contributions by as much as 30%. On the basis of the published literature, it can be concluded, that the average rate of sea-level rise during the 20th century was between 1.0 mm/year and 2.0 mm/year, with a central value of 1.5 mm/ year. Tide gauge data give no evidence for any acceleration of sea level rise during this period (Church et al., 2001).

In contrast to the sparse network of coastal and mid-ocean island tide gauges, measurements of sea level by satellite radar altimetry provides near global and homogenous coverage of the world's oceans, thereby allowing the determination of regional sea-level change (cf. Chapter 2). While the results must also be corrected for isostatic adjustment, satellite altimetry avoids other vertical land movements (tectonic motions, subsidence) that affect local determinations of sea-level trends measured by tide gauges. To date, the TOPEX/Poseidon satellite-altimeter mission, with its (near)

global coverage from 66°N to 66°S (almost all of the ice-free oceans) from late 1992 to the present, has proved to be of highest value for direct estimates of sea-level change.

The TOPEX/Poseidon data suggest a rate of sea-level rise during the 1990s greater than the mean rate of rise derived from the tide gauges. It is not yet clear whether this is the result of a recent acceleration, or of systematic differences between the two measurement techniques, or of the shortness of the record (6 years) (Cazenave et al., 1999).

In order to have confidence in our ability to predict future changes in sea level, we need to confirm that we are able to explain the current rate of change (Figure 3.2.2). According to the Third Assessment Report (TAR) of the Intergovernmental Panel on Climate Change (IPCC; Church et al., 2001), the contributions from all components of sea-level rise during the 20th century can be estimated to range from –0.8 mm/year to 2.2 mm/year, with a central value of 0.7 mm/year. The upper bound is close to the observational upper bound (2.0 mm/year), but the central value is less than the observational lower bound (1.0 mm/year), and the lower bound is negative i.e. the sum of components is biased low compared to the observational estimates. In this assessment, the largest uncertainty (by a factor of more than two) is in the terrestrial storage terms, especially from the effect of dam building. In contrast to earlier assessments, the contribution and range from continental ice masses is smaller, but still considerable (Figure 3.2.2).

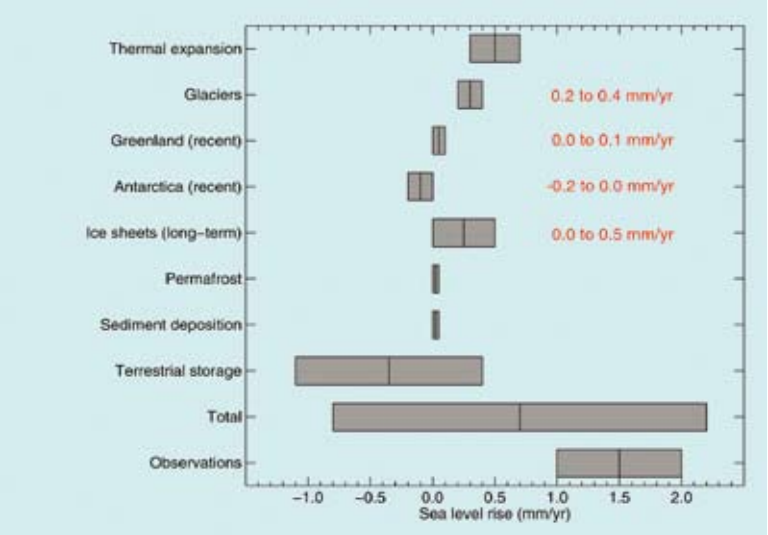

Figure 3.2.2: *Ranges of uncertainty for the average rate of sea level rise during the 20th century and the estimated contributions from different processes (Church et al., 2001) Total sea level rise is the sum of all contributions and uncertainties.*

Improving mass balance estimates with new spaceborne observations

The upcoming satellite missions are expected to greatly improve our knowledge of the state of the continental cryosphere. For the issue of ice mass balance and global sea level these improvements will primarily come from new gravimetry and altimetry data.

Structure of the polar gravity field and gravity field changes

The recent and upcoming gravity field missions CHAMP, GRACE, and GOCE provide global gravity field information with an extraordinary spatial resolution, down to half-wavelengths of about 70 km. For polar regions, the gravity field is an important source to improve the knowledge on both the solid Earth and the ice sheets. Furthermore, the recovery of gravity field changes as outlined in chapter 2.1 allows an independent monitoring of mass changes on spatial scales down to 500 km.

These mass changes are a combined effect of the ice sheets themselves and of the visco-elastic response of the solid Earth due to recent and historical ice load changes (Chapter 3.3). Model pre-

dictions confirm that the new satellite gravity data with their unprecedented accuracy (cf. Chapter 2) allow to validate and to improve the presently existing models (Figure 3.2.3). For example, with a combination of GRACE, ICESat/CryoSat and ground-based GPS measurements the competing effects of postglacial rebound, ice mass balance trends, and firn density changes can be separated (Wahr et al., 2000; Velicogna and Wahr, 2003).

At the same time, GRACE data are expected to greatly improve our knowledge on postglacial rebound elsewhere on the globe. This is important e.g. to correct records of the relative sea level at the coast

Ice surface elevations and elevation changes

The main product of the CryoSat and ICESat altimeter missions (cf. Chapter 2) will be time series of seasonal and interannual variations in surface elevation of inland ice and ice shelves. This will greatly improve existing elevation models and give unprecedented information of its variability. First ICESat data demonstrate already the big step forward in determining spatially highly resolved and accurate ice sheet topography (see Figures 2.19 and 2.20). High precision requires that the accuracy of the ice surface retrieval is known. Therefore the influence of the physical properties of the snow cover such as moisture content, density, crystal size, and roughness on the retrieved signal must be known. This requires the performance of in-situ or ground-truth measurements and elevation retrieval validation in the field.

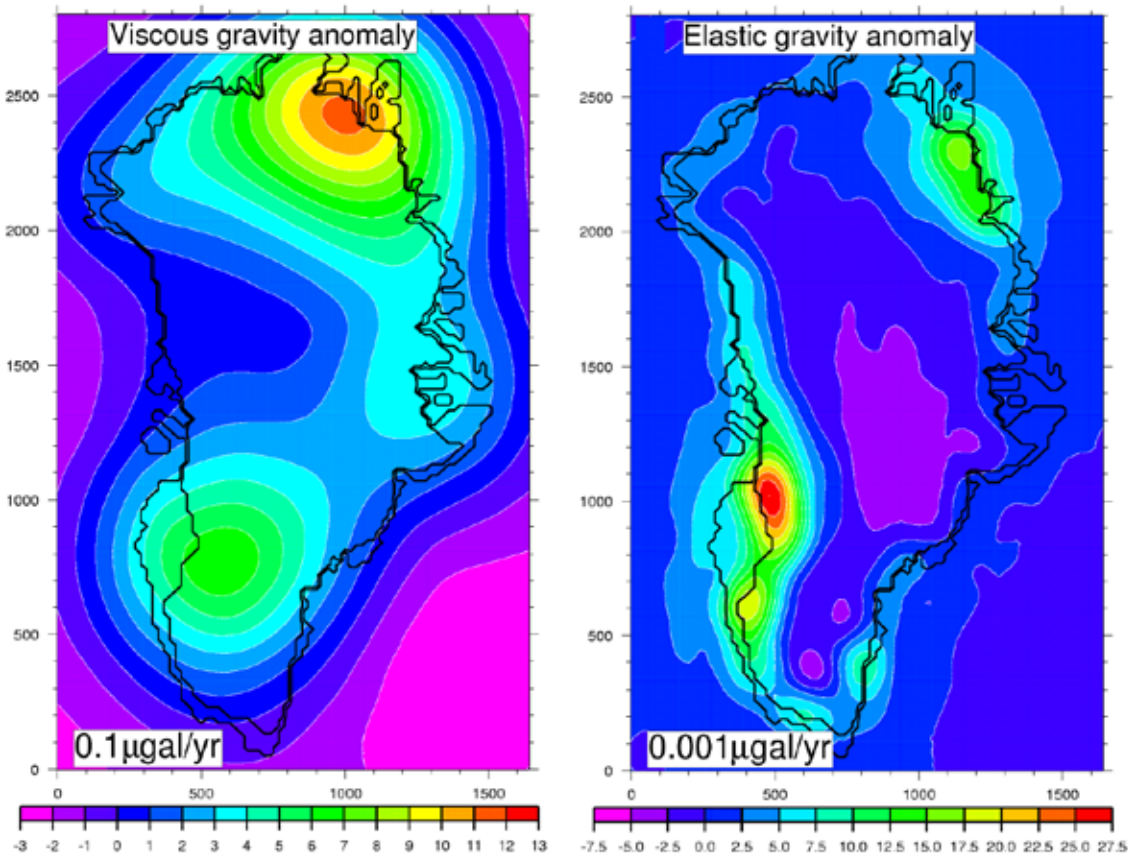

Figure 3.2.3: *Calculations with a coupled ice-sheet/ visco-elastic Greenland ice sheet model over the last glacial cycle indicate that the gravity anomaly trend is dominated by postglacial rebound (represented by the 'viscous effect'), which complicates efforts to extract the contribution from the current ice mass change (represented by the 'elastic effect' from the mean ice thickness background evolution over the last 200 years) from the total response (Le Meur and Huybrechts, 2001).*

However, the main obstacle to further geodetic constraint is the unknown snow accumulation fluctuation. Its spatial covariance is not well known, and this bears directly on the century-scale imbalance uncertainty (Wingham et al., 1998). It is important that recent statistics of accumulation fluctuation are obtained from extensive shallow coring of the ice sheets. In addition, the time series of variations in ice elevations themselves will provide unique data for validation of ice accumulation rates from atmospheric GCM model results. The longer the altimetry record, the clearer short-term variability in ice accumulation and surface melting can be separated from long-term trends in net balance.

Other problems involved to derive ice mass changes from altimetry records include the fact that the surface elevation change includes a signal from both isostatic rebound (Chapter 3.3) and from a variable rate of compaction of snow. Modelling efforts are required to separate these processes. As mentioned above, this can be achieved by a combination of spaceborne gravity, altimetry, and GPS measurements (Velicogna and Wahr, 2003).

Altimetry data are also urgently needed to determine surface elevation of glaciers. Together with aerial photography, high-resolution satellite visible and infrared imagery e.g. from ASTER and Landsat, this will supplement glacier inventory data to determine the distribution of crucial glacier parameters such as elevation, area, and area-altitude relations, so that mass balance, glacier dynamics and runoff/sea-level rise models can be more realistically framed.

Surface velocity field

The interferometric analysis of Synthetic Aperture Radar (InSAR) data provides a tool for mapping the ice surface velocity field from space (Figure 3.2.4). A comparison of these velocities with modelled *balance velocities* (Figure 3.2.5) gives valuable information about the present mass balance status of the ice sheets.

Furthermore, the grounding line as the boundary between the (grounded) ice sheet and the (floating) ice shelves can be mapped accurately using InSAR data and regarding the vertical tidal displacement of ice shelves. With the obtained velocities across the grounding line and additional ice thickness information the mass output of the ice sheet can be inferred. Any changes of the location of the grounding line indicate changes of ice thickness and sea level, respectively, which are key quantities in mass balance studies.

Airborne and surface observations for complementary datasets

Additional data are needed in order to make extensive use of the new satellite data for the improvement of our knowledge on sub-ice, solid-Earth mass anomalies and mass changes of polar ice sheets.

Radio echo sounding (RES) provides information on the sub-glacial bedrock topography, which forms an important boundary condition for ice sheet modelling.

Spatial and temporal features of the accumulation pattern can be obtained by RES (structures of internal layers) in combination with shallow ice coring. This is important for the estimation of the accumulation signal and its variance/covariance both for extracting this signal from different data (altimetry, gravimetry) and for modelling.

Repeated GPS observations at ice-free locations like nunataks (ice-free rock outcrops) allow the determination of glacio-isostatic crustal deformations. With this information possible gravity field changes can be separated into solid Earth and ice sheet contributions. Static and kinematic GPS

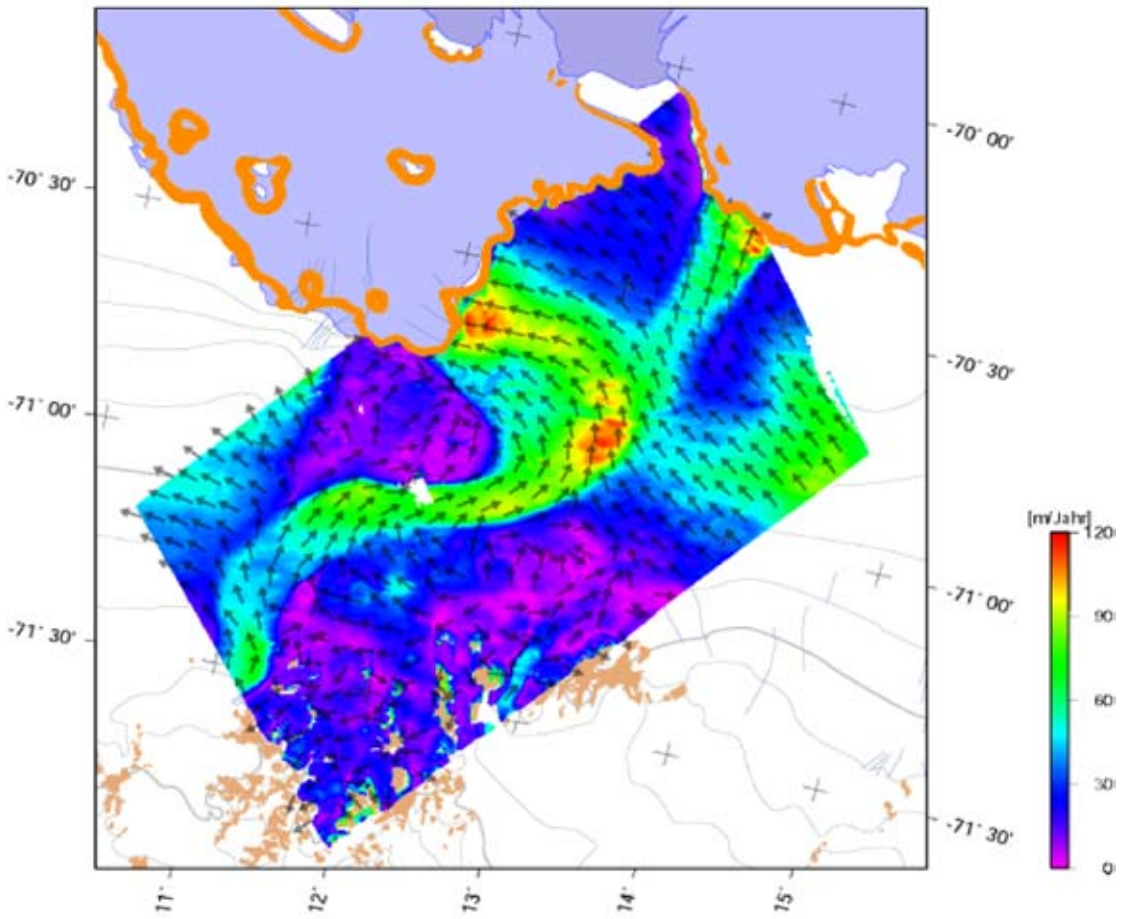

Figure 3.2.4: *Interferometric SAR analysis gives a detailed picture on horizontal ice velocities (region of Schirmacher Oasis, central Dronning Maud Land) (Bäßler and Dietrich, 2002)*

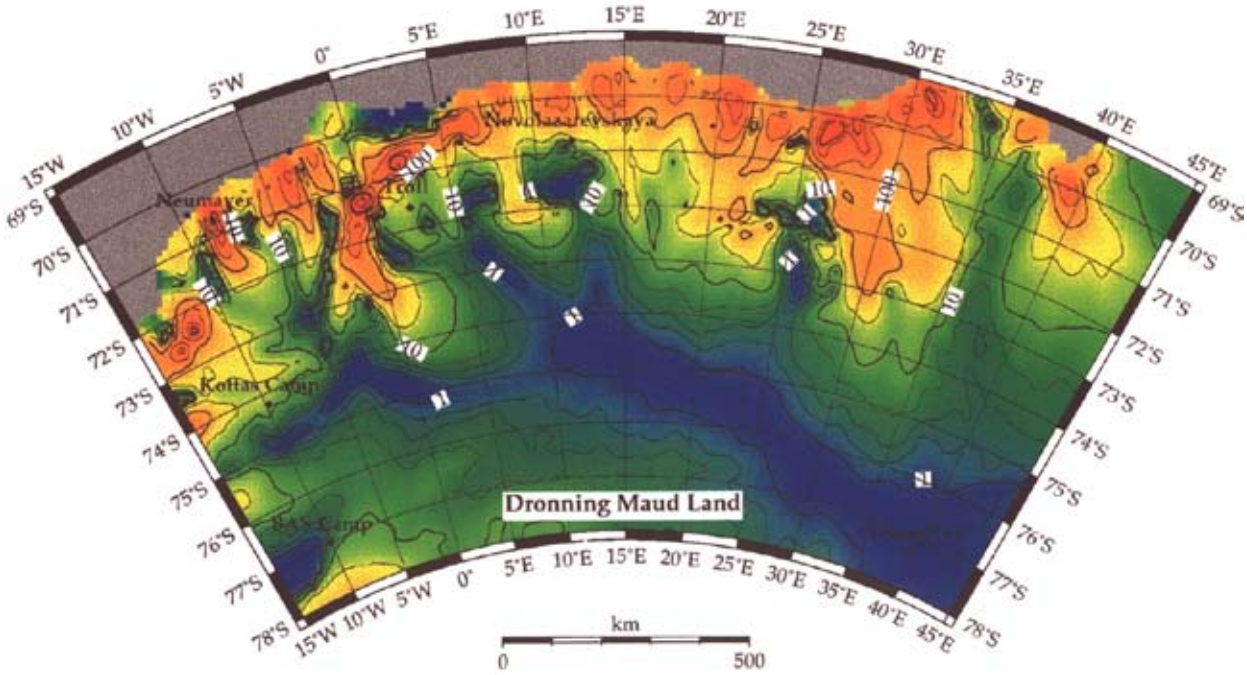

Figure 3.2.5: *Balance velocities in Dronning Maud Land / Antarctica (Huybrechts et al., 2000)*

observations at the ice surface provide valuable ground truth data for surface height, height changes and the velocity field (Figure 3.2.6).

Finally, airborne and surface gravimetry yields important datasets not only for validation, but also for increasing the spatial resolution of the satellite gravity information to improve the knowledge on the underlying Earth crust.

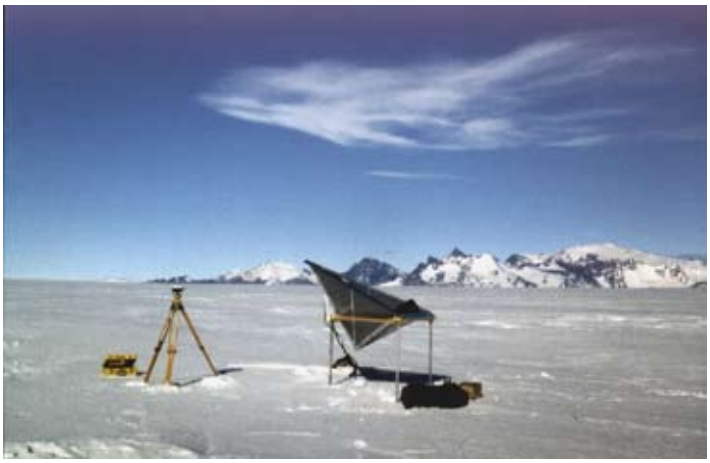

Figure 3.2.6: *Set-up of GPS and a corner reflector as a ground control for ERS-1/2 SAR interferometry (central Dronning Maud Land, Wohlthat Massif, photograph: J. Perlt)*

Role of ice-sheet modelling

A major benefit from the new satellite missions will be greatly improved data sets for ice-sheet model input and model validation. Surface elevation is an important boundary condition to derive the force balance and the distribution of stress and velocities with depth and is furthermore required to determine the bedrock elevation from measured ice thickness. Together with surface velocities and their directions derived from synthetic aperture radar interferometry (ERS1/2, RADARSAT, and ENVISAT), this constitutes a complete set of surface boundary conditions to study the dynamics of ice flow. At the same time, such data yield ice fluxes. Combined with accumulation and ablation observations, it allows to reduce uncertainties of estimates of the mass imbalance of individual drainage basins from todays about 10-15% to probably below 5%.

The role of large-scale numerical ice-sheet models to help with the interpretation of satellite observations is twofold. First, it provides an independent approach to determine the vertical component from isostatic rebound, which is required to transform surface elevation changes into ice thickness changes, and to transform relative sea-level changes from tide gauges into ocean level changes. Second, they provide a glaciologically sound loading history which in combination with visco-elastic Earth models can be used to simulate the gravitational effects of isostatic land movements to distinguish them from ice mass changes.

Improved modelling of the ice sheets during the glacial cycles, taking into account the improved boundary conditions, will also lead to improved simulations of the current evolution of ice sheets. But above all, models are necessary tools to investigate and separate the effects of various processes and are irreplaceable to make predictions into the future.

Global sea-level rise

Satellite altimetry over oceans can be used to generate improved time series of sea-level changes for different regions as well as for the global mean. Long-term tide gauge records may also be interpreted in terms of global sea-level change, provided they are corrected for vertical crustal uplift (which could be obtained by GPS). Altimetry and tide gauge measurements are to a great extent complementary: Tide gauges cover a long time period (in the order of 100 years), but are restricted to coastal areas. Altimetry data cover a shorter time period, but large parts of the world's ocean. Therefore, the combination of both datasets will significantly improve our knowledge on sea-level change and its temporal and spatial behaviour (cf. Chapter 3.1).

Integrated observations of mass balance, gravity, and sea level change

The subject of ice mass balance and sea level represents a complicated ice-ocean-solid Earth interaction within the Earth system. Therefore, it is closely related to other disciplines, in particular to oceanography, geophysics, and geodesy.

Ice melting and accumulation represent mass transfers between ocean and ice sheets (resp. glaciers). Due to the change of the gravity potential caused by these mass redistributions the resulting sea-level change is not globally uniform (see sea-level equation A 3.2 in Annex A3). In addition, the solid Earth response on changing loads (generated by both ice and ocean mass changes) results in vertical crustal deformations. Visco-elastic Earth models (cf. Chapter 3.3) and ice load history models – in combination with recent observations on gravity field changes and vertical crustal deformations – have to be merged together to improve our knowledge about both, mantle viscosity, and about ice load history (Figures 3.2.1 and 3.2.7).

These mass re-distributions within the system Earth introduce not only a time-dependency in the Earth's gravity field in general, but also – related to the harmonics of degree two – in the Earth's inertia tensor. Consequences of the latter are observed in the planet's rotation, both as an acceleration in its rotation rate and as a shift in the position of the rotation axis, which is recently observed by space geodetic methods (GPS, SLR, VLBI) with a high precision. The secular change of the degree two zonal term of the gravity field (the planet's dynamic flattening) is largely dominated by postglacial rebound. Mass shifts within and on the Earth depend on postglacial rebound from past ice sheet geometries, on the Earth's rheology, on ocean circulation, and on recent, past and present rates of melting of the residual ice sheets. Hence, unique estimates of recent mass shifts from ice sheets and glaciers cannot be inferred from such observations alone. However, constraints on the present rate of change of continental ice masses can be obtained through a combination of the rotational observations with geological and tide-gauge estimates of sea-level change. Therefore - also within this context - the polar ice sheets play a key role for the understanding and interpretation of Earth rotation, polar motion and secular gravity field changes.

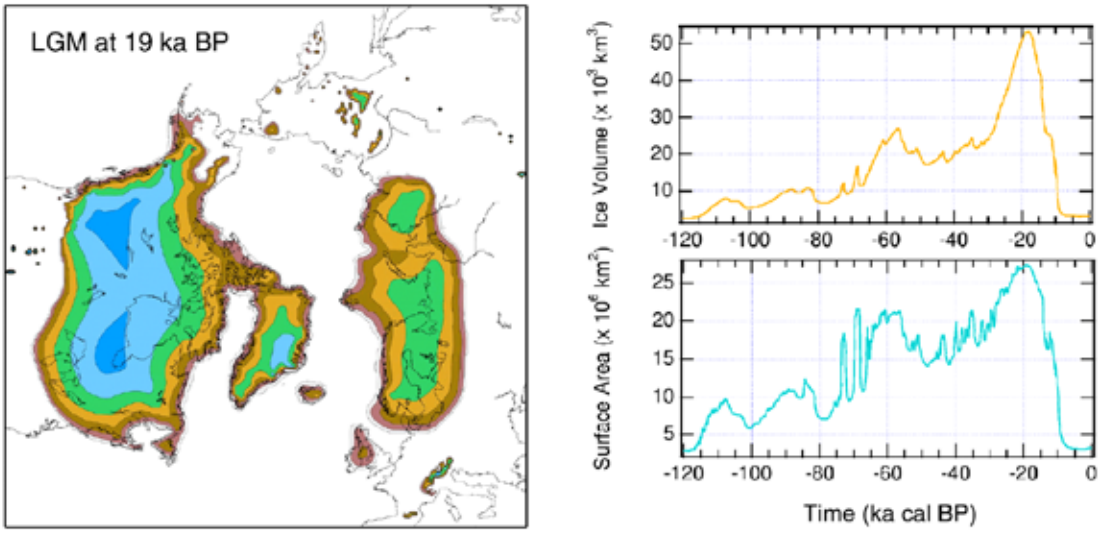

Figure 3.2.7: *Long-term tidal records need to be corrected for vertical land movement due to postglacial rebound. A history of ice loading and unloading to determine the crust's response can be provided by coupled ice-sheet/bedrock/climate modelling. This example shows ice sheet elevation at the Last Glacial Maximum from a time-dependent simulation over the last glacial cycle (Zweck and Huybrechts, 2003)*

Another link between ice-sheet reconstruction and global sea level change concerns the correction of long-term tide gauge records for vertical land movements. The land displacement may be of two types: that caused by active tectonics and that caused by postglacial rebound. On a global scale, the dominant process is the ongoing rebound following the retreat of the last Pleistocene ice sheets. This retarded adjustment of the Earth‘s surface to the unloading is controlled by both the viscosity distribution in the Earth‘s mantle and by the space-time distribution of the Pleistocene ice sheets. Whereas the extent of former ice sheets can often be inferred from geomorphological, stratigraphic, or biological indicators, the past ice thicknesses have only in a few instances been measured directly, and therefore, must be estimated by modelling. This can be done by trial-and-error techniques, in which a loading history is imposed that satisfies constraints on past relative sea level variations inferred from e.g. raised beaches. The resulting ice sheet profiles are however often not glaciologically consistent. Alternatively, the loading history can also be derived from forward modelling of the ice sheet evolution in coupled 3-D ice-sheet/lithosphere/climate models (Figure 3.2.7; cf. Section 3.3).

Improvements of current knowledge

The exploitation of future satellite results is expected to be an important step forward to answer the basic question of the mass balance of the ice sheets and their current contribution to global sea levels. Expected results for the coming 5 years include:

- A significantly improved gravity field for the polar regions, combined from satellite and airborne data, to study mass anomalies in these regions
- A greatly improved elevation model over all of Greenland and most of Antarctica
- An improved set of input and validation data for numerical modelling of ice flow
- Much stronger constraints on the current volume/mass change of the Antarctic and Greenland ice sheets, in particular by combining altimetry data with gravimetric data and the integrated use of numerical models
- Detailed knowledge on recent vertical crustal deformation due to the viscoelastic response of the Earth’s crust on historical and recent ice mass changes
- New insight into the global sea-level change, its spatial and temporal pattern, and signifycantly improved estimates for the contributing processes

It is however equally important that measurements be continued for at least 15 years to establish the climate sensitivities of the mass balance and decadal-scale trends. In view of the average lifetime of 3-5 years of forthcoming missions, this implies a follow-up beyond the current generation of planned missions.

References

Bäßler, M. and Dietrich, R (2002): Investigations of Ice Dynamics at the Grounding Zone of an Antarctic Ice Shelf Utilizing SAR Interferometry. Presentation at the Symposium “50 Years Geodetic Science at the Ohio State University”, Columbus/Ohio, 1-5 October 2002.

Cazenave, A., K. Dominh, L. Soudrarin, F. Ponchaut, and C. Le Provost (1999). Sea level changes from TOPEX-POSEIDON altimetry and tide gauges and vertical crust motions from DORIS. Geophysical Research Letters, 26, 2077-2080.

Charbit, S., Ritz, C., and Ramstein, G. (2002). Simulations of northern hemisphere ice-sheet retreat: sensitivity to physical mechanisms involved during the last deglaciation. Quaternary Science Reviews 21, 243-265.

Church, J.A., J.M. Gregory, Ph. Huybrechts, M. Kuhn, C. Lambeck, M.T.Nhuan, D. Qin, P.L. Woodworth (2001). Changes in sea level. in: J.T Houghton, Y. Ding, D.J. Griggs, M. Noguer, P.J. Van der Linden, X. Dai, K. Maskell, and C.A. Johnson (eds.): Climate Change 2001: The Scientific Basis: Contribution of Working Group I to the Third Assessment Report of the Intergovernmental Panel on Climate Change, Cambridge University Press (Cambridge, New York), 639-694.

Gregory, J. M., and Oerlemans, J. (1998). Simulated future sea-level rise due to glacier melt based on regionally and seasonally resolved temperature changes. Nature 391, 474-476.

Huybrechts, P., and Le Meur, E. (1999). Predicted present-day evolution patterns of ice thickness and bedrock elevation over Greenland and Antarctica. Polar Research 18, 299-308.

Huybrechts, Ph. (2002). Sea-level changes at the LGM from ice-dynamic reconstructions of the Greenland and Antarctic ice sheets during the glacial cycles. Quaternary Science Reviews, 21 (1-3), 203-231.

Huybrechts, Ph., D. Steinhage, F. Wilhelms, and J.L. Bamber (2000): Balance velocities and measured properties of the Antarctic ice sheet from a new compilation of gridded data for modelling. Annals of Glaciology 30, 52-60.

Krabill, W. B., Abdalati, W., Frederick, E., Manizade, S., Martin, C., Sonntag, J., Swift, R., Thomas, R. H., Wright, W., and Yungel, J. (2000). Greenland ice sheet: high-elevation balance and peripheral thinning. Science 289, 428-430.

Lambeck, K., Smither, C., and Johnston, P. J. (1998). Sea-level change, glacial rebound and mantle viscosity for northern Europe. Geophysical Journal International 134, 102-144.

Le Meur, E., and Ph. Huybrechts (2001). A model computation of the temporal changes of surface gravity and geoidal signal induced by the evolving Greenland ice sheet. Geophysical Journal International, 145, 835-849.

Marshall, S. J., James, T. S., and Clarke, G. K. C. (2002). North American ice sheet reconstructions at the Last Glacial Maximum. Quaternary Science Reviews 21, 175-192.

Peltier, W. R., and X., Jiang (1997). Mantle viscosity, glacial isostatic adjustment and the eustatic level of the sea. Surveys in Gephysics, 18, 239-277.

Shepherd, A., Wingham, D. J., and Mansley, J. A. D. (2002). Inland thinning of the Amundsen Sea sector, West Antarctica. Geophysical Research Letters 29, doi:10.1029/2001GL014183.

Thomas, R. H., Csatho, B. M., Davis, C. H., Kim, C., Krabill, W. B., Manizade, S., McConnell, J. R., and Sonntag, J. (2001). Mass balance of higher-elevation parts of the Greenland ice sheet. Journal of Geophysical Research 106 (D24), 33707-33716.

Velicogna, I., and J. Wahr (2003). A method for separating Antarctic postglacial rebound and ice mass balance using future ICESat Geoscience Laser Altimeter System, Gravity Recovery and Climate Experiment, and GPS satellite data. Journal of Geophysical Research 107 (B10),, 2263, doi: 10.1029/2001JB000708.

Wahr, J., Wingham, D. J., and Bentley, C. R. (2000). A method of combining ICESat and GRACE satellite data to constrain Antarctic mass balance. Journal of Geophysical Research 105 (B7), 16279-16294.

Wingham, D. J., Ridout, A. J., Scharroo, R., Arthern, R. J., and Shum, C. K. (1998). Antarctic elevation change from 1992 to 1996. Science 282, 456-458.

Zweck, C., and P. Huybrechts (2003): Modelling the marine extent of northern hemisphere ice sheets during the last glacial cycle, Annals of Glaciology 37, in press.

3.3 Dynamics, structure and isostatic adjustment of the crust and mantle

Mass anomalies at the Earth's surface, in the crust and in the mantle are both the cause and the result of various geodynamic processes such as glacial isostatic adjustment, plate tectonics or mantle convection. In combination with the new generation of seismic tomography and dynamic topography models high precision determinations of the instantaneous gravity field may be used to constrain large and small scale mantle convection models and the rheology of the Earth. The instantaneous gravity field will also be a valuable constraint on modelling crustal structure, particularly in remote areas where limited data exist and access is restricted or difficult (e.g. Antarctica). New available data of the time varying gravity field may provide new constraints on isostatic adjustment, ice models and mantle viscosity. Time dependent mantle convection or plate tectonic processes such as fast plumes, retreating subduction zones or detaching lithospheric roots might produce gravity signals coming close to or exceeding the resolution of the new GRACE data.

Static, instantaneous and temporally varying gravity field

The main parts of the Earth's mantle are assumed to behave as a highly viscous fluid on geological time scales, overlain by a set of elastic or viscoelastic, mobile lithospheric plates. Mass anomalies associated with thermal or compositional heterogeneities or with deflected boundaries between layers of different density produce flow structures and processes known as mantle convection (including plumes, subducting lithospheric slabs and sublithospheric convection), plate tectonics or isostatic ad-

Dynamics of the Earth's Crust and Mantle

Benefits

- The static and time variable gravity field models from CHAMP, GRACE and GOCE allow a much better and more detailed determination of the mantle viscosity, one of the key parameters of the Earth's interior.
- Crust and lithosphere modelling will benefit from the homogeneity of the new gravity field models, without gaps or offsets at coasts or national borders.

Challenges

- Mantle convection models have to be extended to shorter spatial scales.
- The identification of the small effects from mantle plumes and subducting slabs in the GRACE signal is very challenging.
- The combination with the existing terrestrial gravity data sets will be very informative, but laborious, too.

justment (Figure 3.3.1). The processes associated with such mass anomalies may be *static, steady* or time *dependent.*

Examples for essentially *steady* processes include thermally induced mass anomalies associated with thermal convection or cooling oceanic plates, long term temporal variations of such processes occur on time scales of 100 Ma or longer. Examples for *static* mass anomalies are compositional or structural density variations within the lithosphere, or deflected boundaries, such as the "isostatic topography" of the base of the crust (Moho) if kept in place by long-term lithospheric stresses. Strongly *time-dependent* processes may be associated with the transport or advection of compositional or thermal density anomalies, such as glacial isostatic adjustment, orogenic processes, or lithospheric subduction with retreating trenches or starting plumes. Whether density anomalies are in a static or time dependent mode strongly depends on the associated length scales (short wavelengths anomalies may be supported elastically) and the strength of the lithosphere. In any case, static structural density anomalies within the lithosphere or crust are the result of time-dependent geodynamic processes. Thus, explaining structural mass anomalies also requires knowledge of the underlying geodynamic processes.

All mass anomalies associated with static, steady state or time dependent processes produce *instantaneous* gravity and geoid signals on various wavelengths, which may also vary with time. A main objective in solid Earth geophysics is to decompose the composite gravity or geoid signal into its individual contributions and to assign specific geodynamic processes and density structures to them. While it is difficult or impossible to invert for the sources of the instantaneous geoid undulations without further constraints, a new and independent data set will be provided by the temporal variation of the geoid field. Figure 3.3.1 shows schematically that the geoid undulations and their temporal derivatives may be spatially in phase or out of phase. If these two geoid data

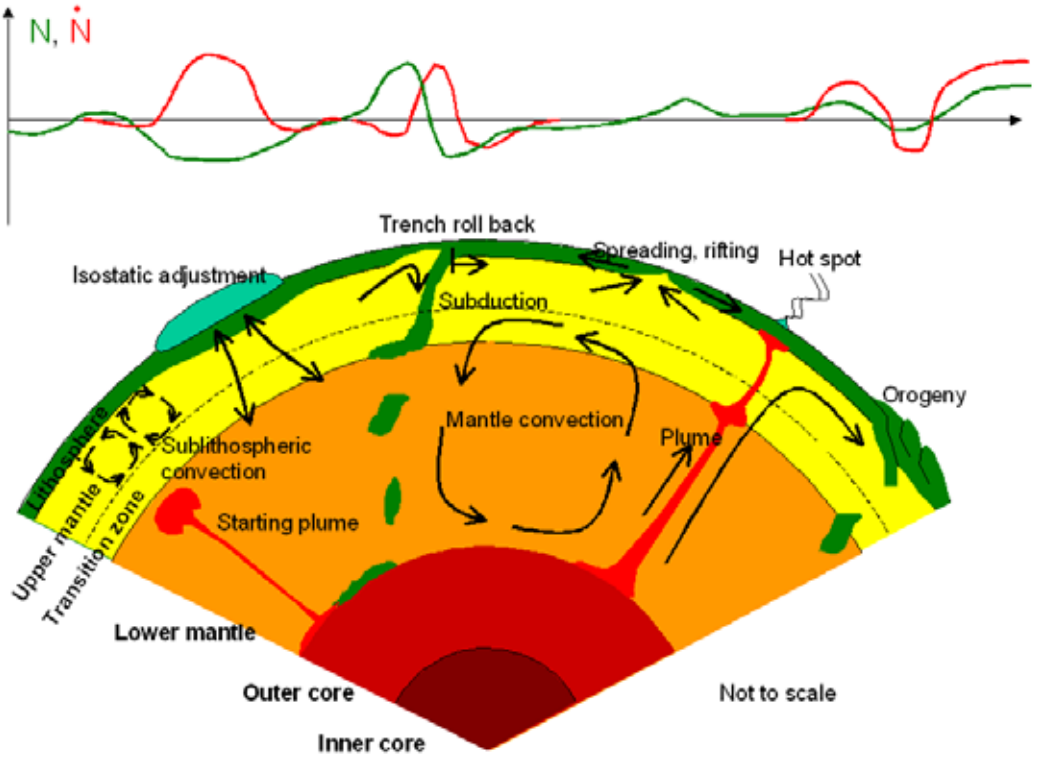

Figure 3.3.1: *Sketch of geodynamic processes associated with mass movements generating steady state (N) and time variable (Ṅ) geoid anomalies. Not to scale*

sets – the instantaneous geoid and its time variations – are complemented by further data sets, such as seismic tomography and topography, new constraints upon dynamic processes, lithospheric structures and rheology will be achieved.

The time-dependent geoid signal does not only contain the contributions of different geodynamic processes, but also of mass anomalies and their movements associated with hydrological, oceanographic and glacial processes. Only by a combined effort of analysing the time dependent and instantaneous gravity data in the spatial and spectral space complemented by additional observations and modelling efforts, a separation of the geoid signal into its various contributions may be possible and the solid Earth effects may be extracted. On the other hand, geodynamic models based on seismic tomography, plate tectonic observations or glacial isostatic models can be used to predict the instantaneous geoid or gravity and its temporal variations providing corrections for the other disciplines.

Solid Earth mass anomalies, transport and the instantaneous gravity potential

Global mantle flows

Mantle flows from seismic tomography

Mantle flows control the Earth's surface, plate tectonic movements, the gravity field and geoid as well as their time dependent variations. If we know the driving density anomalies within the Earth's interior and the gravity potential outside of the Earth, inferences about rheological properties can be made and mantle flows may be determined quantitatively. Whereas the gravity potential is a key parameter for the dynamics of the Earth's interior, the relation between the density distribution and the gravity field is not unique and additional information, such as the seismic velocity structure, is needed. Seismic tomography and the determination of the deflection of the internal boundaries provide supplementary information, which has improved drastically during the last years. The new generation of tomographic models, such as those of Ritsema and van Heijst (2000) or Montelli et al. (2003), has a global resolution of at least 1500 km (Figure 3.3.2a). Regional tomography models have been improved down to resolutions of 200 km or less and show detailed structures, such as slabs and plumes within the upper mantle or in the transition zone. This resolution is comparable to the high resolution to be obtained by the new satellite missions CHAMP, GRACE and GOCE, and new ways of interpretation must be found.

Density-velocity relation

A fundamental problem is the relation between the anomalous seismic velocity and the density or temperature. While a constant factor has often been used in the past, mineral physics provides improved depth dependent constraints (e.g. Karato, 1993) and refinements of density structures based on seismic tomography have become possible. Alternatively, the density-velocity relation may be inverted from gravity (e.g. Kaban and Schwintzer, 2001), but the uncertainties of such inversions are large. In principle, higher quality tomography and geoid data combined with constraints from mineral physics may be used to separate the thermal and compositional contributions of density anomalies in the mantle.

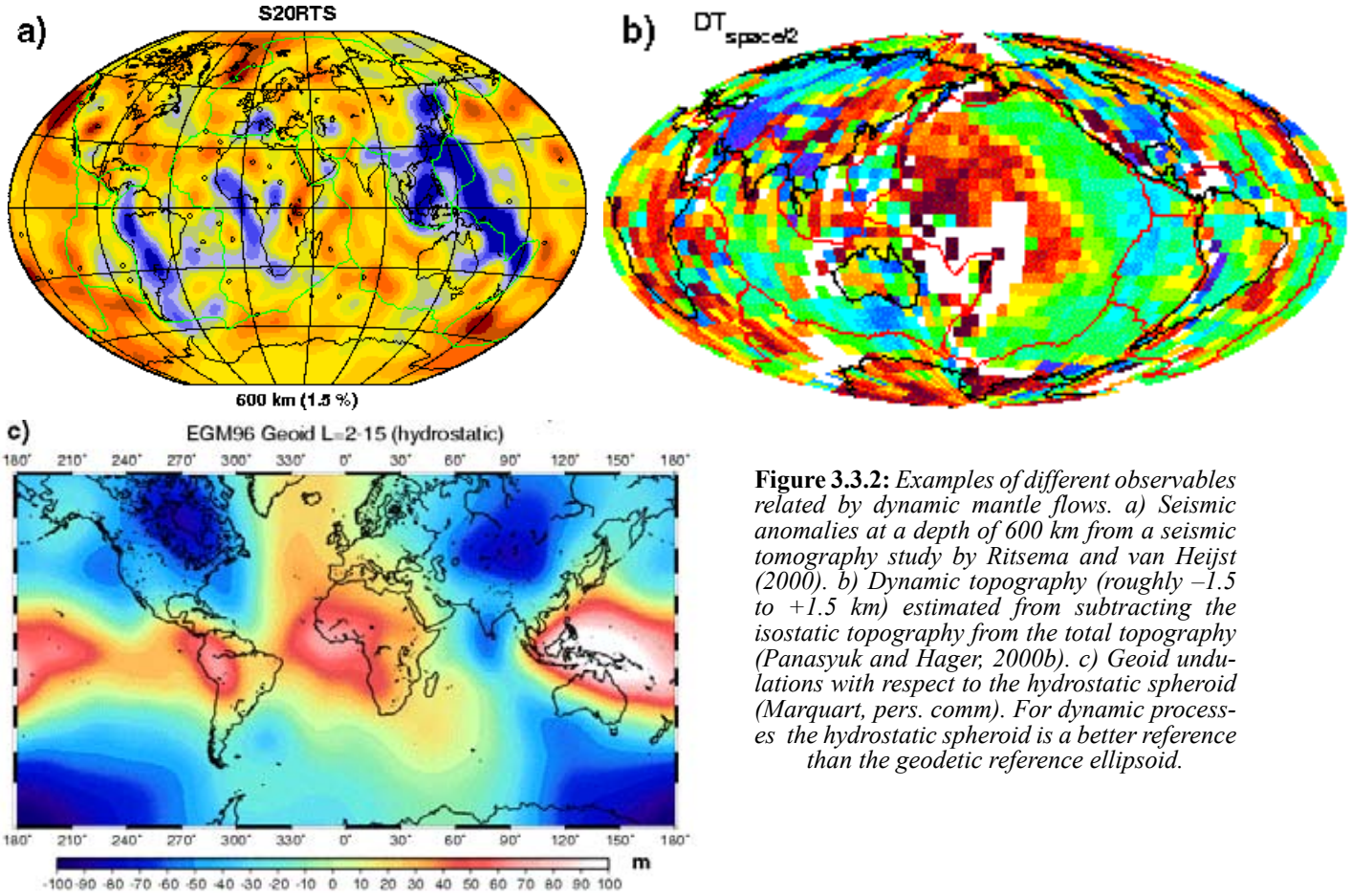

Figure 3.3.2: *Examples of different observables related by dynamic mantle flows. a) Seismic anomalies at a depth of 600 km from a seismic tomography study by Ritsema and van Heijst (2000). b) Dynamic topography (roughly –1.5 to +1.5 km) estimated from subtracting the isostatic topography from the total topography (Panasyuk and Hager, 2000b). c) Geoid undulations with respect to the hydrostatic spheroid (Marquart, pers. comm). For dynamic processes the hydrostatic spheroid is a better reference than the geodetic reference ellipsoid.*

Dynamic topography

Density anomalies produce spatial variations of buoyancy forces, which drive the flow in the Earth's mantle. These flows are associated with stresses, which produce deflections of internal or external boundaries, known as dynamic topography. In contrast, the isostatic topography is the result isostatically compensated density anomalies not associated with mantle flow. The total surface topography is the sum of both. Dynamic topography is difficult to determine, because detailed knowledge of the lithospheric structure (e.g. Mooney et al., 1998) is needed as it controls the "isostatic topography". Figure 3.3.2b shows an estimate of the global dynamic topography, but the uncertainties are large. Moreover, deflected boundaries also contribute to the geoid anomalies. Consequently, both the geoid undulation and the dynamic surface topography reflect the dynamic flow field and the flow properties, i.e. the viscosity of the mantle. In general, the relation between the geoid, dynamic topography and seismic anomalies is complicated, which is illustrated in Figure 3.3.2. While the subducted West Pacific slabs (blue region in the tomographic image) correlate with the geoid and dynamic topography highs, the relation between these quantities in other regions is probably superimposed by mantle dynamics and rheology. Thus, detailed dynamic modelling is required to interpret such signals.

Modelling

So far, long wavelength geoid anomalies (degree $l = 2 – 12$) have usually been explained by global dynamic flow models assuming radially dependent viscosity (see Appendix A4 for the mathematical formulation of this problem). Taking reasonable spatial distributions of subducted slabs or observed seismic tomography, relative viscosity profiles have been estimated (e.g. Panasyuk and Hager, 2000a). Absolute profiles have been determined when using plate velocities as addi-

tional constraint (e.g. Forte et al., 2002). The correlation coefficients between the modelled and observed geoid reach values above 0.8 for very long wavelengths, but the correlation drastically decreases for spherical harmonic degrees above 8. It is somewhat surprising that many successful geoid inversions predict dynamic topographies in disagreement with first estimates, such as the dynamic topography shown in Figure 3.3.2b. Thus, refinements of dynamic topography models and reliable viscosity flow models are needed.

So far, only two investigations (Zhang and Christensen, 1993, Cadek and Fleitout, 2003) have considered lateral viscosity variations with conflicting results. While Zhang and Christensen do not find a significant improvement of the geoid fit, Cadek and Fleitout obtain a considerably improved fit if lateral viscosity variations are allowed within the lithosphere-asthenosphere depth range. The technical problem of models with lateral viscosity variations is mode coupling between source and signal spectrum, which requires forward modelling.

Small-scale sublithospheric convection

The presence of small-scale sublithospheric convection was first postulated already in the 1970s, but direct observations are scarce. While under slowly moving or stagnant plates an irregular cellular pattern is expected, fast moving plates reorganize the flow into convective rolls aligned with the plate movements. Marquart et al. (1999) analysed growth rates and wavelengths of such convective instabilities and suggested that they are weakly visible in the gravity anomalies as linear anomalies crossing faults zones in the Pacific (Figure 3.3.3, e.g. between –15S,225E and –5S, 250E). The expected high-resolution data set of the GRACE and GOCE missions could open new possibilities of identifying sublithospheric convection structures also in other regions.

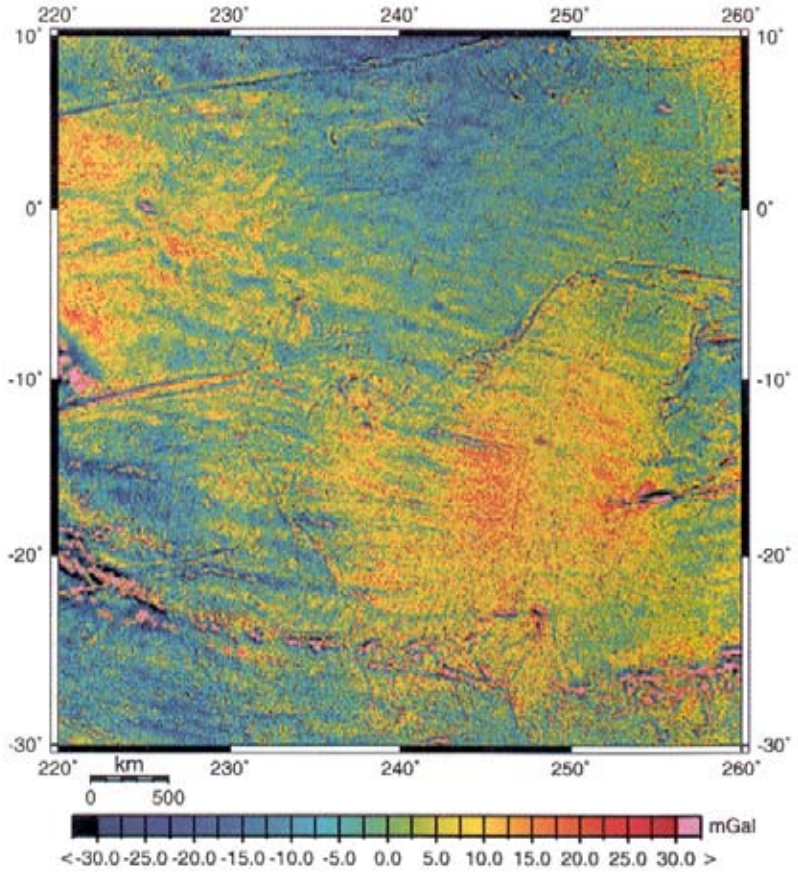

Figure 3.3.3: *Gravity anomalies in the Southeast Pacific derived from ERS-1 geodetic mission data (from Marquart et al., 1999)*

Active, convergent plate boundaries

Mass and energy transports at convergent continent-continent or continent-ocean plate boundaries are characterized by numerous strongly interacting processes, such as active deformation, uplift and erosion, magmatism and crustal accretion, seismic energy release (more than 90% of the global release) and the formation of mineral deposits. While the general plate tectonic concept of mountain building as a consequence of continent-continent or ocean-continent collision has been widely accepted, the underlying complex dynamical, rheological and thermal mechanisms are not well understood yet. Only a combined multidisciplinary effort of utilizing ground based geophysical and geological data combined with regional high-resolution gravity data from GRACE and GOCE as well as structural and dynamic modelling will give new insights into the complex interplay of the controlling mechanisms for the different types of mountain building. In this context, the Andean subduction orogeny constitutes an excellent case study in view of the efforts of several international geophysical and geodetic land- and sea-based programmes in the past years (CINCA, ANCORP and others, e.g. ANCORP Working Group, 2003).

To understand the dynamics of Andean type mountain building, the distribution and evolution of forces and mechanical stresses associated with subduction are of particular interest. Key parameters are the rheology and flexural rigidity of the down going plate and the rheological behaviour of the decoupling zone between the two plates. The effectiveness of the decoupling zone depends on the temperature and the depth of dehydration and subsequent fluid migration. First ideas about the fluid distribution within the decoupling zone are provided by correlating seismic reflectors, discontinuities from seismic receiver functions and zones of high seismicity within the Benioff zones. The three-dimensional and time-dependent nature of these processes results in asperities and strain segmentation along the subduction zones. Recently, GPS and INSAR measurements have provided the first kinematical view of the ongoing surface deformation.

Based on the structural information of the subducting and overriding lithospheres from geophysical studies, the new high resolution gravity data of the GOCE mission call for new dynamical models, which further constrain the rheological properties of the system and quantify the decoupling processes at subduction zones. Importantly, the GOCE data will provide the opportunity to extend interpretations to regions that currently lack data.

Asperities, areas of greater seismic slip and moment release with respect to surrounding regions, have been recognized for many subduction zones. The origin of these areas of high slip and their role in earthquake recurrence are much debated (e.g. Wells et al, 2003). Global bathymetric and gravity data show that asperities are commonly correlated with forearc basins and strong, rigid upper-plate blocks. Along the Nankai Trough of SW Japan, well constrained regions of maximum co-seismic slip correlate with the bathymetric and gravity lows of forearc basins. Off southern Chile, offshore basins are also marked by negative free-air gravity anomalies, but are also evident in seismic profiles. Slip maxima during the 1960 Valdivia earthquake, the largest earthquake ever recorded, coincide with the extent and distribution of the basin-centred forearc gravity lows. This correlation suggests a link between basin formation and the slip process whereby basins grow by interseismic subsidence driven by tectonic erosion at depth.

Song and Simons (2003) found that trench-parallel gravity anomalies and trench-parallel anomalies of topography are positively correlated in most areas. This correlation is expected because gravity anomalies are intrinsically tied to topographic variations by a given compensation mechanism. Results from viscous models, viscoelastic models and laboratory experiments suggest that spatial variations in the magnitude of shear traction on the plate interface can modulate surface topography and hence gravity in the fore-arc. In particular, these models indicate that increasing shear tractions on the plate interface induce a decrease in vertical compressive stress, thereby depressing forearc topography and gravity.

Identifying positive and negative gravity anomalies associated with the processes described above requires high precision gravity field measurements. The uniform nature of the GOCE gravity/gradient database will overcome the problems associated with combining sea- and land-based data across the ocean–continent transition and greatly aid the determination of asperity distribution at convergent margins.

This new database from GRACE and GOCE will also provide constraints for forward and inverse modelling of the geoid, the isostatic gravity anomaly and its gradient in various segments along active continental margins, but also for other regions of interest. New insights are expected for

1) the detailed structure of the lithospheric ocean-continent contact zone,
2) the flexural rigidity of the associated lithospheres and the viscosity distribution in the subduction zone,
3) the distribution of stresses and buoyancy forces at specific active continental margins based on 3D density models and dynamical modelling,
4) the state of isostasy and the flexural rigidity of the lithosphere in other active or passive regions, such as the Antarctic margin, Ural mountains, eastern Alps, northern German basin etc.

Temporal gravity field variations due to glacial isostatic and geodynamic processes

Ice mass balance and glacial isostatic adjustment

An important process in the solid earth is its glacial isostatic adjustment in response to past and present changes of the continental ice loads. This topic has been briefly addressed in Section 3.2, where it has been pointed out that ice load changes cause elastic or viscoelastic deformations of the earth. The calculation of the earth‘s elastic response to the present ice redistributions over Greenland and Antarctica is a standard problem. The result is that, for a given ice mass loss, the total mass deficit is reduced by about 10 per cent.

More difficult is the consideration of changes in the polar ice masses during the past hundreds to thousands of years. The reason for this is that the history of the Greenland and Antarctic ice sheets is recorded as an ongoing viscoelastic relaxation of the earth (e.g. Nakada et al., 2000, Tarasov and Peltier, 2002, see Appendix A5 for the mathematical formulation of this problem). In principle, the calculation of the associated vertical motion requires a detailed knowledge of both the viscosity stratification in the earth‘s mantle and the evolution of the ice sheets since the Pleistocene. But whereas the earth‘s viscosity profile has been determined within certain bounds from studies of the glacial isostatic adjustment following the melting of the major Pleistocene ice sheets on the northern hemisphere, much less is known about the history of the present day polar ice sheets. This situation applies in particular to Antarctica, where the development of the West Antarctic ice sheet has been controversially discussed for years (see Figure 3.2.1 for a 3-D numerical model). As a consequence, the uncertainties in calculating the bedrock responses for Greenland and Antarctica are significant and may be comparable with the signals directly associated with the present day ice mass fluctuations.

An alternative and possibly more promising method of allowing for the bedrock response is to determine it by terrestrial measurements. The most direct approach involves the installation of permanent GPS receivers on exposed bedrock along the margins of the Greenland and Antarctic ice sheets (e.g. Tregoning et al., 2000, Wahr et al., 2001). Experience gained from the BIFROST

GPS network installed in Fennoscandia has shown that, with vertical displacement rates of the order of several millimetres per year, reliable linear trends can be extracted from the GPS time series after a record length of about 5 to 8 years (Milne et al., 2001). Recently, absolute gravity measurements have been used as a control for the GPS vertical motion results. However, although the sensitivity of terrestrial gravity measurements to ice mass fluctuations is less pronounced than that of satellite gravity measurements, the influence of such variations on the absolute gravity measurements cannot be completely ignored. A different problem shared by GPS and absolute gravimetry is that the measurements are restricted to the peripheries of the ice sheets, where the pattern of vertical motion tends to be complicated. This is a result of the presence of a peripheral bulge at some distance from the ice margin at the last glacial maximum. After the ice sheet starts melting, the peripheral bulge gradually collapses and may also migrate laterally. The details of this behaviour strongly depend on the shallow viscous stratification. As a consequence, the vertical motion in the peripheral regions is usually not representative and also not easily extrapolated toward the centres of the ice sheets.

Apart from the gravity change associated with present day ice mass changes in Greenland and Antarctica, the secular gravity signal is influenced by the ongoing glacial isostatic adjustment following the retreat of the major Pleistocene ice sheets in Fennoscandia and Canada. The main surface features associated with this process are the residual depressions in the Hudson Bay and Gulf of Bothnia, both of which give rise to negative free air gravity anomalies. The benefit of these signatures is, however, imparted by their superposition with the gravity anomalies caused by mantle convection. So far, this has prevented their use as an additional constraint when inverting glacial isostatic adjustment data in terms of the viscosity distribution in the earth‘s mantle, although the new generation of seismic tomography inversions and associated mantle flow models might provide some useful constraints. The conventional procedure of modelling glacial isostatic adjust-

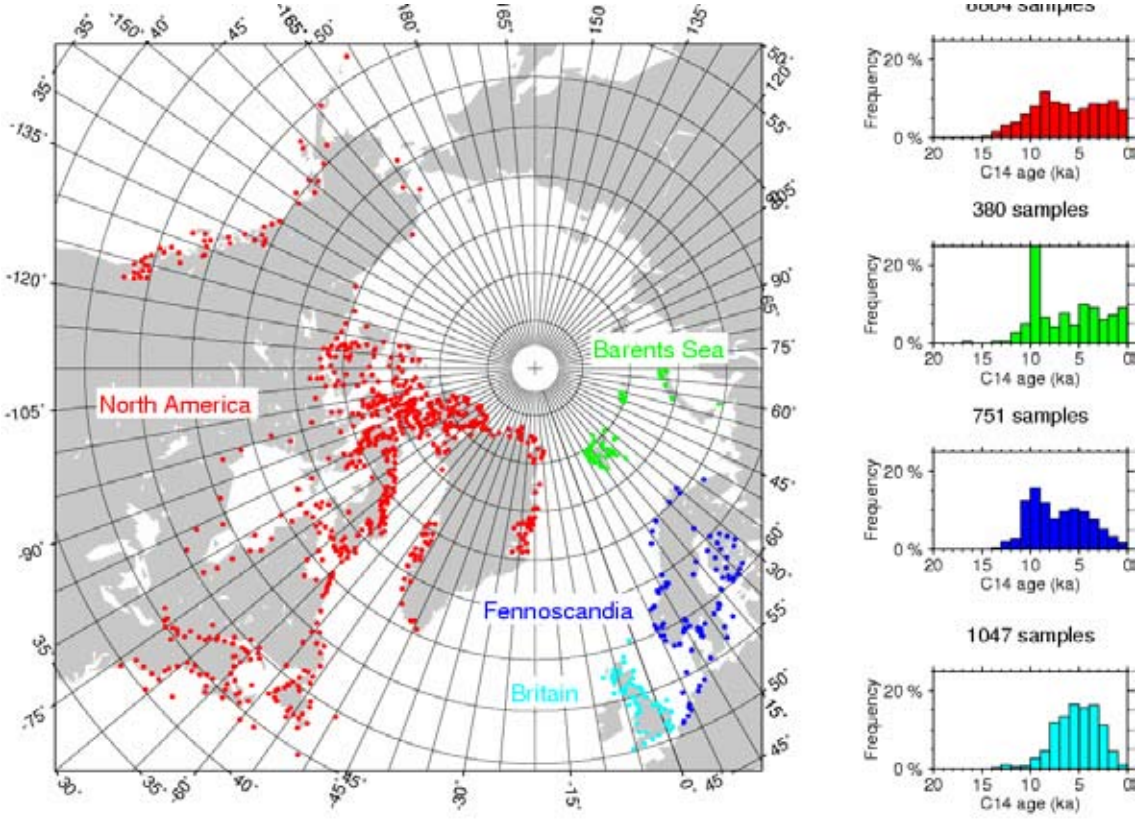

Figure 3.3.4: *Spatial (left) and age (right) distributions of radiocarbon-dated postglacial shorelines on the northern hemisphere.*

ment followed over the last three decades has been to invert raised postglacial shorelines in terms of the viscosity of the earth's mantle (e.g. Wu and Peltier, 1983, Lambeck et al., 1990, Kaufmann and Wolf, 1996, Martinec and Wolf, 1994). Figure 3.3.4 shows the spatial and age distributions of dated shorelines mapped on the northern hemisphere. The modelling of the postglacial uplift recorded by them is based on using viscoelastic earth models loaded by surface masses representing the Pleistocene ice cover. A principal problem of this procedure has been our uncertainty about the space-time distribution of the continental ice cover during the Pleistocene. This has resulted in the development of a series of global ice models, which, however, simulate the actual Pleistocene conditions only crudely. Widely used is still the global model ICE-3G (Tushingham and Peltier, 1991) shown in Figure 3.3.5.

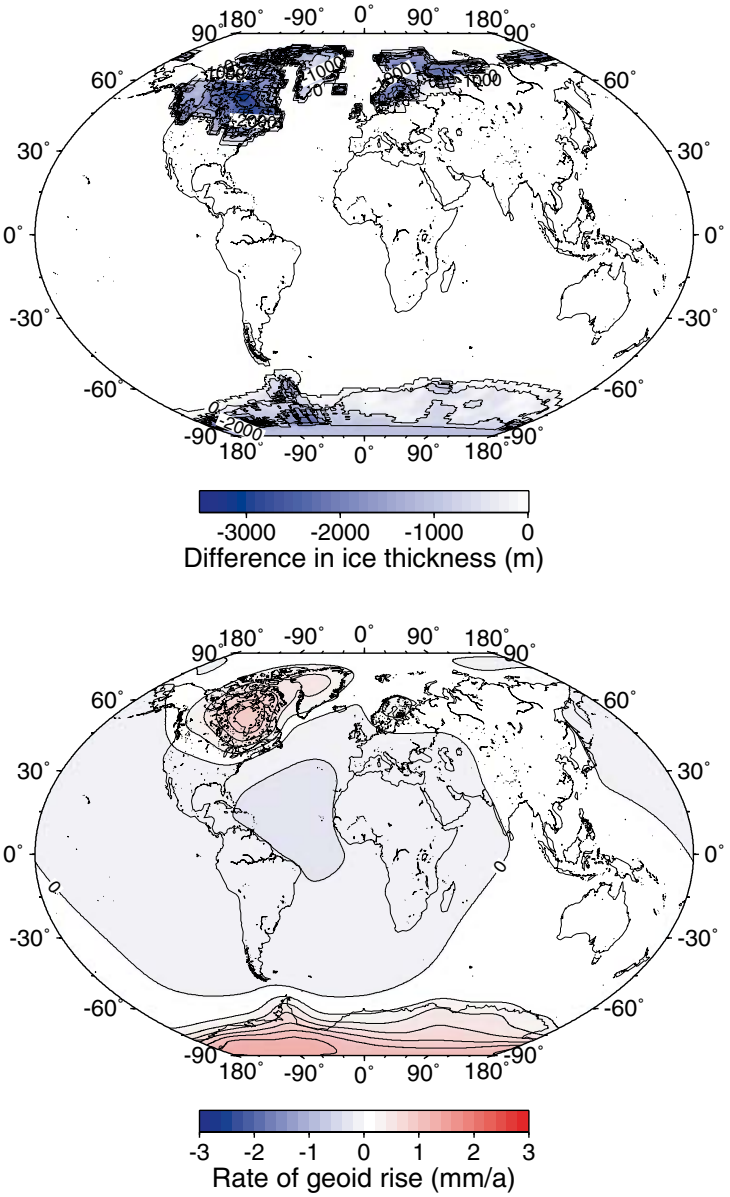

Figure 3.3.5: *Difference in ice thickness for ice model ICE-3G between 21 ka BP and today (top) and associated present day geoid rise (bottom).*

Recently, additional types of data have been used to impose tighter constraints on the earth's viscosity profile. Most important among them are tide gauge and GPS measurements. With time series sufficiently long, linear trends may be extracted and interpreted (e.g. Lambeck et al., 1998, Scherneck et al., 2002, Velicogna and Wahr, 2002a, Milne et al., 2004). An advantage of tide gauge and GPS measurements is that they refer to the present time. In contrast to postglacial shorelines reflecting the uplift history since the last deglaciation, they are thus less affected by our inadequate knowledge of the Pleistocene ice cover. So far, longer time series of GPS data have been obtained only at a small number of locations. The situation is more favourable for tide gauge stations, where time series extending over decades or even more than a century exist. However, tide gauge records monitor relative sea level change, i.e. a combination of land movement, geoid change and absolute sea level change, which complicates their use in studies of glacial isostasy.

A more promising constraint on the earth's viscosity profile is expected to result from the GRACE satellite mission. According to sensitivity studies, the mission is capable of resolving the temporal variations of gravity associated with the ongoing glacial isostatic recovery. This, in particular, applies to Canada, where the largest Pleistocene ice sheet was located and where reliable estimates of the current land uplift are still missing because of inadequate GPS coverage of the Hudson Bay region. The GRACE gravity data, therefore, provide a new and independent constraint on the mode of readjustment, which will allow us to impose tighter constraints on the viscosity distribution in the earth's mantle.

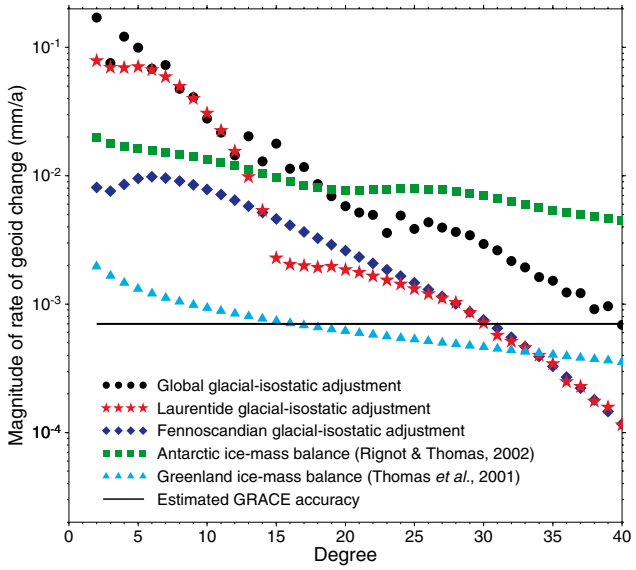

Figure 3.3.6: *Present day geoid change predicted for different glacial isostatic processes and ice mass balances.*

However, temporal variations of gravity are not restricted to the Pleistocene centres of glaciation in Fennoscandia and Canada, but encompass the whole earth. This is shown in Figure 3.3.5, where the present day geoid rise is predicted on the basis of combining ice model ICE-3G and viscosity model VM-2 (Peltier, 1998). The calculation also includes effects due to the redistribution of melt water in the oceans, which requires the solution of the sea level equation (e.g. Peltier et al., 1978, Wolf et al., 2002). As explained above, geoid variations also enter into relative sea level variations. Hence, their contribution must be taken into account when attempting to extract absolute sea level changes from the tide gauge record.

An important problem to be solved is the differentiation between the individual processes contributing to the linear trend in the GRACE gravity signal. Of some assistance is the fact that the GRACE satellite mission is sensitive to temporal gravity variations down to fairly short wavelengths. This is illustrated in Figure 3.3.6, where the signal components of the main processes responsible for secular gravity changes are seen to be above the GRACE error up to fairly high spherical harmonic degrees (see also Fleming et al., 2005). The benefit of this sensitivity to smaller scale features is that a rather detailed spatial distribution of gravity variability is expected to evolve from the analysis of the GRACE data. With this, it will become possible to associate particular patterns with the individual processes mentioned above and, therefore, to decouple them when interpreting the gravity variations.

Convecting mass anomalies in the mantle and other plate tectonic processes

So far, the temporal variations of the geoid due to mantle convection and plate tectonic processes have not attracted much attention. As mentioned above, many geodynamic processes are time-dependent and, consequently, produce a time-dependent geoid signal. Thus, Ricard et al. (1993) calculated temporal variations of long wavelength (degree $l = 2 – 12$) geoid anomalies due to mantle flow induced by sinking slabs and predicted variations up to 5×10^{-3} mm/a in the spatial domain. A similar model by Marquart et al. (2004) is shown in Figure 3.3.7. If decomposed into the spectral domain, the variations almost reach the same order of magnitude as the resolution limit of the

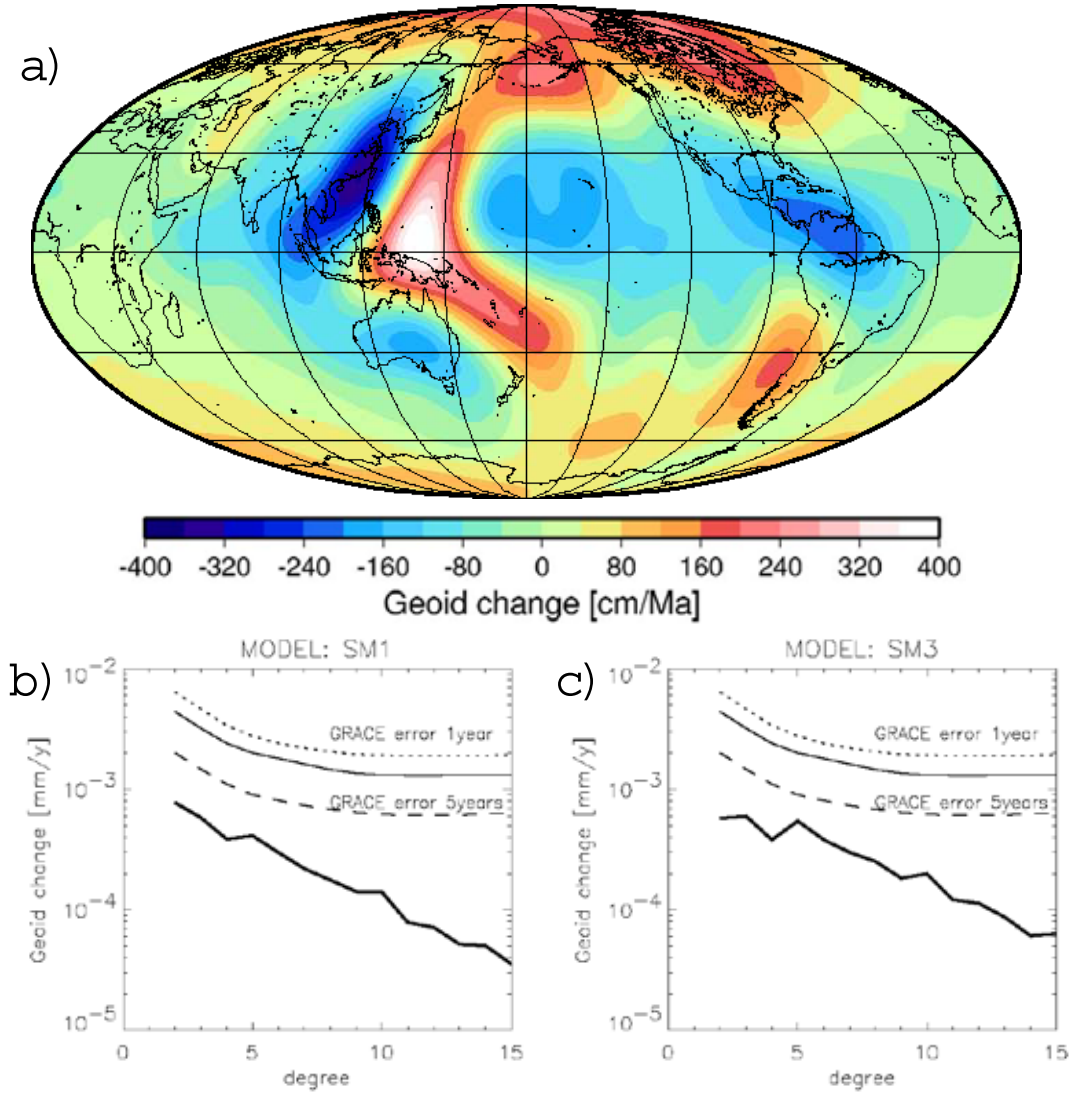

Figure 3.3.7: *Temporal variations of the geoid inferred from the slab sinking model. a) Variations in the spatial domain of a model with a reduced asthenosphere viscosity (400 cm/Ma = 4×10-3 mm/a). b) Rates of change in the spectral domain for a model without a low viscosity channel, c) as b) but with a low viscosity channel. Also shown is the degree resolution expected for a 1 and 5 year GRACE satellite mission duration following Kaufmann (2002) (thin solid and dashed line) and for 1 year flight duration accuracy according to Wahr et al. (1998) (dotted line).*

GRACE mission (5 years). Different radial viscosity distributions result in different spectra (c.f. Fig. 3.3.7 b and c), hence the question arises whether new tomography models, other viscosity distributions or rheological laws or other plate boundary conditions might lead to temporal geoid variations resolvable by GRACE.

Regionally, several geodynamic processes may be characterized by high velocities of the moving masses. For example, plate boundaries may migrate with velocities above 20 cm/a (e.g. the retreating Tonga subduction zone). Models of detaching lithospheric roots within collision zones or of rising plumes have shown that a non-linear viscous mantle rheology may result in vertical flow velocities between 10 cm/a and 1 m/a. Associated rates of change of the geoid resulting from such processes are estimated to range between 10^{-3} and 10^{-2} mm/a for degrees $l = 30 – 50$, which could possibly be identified in the GRACE signal.

Uplift and erosion rates in active orogenic areas may not always be in a steady state. Measurements of uplift rates are based on geodetic methods, while denudation rates are determined from estimates of sediment discharge and thermo-chronometry of minerals with low closing temperatures, which allow the reconstruction of recent unroofing histories during exhumation. Uplift and denudation estimates for active orogenic areas range between 0.2 and 10 mm/a. If these rates apply to steady state conditions, they must be equal and opposite, and no temporal gravity signal should be expected (e.g. the southern Alps in New Zealand). Any departure from steady state – both secular and seasonal – will produce a time-dependent gravity signal. Deviations from steady state are observed for several orogens. An example is the uplift rate of the Alps, which is about 5 times higher than the denudation rate. Non-steady state uplift-denudation rates of several mm/a are expected to produce gravity signals of several μGal/a. Measuring temporal variations of gravity by GRACE should provide an additional constraint on the unresolved question of steady state versus non-steady state uplift rates in orogens.

While the above-mentioned geodynamic and plate tectonic processes are associated with long-term velocities of the order of 1 mm/a to more than 10 cm/a, the short-term scale of these processes may be episodic. This is particularly the case along plate boundaries, where the relative movement of the plates is accomplished by Earthquakes. Continuous GPS measurements near plate boundaries, such as the San Andreas fault system or the rift system in Iceland, reveal that, within a band of several 100 km width, the plate tectonic concept of steady plate velocities is no longer applicable and episodic motions associated with seismic and post-seismic deformations or volcanic activity are dominating. Depending on the style of deformation, such "episodic plate tectonics" may show up in the gravity field, with temporal variations of several μGal/a. Monitoring the gravity field along plate boundaries using GRACE data may therefore provide additional constraints on the episodicity of plate tectonics along plate boundaries.

Combining and validating satellite gravity with complementary data

As a result of various geodynamic processes, such as continental collision or subduction, complex crustal or lithospheric structures have evolved during geological history and continue to evolve at present. Such structures produce gravity signals, which provide important constraints for any geological model. A major problem is, however, the fact that Earth based gravity measurements in different continental areas have different resolutions and non-compatible reference systems, sometimes resulting in discrepancies of up to 60 mGal. Changes of resolution and reference system often occur at political borders, which may coincide with tectonic boundaries. Thus, a better understanding of tectonic processes and resulting structures requires a gravity anomaly field with uniformly high resolution for wavelengths down to the order of 100 km.

To combine measurements from sea, land, air and satellites, a homogeneous set of gravity data for the Earth's surface and different altitudes is needed. This "test box" should be chosen for a region showing considerable gravity variations and high coverage of measurements, which allows its use for the validation and calibration of satellite missions. Because of the high density of terrestrial data, possible "test boxes" are the active or passive continental margins of South America and other appropriate regions. Complementary intraplate "test boxes" are also desirable. Of significance is the development of methods to combine, analyse and interpret the gravity measurements from the different platforms, with particular emphasis on horizontal and vertical gradients. These are also directly measured by the GOCE satellite mission. The new algorithms should then be tested and applied to the new satellite data.

The signals measured by GOCE correspond to the gradient components of the gravity acceleration, that is, the second derivatives of the gravitational potential. In the final product, the gradients will be transformed to give a global gravity field expressed by a set of spherical harmonic coefficients (see Appendix A). However, the six independent components of the Eötvös tensor can also be used for modelling lithospheric mass variations.

In contrast to gravity potential and the gravity field, the gravity gradients respond more sensitively to lateral density variations. Therefore, gravity gradients have frequently been used to detect and investigate fault systems and gravity lineaments. Previously, horizontal gradients have been quantified by calculating gravity differences between different gravity observation points. However, horizontal gradients and other derivatives of the gravity potential can be also determined using both older torsion balances (Eötvös, 1908) and modern gradiometers (Metzger and Jircitano, 1981; Bell et al., 1997; van Leeuwen, 2000; Tóth and Völgyesi, 2003).

It has recently been suggested that „old“ surface torsion balance measurements will be valuable for calibrating the GOCE gradient measurements. Because of the long tradition of torsion balance observations in Germany and Hungary, a large number of ground-based gradient and curvature measurements are available (Götze and Golz, in press). Therefore, Germany and Hungary provide ideal test-beds for calibration purposes. Collocation methods with adequate covariance functions can be used to calculate deflections of the vertical, geoidal undulations and gravity anomalies from the horizontal gradients and curvature obtained directly from the torsion balance observations. 3D forward modelling of independently measured Eötvös tensor components will complement gravity modelling and provide model constraints in a different part of the gravity spectrum. Furthermore, the torsion balance measurements can be transferred from the Earth‘s surface to satellite height (250 km) by analytical upward continuation. This will allow a direct comparison with gradients measured by the GOCE gradiometers.

Particular emphasis must be placed on the representation of the geoid or gravity field in geophysical interpretations. While, for long wavelengths, the spherical harmonic representation is most appropriate, global base functions may not be optimal for analyses of regional geologic structures or processes. Here, a wavelet analysis may provide improvements, as target regions may be analysed in the spectral domain without loosing the spatial information (e.g. Freeden et al., 1999). Geologic features, such as ancient suture zones (zones where an ocean has been closed), may be resolved in this way, which can be detected in the spatial domain only with very high-resolution gravity data (Vecsey et al., 2002).

Essential complementary data sets for interpretations of geoid or gravity data include seismic and topographic data (dynamic and isostatic). As mentioned above, a distinction between the dynamic and isostatic topography requires global crustal models (e.g. Mooney et al., 1998), whose resolution is still insufficient. For example, in some regions the errors of the dynamic topography are of the order of the signal itself. Here, an improvement is expected from a new global crustal model based on a better coverage by seismic stations combined with the use of receiver functions and reflected seismic phases. Such seismological data may also be used to constrain the thickness of the transition zone and the deflections of the phase boundaries at 410 and 660 km depth. In addition to tomography models, these data are also important constraints or even input for dynamic geoid models. On the other hand, the new gravity data from GRACE and GOCE must also be used to refine the global crustal model in regions where seismic information is missing.

Separation of the solid Earth gravity signal from other signals

As all mass anomalies and movements within the system Earth produce gravity signals that add up to the total gravity or geoid signal, the different disciplines have a natural connection. However, analysing the data in different spatial, spectral and temporal domains, the decomposition of the total signal into its individual contributions should be possible to some extent.

One objective is the analysis of temporal gravity potential variations caused by long-term geodynamic processes and episodic plate tectonic events. While the glacial isostatic adjustment signals are well above the resolution of GRACE, the other solid Earth processes produce rates near or only slightly above it. Ideally, it would be desirable that oceanography, hydrology, meteorology and glaciology provide corrections to be used to isolate solid Earth generated temporal gravity signals. Both global and regional predictions are required, depending on the geophysical target region or process. For example, separation of the temporal geoid signal of a retreating subduction zone, such as the Tonga trench, may only be extracted from the observational data if gravity changes due to sea level changes and ocean currents in that region are removed from the GRACE signals.

On the other hand, forward models of time-dependent geodynamic processes have the potential to predict longer wavelength gravity or geoid variations. Although these are expected to be close to the resolution limit of GRACE, they may still be useful as corrections for other disciplines using secular geoid variations, such as oceanography, hydrology or glaciology. Regional dynamic or structural models of active or passive continental margins allow us to predict the tectonic contribution to the gravity potential signal and its gradients. As these signals cover also ocean areas, they may also be used as corrections for oceanographic purposes.

Episodic variations of the gravity potential along active plate boundaries will be monitored. If they can be associated with tectonic, seismic or erosional effects, these contributions to the total signal will serve as an important correction for hydrological, oceanographic and glacial processes.

As an important by-product of large-scale geodynamic models, temporal variations of the global or regional dynamic topography will be predicted. In the spatial domain, such variations are of the order of 0.1 to 1 mm/a globally or 1 to 10 mm/a regionally, which is important for the determination of secular sea level variations.

Separation of the gravity signal into different components is also important in geological and tectonic applications. For example, crustal studies require only the shortest-wavelength parts of the gravity field. In surface-measured datasets, these short-wavelength components are masked by longer-wavelength anomalies associated with density anomalies at mantle depth and deeper. These regional and local effects can be isolated using “regional–residual separation”. The residual field reflecting smaller-scale features within the crust is typically determined by subtracting from the surface measurements a regional field defined by upward continuation or an isostatic model, or by high-pass filtering the surface data. However, the ambiguties inherent in these techniques can potentially be avoided by using a longwavelength (regional) field defined by GRACE or GOCE gravity models. The resulting residual anomalies probably better reflect crustal structure (see Figure 3.3.8).

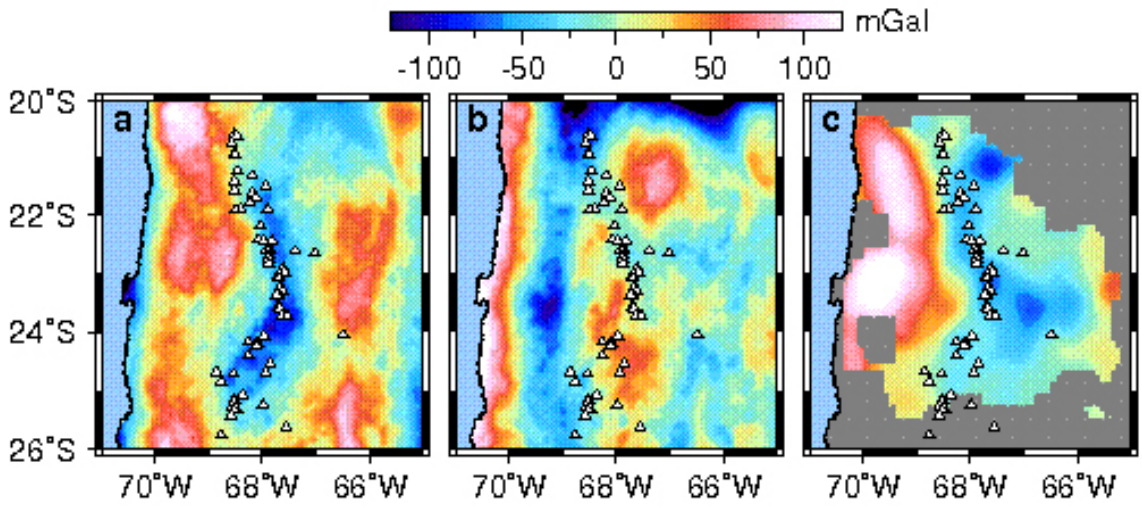

Figure 3.3.8: *(a) residual gravity field in the central Andes derived by subtracting the EIGENGRACE01S gravity model (to degree and order 120, minimum wavelength ~300 km) from surface data, (b) residual field for the same area derived by high-pass filtering of surface gravity data (cut-off wavelength 300 km), and (c) crustal gravity effect predicted from a seismic tomography model (Ivan Koulakov, pers. comm., 2004). The filtered data do not correlate well with the field predicted from the tomography model. This suggests that the residual computed by subtracting a satellite-derived regional gravity field is more realistic. Triangles mark active volcanoes of the Andean volcanic arc.*

Impact of the new satellite missions on solid Earth mass anomalies and movements

Instantaneous global and regional gravity potential field

The instantaneous global gravity potential field may be used in combination with seismological and mineral physics data to refine global flow models with laterally varying viscosity. Such refinements include deflections of internal boundaries, such as the 410 km and 660 km discontinuity.

New structures in the wavelength range of 50 to 500 km are expected to show up in the high-resolution gravity potential field of GOCE and its gradient. These structures include active and passive continental margins, ancient suture zones, buried continental faults, asperities at subduction zones, sublithospheric convection cells beneath oceanic and continental plates and other features.

With complementary terrestrial data, e.g. from seismology, the new GOCE data may be used to improve the global crustal model in areas with sparse terrestrial observations.

Temporal changes of the gravity field

The combined data sets of geoid and geoid variation may be used to infer not only relative, but also absolute viscosity distributions within the Earth. In combination with improved seismological data (seismic tomography and deflected internal boundaries) and dynamic topography data (from improved crustal models), such data sets may allow us to infer also lateral variations of the viscosity within the asthenosphere. In addition, the spectral modes of the geoid variation seem to be more sensitive to a low viscosity zone beneath the lithosphere than the instantaneous geoid itself. Thus, for the first time, temporal geoid variations may provide a data set that further constrains mantle rheology and mantle flows. While viscosity estimates from glacial isostatic ad-

justment are expected to be biased by continental influences, the GRACE data provide an evenly distributed coverage.

The measured temporal gravity variations can be analysed in the spatial and spectral domains and separated into drifting and non-drifting contributions. Correlations with drifting lithospheric plates should provide some interesting clues.

Another interesting question is the possible correlation between the instantaneous gravity field and its rate of change. Such correlations potentially contain additional information about the geodynamic processes involved. For example, the correlation between geoid and geoid rate is expected to be different for retreating subduction zones, detaching slabs and developing plumes.

An important new field will also be the monitoring of episodic and steady mass movement processes along active plate boundaries or in orogens.

Forward modelling

Future forward modelling of the new satellite based gravity data should focus on the following:
Global:

- Global models will include laterally variable or stress- and temperature-dependent viscosity
- Improvements of the seismological models and mineral physics relations may push geoid modelling towards higher degrees ($l = 20 – 40$ rather than $10 – 20$)
- Non-linear relations between the density distribution in the mantle and the resulting satellite gravity signals based on tomography or deflection of internal boundaries from seismology may be detected
- Modelling of temporal geoid variations may become important in the light of the high resolution GRACE data
- The new GOCE gravity field and gradients can be used for 3D whole-Earth forward modelling. In this way, the gravity effect of global Earth models derived from seismol-ogical databases and gross petrological models (e.g. Dziewonski and Anderson, 1981; Kennett et al., 1995) can be compared to “normal gravity”, the gravity field of the refer-ence ellipsoid used in gravity field research (currently GRS80: see Moritz, 1980).

Regional:

- Subduction zones are characterized by high seismicity and, as a consequence, high tomographic resolution. Detailed structural and dynamic models (steady state or time-dependent) may predict the seismic signal to be correlated with the satellite gravity signal
- What is the effect of slabs lying flat at the 660 km discontinuity (Figure 3.3.1) on gravity?
- What is the effect of plumes interacting with the lithosphere, do they show up in the gravity data?
- What are the fine features of the gravity signal of continent-ocean transitions?
- How do temporal gravity fields of developing plumes, detaching slabs, collision zones and subduction zones look like, and do they show up in the GRACE data?

Inversions

In selected regions with good seismic coverage, joint inversions of seismic and satellite gravity data may result in improved models of lithospheric (Moho depth) or upper mantle structures

References

ANCORP Working Group, 2003. Seismic imaging of a convergent continental margin and plateau in the central Andes (Andean Continental Research Project 1996 (ANCORP´96)). J. Geophys. Res., 108:B7, ESE 3–1 to ESE 3–25, pp. 25.

Bell, R. E., Anderson, R. and Pratson, L., 1997. Gravity gradiometry resurfaces. The Leading Edge, 16:55–59.

Cadek, O. and L. Fleitout, 2003. Effect of lateral viscosity variations in the top 300 km on the geoid and dynamic topography. Geophys. J. Int., 152:566–580.

Dziewonski, A. M. and Anderson, D. L. 1981). Preliminary reference Earth model. Phys. Earth Planet. Int., 25:297–356.

Eötvös, R., 1908. Bestimmung der Gradienten der Schwerkraft und ihrer Niveauflächen mit Hilfe der Drehwaage. in: H. G. van de Sande Bakhuyzen (Ed.), Verhandlungen der fünfzehnten allgemeinen Konferenz der Allgemeinen Erdmessung. September 20-28, 1906, Budapest, Verlag von Georg Reimer, Berlin.

Fleming, K., Z. Martinec, J. Hagedoorn and D. Wolf. 2005. Contemporary changes in the geoid about Greenland: predictions relevant to gravity space missions. In: Reigber, C., H. Lühr, P. Schwintzer and J. Wickert (eds): Earth Observations with CHAMP: Results from Three Years in Orbit, Springer, Berlin, 217-222.

Freeden, W., O. Glockner and M. Thalhammer, 1999. Multiscale field recovery from GPS-Satellite-to-Satellite Tracking. Stud. Geophys. Geod., 43:229–264.

Forte, A.M., J.X. Mitrovica and A. Espesset, 2002. Geodynamic and seismic constraints on the thermochemical structure and dynamics of convection in the deep mantle. Phil. Trans. R. Soc. Lond. A, 360:2521–2543.

Götze, H.-J. and Golz, G., in press. Old torsion balance measurements: too old for modern exploration? in: Talwani, M. and Biegert, E., Gravity Gradiometry – Instrumentation, Processing, and Case Studies, SEG Geophysical Developments Series.

Kaban, M.K. and P. Schwintzer, 2001. Oceanic upper mantle structure from experimental scaling of Vs and density at different depths. Geophys. J. Int., 147:199–214.

Karato, S.-I., 1993. The importance of anelasticity in the interpretation of seismic tomography. Geophys. Res. Lett., 20:1623–1626.

Kaufmann, G. and D.Wolf, 1996. Deglacial land emergence and lateral upper-mantle heterogeneity in the Svalbard Archipelago-II. Extended results for high-resolution load models. Geophys. J. Int., 127:125–140.

Kennett, B. L. N., Engdahl, E. R. and Buland, R., 1995. Constraints on seismic velocities in the Earth from travel times. Geophys. J. Int., 122:108–124.

Lambeck, K., P. Johnston and M. Nakada, 1990. Holocene glacial rebound and sea-level change in NW Europe. Geophys. J. Int., 103:451–468.

Lambeck, K., C. Smither and M. Ekman, 1998. Tests of glacial rebound models for Fennoscandinavia based on instrumental sea- and lake-level records. Geophys. J. Int., 135:375–387.

Marquart, G., H. Schmeling and A. Braun, 1999. Small Scale Instabilities below the cooling oceanic lithosphere. Geophys. J. Int., 138:655–666.

Marquart, G., B. Steinberger, and K. Niehuus, 2004: On the Effect of a Low Viscosity Asthenosphere on the Temporal Change of the Geoid - A Challenge for Future Gravity Missions, submitted to J. Geodynamics

Martinec, Z. and D. Wolf, 2004. Inverting the Fennoscandian relaxation-time spectrum in terms of an axisymmetric viscosity distribution with a lithospheric root. J. Geodyn., in press.1.1.5 Dynamics of crust and mantle

Metzger, E.H. and Jircitano, A., 1981. Application of Bell rotating accelerometer gravity gradiometers and gravity meters to airborne or land vehicle gravity surveys, in: Proceedings of the 2nd International Symposium on inertial surveying and geodesy. Banff, Canada.

Milne, G.A., J.L. Davis, J.X. Mitrovica, H.-G. Scherneck, J.M. Johansson and M. Vermeer, 2001. Spacegeodetic constraints on glacial isostatic adjustment in Fennoscandia. Science, 291:2381–2385.

Milne, G.A., J.X. Mitrovica, H.-G. Scherneck, J.L. Davis, J.M. Johansson, H. Koivula and M. Vermeer, 2004. Continuous GPS measurements of postglacial adjustment in Fennoscandia: 2. Modeling results. J. Geophys. Res., 109, B02412, doi:10.1029/2003JB002619.

Montelli R., G. Nolet, F.A. Dahlen, G. Masters, E.R. Engdahl and S.-H. Hung, 2003. Finite-frequency tomography reveals a variety of plumes in the mantle. Published online December 9, 10.1126/science.1092485 (Science Express Research Article).

Mooney, W.D., G. Laske and T.G. Masters, 1998. CRUST 5.1: A global crustal model at 5 × 5 degrees. J. Geophys. Res., 103:727–747.

Moritz, H., 1980. Geodetic Reference System 1980. Bulletin Géodésique, 54:395–405.

Nakada, M., R. Kimura, J. Okuno, K. Moriwaki, H. Miura and H. Maemoku, 2000. Late Pleistocene and Holocene melting history of the Antarctic ice sheet derived from sea-level variations. Mar. Geol., 167:85–103.

Panasyuk, S.V. and B.H. Hager, 2000a. Inversion from mantle viscosity profiles constrained by dynamic topography and the geoid, and their estimated errors. Geophys. J. Int., 143:821–836.

Panasyuk, S.V. and B.H. Hager, 2000b. Models of isostatic and dynamic topography, geoid anomalies and their uncertainties. J. Geophys. Res., 105:28199–28209.

Peltier, 1998. Postglacial variations in the level of the sea: implications for climate dynamics and solidearth geophysics. Rev. Geophys., 36:603–689.

Peltier, W.R., W.E. Farrell and J.A. Clark, 1978. Glacial isostasy and relative sea level: a global finite element model. Tectonophysics, 50:81–110.

Ricard, Y., M.A. Richards, C. Lithgow-Bertelloni and Y. LeStnuff, 1993. A geodynamic model of mantle density heterogeneity. J. Geophys. Res., 98:21895–21909.

Rignot, E., Thomas, R.H., 2002. Mass balance of polar ice sheets. Science, 297, 1502 -1506.

Ritsema, J. and H.-J. van Heijst, 2000. Seismic imaging of structural heterogeneity in earth‘s mantle: evidence for large-scale mantle flow. Science Progress, 83:243–259.

Scherneck, H.-G., J.M. Johansson, G. Elgered, J.L. Davis, B. Jonsson, G. Hedling, H. Koivula, M. Ollikainen, M. Poutanen, M. Vermeer, J.X. Mitrovica and G. Milne, 2002. BIFROST: observing the three-dimensional deformation of Fennoscandia, in: J.X. Mitrovica, B.L.A. Vermeersen (eds.): Ice Sheets, Sea Level and the Dynamic Earth, American Geophysical Union, Washington, 69-93.

Song, T.-R. A. and Simons, M., 2003. Large trench-parallel gravity variations predict seismogenic behavior in subduction zones. Science, 301:630–633.

Tarasov, L. and W.R. Peltier, 2002. Greenland glacial history and local geodynamic consequences. Geophys. J. Int., 150:198–229.

Thomas, R., Csatho, B., Davis, C., Kim, C., Krabill, W., Manizade, S., McConnell, J., Sonntag, J., 2001. Mass balance of higher-elevation parts of the Greenland ice sheet. J. Geophys. Res., 106, 33707 - 33716.

Tóth, G. and Völgyesi, L., 2003. Importance of Eötvös torsion balance measurements and their geodetic applications. EGS 2003, Geophysical Research Abstracts, 5:13217.

Tregoning, P., A. Welsh, H. McQueen and K. Lambeck, 2000. The search for postglacial rebound near the Lambert glacier. Earth Planet. Space, 52:1037–1041.

Tushingham, A.M. and W.R. Peltier, 1991. Ice-3G: a new global model of late Pleistocene deglaciation based upon geophysical predictions of post-glacial relative sea level change. J. Geophys. Res., 96:4497–4523.

Vecsey, L., C.A. Hier Majumder and D.A. Yuen, 2002. Multi resolution tectonic features over the earth inferred from the wavelet transformed geoid. Submitted to Electronic Geosciences, Sept. 25.

Velicogna, I. and J. Wahr, 2002a: A method for separating Antarctic postglacial rebound and ice mass balance using future ICESat Geoscience Laser Altimeter System, Gravity Recovery and Climate Experiment, and GPS satellite data. J. Geophys. Res., 107, 2263, doi:1029/2001JB000708.

Velicogna, I. and J. Wahr, 2002b: Postglacial rebound and Earth‘s viscosity structure from GRACE. J. Geophys. Res., 107, 2376, doi:10.1029/2001JB001735.

van Leeuwen, E. H., 2000. BHP develops world‘s first airborne gravity gradiometer for mineral exploration. Preview, 86:28–30.

Wahr, J., M. Molenaar and F. Bryan, 1998. Time variability of the earth‘s gravity field: hydrological and oceanic effects and their possible detection using GRACE. J. Geophys. Res. 103:30205–30229.

Wahr, J., T. van Dam, K. Larson and O. Francis, 2001. GPS measurements of vertical crustal motion in Greenland. J. Geophys. Res., 106:33755–33759.

Wahr, J. and I. Velicogna, 2003: What might GRACE contribute to studies of postglacial rebound? Space Sci. Rev., 108:319–330.

Wells, R. E., Blakely, R. J., Sugiyama, Y., Scholl, D. W. and Dinterman, P. A. 2003, Basincentred asperities in great subduction zone earthquakes: A link between slip, subsidence, and subduction erosion, J. Geophys. Res., 108, 2507, doi:10.1029/2002JB002072.

Wolf, D., J. Hagedoorn and M. Martinec, 2002. A new time-domain method of implementing the sealevel equation in glacial-isostatic adjustment. EOS, 83(47), Fall Meet. Suppl.: Abstract G12A–1059.

Wu, P. and W.R. Peltier, 1983. Glacial isostatic adjustment and the free air gravity anomaly as a constraint on deep mantle viscosity. Geophys. J. R. Astr. Soc., 74: 377–449.

Zhang, S. and U. Christensen, 1993. Some effects of lateral viscosity variations on geoid and surface velocities induced by density anomalies in the mantle. Geophys. J. Int., 114:531–547.

3.4 Continental hydrology

In view of the pivotal role that continental water storage plays in the Earth's water, energy and biogeochemical cycles, the temporal and spatial variations of water storage for large areas are presently not known with satisfactory accuracy. GRACE observations of the time-variable gravity field will, for the first time, allow to directly quantify mass changes on the continents that are caused by changes in water storage. This will considerably enhance the knowledge about continental water storage variations and will contribute to closing the water balance at different scales in space and time. In addition, it will help to validate and improve the predictive capacity of large-scale hydrological models.

The hydrological cycle

The system of water redistribution within the global water cycle is the main driving force for life on the land masses. By transformation and transport processes in the hydrological cycle, water is changing its phase from liquid or ice to vapour and back. Water fluxes within and between land and ice masses, oceans and atmosphere are closely coupled to each other. In the form of a complex system of nested cycles from local up to global scales (cf. Figure 3.4.1), mass and energy is transported over large distances. Atmospheric water vapour originating from evaporation at the ocean surface returns as precipitation on the oceans and, after vapour transport, on the land masses.

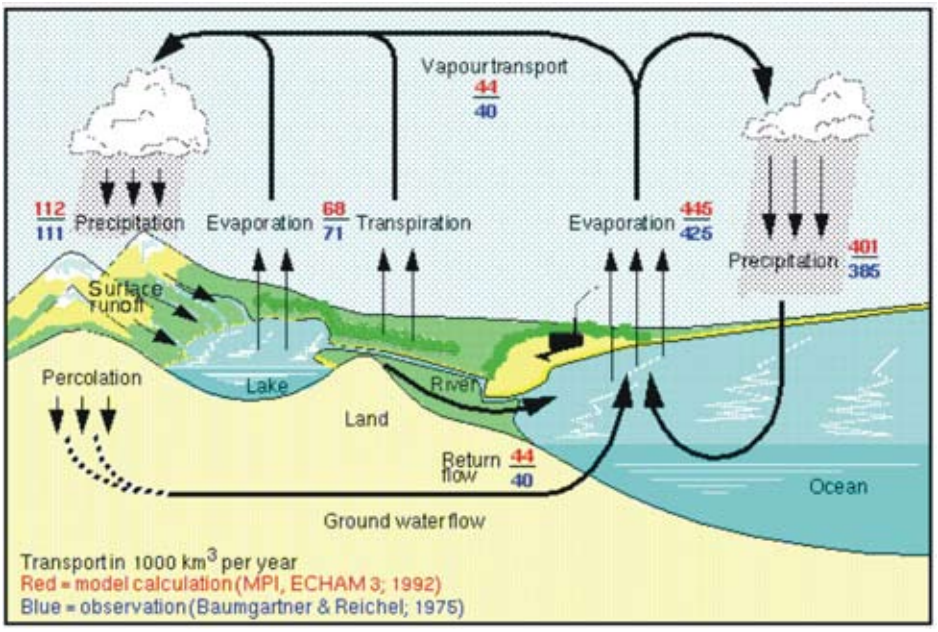

Figure 3.4.1: *The global hydrological cycle (Max-Planck-Institute for Meteorology, Hamburg)*

The Hydrological Cycle

Benefits

- For the first time, temporal and spatial variations of the continental water storage can be quantified for large areas.
- This will allow to close the water balance of large river basins and continents, and to validate and improve existing simulation models towards an enhanced description of the hydrological cycle and the impacts of climate / environmental change.

Challenges

- The methodology of deriving water storage changes from GRACE gravity data must be verified for well observed areas of appropriate size before it can be applied to ungauged river basins. This is a prerequisite for the separation of the hydrological component from the gravity signal.
- The separation of different water storage components such as groundwater, surface water and snow or ice by help of complementary hydrological data is a complex and comprehensive task for large catchment areas.

Mass changes observable by gravity measurements are not directly related to single processes like precipitation, but are the result of the mass balance of numerous transport processes with different time constants. On the continents, water from precipitation is recycled locally to the atmosphere by ongoing evaporation from open water surfaces or soils and by transpiration from plants and is returned again by precipitation as rain or snow. These evapotranspiration processes are complex and vary considerably in time and space. They depend on the type of land use, i.e., the vegetation type, its vegetation period and leaf area, on available soil water storage and on local atmospheric conditions. Depending on the available energy, precipitation is recycled several times via evapotranspiration (about 10 times for tropical, and 1-2 times for temperate climate conditions) without being observable in mass signals.

After evapotranspiration, the remaining rain or snow melt is split up into a surface runoff component, a fast interflow component in the shallow soil zone and into percolation to deeper subsurface zones resulting in a slow groundwater flow component. The relative contribution of the different flow components to total runoff is governed by topography, vegetation, soil characteristics, underlying hydrogeological conditions and the actual status of the related storage. In other words, these factors determine the relative contribution and the residence time of water masses in the different soil and rock storage compartments and, thus, the time-variable soil moisture and groundwater storage volumes. Runoff from the landscape is concentrated into the river drainage system. River runoff as well as groundwater flow at large spatial scales passes various intermediate storages, such as retention in the river network itself, in lakes or wetlands. There, it is partly subject to evaporation or extraction for human consumption, before being fed back into the oceans.

For a catchment area, being the basic spatial unit of hydrological analysis and water management issues, the water balance can be written as:

$$P = Q + ET + \Delta S \tag{3.4.1}$$

P	[mm]	Precipitation,
Q	[mm]	Discharge,
ET	[mm]	Evapotranspiration,
ΔS	[mm]	Storage change

in units of the height of water column per time interval.

However, the rates of water fluxes between the different components of the hydrological cycle vary considerably and show a specific temporal behaviour due to the different storage characteristics. This storage in the form of snow or ice cover, vegetation interception, surface water, soil

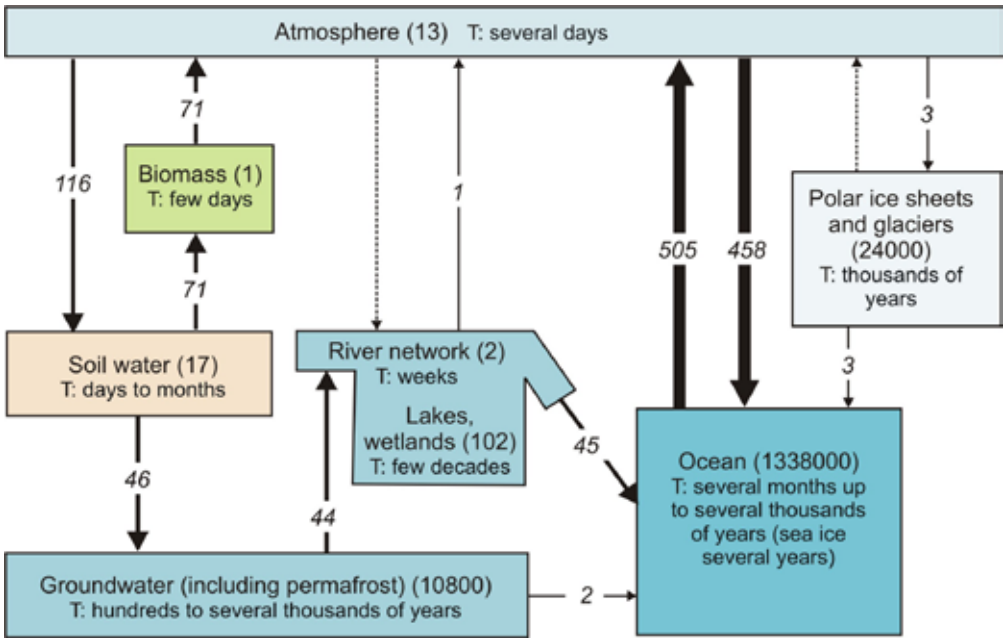

Figure 3.4.2: *Storage in the global hydrological cylce. Storage volumes (1000 km³, in brackets), fluxes (1000 km³/year, in italics) and order of magnitude of mean water residence times (T) (after WBGU, 1997)*

moisture and groundwater all exhibit individual residence times, maximum storage levels and paths for water input and output. Characteristic average residence times of continental water storage, for instance, range from a few days for the biomass or upper soil layers to several hundreds or thousands of years for deep groundwater storage (cf. Figure 3.4.2).

Although making up only about 3.5% of total water in the hydrologic cycle, continental water storage and related mass redistribution processes have a huge importance for the dynamic Earth system. Soil moisture, for instance, has frequently shown to be a key parameter as it links the water and energy cycles via the transport of latent heat envolved in the evapotranspiration process and, in addition, the biogeochemical cycle by transport of solutes and suspended load being associated with water mass redistribution.

Furthermore, continental water storage is of highest importance for civilization on Earth. The replenishment of surface and groundwater storage provides the basis for water supply to a wide range of uses in the domestic, industrial and agricultural sectors. Soil moisture is essential for plant growth, including agricultural crops and thus food supply. About two-thirds of global water use is attributed to irrigation in agriculture. Population growth and economic development lead to an increasing water demand and rising extractions from continental water storage. However, the physiographic settings of many regions in the world together with climate variability often constrain water availability to amounts being below the actual demand. About two-thirds of the population of the world live at least temporarily in such a condition of water stress.

Global climate change associated with a projected increase of global surface temperature in the range of 1.5 to 5.8°C between 1990 and 2100 (IPCC, 2001) provides an increase of available energy for evapotranspiration and is expected to change volumes and flux rates between the storages of the hydrological cycle. Within a general tendency of increasing variability, global atmospheric water vapour and precipitation is expected to increase, although effects at the regional scale may deviate from the global tendency and are highly uncertain (IPCC, 2001). These changes, together with other aspects of global change such as land use changes which directly affect evapotranspiration and mass transport at the land surface, affect water availability in surface and groundwater water storage being essential for human use.

Thus, the knowledge and understanding of temporal and spatial variations in continental water storage is of crucial environmental and economic importance. It forms the basis for a reasonable description of mass redistribution processes in the hydrological cycle for current conditions and consequently also for reliable estimates of the future development by scenario simulations. This, in turn, is essential for the implementation of adequate long-ranging water management strategies at the regional scale of river basins in view of both changing water availability and water demand. Going even beyond the regional scale, a global scale analysis is required due the close interaction of changes in the continental water storage and the climate system and its feedback on future climate conditions.

Before the launch of the GRACE satellites, a large-scale monitoring system of changes in continental water storage, however, did not exist. Ground-based observations of soil moisture or groundwater levels give only point estimates of the water storage and are hard to be interpolated to larger areas in view of the sparse measurement network and the multitude of influencing factors. For large areas, estimates by remote sensing have been made for snow cover and by altimetry for water levels for continental surface waters, but so far only for selected lakes, reservoirs or wetlands. Also data on soil moisture are given by remote sensing methods for larger areas, however they are limited to the uppermost centimetres of the soil and do not capture the important deeper soil water and groundwater storage. While adequate measurements of precipitation and runoff may be available in some cases at the river basin scale, a calculation of storage changes by use of the water balance equation (see equation 3.4.1) usually is not feasible as no reliable estimates of evapotranspiration are available for large scales. The shortage of adequate data (for model input and validation) also limits the applicability of hydrological simulation models to quantify water storage components for large areas.

Temporal variations of continental mass measured by the GRACE mission are of extraordinary importance to overcome the lack of direct measurements of changes in the continental water storage at large scales. Simultaneous altimetric measurements of surface water level changes and of changes in snow or ice cover will allow for a further separation of the involved storage components. In the following chapters an overview is given on present open questions in hydrology and on the perspectives which are opened up by the use of gravitational and altimetric measurements.

Global water balance

Until present, the global and continental water balance is not known with sufficient accuracy neither in its temporal variation nor for its mean annual values. Values differ considerably for different data sources (see Figs. 3.4.1, 3.4.3). This uncertainty is due to the difficulty of direct measurements of the climatic components of the water cycle (precipitation and evaporation) at the land surface in terms of the spatial coverage and density of measurement points. Problems also arise with the accurate measurement of river discharge on the global scale, especially for the main contributing river systems of the world with large discharge volumes. Estimates of total continental discharge into the oceans vary by about 20% (cf. Figure 3.4.3).

Even more uncertain is the quantification of the considerably smaller net flux between oceans and land masses. It is defined by the imbalance between water vapour transport to the land masses and total runoff, and contributes to estimates of sea level change. Similar problems exist for the mass balance of ice masses (here the Antarctic and Greenland ice sheets), for which the mass output cannot be determined better than +/- 20% of the mass input (see Chapter 3.2). However, these mass balances and the resulting net mass fluxes are essential for the determination of changes in the oceanic mass storage.

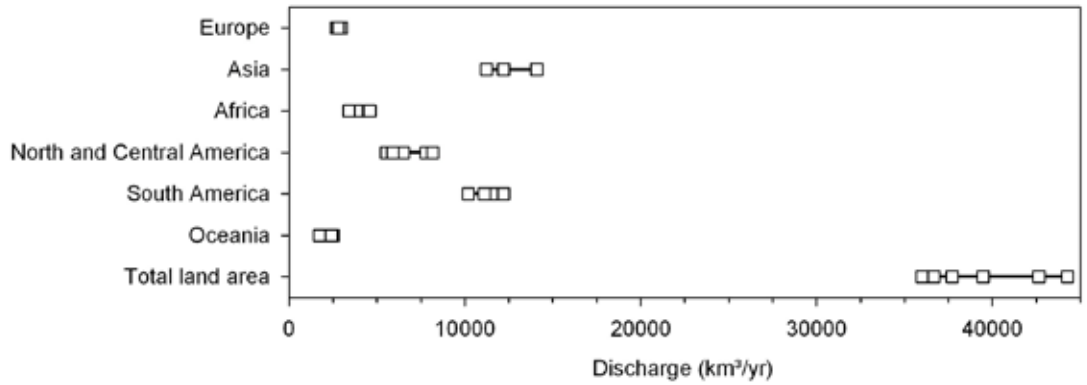

Figure 3.4.3: *Long-term average annual continental discharge into oceans (Estimations of six observation-based and model-based studies compared in Döll et al. 2003)*

Observations of gravity changes by GRACE measurements allow a direct determination of mass variations and, thus, of net fluxes between the three compartments land masses, oceans and ice (cf. Figure 3.4.2). As the mass loss from land and ice areas does not only occur via liquid water but also via the release of water vapour to the atmosphere (evapotranspiration), the exchange with the atmosphere as an additionally flow path has to be accounted for. These four compartments of global water storage are closely coupled.

Large-scale variations of the continental water storage

Intra-annual and inter-annual dynamics of continental water storage vary substantially between environments of different physiographic and climatic conditions (Figures 3.4.4 and 3.4.6). For example, the intra-annual variation between maximum and minimum water storage amounts to about 50 mm of water column in river basins with rather uniform climatic conditions, whereas it is up to 450 mm in tropical river basins with a strong seasonal variation of climatic forcing, in particular precipitation input. These mass variations turn continental hydrology into one of the strongest signal components of the time-variable gravity fields measured by GRACE.

In general, however, the spatial and temporal variability of water storage is not sufficiently known until now (Rodell and Famiglietti, 1999; Alsdorf et al., 2003). Observations of variations in continental water storage such as soil moisture or groundwater are rarely available even on small scales of sub-areas of river basins due to the limitations of the measurement methods with regard to sample density, spatial coverage or soil penetration depth as in the case of radar remote sensing of soil moisture. GRACE, in contrary, provides a global, vertically integrating and, thus, unprecedented measure of storage changes. Yet even more difficult than to assess water storage is to quantify the water fluxes between the storages which often include complex interactions. Not all water fluxes, however, cause a net change in water storage. Steady-state groundwater flow, for instance, transports water masses without changing the water volume stored in a certain section of the aquifer. Consequently, such water transport processes without net mass variations cannot be captured by gravimetric measurements such as GRACE, but require additional ground-based observations.

A complementary way to quantify hydrological processes, i.e., transport processes of water that affect water storage, is by using hydrological models. Only models allow to represent the multitude of processes in an integrative form and for prognostic purposes. A wide range of hydrological models exists, reaching from detailed physically-based process models up to simplified water

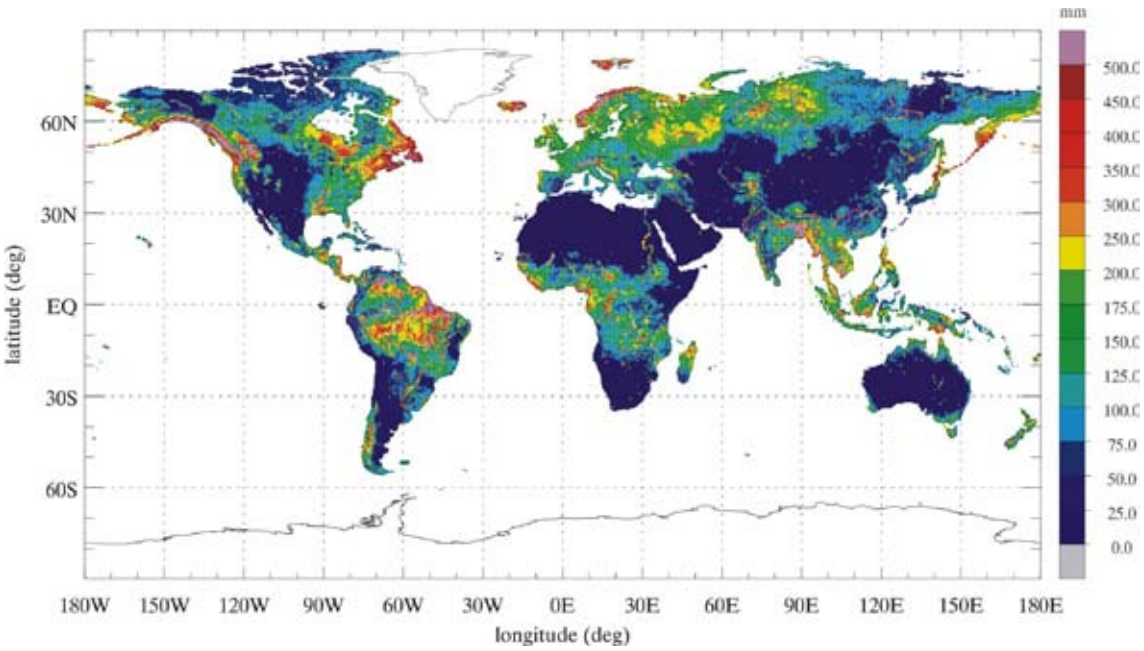

Figure 3.4.4: *Average seasonal changes (changes between the months of maximum and minimum storage) of the total continental water storage (composed of the storage components snow, soil water, groundwater, river, lakes and wetlands), simulated on a 0.5° global grid with the model WGHM (Döll et al., 2003), period 1961-1995.*

balance models which make use of interrelated conceptual storages and transfer functions to represent water fluxes (e.g., evapotranspiration, percolation, runoff generation, river network routing). More comprehensive models of water management also address anthropogenic, time variant influences on water storage, such as pumping from groundwater or withdrawal from surface reservoirs for irrigation or other uses (cf. Figure 3.4.5).

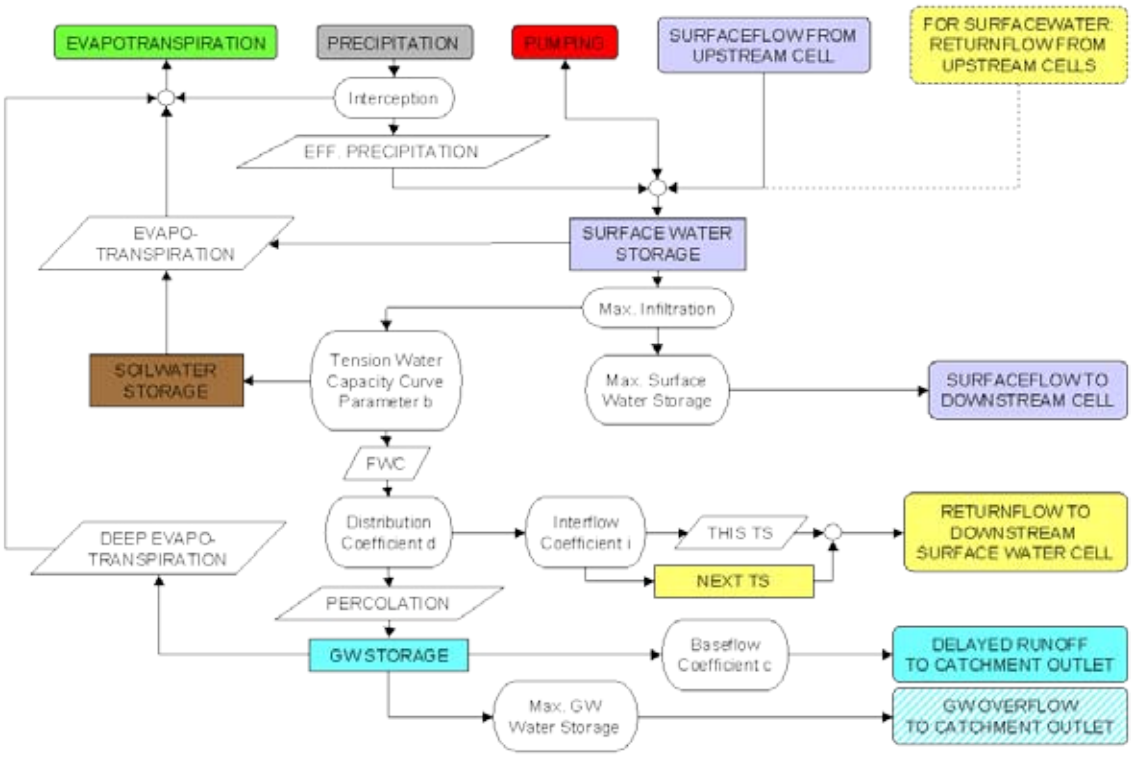

Figure 3.4.5: *Flow chart of a water balance model (Riegger et al., 2001)*

The applicability of a specific model type depends, among others, on the spatial scale and the available information on soils, hydrogeology, land use and climate. On small scales with detailed spatially distributed information, models can address a complex system of various interacting hydrological processes. These models often use a spatial discretization based either on a raster representation of all relevant parameters or on a sub-division of the river basin into areas of similar hydrological response.

With an increase in scale and a related decrease of detail in the available data, the actual landscape heterogeneity can no longer be explicitly represented in the model. Thus, scaling approaches are used to describe the sub-scale variability, e.g., by means of average parameters, distribution functions or simplifying lumped process formulations.

In general, the capability of hydrological models to represent the hydrological cycle and, thus, their predictive power to quantify current and future variations in continental water storage, is dependent on the accuracy of input data, on the appropriateness of process formulations and on the availability of data for model calibration and validation. Large differences between regions of different climate or physiography in terms of hydrological processes and storage dynamics prevent hydrological models from being easily transferred from one region to another. In particular for large-scale applications, the only available variable for model validation usually is river discharge. Although satisfactory results may be obtained when comparing mean simulated and observed river discharge, the temporal variability and the state of soil, groundwater and surface water storage volumes may be unsatisfactorily simulated in the model. As an example, current limitations of hydrological models to accurately quantify continental storage changes are shown in Figure 3.4.6 in terms of large differences in temporal storage variations between model results and water balance studies for large river basins.

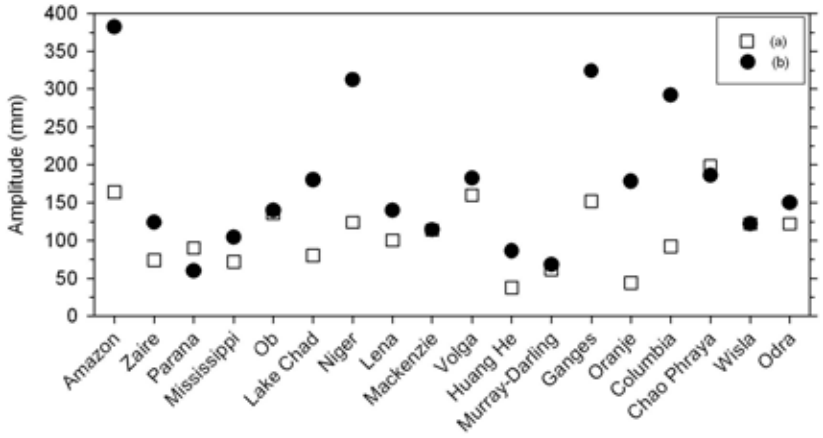

Figure 3.4.6: *Mean difference between annual maximum and minimum continental water storage for large river basins, (a) median value of 10 global land-surface models, years 1987-1988, (b) value derived from a water balance study, years 1989-1992 (data summarized in Rodell & Famiglietti, 1999).*

In view of the existing uncertainties mentioned above, a multi-variable validation of hydrological models going beyond river discharge as validation variable has often been called for. In this respect, measurements of continental water storage changes by the GRACE mission can provide a unique additional data source for model validation and calibration. Accuracies are higher when averaging for larger regions, and are expected to increase in future due to advances in data processing and due to the decreasing GRACE orbit altitude. Thus, storage variations at monthly and longer time scales observed by GRACE are of sufficient accuracy for large river basins to constrain uncertainties of existing estimates and model results

First results from GRACE time-variable gravity fields reduced to the hydrological signal component (Tapley et al., 2004; Wahr et al., 2004; Schmidt et al., 2004) clearly show a seasonal continental-scale pattern of water storage changes that corresponds to estimates by global hydrological models, such as the WaterGap Global Hydrology Model WGHM (Döll et al., 2003) (Figure 3.4.7, see also Figure 2.12). The largest storage change signals occur in the tropical areas of South America and Africa, in the monsoon region of South-East Asia, and in high latitudes of northern

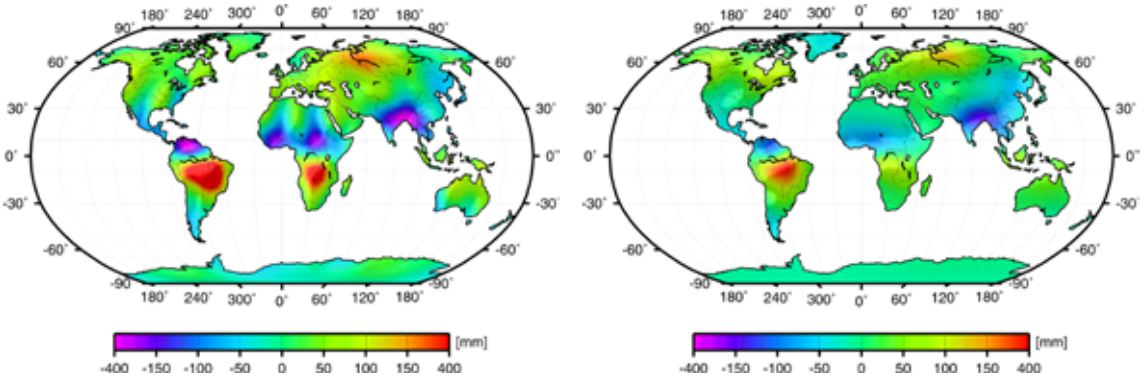

Figure 3.4.7: *Global continental pattern of differences between two monthly GRACE gravity field solutions (April/May 2003 minus Aug. 2003) reduced to the hydrological mass signal (left) and water storage differences for the same time period simulated with the global hydrological model WGHM (right).*

Russia / Sibiria. While the spatial pattern is reflected in the model results, the amplitude of storage changes as derived from GRACE is markedly larger than that of the hydrological model. Similar results were obtained for the comparison with other global hydrological models (Schmidt et al., 2004). Also at the scale of large river basins, first GRACE results allow to represent the characteristic temporal dynamics of storage change of basins in different environments (Figure 3.4.8). The overall seasonal behaviour corresponds to simulation results of hydrological models, while the amplitudes usually are larger for GRACE than for the simulations.

These discrepancies between water storage variations from GRACE and from hydrological models highlight, on the one hand, residual errors in the GRACE solutions (e.g., errors in reducing

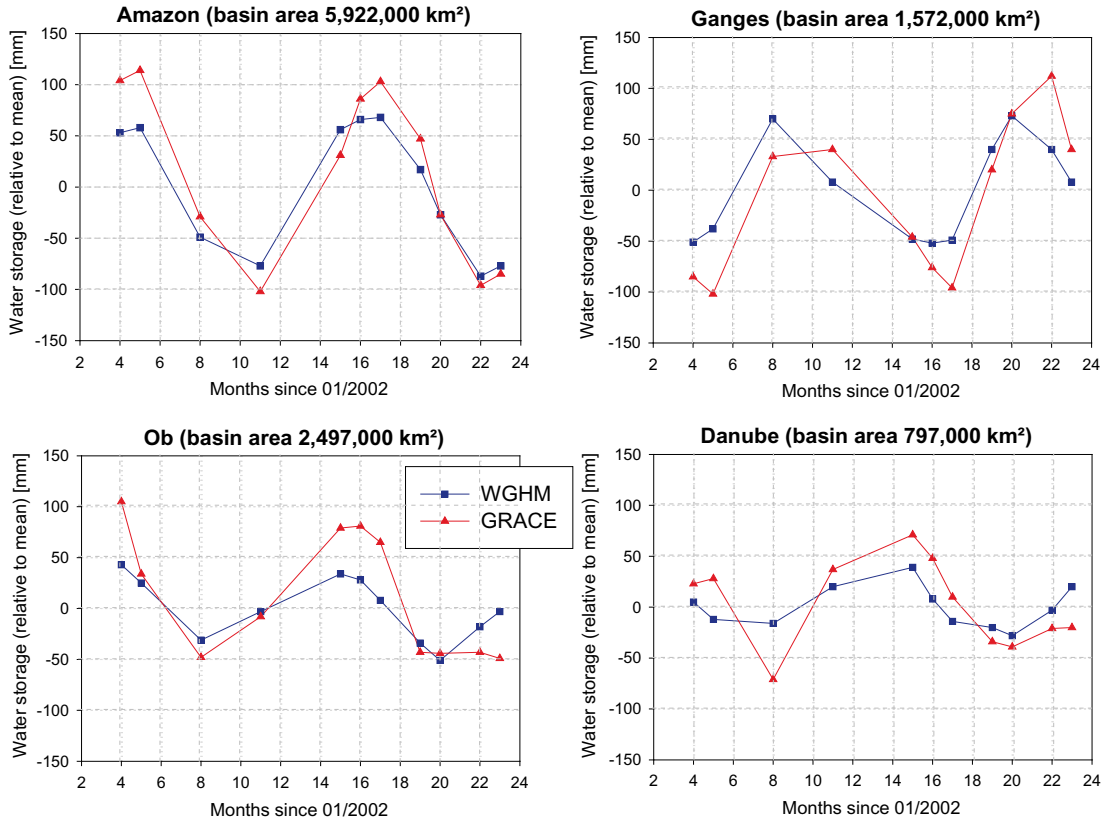

Figure 3.4.8: *Time series of water storage for large river basins for 11 monthly GRACE gravity field solutions (red) and for simulations with the global hydrological model WGHM (blue).*

other than hydrological mass signals), and, on the other hand, limitations of the hydrological models. One limitation is that models usually represent only selected water storage components whereas GRACE gives a vertically integrated storage signal. Other limitations are non-adequate process formulations or parameterizations in the model, or errors in the input data such as a systematic underestimation of snow precipitation which may lead to underestimated storage change in the case of high latitude basins (e.g., River Ob in Figure 3.4.8).

The validation of GRACE measurements of continental water storage variations by ground-based measurements and the quantification of related uncertainties is of fundamental importance for hydrological modelling and forecasting and, as a consequence, for the separation of other contributions to gravity signals like the Earth's mantle and crust dynamics (see Chapter 3.3). In principle, the validation consists of investigating the consistency between climatic and hydrological data on the one hand, and observed mass changes from GRACE on the other hand. For this comparison well observed catchments are to be selected where measurements of soil moisture, groundwater levels, surface water storage and possibly snow cover exist with sufficient density and for which the processes are understood and reliable model estimates of water storage variations are available. An example is the Rhine catchment (Bardossy A., Hundecha J., 2004) (Figure 3.4.9), although its spatial extent of about 200 x 600 km is at the limit of the observable resolution of GRACE mass changes.

As gravity-based observations of continental mass variations deliver integral values of storage changes of groundwater, soil moisture, snow and surface water, additional storage data help to disaggregate the signal into its individual storage components. This is feasible in well-observed catchments as that mentioned above (Figure 3.4.9, see also Rodell and Famiglietti, 2001). Complementary large-scale measurements of water levels in surface waters by satellite altimetry provide the outstanding opportunity of quantifying changes in surface water storage and of separating this component from total water storage data. Other remote sensing data for signal separation are in particular data on snow or ice covers, surface soil moisture, as well as ground-based measurements of variations in the groundwater table, for instance. Given any independent a-priori information, inversion techniques such as present by Ramilien et al. (2004) may help to separate different hydrological contributions to the time-variable gravity field solutions.

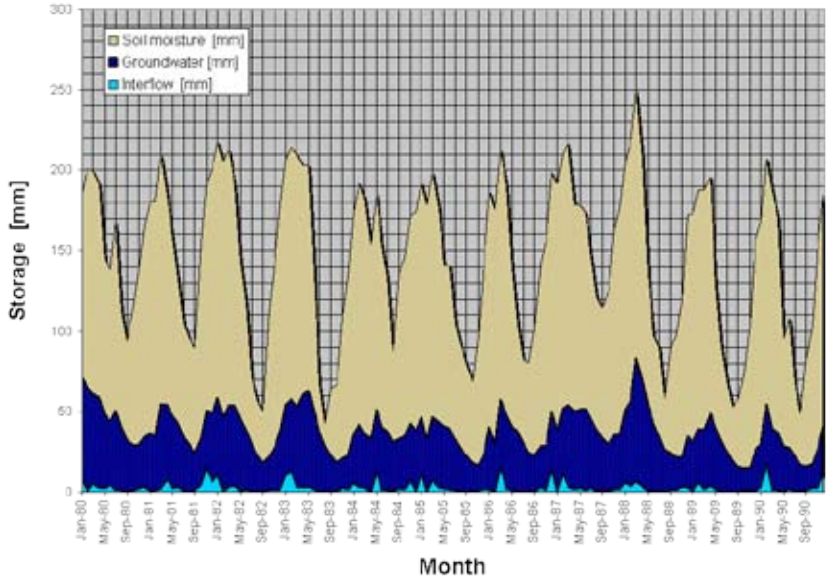

Figure 3.4.9: *Time series of continental water storage averaged over 90525 km² of the Rhine catchment for soil moisture, interflow and groundwater, according to simulations with the HBV model (Bardossy A., Hundecha J., 2004).*

In summary, the knowledge of continental water storage variations measured by GRACE considerably improves the understanding of the hydrological cycle and of water transport processes and their relation to climate or physiography. Starting out from the continental scale and going to a higher spatial resolution corresponding to that attained by GRACE, the investigation of a large number of different environments and river basins will allow to cover the maximum diversity in basin characteristics and storage responses, ranging from humid tropical, arid and semi-arid, humid temperate to snow- and ice-dominated regions. In this way, relationships between storage variations and climate variability can be quantified for different basin characteristics and used to improve model transferability and to reduce related uncertainty. This is of particular importance for model transfer to ungauged catchments, where no calibration and validation with discharge data is possible.

Large-scale evapotranspiration

Evapotranspiration fluxes and their temporal distribution, depending on climatic conditions, soil moisture availability, the vegetation type and period and the time-variable area of surface water bodies such lakes, reservoirs and wetlands, are poorly known for large scales. Different modelling approaches may deliver substantially dissimilar results at the monthly, seasonal or even annual time scale. GRACE measurements of water storage changes together with the altimetric monitoring of changes in surface water levels, however, will enable to close the water balance and resolve the water balance equation for evapotranspiration (see Equation 3.4.1) (Rodell et al., 2004). This will allow for an evaluation and improvement of evapotranspiration models with respect to a realistic description under different hydrological situations (different climate zones, soil and vegetation conditions). Thus, GRACE observations of the temporal variability of continental water storage should be suitable for the validation of existing evapotranspiration modules in hydrological models. This reduces the degree of freedom in conceptional models and considerably enhances the quality of parameter estimations and the prognostic power of the models. The transfer of this knowledge to ungauged catchments will then allow a calculation of discharge on the basis of known water storage changes from GRACE and climatic data and thus deliver an essential input to the assessment of the global water balance.

Trends and anomalies in continental water storage

Processes of environmental change may cause gradual changes in continental water fluxes and storage volumes, which are of high importance for ecosystems and human water and food supply. Similarly, large-scale modifications of the oceanic and atmospheric circulation patterns such as in the course of El-Nino - Southern Oscillation (ENSO) also have marked effects on the continental hydrology at inter-annual scales in terms of anomalies of precipitation, soil moisture and runoff. Inter-annual changes in the hydrological contribution to the gravity field measured by GRACE will allow to investigate slowly changing storage, i.e. of groundwater or continental ice masses, and thus contribute to the detection of long-term trends for large spatial scales. New signals of climate change may become observable. In high latitudes, for instance, increasing temperature is expected to lead to a thinning or disappearance of permafrost. A long-term storage decrease will contribute to continental net discharge and thus to sea level rise. In arid to sub-humid areas, cli-

mate change is likely to decrease soil moisture, causing runoff changes, land degradation or desertification. The gravity-based observations of inter-annual water storage changes will also help to better understand the impact and persistance of global ENSO-type of circulation anomalies on continental hydrology.

Large scale anthropogenic impacts on water storage are expected to become observable by changes in the gravity field. Direct impacts by water management like withdrawal use of groundwater and surface water for irrigation as well as indirect impacts via changes in land use like deforestation or drainage of wetlands could be detected in areas where these data are not available by other means (Rodell, M., & Famiglietti, J. S., 2002). Excessive water use from lakes and reservoirs or from their contributing rivers leads to a decreasing trend in their storage volumes (Aral Sea, Lake Nasser etc.). Huge new reservoirs, in particular the Three Gorges Dam in China, lead to an accumlation of water masses that might be represented in the GRACE data. For a differentiated description of trends or anomalies in one of the water storage components, they have to be separated by means of complementary data from remote sensing like altimetry, ground-based measurements and/or hydrological models.

The investigation of the relation between the observed continental storage changes and changing environmental boundary conditions in the context of climate change or human impacts is not only important for the understanding of hydrological processes and the evaluation of hydrological models, but also for the separation of geophysical contributions (by Earth's mantle and crust dynamics), as both are contributing to mass changes on this long-term time scale. In areas which are insufficiently observed in terms of their hydrological behaviour it is inevitable to determine long-term changes in water storage from climatic data on the basis of models. Only after the separation of hydrological gravity changes based on hydrological models, a separate analysis of other geophysical components is possible.

Long-term environmental change is not only expressed by changes in the mean, but also by changes in the temporal distribution or variability. In this respect, another potential contribute to the detection of gradual changes in the hydrological cycle by gravity measurements is via the analysis of changes in the intra-annual regime of storage variations on a monthly basis. Possible areas of investigation are temporal shifts in the soil moisture regime due to an increasing fraction of rainfall relative to snow in the course of global warming, or changes in water storage due to changing frequencies of different atmospheric circulation patterns can potentially be detected. These analyses help to quantify the impact of environmental change, either due to natural climate variability or various anthropogenic influences, on long-term continental mass variations and changes in the hydrological cycle.

References

Alsdorf, D., D.P. Lettenmeier and C. Vörösmarty, 2003: The need for global, satellite-based observations of terrestrial surface waters. EOS, 84(29):269-276.

Bárdossy, A . and Y. Hundecha, 2004: Modelling of the effect of landuse changes on the runoff generation of a river basin through parameter regionalization of a watershed model. Journal of Hydrology, 292 (2004):281-295

Dickey, J. O., C. R Bentley, R. Bilham, J. A. Carton, R. J. Eanes, T. A. Herring, W. M. Kaula, G. S. E. Lagerloef, S. Rojstaczer, W. H. F. Smith, H. M. van den Dool, J. M. Wahr and M. T. Zuber, 1999: Gravity and the hydrosphere: new frontier. Hydrological Sciences Journal 44(3): 407-415.

Döll, P., F. Kaspar and B. Lehner, 2003: A global hydrological model for deriving water availability indicators: model tuning and validation. Journal of Hydrology, 270:105-134.

IPCC (2001): Intergovernmental Panel on Climate Change. 3rd Assessment report. Cambridge University press, UK.

Ramillien, G., Cazenave, A. and O. Brunau, 2004: Global time variations of hydrological signals from GRACE satellite gravimetry. Geophysical Journal International 158: 813-826, doi: 810.1111/j.1365-1246X.2004.02328.x.

Riegger, J., H. Kobus, Y. Chen, J. Wang, M. Süss and H. Lu, 2001: The water system. IREUS Research report 22, „Sustainable development by integrated land use planning“, pp. 112-139, Institut für Raumordnung und Entwicklungsplanung, Universität Stuttgart.

Rodell, M. and J. S. Famiglietti, 1999: Detectability of variations in continental water storage from satellite observations of the time dependent gravity field. Water Resources Research 35(9):2705-2723.

Rodell, M. and J. S. Famiglietti, 2001: An analysis of terrestrial water storage variations in Illinois with implications for the Gravity Recovery and Climate Experiment (GRACE). Water Resources Research 37(5):1327-1339.

Rodell, M. and J. S. Famiglietti, 2002: The potential for satellite-based monitoring of groundwater storage changes using GRACE: the High Plains aquifer, Central US. Journal of Hydrology 263:245-256.

Rodell, M., Famiglietti, J. S., Chen, J., Seneviratne, S. I., Viterbo, P., Holl, S. and C.R. Wilson, 2004: Basin scale estimates of evapotranspiration using GRACE and other observations. Geophysical Research Letters, 31, L20504, doi:10.1029/2004GL020873.

Schmidt, R., P. Schwintzer, F. Flechtner, C. Reigber, A. Güntner, P. Döll, G. Ramillien, A. Cazenave, S. Petrovic, H. Jochmann, and J. Wünsch, 2004: GRACE observations of changes in continental water storage, Global and Planetary Change, in print.

Swenson, S., J. Wahr and P.C.D. Milly, 2003: Estimated accuracies of regional water storage variations inferred from the Gravity Recovery and Climate Experiment (GRACE). Water Resources Research, 39(8):1223, doi:10.1029/2002WR001808.

Swenson, S. and J. Wahr, 2002: Methods for inferring regional surface-mass anomalies from Gravity Recovery and Climate experiment (GRACE) measurements of time-variable gravity. Journal of Geophysical Research, 107 (B9), 2193, doi: 10.1029/2001JB000576.

Tapley, B. D., Bettadpur, S. V., Ries, J. C., Thompson, P. F. and M. M. Watkins, 2004: GRACE measurements of mass variability in the Earth system. Science, 305: 503-505.

Velicogna, I., J. Wahr. and D. H. Van, 2001: Can surface pressure be used to remove atmospheric contributions from GRACE data with sufficient accuracy to recover hydrological signals? Journal of Geophysical Research B: Solid Earth 106:16415-16434.

Wahr, J., M. Molenaar and F. Bryan, 1998: Time variability of the Earth's gravity field: Hydrological and oceanic effects and their possible detection using GRACE. Journal of Geophysical Research – Solid Earth 103(B12):30205-30229.

Wahr, J., Swenson, S., Zlotnicki, V. and I. Velicogna, 2004: Time-variable gravity from GRACE: First results. Geophysical Research Letters, 31: L11501, doi:10.1029/2004GL019779.

WBGU, 1997: Welt im Wandel – Wege zu einem nachhaltigen Umgang mit Süßwasser.

Wissenschaftlicher Beirat der Bundesregierung Globale Umweltveränderungen, Springer-Verlag, Berlin-Heidelberg.

3.5 Atmosphere, tides and Earth core motion

Mass transports by the atmospheric circulation and by tides make up an integral part of mass variations and transports in the Earth system. For the purpose of the proposed program, both components are regarded as known from observations and models. They are treated as correction terms during gravity field analysis. However, the contribution of their uncertainty to the total error budget of mass variation estimates has to be assessed. Furthermore, the atmospheric conditions are required as input for models of the oceans, the continental hydrosphere and the cryosphere to drive mass transport and mass exchange processes. Mass variations caused by Earth core motion will be taken into account for the lowest harmonic degrees.

Atmosphere

Atmospheric mass variations and mass transports are interconnected in many ways to the mass signals and transport processes in other segments of the Earth system discussed in this report. In the proposed research program, the atmosphere plays two distinct roles: First, atmospheric forcing fields are essential in driving ocean circulation models, models of the terrestrial cryosphere and of continental hydrology. Atmospheric exchange processes are an essential part of the hydrological cycle. Second, atmospheric mass variations will inevitably influence the satellite estimates of geoid and gravity anomalies, and, thus, they have to be separated from the total gravity signal before studying mass variations in the oceans, ice masses, continental hydrology or solid Earth.

Atmospheric forcing and mass exchange

Ocean models are driven by surface forcing fields of momentum fluxes, net heat and net freshwater. Usually those forcing fields are provided by numerical weather prediction centers such as ECWMF and NCEP on a daily basis. While all those fields are only estimates of the true forcing fields, they are valuable first guess fields that lead to reasonable simulations of the ocean circulation on time scales of days to weeks to years and beyond. Ocean data assimilation has as one of its goals to improve those surface forcing fields in such a way that ocean models better simulate observed conditions. It is hoped that those estimated forcing fields will help to improve atmospheric models not only over the ocean but also over continents.

On the continents, the atmospheric forcing is an essential input for hydrological models and for models of the cryosphere. The main climate elements used by these models are precipitation, available energy (radiation, air temperature), near-surface atmospheric moisture content and wind velocities. These variables drive processes that govern the water and energy balance of the land surface, such as snow or ice accumulation and melt, evapotranspiration, and water and heat fluxes in the soil. The atmospheric forcing data for these models are provided from atmospheric model outputs, ground-based or air-borne meteorological measurements, or combinations of both (reanalysis data of atmospheric circulation models).

These interactions between atmosphere, oceans, continental hydrology and cryosphere are discussed more explicitly in Chapters 3.1, 3.2 and 3.4. In the following, we concentrate on the second research topic, the correction of the observed gravity field signal for atmospheric mass variations.

Atmospheric mass variations and atmospheric de-aliasing

Atmospheric mass variations due to atmospheric circulation and the related movement of pressure systems cause one of the strongest components of the time-variable gravity field signal over the continents. Over the oceans, in contrary, the atmospheric mass variations are to a large extent isostatically compensated by the so-called inverse barometer effect.

To avoid contamination of the other gravity signal components over the continents, it is essential to correct gravity field observables using the best available air pressure data and atmospheric models. These play an important role for the gravity field determination, as their errors are propagated to the solutions via the corrections to be applied or via the assumptions made for the inverse barometer effect. In order to estimate their specific error budget, an independent validation of both the atmospheric model and the inverse barometer assumption is required.

Due to orbit characteristics of the gravity field missions the spatial sampling over a specific period of time (e.g. monthly) is not uniform over the whole mission lifetime. This means mass variations occurring on shorter time scales generally are not eliminated by computing a mean value of spatially repeated observations at different local times. For this reason these short-term, mass variations have to be corrected before or during the gravity field analysis in order to compute a representative mean value of the gravity field for a specific time period. This process is called gravity field de-aliasing. Here we address the gravity field de-aliasing for atmospheric masses together with the inverse-barometer assumption and its validation.

Local mass changes of the atmosphere are reflected in changes of the local pressure values at the Earth's surface. The surface pressure at a specific time represents the mass of the atmospheric column including its water content above a point on the Earth's surface at this time. The height of the atmospheric centre of gravity has to be taken into account for the determination of the de-aliasing gravity field spherical harmonic coefficients. Variations of the atmospheric masses are computed with respect to a mean atmosphere. The definition of this mean atmosphere is dependent on the de-aliasing concept to be used for the data analysis. If the static gravity field shall be determined a multi year mean atmosphere shall be used as reference. In case monthly gravity fields shall be computed the de-aliasing shall refer to a monthly mean of the atmosphere too. Any other combination is correct as long as the mean atmosphere covers the time period of the gravity field analysis. In case the mean atmosphere covers a longer period than the gravity analysis period, one can assume that the complete atmospheric gravity variations with respect to this mean atmosphere are taken into account. This is the procedure which is currently implemented for the GRACE monthly

mean fields, where a one year mean atmosphere is used (for year 2001). In other words, the current GRACE monthly gravity field solutions are corrected for atmospheric mass variations with frequencies from 6 hours (highest resolution of atmospheric models) to one year.

The atmospheric parameters required for the de-aliasing are extracted from global atmospheric models as they are operated by the European Centre for Medium Range Weather Forecast (ECMWF) or the National Centre for Environmental Prediction in the US (NCEP). To estimate the quality of the atmospheric models one can compare for example pressure fields from ECMWF and NCEP for the same time stamps. Such comparisons yield a RMS of the global differences of 1 to 1.5 mbar. However, this number has to be regarded as a lower bound, because systematic errors present in both models are not accounted for. Assuming that the above values are representative, errors in atmospheric corrections to gravity field coefficients can be estimated from the differences between both models and compared against the mission error predictions (see Figure 3.5.1). The figure shows that the atmosphere plays a significant role for the GRACE data analysis, while for CHAMP only the very long wavelengths and for GOCE gradiometry only a few terms are above the predicted error curves.

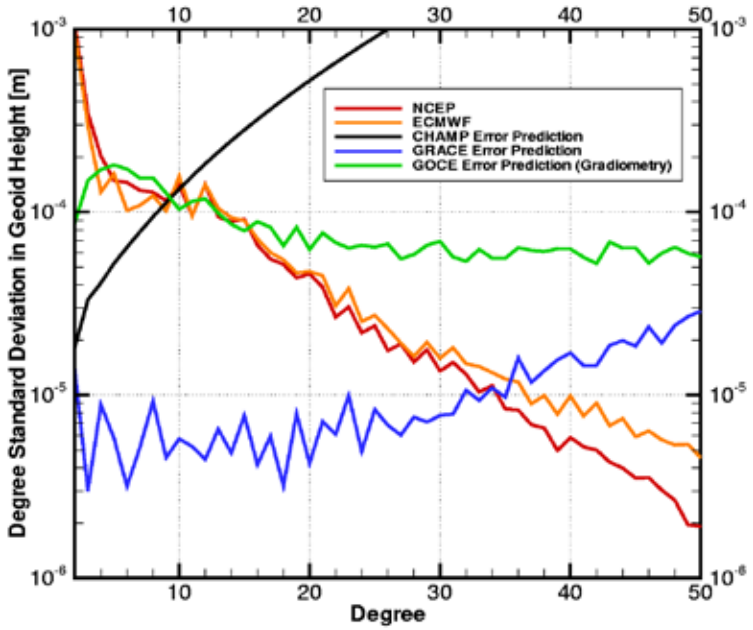

Figure 3.5.1*: Gravity signals computed from atmospheric models compared to mission predictions*

From Figure 3.5.1 one can also identify that there is a visible difference in the gravity field de-aliasing signals depending if ECMWF or NCEP data were used as input (all computations were made for the same date and time). These differences represent an estimate of the error that the atmospheric models induce to the final gravity field solutions for the missions.

As an example, Figure 3.5.2 shows the differences in terms of geoid heights that were obtained when using the ECMWF or the NCEP atmospheric data set for an arbitrary 6-hour period. Differences in the geoid height variations of up to ±1 mm are present which can be regarded as the 6-hourly error introduced by atmospheric models during de–aliasing. As GRACE is designed to observe geoid heights with mm accuracy up to degree and order 50 there are indications that such errors will fully be incorporated into gravity field solutions of this level of accuracy.

As the error estimates of the atmospheric models are somehow speculative, a validation of them shall be performed in order to better understand, what their level of uncertainty and what their im-

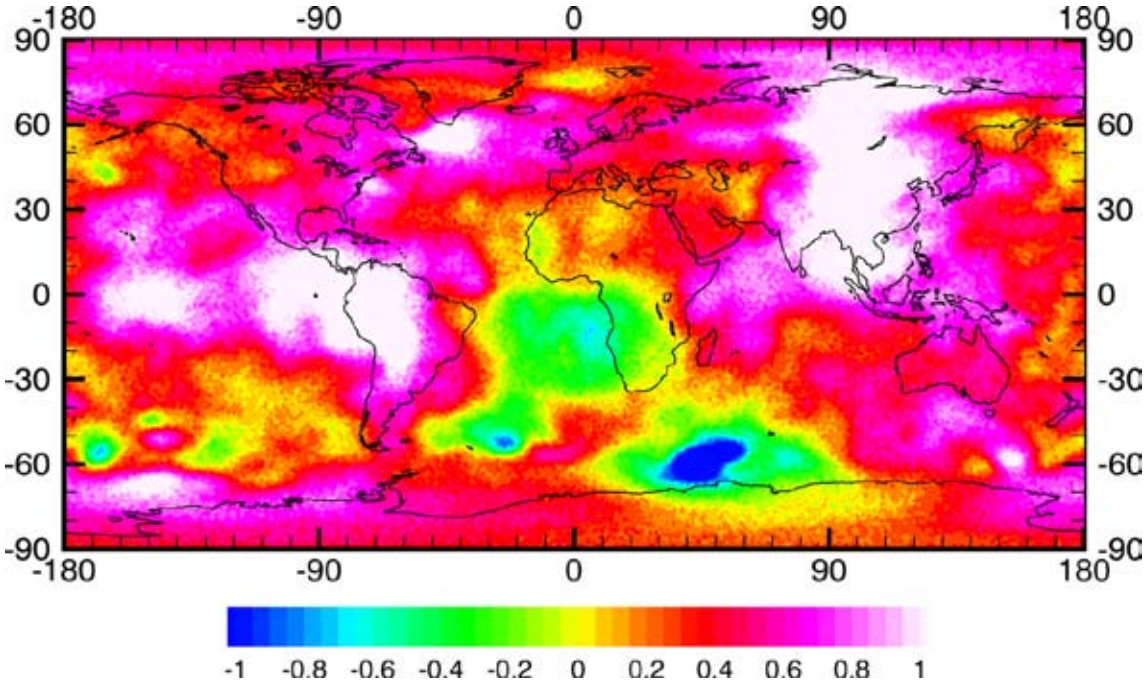

Figure 3.5.2*: Differences of geoid height variations between NCEP re-analysis and ECMWF operational analysis for an arbitrary 6-hourly time interval [mm].*

pact to the gravity field solutions is. The preliminary results shown above indicate such an influence, but are all based on the differences between two models. Such a validation shall be based on independent data from other Earth observing missions or ground based observations.

For this purpose ENVISAT with its atmospheric sensors MIPAS, and SCIAMACHY could provide independent validation data sets. Also the GPS radio occultation results from the in-orbit missions CHAMP and GRACE and from the planned COSMIC mission could significantly contribute to such a validation activity. If we can derive realistic error estimates from comparisons of the atmospheric models with in situ observations, their impact to the de-aliasing gravity coefficients can be estimated and finally also the error induced to the final gravity field solutions can be quantified.

A direct check of the consistency of atmospheric mass changes derived from gravitational signals with that derived from surface pressure and thus a quantification of the resulting accuracy of atmospheric corrections is feasible in areas where all other fluxes causing mass changes are known or negligible. This may apply to arid zones or deserts, where after long periods without rainfall any mass redistribution by evaporation or runoff can be excluded and changes in the gravity signal are due to atmospheric mass fluxes only.

Inverse barometer assumption

Up to now it was assumed that no compensation of the atmospheric masses by water mass redistribution over the oceans is present. This is the non inverse barometric assumption (non-IB). In reality this is not the case. The oceans respond within some time delay to the atmospheric mass variations by mass redistribution. If this time delay would be zero the ocean would immediately react on atmospheric mass variations by water mass redistribution such that it fully compensates them. This is called the full inverse barometer response (full-IB) of the ocean. Several investiga-

tions based on satellite altimeter data pointed out, that there is a significant deviation of the oceanic response to atmospheric mass variations from the full-IB assumption. This deviation in the mid and high latitudes mainly is caused by wind effects on the oceans. In opposite it was also identified, that true non-IB effects are present in the tropics. This implies that none of both assumptions (full-IB or non-IB) is fully correct. In order to correctly handle mass variations over the oceans an ocean model providing ocean bottom pressure with the same time and spatial resolution has to be used. This model shall use wind and other data in order to determine the real not compensated ocean mass variations, which represents the deviation from the full-IB case. These mass variations will again be validated by independent means. This could be done for example by combining altimetry with sea surface temperature and salinity observations from space (the latter are planned to be observed with the SMOS mission).

Tides

The presence of sun, moon and planets causes time variable gravity effects, which have to be considered before or during gravity field analysis. We distinguish between direct tides, which are the gravitational attractions of these bodies on the satellite itself and indirect tides, which cause deformations of the fluid and solid Earth as result of the tide generating forces. The quality of the direct tides depends on the knowledge of the gravitational constants of the Earth, sun, moon and the planets and the relative position between the satellite and these external bodies. As planetary ephemeris and the gravity constants of all bodies are known sufficiently well, the direct tides influence on the gravity field can be computed on a level of 10^{-8} and better corresponding to micrometer accuracy in terms of geoid heights. Indirect solid Earth tides are dependent on the same information than direct tides except that the Love numbers, which describe the elastic solid Earth response to external forces. The knowledge of the Love numbers as of today is sufficiently good for analysis of the new gravity mission data. It might turn out during gravity field analysis and comparisons with GPS station data that some Love numbers shall be readjusted.

The modelling of the indirect ocean tides is much more complicated. The ocean responds hydrodynamically to external tidal forces. This means, that several other parameters have to be taken into consideration in order to estimate the gravity effect of such water movements in the oceans (e.g. ocean depth). The whole correction is strongly dependent on local features in the oceans and therefore requires a much more complicated modelling. Actual ocean tide models strongly are based on the analysis of altimeter mission data with a suitable repeat orbit (e.g. TOPEX/POSEIDON and JASON-1). These models are known to be better than 3 cm RMS in terms of water heights in the open oceans. This error significantly increases on continental shelves and in coastal seas. The uncertainty of the ocean tide models and its impact on the gravity field determination can be estimated by differencing two actual models and regarding the residual effects in terms of gravity signal. Such an investigation shows, that the tide models significantly differ in coastal areas and towards the polar regions. These differences are larger than the measurement accuracy, which can be reached with GRACE. From this we can conclude that ocean tide models have to be improved for the purpose of time variable gravity field analysis. As the current gravity missions due to their orbit design are not well suited for tide modelling, other missions like the planned JASON-2 with a wide-swath altimeter could support this task. For the time being a map showing the uncertainty level induced from the existing tide models shall be generated, such that the user can identify in which areas there might be problems from the tide model in the data.

Earth core motion

In the Earth's core, there is a wide range of mass movements and oscillations such as core modes, inner and outer core nutation, and coupling at the core-mantle boundary. They cause gravity field variations, although their effect on the magnetic field is much more important (see chapter 4.2). The gravity field variations are very small, and most of them occur at short time scales that are not resolved by the CHAMP mission. For GRACE, recent work revealed that the sensitivity of the GRACE mission for the lowest harmonic degrees (degree 2 coefficients) is close to the time-variable gravity signal expected from the Earth core (Greiner-Mai et al., 2003). Nevertheless, as the signal to be resolved and the expected error budget for GRACE are on the same level it is not expected that these signals can be discriminated with the current gravity field missions. Therefore, the total effect of mass variations caused by Earth core motion will be taken into account, but the Earth's core is not included as a subject of research on its own within the proposed framework structure.

References

Chao, B.F. and Eanes, R., 1995. Global gravitational changes due to atmospheric mass redistribution as observed by the Lageos nodal residual. Geophys. J. Int., 122:755-764.

Dumberry, M. and Bloxham, J., 2004. Variations in the Earth's gravity field caused by torsional oscillations in the core. Geophys. J. Int., 159:417-434.

Földvary, L., and Fukuda Y., 2001. IB and NIB hypotheses and their possible discrimination by GRACE. Geophys. Res. Lett., 28(4):663-666.

Földvary, L., and Fukuda, Y., 2002: Effects of atmospheric variations on the marine geoid determined by forthcoming gravity satellite missions. IAG Symposia Proceedings, No. 125, 187-192, Vistas for Geodesy in the New Millenium, Ed. Adam, Schwarz, Springer Verlag.

Gaspar, P., and Ponte R.M., 1997. Relation between sea level and barometric pressure determined from altimeter data and model simulations. J. Geophys. Res., 102(C1):961-971.

Greiner-Mai, H., Jochmann, H., and Barthelmes, F., 2000. Influence of possible inner-core motions on the polar motion and the gravity field. Physics of the Earth and Planetary Interiors, 117, 81-93.

Greiner-Mai, H., and Barthelmes, F., 2001. Relative wobble of the Earth's inner core derived from polar motion and associated gravity variations. Geophys. J. Int., 144:27-36.

Greiner-Mai, H., Jochmann, H., Barthelmes, F., and Ballani, L., 2003. Possible influences of core processes on the Earth's rotation and the gravity field. J. Geodyn., 36:342-358.

Gruber, Th. and Peters, Th., 2003. Time variable gravity field: using future Earth observation missions for high frequency de-aliasing. Proceedings of IERS Workshop on Combination Research and Global Geophysical Fluids, Munich, IERS Technical Note No. 30, 157-160 Ed. B. Richter, Verlag des Bundesamtes für Kartographie und Geodäsie, Frankfurt/Main.

Hirose, N., Fukimori, I., Zlotnicki, V., and Ponte, R.M., 2001. Modeling the high-frequency barotropic response of the ocean to atmospheric disturbances: sensitivity to forcing, topography, and friction. J. Geophys. Res., 106(C12):30987-30995.

Knudsen, P., Andersen, O., Abbas Khan, S. and Høyer, J., 2001. Ocean tides effects on GRACE gravimetry. IAG Symposia Proceedings, Vol. 123, Ed. M. Sideris, p. 159-164, Springer Verlag.

Knudsen, P. and Andersen, O., 2002: Correcting GRACE Gravity Fields for Ocean Tide Effects. Geophys.Res. Lett., 29(8), doi:10.1029/2001GL014005.

Knudsen, P., 2003. Ocean tides in GRACE monthly averaged gravity fields. Space Science Reviews, 108:261-270, Kluwer Academic Publishers.

Ponte, R.M., and Gaspar, P., 1999. Regional analysis of the inverted barometer effect over the global ocean using Topex/Poseidon data and model results. J. Geophys. Res., 104(C7):15587-15601.

Ponte, R. M. and Ray, R.D., 2002. Atmospheric pressure corrections in geodesy and oceanography: A strategy for handling air tides. Geophys. Res. Lett., 29(24):2153, doi: 10.1029/2002GL016340.

Ray, R.D., Eanes, R.J., Egbert, G.D., and Pavlis, N.K., 2001. Error spectrum for the global M2 ocean tide. Geophys. Res. Lett., 28(1):21-24.

Ray, R.D., Rowlands, D.D., and Egbert, G.D., 2003. Tidal models in a new era of satellite gravimetry. Space Science Reviews, 108:271-282, Kluwer Academic Publishers.

Ray, R.D. and Ponte, R.M., 2003. Barometric tides from ECMWF operational analyses. Annales Geophysicae, 21:1897-1910.

Reigber, Ch., Barthelmes, F., Greiner-Mai, H., Gruber, Th., Jochmann, H., and Wünsch, J., 1999. Temporal gravity field variations from oceanic, atmospheric and inner core mass redistributions and their sensitivity to new gravity missions CHAMP and GRACE. Bolletino di Geofisica Teorica ed Applicata, 40(3-4):329-340.

Schrama, E.J.O., 1995. Gravity missions reviewed in the light of the indirect ocean tide potential. IAG Symposia Proceedings No. 116, pp. 131-140, Springer Verlag.

Schrama, E.J.O.. 2004. Follow-on gravity missions and their physical limitations. Paper submitted to Earth, Moon, and Planets.

Swenson, S. and Wahr, J., 2002. Estimated effects of the vertical structure of atmospheric mass on the time-variable geoid. J. Geophys. Res. 107(B9):2194, doi:10.1029/2000JB000024.

Thompson, P.F., Bettadpur, S.V., and Tapley, B.D., 2004. Impact of short period, non-tidal, temporal mass variability on GRACE gravity estimates. Geophys. Res. Lett., 31:L06619, doi: 10.1029/2003GL019285.

Velicogna, I., Wahr, J., and van den Dool, H., 2001. Can Surface Pressure be used to remove atmospheric contributions from GRACE data with sufficient accuracy to recover hydrological signals. J. Geophys. Res., 106(B8):16415-16434.

4 A common frame for the Earth system: integration and synergies

The gravity field and altimetry missions give us a new tool to observe mass signals. However, in order to study and understand each individual mass phenomenon, the interrelations with all others have to be considered. Mass exchanges between the system components must be modelled consistently. Major challenges are the separation of superimposed mass signals and the homogeneity of reference systems and standards in all involved disciplines.

4.1 Mass transport processes: parts of a comprehensive system

In Chapter 3, mass transport and mass distribution associated with a wide range of processes from the various parts of the Earth system have been discussed in detail, outlining the current status of modelling and future perspectives for each of them. It has been shown that by the new satellite gravity and altimetry data mass signals can be detected which cannot be detected by other means, and thus a fundamentally new research field for modelling and understanding of very central processes in the Earth system is opened.

Now the question will be addressed, why an intensive cooperation between the different research areas is required in order to reach substantial progress on each individual field. It will be pointed out that research on each of the individual processes described in this report would benefit considerably from the integration into a *joint research framework*.

The overall structure of the proposed research framework is, once again, outlined in Figure 4.1. The new satellite data, shown on the left hand side of the Figure, are the common basis for all applications. The central research fields, represented by the boxes to the right, are now complemented with some keywords taken from Chapter 3. The colour circles connecting the central research fields symbolize the interactions and interconnections between the fields. The atmosphere with its special role (cf. Chapter 3.5) surrounds the system components. The yellow box contains the key elements of geodetic analysis of the satellite data which will warrant the consistent use of the data in all applications and enable the separation of effects and the mutual exchange of model results.

The individual research projects in this common framework are connected due to three basic facts, which are:

1. Complementarity of gravity and altimetry missions: For many of the proposed applications, the exploitation of satellite gravity or altimetry data alone is not sufficient, but the combination of both is needed, as well as the combination with other complementary missions. This is particularly challenging, because the mass signals to be determined are so small, and because the sensor systems and data types to be combined are profoundly different.

2. Mass exchange: For many of the described processes, the exchange of masses between system components, i.e. between oceans, ice and land masses is of central importance. Output from one process represents intput for other processes.

3. Separation of integral signals: The satellite observations result from the sum of all mass changes in the Earth system. A strategy has to be established to identify the contribution of each individual mass change. The better we understand all other signal components, the better we can extract and use one single component of interest.

The long term goal must be to build a *comprehensive global model for mass transport and mass balance* in the Earth system. This will lead to a much deeper understanding of the individual processes, and will enable forecasts of Earth system behaviour. The authors agree that such a comprehensive model is not feasible on the short run. A valid starting point is the coupled modelling of some processes, such as the combined modelling of glacial isostatic adjustment and recent ice mass change in the polar regions. In other cases, closed sub-systems will be dealt with whereby the interface with other system components is to be defined, and exchange of results will take place by means of correction terms. In this sense, the aim of the proposed framework is to develop methods for an interactive modelling of the involved Earth system components.

4.2 Neighbouring fields: magnetic field and Earth rotation

This report does not cover all mass transport processes and mass distributions in the Earth system. The fields proposed as core elements of this joint research framework (Figure 4.1) are those, for which the gravity field missions in combination with satellite altimetry enable completely new approaches.

On purpose, the framework will not include projects on magnetic field effects (because these are subject to a DFG priority program on its own), and Earth rotation (which is subject of a DFG research group). The interrelations with these fields will be taken into account, however, to the necessary extent.

The combination of gravity and magnetic field data for a more complete Earth system understanding could be very interesting for future research, not only for the study of the Earth's core, but also for the atmosphere and possibly for ocean circulation and tides. On CHAMP, this combination is realized from the observational side. However, due to the currently running DFG priority program, for the proposed framework it is recommended to restrict to gravity and altimetry as core data.

Variations of Earth rotation are subdivided into nutation, variation in spin rate and polar motion. Any mass change in Earth system and any relative forcing between Earth system components result in variations of Earth rotation. As gravitation, the observed Earth rotation parameters (length-of-day and polar motion) reflect the integral effect of all exchanges of angular momentum in Earth system. The separation of effects is possible by means of typical time periods of the indi-

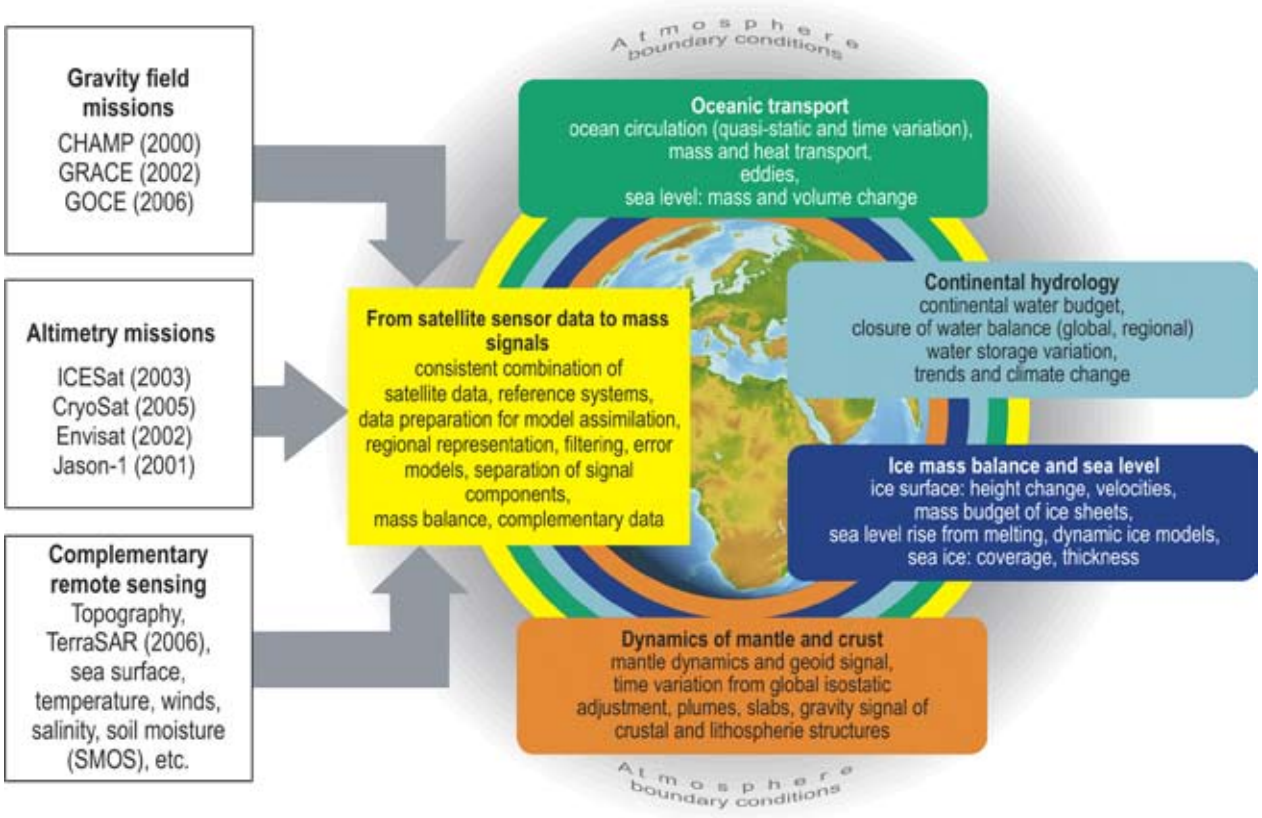

Figure 4.1: *The new satellite data serve as common basis for the modelling of mass transport and mass distribution in the Earth system. The right hand side of the figure gives an overview of the main research fields. The coloured rings symbolize the interconnections which are due to physical reasons, but also resulting from observational data characteristics.*

vidual effects or based on external models. Earth rotation analysis ideally complements the gravity field and altimetry approach to mass transports. At the time of writing, a special research group on *Earth rotation and global geodynamic processes* is being established by the DFG, based on a concept document by Schuh et al. (2004). A close cooperation with this group is planned.

4.3 Synopsis of signal components and amplitudes

In Chapters 2 and 3, numbers of required accuracies and estimated signal amplitudes are discussed in various places. For the gravity field, a summary of this information is compiled in Tables 4.1 and 4.2, augmented by some further estimates from other sources (NRC 1997, Rummel et al., 2003). Table 4.1 shows the requirements on the *static* gravity field in terms of geoid heights and gravity anomalies, and the required spatial resolution, from the main areas of modelling. These requirements will essentially be met by the GRACE and GOCE gravity field models.

Table 4.2 lists the gravity field *time variations*, showing the typical signal amplitudes, typical spatial scales and time periods, as estimated today. The signal amplitudes are still subject of discussions, as simulation results vary considerably, some giving regional extreme values, others global standard deviations. The consolidation of these numbers will be among the tasks of the proposed

research program. Therefore, in Table 4.2 (as in Table 4.1) only orders of magnitude are given, which are rather certain in most cases.

The comparison of these signal amplitudes with the expected mission performance of CHAMP, GRACE and GOCE as discussed in Chapter 2 (see Table 2.1, Figures 2.7, 2.8 and 2.9) shows that the amplitudes of most signal components exceed the gravity field errors and are thus in the measurable range, at least for large spatial scales. For the small numbers for secular changes in Table 4.2, it has to be taken into account that the accuracy of linear trend determination improves fast with increasing mission duration: From 5 years of monthly gravity field solutions, each of them with an accuracy of 0.01 mm in terms of geoid for the best resolved spherical harmonic degrees (see Figure 2.9), a linear trend in geoid variation can be estimated with an extremely high accuracy of about 0.8 μm/y for these degrees. Thus, also very small secular changes such as the signals expected from mantle plumes will possibly be detectable.

When looking at the numbers for the time variations in Table 4.2, one should keep in mind that any observation even being only slightly above the error level is already very valuable and represents a completely new piece of information on mass transport processes.

An impression of the type of interconnections between the processes and disciplines is given by Figure 4.2, which is showing the spatial and temporal scales of geoid signals caused by the various Earth system processes in synoptic way (adapted from Rummel et al., 2003). For both, space and time, one has to deal with a wide variety of scales, ranging from static down to very high frequent signals in the time domain, and from local to global scales in the space domain. The bubbles of the various signals superimpose each other in many places. Some processes have signals ranging over nearly the entire spectrum, such as ocean circulation, or hydrology. The Figure also shows the expected limits of spatial and temporal resolution for the gravity field missions CHAMP, GRACE and GOCE. It becomes clear that the signal of some processes is partly or entirely beyond the time or space resolution of these satellite missions. Signals with spatial scales smaller than 70 km will not be resolved in the next few years, although we hope to extend this limit with future missions. In the time domain, the current resolution limit is given by the monthly GRACE gravity field solutions. Higher frequency signal components, with periods from hours to days, e.g. tides or high frequency atmosphere variations, tend to alias into the observed time series. To keep this under control, for these components reductions using the best available models have to be applied. Altogether, with the current missions we can achieve considerable progress in

Table 4.1: *Static gravity field requirements for mass transport and mass distribution modelling*

Application		Accuracy		Resolution
		geoid [cm]	gravity [mGal]	[km half-wavelength]
ocean circulation and transport	short scale sea surface topography	1		100
	basin scale sea surface topography	0.1		1000
ice dynamics	rock basement		1	50
	ice height reference	1		100
Earth mantle and crust	crust and lithosphere structure, plate boundaries	10	1	50
	mantle convection	10	1	200
	mantle plumes	10	1	50
	sublithospheric convection, oceanic asthenosphere	10	1	100
geodesy	unified height systems, tide gauges	1		100
	GPS levelling	1		100
	orbits (LEO)		0.01	200

Table 4.2: *Time variable gravity field signal components: amplitude, spatial scales and main periods. Secular signal amplitudes are given in mm/year, µm/year or µGal/year. Amplitudes referring to other time periods are given in mm or µGal.*

Application		Amplitude		Spatial scales	Main periods
		geoid	gravity	(km)	
ocean circulation and transport, sea level	ocean currents, deep circulation, eddies, sea level	10 mm 0.01 mm/year	10 µGal	30-5000 1000-5000	(sub-) seasonal to interannual, secular
ice	ice sheet mass balance	1 mm 0.01 mm/year	1 µGal	100-4000 5000	(sub-) seasonal to interannual secular
Earth mantle and crust	glacial isostatic adjustment	1 mm/year	1 µGal/year	500-10000	secular
	mantle plumes, slabs	1 µm/year	0.01 µGal/year	100-2000	secular
	tectonics, orogens	1 µm/year	1 µGal/year	100-2000	secular
continental hydrology	water storage, evapotranspiration, runoff, exchange with oceans	10 mm	10 µGal	100-5000	some weeks to interannual
atmosphere		10 mm	10 µGal	50-5000	annual, seasonal, daily, others
tides	solid Earth and ocean tides	1000 mm	100 µGal	10-10000	daily, semi-daily, semi-monthly

many areas, but we will not be able to cover all processes relevant for mass transport and mass distribution. The present missions are a first important step for mass transport and mass distribution monitoring in Earth system research.

4.4 Common challenges for satellite data analysis

This section addresses the topics in the yellow rectangle of Figure 4.1, which are prerequisite for the derivation of mass signals from the satellite data products, and concern all geophysical applications. The box represents the interface between the satellite geodetic sensor data and the various geophysical disciplines. It provides the processing chain from sensor data to mass signals, and supports geophysical modelling in transforming the mission data into a format and representation adequate to data assimilation requirements.

Consistent combination of missions

The combination of data products from different satellite missions allows some of the most interesting and novel applications:

- The static geoid from GRACE and GOCE will be combined with the sea surface as derived from the ocean altimetry missions in order to determine global dynamic sea surface topography, which is the deviation of the sea surface from a state of rest. This allows a completely new and direct way of modelling the quasi-static ocean circulation, and has important implications for the determination of mass and heat balance, for climate and ocean forecasting (cf. Chapter 3.1).

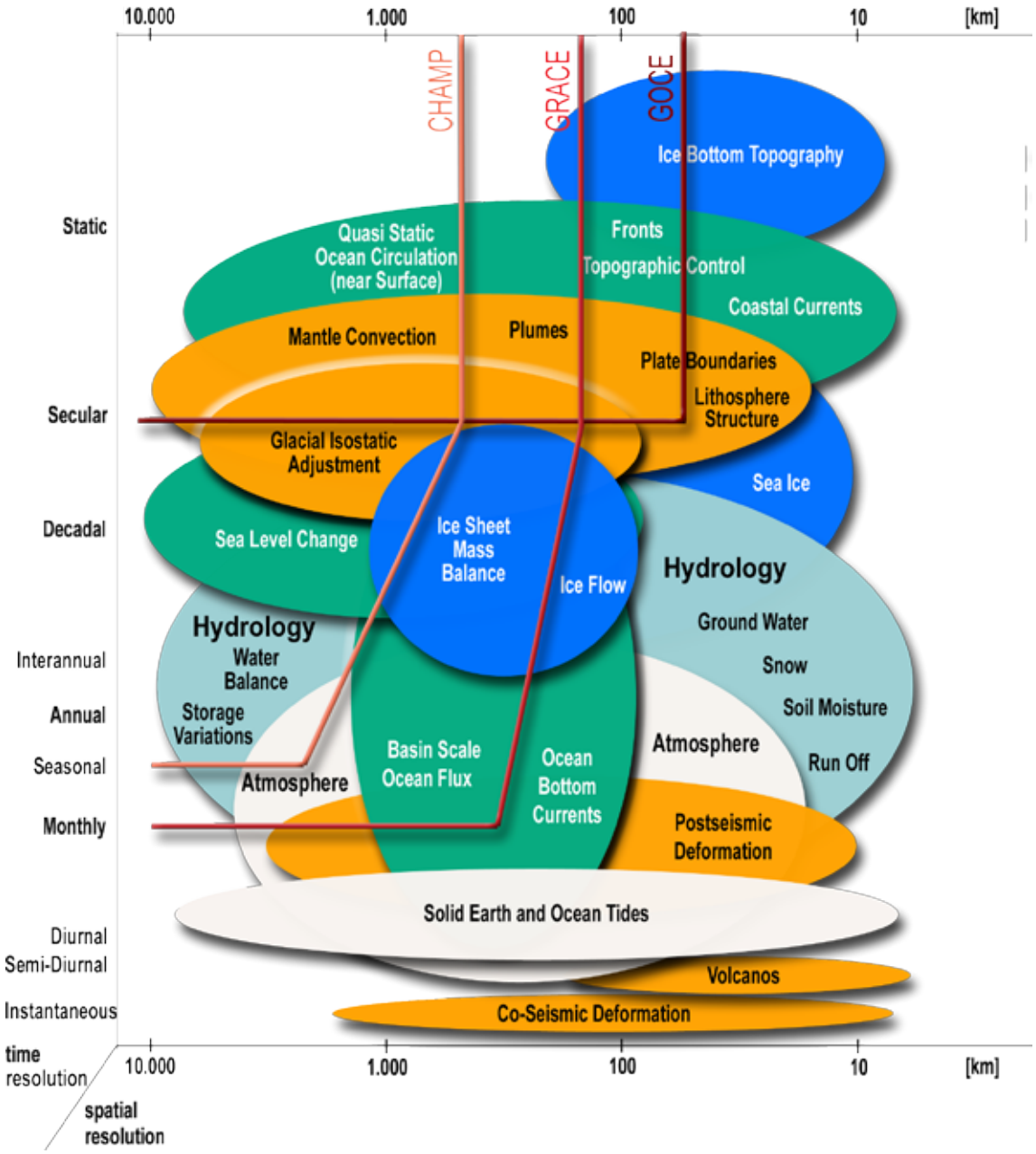

Figure 4.2: *Spatial and temporal scales of geoid signals associated to solid Earth (orange), ocean (green), ice (dark blue) and continental hydrology (light blue) processes. The red lines show the spatial and temporal resolution limits of the CHAMP, GRACE and GOCE missions.*

- Mass variations as derived from GRACE over the oceans can be combined with geometric variations of the sea surface height from altimetry in order to identify the temperature dependent (steric) component of sea level variations (cf. Chapter 3.1).
- Mass variations from GRACE over ice sheets in combination with height changes from ICESat and CryoSat, together with ground based GPS, will allow to analyse the complex superimposition of glacial isostatic adjustment, recent ice mass changes and ice compaction (cf. Chapter 3.2 and 3.3).

With such combinations, a number of new research tasks arise: Each satellite mission has its specific sampling and resolution in space and time. In particular, gravity missions – measuring

a field quantity – have characteristics very different from those of altimetry missions. Thus, an optimal fusion of time series from both types of missions is to be found – with minimum loss of signal content – and to be adjusted to the requirements of the assimilation models. To adapt the sampling, interpolation in space and time is required. To adapt the resolution, filtering may be required. As an example, the results for dynamic sea surface topography would be heavily disturbed without a consistent low-pass filtering of geoid and altimetric data. For satellite altimetry, special focus will be given on multi-mission combinations exploiting the sampling characteristics of the various missions, in order to obtain long time series for the ocean and ice surface geometry, with both high temporal *and* spatial resolution, a task which single satellite missions cannot fulfil.

Not only the signal data, but also the corresponding stochastic models have to be established and combined in a consistent way. This is an ambitious task because the error characteristics of the data sets vary considerably.

Reference systems and standards

The geometric and gravimetric signals to be analysed are very small. Only due to the enormous technological progress of recent years they became observable with adequate precision, and spatial and temporal resolution. The required relative precision is close to 1 p.p.b. (10^{-9}), corresponding to 1 mm for distances of 1000 km or 1 μGal relative to "*g*". It is a great challenge to transport the 1 p.p.b. precision from the sensor systems through various transformations into the geophysical mass related models, and to maintain this standard when exchanging data between all involved models.

The link of the various space segments (satellite sensors) is established via the orbits, i.e. via the tracking systems and ground stations. The objective will be to combine all data, from space segments and terrestrial systems, with a precision of 10^{-8} to 10^{-9}, relatively, in one global reference system, and to keep this combination consistent in space and in time over decades. This objective is precondition in particular for the detection of anomalous trends in time and space.

The lowest degree coefficients of the satellite gravity models, where the reference system and the scale are imprinted, have to be analysed carefully. The global height system requires particular attention, as it provides the connection between land surface, ice and ocean, by means of tide gauges and control markers on land and ice. Furthermore, all included reduction models such as solid Earth and ocean tides, polar tides, and ocean loading have to be applied in a consistent manner for all quantities to be determined. These problems are probably greatly underestimated at present. Any violation of a consistent processing will lead to systematic distortions, with the danger of an erroneous interpretation in terms of geophysical significance.

The efforts for a high precision and consistent reference system fit to the aims of the international geodetic-geodynamic community to establish an Integrated Geodetic-Geodynamic Observing System (IGGOS). Such a system will integrate the observables of the geometric shape, the gravity field and the rotation of the Earth, with the reference system as the very central issue. In the past, the gravity field was a weak element of such an integrated observing system, which is changing now due to the present gravity missions.

Data preparation for model assimilation

The mass signals derived from the satellite data are given in a certain appropriate mathematical representation, typically in spherical harmonic representation, as global grids, or along satellite tracks. These have to be made compatible with the mathematical representation (in space and time) that is chosen for the geophysical models, such as triangular meshes or 3D grids for ocean

circulation models, river catchment boundaries for hydrological modelling, point values, profiles, and others. This, again, has to be accomplished with minimum loss of information. It also includes the appropriate treatment of truncated high frequency signal and of aliasing.

The study of representation and parameterization when introducing satellite data into the application models must become a central task in the proposed joint research framework. Similar considerations apply when introducing complementary data (see below).

Separation of signal components

The satellite observations represent integral signals containing components of all mass related processes. To separate them and to identify the contributions of each individual process is generally seen as one of the most challenging scientific issues for the coming years. Time variations from oceanic variability, from glacial isostatic adjustment, tectonics at plate boundaries, ice mass changes, variations in continental water storage and from atmospheric mass sum up to an integral signal. The superposition of effects can be seen in Figure 4.2. This applies certainly to the gravity field signal, but to some extent to the geometry signal from altimetry, too: For example, in Antarctica, height changes measured by ICESat and CryoSat contain the sum of vertical movements due to the glacial isostatic adjustment and of ice thickness changes. GRACE, in turn, is measuring the superimposed mass effect of glacial isostatic adjustment mass variations and ice mass changes. The signal superposition is particularly pronounced for sea level change. The measured sea level variations contain contributions from thermal expansion, ocean current changes, ice melting, changes in precipitation and river runoff, and from vertical land and ocean floor movements.

A strategy for signal separation has to be developed based on the following available elements:

- Separation in space domain using regional signal characteristics, e.g. by filtering out the signal component for a river catchment or a certain tectonic unit,
- Separation in time domain based on long time series, isolating typical time periods such as annual and semi-annual periods,
- Separation in spectral domain using spectral characteristics in space (e.g. for the separation of glacial isostatic adjustment and ice mass changes) and time (e.g. for hydrology using characteristic response times, cf. Chapter 3.4),
- Use of known geophysical contributions based on models such as atmospheric models,
- Use of complementary terrestrial / in-situ data. Important examples are deep sea pressure gauges in the case of ocean bottom pressure variations, GPS vertical land movement observations for glacial isostatic adjustment, hydrological data from well observed areas, terrestrial gravity data for continental plate boundaries, or permanent superconducting gravimetry for the identification of local gravity variations e.g. due to ground water variations,
- Use of complementary remote sensing mission data: sea surface temperature, salinity, winds, soil moisture, snow, deformations, see the corresponding box in Figure 4.1,
- Mutual exchange of mass transport estimates as derived from models of individual Earth system components (ocean, hydrology, solid Earth and ice). In general, the process modelled with the inferior accuracy will benefit from the output of all other areas in order to isolate its own contribution,
- Use of special satellite configurations, crossovers, and repeat orbits, in order to reduce high frequency variations (periods of hours or days in tides, atmosphere, hydrology, etc.) and to avoid aliasing.

For the separation approaches, see also Tables 4.4 to 4.11 below.

Mass balance determination

Besides the extreme accuracy, one of the strongest advantages of the new satellite data is the completeness of coverage. Geoid, gravity and their time variation are measured with global coverage by the gravity field missions. From the new generation altimetry satellite missions, the surface geometry and its time variation are obtained for the entire oceans (ice-free and ice-covered), for the entire ice sheets and for glaciers, with the exception of very tiny polar gaps. The issue of completeness is particularly important for the study of mass transport balance. In-situ data may sometimes be more accurate or cover a longer time span, but only for single points or regions. They are very valuable, e.g. for the separation strategy. But a reliable knowledge of mass balance requires the observation of the processes as a whole, i.e. for the complete oceans, for whole continents or ice sheets, which can only be realized by the new satellite missions.

4.5 Interconnection tables for the individual processes

In the following, for all major mass related processes the interconnections between processes and data sets are collected, see Tables 4.3 to 4.11. The number and intensity of interconnections underlines the need for interactive modelling between the involved research disciplines, and the necessity of a joint research framework. The collection is based on the discussion of the individual processes in Chapter 3.

Table 4.3 gives an overview in matrix form. The matrix entries show processes, for which interconnections exist. The matrix is well filled. The number of entries demonstrates that all these processes form one unity.

Tables 4.4 to 4.11 contain the following entries for each of the main processes and research fields:

- *interacting processes*, by exchange of mass and energy (heat), or by interaction of forces;
- *superimposed signal components*, mass and/or geometry signals, caused by other processes acting in the same geographical region, which have to be considered and separated from the signal component of interest; these cases require an interactive modelling of all involved processes and an exchange of results;
- *data products from the new satellite missions*; in many cases the combination of two or three data types is needed;
- *complementary data and models*, and
- *approaches for the separation of signal components*.

The tables reflect an assessment of the current status and will probably undergo changes with time. After each of Tables 4.4 to 4.11, the most important interconnections and synergies are explained. Some aspects appear repeatedly, as it is natural for interconnections between several fields.

Table 4.3: *Interconnection matrix; black dots on red cells indicate considerable interactions between processes or superposition of signal components, circles on light red cells indicate less intensive interconnection.*

	quasi-static ocean circul.	time variable ocean circul.	ice mass balance	glacial isost. adjustment	sea level change	mantle convection	subduction zones	hydrological cycle
time variable ocean circulation	●							
ice mass balance		●						
glacial isostatic adjustment		●	●					
sea level change	○	●	●	●				
global mantle dynamics				●	○			
subduction zones		○		●		●		
hydrological cycle	○	●	●	○	●		○	
atmosphere mass variation	●	●	●		●			●

Table 4.4 Quasi-Static Ocean Circulation	
Research Topics: major questions of global climate: how much heat does the ocean transport and redistribute; determination of global absolute surface velocities, climatologic 3D circulation and associated transports of heat, mass, nutrients and trace substances, ocean – atmosphere exchange of heat and mass, interaction of mean flow and eddy field, role of ocean bottom topography	
Interacting Processes, Superimposed Signals:	
time variable ocean circulation, sea level anomalies (time variation of sea surface), eddies, tides, loading effects, coastal bathymetry	
Data from the New Missions:	**Complementary Data and Models:**
static high resolution geoid altimetric sea level: mean and time variation precise gravity field for altimeter orbit corrections	ocean circulation models hydrographic in-situ data (ocean temperature, salinity) velocities from moored instruments and drifters sea surface temperature and salinity from remote sensing (e.g. SMOS) tide models, tide gauges marine gravimetry, bathymetry future: altimetry by GNNS reflections, wide swath altimetry
Approaches for Separation of Signal Components:	
accurate and consistent modelling of sea surface time variability (consistent time series, improvement of spatial-temporal interpolation) comparison of long time averaged observations with solutions from steady state forward and inverse models improvement of tide and loading modelling	

In the past, when oceanographers approached questions concerning the climate, they had no possibility to use measured dynamic sea surface topography for their purpose. Until now dynamic topography could only be measured at coastal tide gauges. With the new and accurate geoid information a reference surface for altimetry is available and oceanographers can use a novel type of data for comparison and assimilation into circulation models. It is expected that when assimilating the absolute sea surface topography into ocean circulation models, many features will appear that have not been visible in the past, when modelling was only based on oceanographic in-situ data. The in-situ data, however, remain very important for the deep ocean, and the optimal combination of these very different data types (satellite gravity, satellite altimetry and in-situ data) is one of the major challenges in this field.

The altimetric sea surface necessary for this approach cannot be derived from a single satellite mission, but one has to advance the strategies for multi-mission combination in order to get the best possible spatio/temporal coverage of the dynamic sea surface topography. Here another synergy effect is the accuracy improvement for the past altimetry missions when using the new satellite gravity field models for orbit recomputation and reanalysis.

Table 4.5 Time Variable Ocean Circulation	
Research Topics: intraseasonal and interannual variations of the ocean in relation to mean flows and transports, global and regional sea level change, distinction between mass and volume changes, increase in heat storage related to global climate change, ocean response to El Nino, the North Atlantic Oscillation and changes in the atmosphere, ocean bottom pressure anomalies and associated changes in shape of the Earth and Earth rotation, eddy induced mean flow, generation of eddies by instability of the mean flow	
Interacting Processes, Superimposed Signals:	
mass exchange between atmosphere, ocean, land and cryosphere atmospheric mass variation over land and ocean, deviation from inverse barometer model tides, loading oceanic response to varying atmospheric conditions sea ice coverage and freshwater transports by sea ice	
Data from the New Missions:	**Complementary Data and Models:**
time variation of the geoid time variation of altimetric sea level time variation of shape of inland ice time variation of sea ice coverage and thickness	ocean circulation models hydrographic in-situ data deep sea pressure gauges velocities from moored instruments and drifters sea surface temperature and salinity from remote sensing tide models, tide gauges Earth orientation parameters future: altimetry by GNNS reflections, wide swath altimetry
Approaches for Separation of Signal Components:	
separation of volume and mass changes based on gravity and sea surface height changes combination with deep sea pressure gauges support by atmospheric models and data support by continental water balance results and ice sheet modelling improvement of tidal and loading modelling	

Time varying ocean circulation can only be studied reasonably if the mean circulation is known sufficiently well. Realistic ocean modelling always includes time dependence and interaction between mean (i.e. average) circulation and temporal variations. Their interaction is a key research topic in oceanography at present. Therefore, both the study of high resolution mean conditions based on GOCE as well as mass changes derived from GRACE offer unprecedented opportunities to oceanographers.

For time variable circulation, satellite gravity and altimetry missions support each other. The sea surface height changes (anomalies) observed by altimetry satellites contain a volume (density) and a mass component, which cannot be distinguished by altimetry alone. With mass change observations from GRACE, the distinction becomes possible. Thus, by the combination of satellite data, one can determine (1) mass changes due to circulation variations, e.g. from deep ocean circulation variations, and due to melting and other freshwater inflow, and (2) the steric volume expansion of water due to variations in temperature and salinity in the deep ocean and at its surface. Both results are needed for ocean circulation modelling, and they are necessary in order to understand present sea level rise.

Due to the mass exchange between the ocean, the continental water cycle (river runoff), the atmosphere (precipitation, evaporation) and the ice masses (discharge, melting, sea ice transport), ocean modelling depends very much on a better understanding of processes on these fields.

Table 4.6 Ice Mass Balance	
Research Topics: altitude change of ice sheets and ice caps, ice flow velocity, accumulation/mass discharge, sea level change	
Interacting Processes, Superimposed Signals:	
glacial isostatic adjustment (GIA) snow / ice compaction atmospheric and oceanic mass variation tectonic motions	
Data from the New Missions:	**Complementary Data and Models:**
ice altitude changes time variable and static geoid and gravity	altitude change from GPS ice velocity from GPS, INSAR and modelling radar echo sounding data sea level change from tide gauges and modelling glaciological and climatological data from ice cores meteorological data absolute gravimetry, airborne gravimetry dynamic ice flow models viscoelastic Earth models atmosphere and ocean models
Approaches for Separation of Signal Components:	
joint determination of altitude change, firn density change and ice mass balance consideration of glacial isostatic adjustment using viscoelastic Earth models and 3D GPS displacements corrections from atmosphere and ocean models corrections from compaction models	

The signals of the recent ice mass balance of the ice sheets are superimposed by the strong secular glacial isostatic adjustment signal (see Table 4.7). Both processes cause mass changes as well as surface height changes. The latter are also caused by densification of the surface firn layer. The combination of GRACE mass change observations together with surface height changes from ice altimetry missions and GPS measurements of bedrock uplift is expected to be particularly valuable to resolve this complex superimposition. With this combination also ice compaction (ice density) models could be validated, which is considered as one of the key uncertainties for ice mass balance determination today.

For the polar regions, the combination and mutual validation of satellite data and ground data is of particular importance. Table 4.7 shows that a broad range of complementary terrestrial data can be introduced. These data sets have to be extended in the near future for a sufficient spatial and temporal coverage of mass variations. The impact of each data type for ice mass balance modelling has to be carefully assessed.

A very central issue is, of course, the interconnection between ice mass balance and all sea level observations. With the improved results expected from the new satellite data, substantial progress on this field will be achievable.

Table 4.7 Glacial Isostatic Adjustment (GIA)	
Research Topics: vertical movement, 3D displacement, internal mass redistribution, sea level change, 3D distribution of mantle viscosity, development of Pleistocene land ice	
Interacting Processes, Superimposed Signals:	
recent ice mass balance absolute sea level change tectonic vertical movement hydrological and oceanic mass variations	
Data from the New Missions:	**Complementary Data and Models:**
time variation of the geoid ice altitude changes	vertical movement from repeated levelling and from paleo-shorelines 3D displacement from GPS mass redistribution from absolute gravimetry and modelling sea level change from tide gauges, GPS and modelling mantle viscosity from viscoelastic Earth models Pleistocene land ice from geomorphology and modelling dynamic ice flow models viscoelastic Earth models hydrological and ocean models
Approaches for Separation of Signal Components:	
joint determination of 3D displacement, internal mass redistribution and sea level change consideration of recent ice mass balance and absolute sea level change consideration of tectonic vertical movement corrections from hydrological and ocean models	

The aspects of glacial isostatic adjustment (GIA) are manifold. One of them concerns the prediction of various signatures related to GIA. An important signature is the relative sea level change induced by GIA. This is of particular significance for estimating the global sea level rise caused by the recent melting of the polar ice sheets and ice caps and the mountain glaciers. Therefore, the interconnection between GIA and all sea level related observations is very close. Another GIA signature is the temporal gravity variation associated with readjustment processes. In view of their size, the rebounding areas of Canada, Fennoscandia and Antarctica are of particular importance, and the resulting secular gravity trends are expected to be part of the gravity variation recorded by GRACE. Forward calculations therefore serve to correct monthly GRACE solutions for the influence of ongoing GIA. On the other hand, after a satellite mission duration exceeding five years it should become possible to extract the GIA induced secular gravity change over Canada directly from the GRACE data. For Antarctica and Greenland, the GIA mass change is superimposed by present ice mass changes. Therefore, ice mass balance results based on ice altimetry can support GIA modelling. Together with complementary data, such as GPS, it will be possible to invert for the viscoelastic stratification of the Earth's mantle and, thus, to improve our constraints on the viscosity model. The viscosity model, in turn, represents the interconnection to global mantle dynamics, because it is vital for models of mantle convection and the evolution of the Earth.

Table 4.8 Sea Level Change	
Research Topics: global sea level change, pattern of spatial variation, distinction of mass exchange from volume change, quantification of single contributions, separation of recent variations from long term change	
Interacting Processes, Superimposed Signals:	
vertical land movement: tectonics, glacial isostatic adjustment melting of ice sheets and glaciers hydrological cycle volume change due to temperature changes change in composition of ocean properties, velocities, dynamical sea surface topography tides, loading effects, atmospheric mass variations, water exchange with atmosphere	
Data from the New Missions:	**Complementary Data and Models:**
quasi-static and time variable geoid altimetric sea surface: mean and time variation ice surfaces: elevation and extension changes from altimetry	core probes from ocean drilling, geological and climatological data, corals paleo-shorelines GPS elevation change, levelling tide gauges ocean surface temperature and salinity from remote sensing and in-situ data ocean circulation model results runoff, hydrological models
Approaches for Separation of Signal Components:	
Modelling the thermo-haline expansion of sea water using climatological data (temperature/salinity profiles), drifters, XBT data or remotely sensed salinity (SMOS-mission) or sea surface temperature Comparison between tide gauge recordings and altimetric time series Modelling sea-air interaction, evapotranspiration, river run-off	

Global sea level, the most prominent indicator of global change, is interconnected to nearly all of the processes discussed in this report. Mass balance changes of the polar ice, of the atmospheric water content and in the continental hydrological cycle – all reappear as sea level change. Absolute or relative sea level is also changed by ocean circulation variations, by thermal ocean volume expansion and by vertical movements due to glacial isostatic adjustment. Thus, the total sea level change signal is very complex and has a large range of spatial and temporal scales.

Drilling at ocean sediments, for example, indicate sea level changes of about 120 m for the geological sequence of glacial era and intermediate warming periods. The last deglaciation causes vertical crustal movements of up to 1 cm/year, visible at paleo-shorelines or observable by repeated or continuously performed precise point positioning. Today, sea level is monitored by tide gauges and satellite altimetry, two observation systems that complete each other. Tide gauges provide very precise records of mean sea level for time periods up to 100 years or even more, limited, however, to sites of an inhomogeneously distributed network. Satellite altimetry, on the other hand, provides fast, repeated, precise and nearly global observation of the sea level. ICESat and CryoSat, will extend the coverage to nearly the entire global oceans. However, vertical control and long-term stability of altimeter systems is available only since the last decade. A careful calibration and cross-calibration of altimeter systems is as necessary as the knowledge about the actual vertical crustal movement at tide gauges to ensure that both systems really observe the same sea level signal.

Altimeter data of the last decade show large areas with completely different evolution of the sea level, the rates of change reaching ±15-20 mm/year. Most of these changes are attributed to the thermo-haline expansion of the upper layer water. The combination of satellite altimetry and GRACE observations will help to clarify associated mass changes; see also the comment on Table 4.5.

Table 4.9 Global Mantle Dynamics	
Research Subjects: global mantle flow and dynamic topography of Earth surface and internal boundaries from seismic and geoid data, time-dependent mantle convection and plate rearrangements, plumes,3D viscosity models, small scale sublithospheric convection processes, improvement of crust and lithosphere models	
Interacting Processes, Superimposed Signals:	
structure and gravity field signal of the lithosphere viscosity models from glacial isostatic adjustment models thermally, compositionally and water induced variations of seismic velocities and density phase transformations in the mantle kinematics of the plates plume – lithosphere interaction	
Data from the New Missions:	Complementary Data and Models:
quasi-static geoid and gravity time-dependent geoid	crust and lithosphere models dynamic and isostatic topography seismic velocities, seismic tomography PREM seismic velocity – density conversion models viscosity models (vertical, lateral) experimental viscosity data
Approaches for Separation of Signal Components:	
independent modelling of dynamic Earth surface topography using crust and lithosphere models combination with seismic tomography correlation gravity – topography – plate kinematics to identify sublithospheric convection correlation with heat flow relate quasi-static with time-dependent geoid variations	

Mass anomalies associated with global convective mantle flows lead to a complex system of dynamic and rheological interactions with observables such as gravity, geoid, long term variations of these fields, dynamic topography, seismic velocities, heat flow etc. Interpretation of new gravity potential data in terms of such mantle dynamic processes requires a combined effort of dynamic forward modelling, including 1D or 3D-variations of mantle viscosities based on models of glacial isostatic adjustment models, as well as plate kinematics, and accounting for seismic tomography and crustal and lithospheric structures. Thus, seismic tomography, dynamic topography, surface deformations, gravity and the vertical and lateral viscosity structure of the mantle are the key observables and parameters for a three and four dimensional modelling of mantle dynamics.

The worldwide seismic station network enables the improvement of global models of the Earth's crust (density distribution and thickness) and of tomographic velocity models of the Earth's mantle. The spatial structure of the gravity field gives boundary values for (1) an isostatic model of the Earth's lithosphere to investigate its static equilibrium (medium to short-scale) and (2), by this, to infer the dynamic topography due to mantle dynamics for the mantle's temperature and density distribution. The knowledge of the Earth's crustal structure and the resolution and accuracy of tomographic models is, compared to the knowledge of the quasi-static gravity field, rather low. Therefore, there is a need for improving the seismologic monitoring and modelling. This situation changes, when turning to smaller wavelengths appropriate e.g. for sublithospheric convection, plume – lithosphere interactions or to regional tectonic modelling. In the latter case accurate gravity down to wavelengths of some kilometres is required, and satellite gravity field missions will provide the longer wavelengths frame for a reliable detailed geoid and gravity field modelling with a data coverage densified by terrestrial and ship- and airborne measurements.

Table 4.10 Subduction Zones, Tectonics	
Research Subjects: sinking slabs in Earth mantle, roll back of subduction zones, active and passive continental margins, orogeny, episodic mass shifts,	
Interacting Processes, Superimposed Signals:	
topography, bathymetry mass changes from ocean, continental hydrology, and atmosphere mantle gravity field phase boundaries in the mantle viscosity stratification of the mantle and viscosity structure of the slabs	
Data from the New Missions:	**Complementary Data and Models**:
time variable and static geoid time variable and static gravity anomalies	surface deformation and uplift/subsidence rates from INSAR, GPS, levelling viscosity parameters rigidity, elasticity seismic data PREM tide gauges absolute gravimetry, airborne gravimetry terrestrial gravimetry
Approaches for Separation of Signal Components:	
forward modelling of subduction and orogenic processes correlation with seismicity reduction of time-dependent gravity signals from hydrology and oceanography	

A challenging task will be the search of time dependent signals near plate boundaries such as subduction zones or orogens, and to identify processes such as vertical mass movements in the mantle associated with subduction or delamination, trench roll back or other episodic mass movements. Such time variations will be near the resolution limit of GRACE. Therefore careful analyses of temporal variations of the gravity field in the space domain in combination of dynamic forward modelling utilizing geometric, kinematic or seismic observations will be necessary.

Table 4.11 Continental Hydrological Cycle	
Research Subjects: global and continental water balance (water fluxes between atmosphere, continents, oceans and ice masses), spatial and temporal variations of the terrestrial water storage, evapotranspiration of the land surface, effects of climate change / environmental change on the terrestrial water storage	
Interacting Processes, Superimposed Signals:	
atmospheric mass variations mass variations in the ocean adjacent to the land surface atmospheric circulation (meteorological and climatological conditions as forcing of the hydrological cycle) mass change in continental snow and ice zones change of land use and vegetation zones human water use mass changes by glacial isostatic adjustment	
Data from the New Missions:	**Complementary Data and Models:**
time variation of geoid and gravity altimetry of water levels in lakes, reservoirs, wetlands and rivers (time-variations)	meteorological data hydrological data (river discharge, soil moisture, groundwater) data from remote sensing of the land surface (land use, snow cover, ice cover, surface temperature) large-scale hydrological models (global) circulation models of the atmosphere and the oceans (GCMs) snow and ice balance models
Approaches for Separation of Signal Components:	
corrections of the gravity signal with results from ocean and atmosphere circulation models and with meteorological data separation of components of the terrestrial water storage by using hydrological data and models separation of mass variations in surface water and snow-/ice cover with the help of altimetry and other remote sensing data spatial filtering for the geometry of river basins temporal filtering by process-specific time constants	

The continental hydrological cycle is coupled to a large number of concurrent processes which affect mass variations at a broad range of space and time scales. Exchanges between the terrestrial water storage and the atmosphere are driven via precipitation and evapotranspiration processes. Variations of the ice or snow mass balance of glaciated areas contribute to changes in the water balance of river basins. Long-term variations in the freshwater runoff from continental areas induced by climate variability and climate change are directly connected to oceanic processes such as sea level change or the time-variable oceanic circulation due to salinity changes. Glacial isostatic adjustment may interact with a gravity signal due to hydrological processes at high latitudes for longer time scales. In addition, human impacts by land use changes or water use affect the hydrological cycle and the terrestrial water storage.

Due to these numerous couplings, there is an indispensable need for a joint analysis including data and models from a variety of disciplines in order to separate the contributions to mass variations induced by the involved processes. Measured mass changes from GRACE, monitored surface water levels from altimetry missions as well as ground based hydrological measurements allow to quantify changes in the water storage, to separate the different storage components and to eliminate the hydrological component of the time-variable gravity signal as a basis for the investigation of other processes.

References

NRC Committee on Earth gravity from space, 1997. Satellite gravity and the geosphere, National Academy Press Washington.

Rummel, R., J. Flury, R. Haagmans, C. Hughes, P. Le Grand, J. Riegger, E. Schrama, N. Sneeuw, B. Vermeersen, and P. Woodworth, 2003. Scientific objectives for future geopotential missions, ESA contract "Enabling observation techniques for future geopotential missions", document SolidEarth-TN-TUM-001.

Schuh, H., R. Dill, H. Greiner-Mai, H. Kutterer, J. Müller, A. Nothnagel, B. Richter, M. Rothacher, U. Schreiber, and M. Soffel, 2004. Erdrotation und globale dynamische Prozesse. Concept report of the DFG research project "Rotation der Erde", Mitteilungen des Bundesamtes für Kartographie und Geodäsie, Frankfurt/Main, No 32.

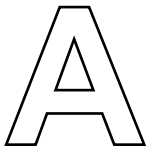

Annex

The following annexations provide the concepts and the state-of-the-art in physical and mathematical methods applied in global gravity field analysis and in the research fields that are addressed in this report. The satellite mission fact sheets (A7) summarize the characteristics of the relevant recent and coming missions.

A1 Gravity field tutorial

The formulae and derivations in the following Chapters A1.1 to A1.3 are based on Heiskanen and Moritz (1967) and Lambeck (1990). For the sake of simplicity, problems dealing with topographic reduction and ellipsoidal corrections when using spherical approximations are not addressed. As such, most of the formulae given below are first order approximations of the exact expressions.

A1.1 Expansion of the gravitational potential into spherical harmonics

The stationary part of the **Earth's gravitational potential U** at any point P(r,φ,λ) on and above the Earth's surface is expressed on a global scale conveniently by summing up over degree and order of a spherical harmonic expansion. The spherical harmonic (or Stokes') coefficients represent in the spectral domain the global structure and irregularities of the geopotential field or, more generally spoken, of the gravity field of the Earth. The equation relating the spatial and spectral domain of the geopotential is as follows:

$$U(r,\varphi,\lambda) = \frac{GM}{R}\left[\frac{R}{r}\bar{C}_{00} + \sum_{l=1}^{l_{max}}\sum_{m=0}^{l}\left(\frac{R}{r}\right)^{l+1}\bar{P}_{lm}(\sin\varphi)\left(\bar{C}_{lm}\cos m\lambda + \bar{S}_{lm}\sin m\lambda\right)\right] \qquad \text{(A1.1.1)}$$

where r,φ,λ - spherical geocentric coordinates of computation point (radius, latitude, longitude)
R - reference length (mean semi-major axis of Earth)
GM - gravitational constant times mass of Earth
l,m - degree, order of spherical harmonic
$\bar{P}_{lm}$ - fully normalized Lengendre functions
$\bar{C}_{lm}, \bar{S}_{lm}$ - Stokes' coefficients (fully normalized)

The $\bar{C}_{00}$ -term is close to 1 and scales the value GM. The degree 1 spherical harmonic coefficients $(\bar{C}_{10}, \bar{C}_{11}, \bar{S}_{11})$ are related to the geocentre coordinates and zero if the coordinate systems' origin coincides with the geocentre. The coefficients $(\bar{C}_{21}, \bar{S}_{21})$ are connected to the mean rotational pole position that is a function of time.

Subtracting from the low-degree zonal coefficients (order 0) the corresponding Stokes' coefficients $(\bar{C}^{ell}_{00}, \bar{C}^{ell}_{20}, \ldots \bar{C}^{ell}_{80})$ of an **ellipsoidal 'normal' potential** $V(r,\varphi)$ leads to the mathematical representations of the **disturbing potential** $T(r,\varphi,\lambda)$ in spherical harmonics, related to a conven-

tional ellipsoid of revolution that approximates the Earth's parameters. Close to the Earth surface with $r = R$ (in spherical approximation) the disturbing potential reads:

$$T(R,\varphi,\lambda) = U(R,\varphi,\lambda) \; - \; V(R,\varphi) \tag{A1.1.2a}$$

$$T(R,\varphi,\lambda) = \frac{GM}{R}\left[\bar{C}'_{00} + \sum_{l=1}^{l_{max}} \sum_{m=0}^{l} \bar{P}_{lm}(\sin\varphi)\left(\bar{C}'_{lm}\cos m\lambda + \bar{S}_{lm}\sin m\lambda\right)\right], \tag{A1.1.2b}$$

with $\bar{C}' = \bar{C} - \bar{C}^{ell}$. Note, that $\bar{C}'_{00}$ is close to zero.

The maximum degree l_{max} of the expansion in Equation (A1.1.1) correlates to the spatial resolution at the Earth surface by

$$\lambda_{min} \approx 40000\ km\ /(\ l_{max} + 0.5)\ , \tag{A1.1.3}$$

where λ_{min} is the minimum wavelength (or twice the pixel side length) of gravity field features that are resolved by the $l_{max}\cdot(l_{max}+1) \approx (l_{max} + 0.5)^2$ parameters $\bar{C}_{lm}, \bar{S}_{lm}$.

Equation (A1.1.1) contains the upward-continuation of the gravitational potential at the Earth's surface for $r > R$ and reflects the attenuation of the signal with altitude through the factor $(R/r)^{l+1}$.

Figure A1.1.1 gives examples for the three different kinds of spherical harmonics $P_{lm}(\sin\varphi)\cdot\cos m\lambda$: (a) zonal with $l \neq 0$, $m = 0$, (b) tesseral with $l \neq 0$, $m \neq 0 < l$ and (c) sectorial harmonic with $l = m$. Amplitudes and phase of the individual spherical harmonics then are determined by multiplication with the C_{lm} and S_{lm} coefficients.

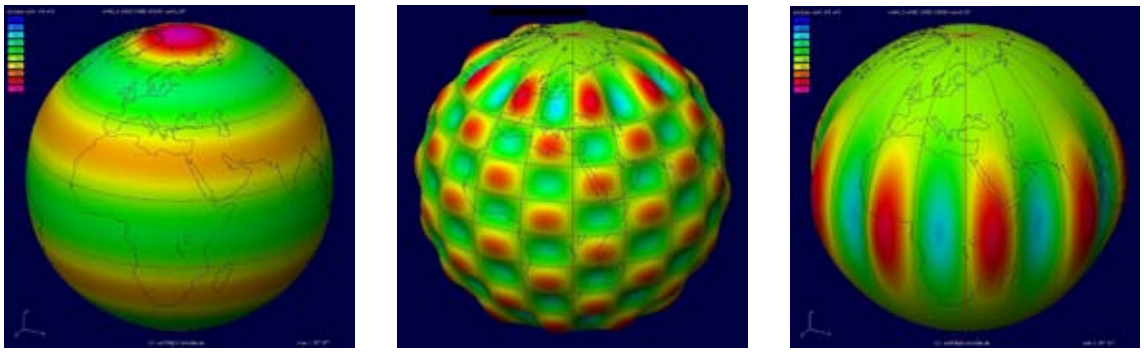

zonal: l=6, m=0 *tesseral: l=16, m=9* *sectorial: l=9, m=9*

Figure A1.1.1: *Examples for spherical harmonics* $P_{lm}(\sin\varphi)\cdot\cos m\lambda$ *[from –1 (blue) to +1 (violet)].*

A1.2 Functionals of the disturbing gravitational potential

The **geoid undulation** N (Figure A1.2.1) is the distance between the special equipotential surface $U(R,\varphi,\lambda) = \text{const}$ that is close to the mean sea level and the surface of the conventional ellipsoid of revolution. As such the geoid is derived from the disturbing potential T applying *Bruns formula*

$$N = \frac{T}{\gamma}\ , \tag{A1.2.1}$$

where γ is 'normal' gravity on the surface of the ellipsoid. With $\gamma = GM/R^2$ in spherical approximation, the geoid undulations (or geoid heights) can be computed from the spherical harmonic coefficients in Equation (A1.1.2) by

$$N(R,\varphi,\lambda) = \frac{R^2}{GM} \cdot T(R,\varphi,\lambda)\ , \tag{A1.2.2a}$$

$$N(R,\varphi,\lambda) = R\left[\bar{C}'_{00} + \sum_{l=1}^{l_{max}}\sum_{m=0}^{l}\bar{P}_{lm}(\sin\varphi)\left(\bar{C}'_{lm}\cos m\lambda + \bar{S}_{lm}\sin m\lambda\right)\right]. \qquad \text{(A1.2.2b)}$$

Strictly speaking, Equation A1.2.2 applies only over the oceans, where no topographic masses exist above the geoid. Over land areas, the disturbing potential must be computed at the bottom of the topography, i.e. inside the masses. Without considering topography, Equation A1.2.2 yields (in spherical approximation) the so-called height anomalies, which are close to geoid heights but of different conceptual background.

The negative of the vertical derivative of the disturbing potential $\delta g = -\partial T/\partial r$ is called **gravity disturbance** δg (Figure A1.2.2) that is equal to gravity at a point *P* (negative of vertical derivative of *U*) minus 'normal' gravity at point *P* (negative of vertical derivative of *V*). Close to the Earth surface and in spherical approximation *(r = R)* the gravity disturbance then is expressed by

$$\delta g(R,\varphi,\lambda) = \frac{GM}{R^2}\left[\bar{C}'_{00} + \sum_{l=1}^{l_{max}}(l+1)\sum_{m=0}^{l}\bar{P}_{lm}(\sin\varphi)\left(\bar{C}'_{lm}\cos m\lambda + \bar{S}_{lm}\sin m\lambda\right)\right]. \qquad \text{(A1.2.3)}$$

The difference between gravity at a point *P* at the Earth surface with potential U_p and ‚normal' gravity at the corresponding point Q with ‚normal' potential $V_p = U_p$ is called (free-air) **gravity anomaly** Δg (Figure A1.2.3) and related to the disturbing potential by

$$\Delta g = -\frac{\partial T}{\partial r} - \frac{2}{r}T \qquad \text{(A1.2.4)}$$

The vertical distance between P and Q is the height anomaly. Again in spherical approximation, one gets for the spherical harmonic expansion of the gravity anomalies (note: no degree 1 terms appear in Equation A1.2.5)

$$\Delta g(R,\varphi,\lambda) = \frac{GM}{R^2}\left[-\bar{C}'_{00} + \sum_{l=2}^{l_{max}}(l-1)\sum_{m=0}^{l}\bar{P}_{lm}(\sin\varphi)\left(\bar{C}'_{lm}\cos m\lambda + \bar{S}_{lm}\sin m\lambda\right)\right], \qquad \text{(A1.2.5a)}$$

thus

$$\Delta g = \delta g - \frac{2}{R}T\ . \qquad \text{(A1.2.5b)}$$

The second derivatives of the potential leads to the **gravity-gradient tensor**. The most important vertical gradient $g_r = \frac{-\partial^2 U}{\partial r^2}$ of the tensor component can be represented as

$$g_r = -\frac{GM}{R^3}\left[\left(\frac{R}{r}\right)^3 2\bar{C}_{00} + \sum_{l=1}^{l_{max}}\sum_{m=0}^{l}(l+1)(l+2)\left(\frac{R}{r}\right)^{l+3}\bar{P}_{lm}(\sin\varphi)\left(\bar{C}_{lm}\cos m\lambda + \bar{S}_{lm}\sin m\lambda\right)\right]. \qquad \text{(A1.2.6)}$$

Once the spherical harmonic coefficients $\bar{C}_{lm}, \bar{S}_{lm}$ of a global gravity field model are given, the quantities of the various functionals described above can be computed in its geographical distribution. If computed in terms of gravity disturbances or anomalies and gravity gradients, the higher frequency regional to local content is emphasised through the degree-dependent factors $(l + 1)$, $(l - 1)$ and $(l + 1)(l + 2)$, respectively, whereas the potential and geoid representations of the gravity field show the broad and generalized features of the gravity field. Vice versa, a gradiometer measuring gravity gradients is capable to better resolve detailed structures of the gravity field rather than the long wavelength part.

The fully normalized spherical harmonic coefficients in Equation (A1.1.1) are related to the mass distribution within the Earth by

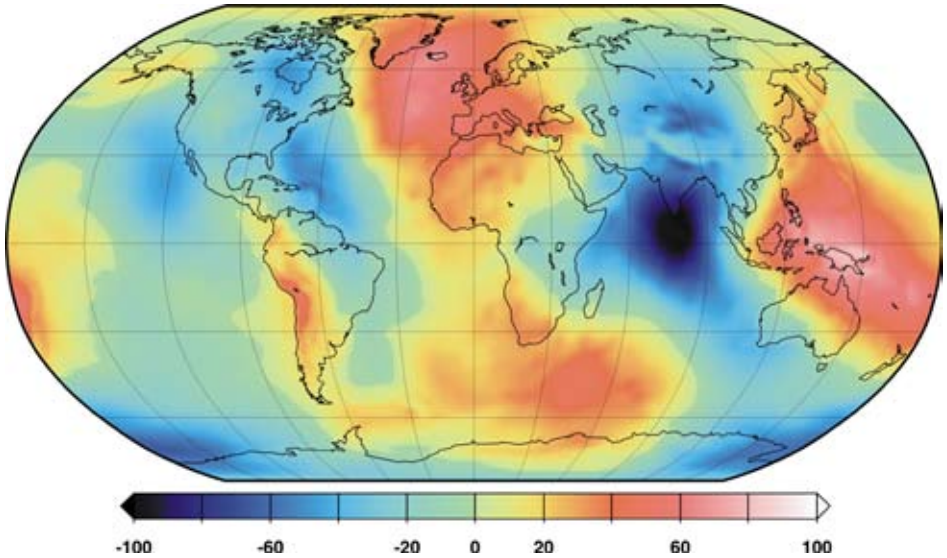

Figure A1.2.1: *Geoid undulations N [m]: resolution λ=500 km, rms (N √cos φ) = 30.6 m*

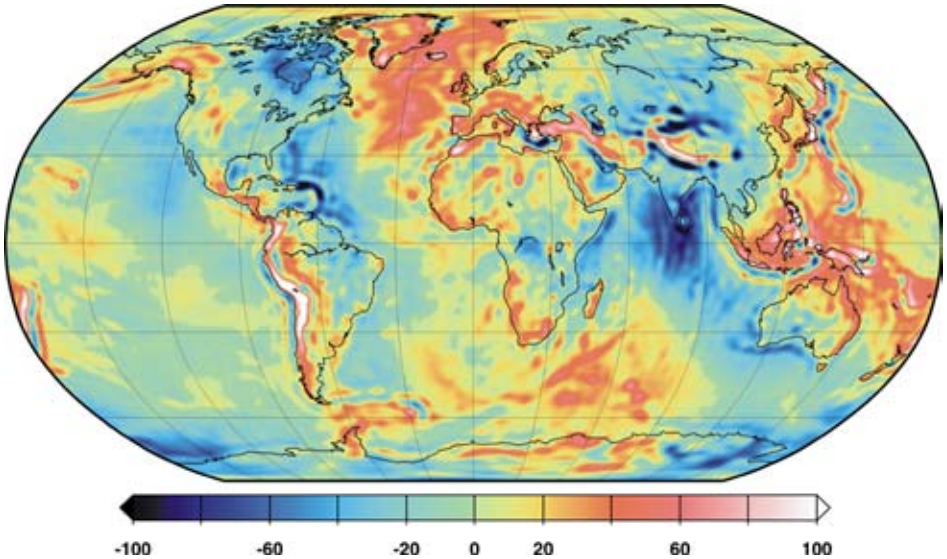

Figure A1.2.2: *Gravity disturbances δg [mGal]: resolution λ=500 km, rms (δg √cos φ) = 27.2 mGal.*

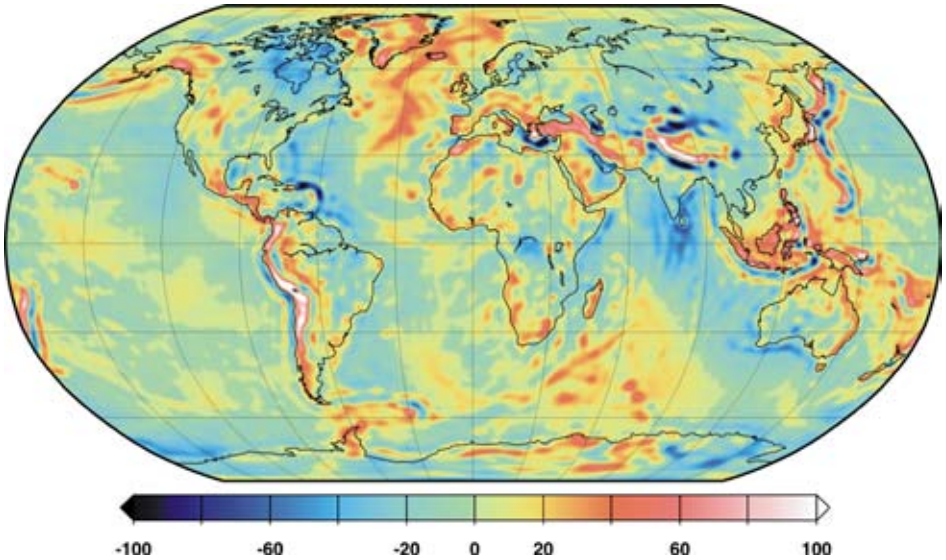

Figure A1.2.3: *Gravity anomalies Δg [mGal]: resolution λ=500 km, rms (Δg √cos φ) = 20.6 mGal.*

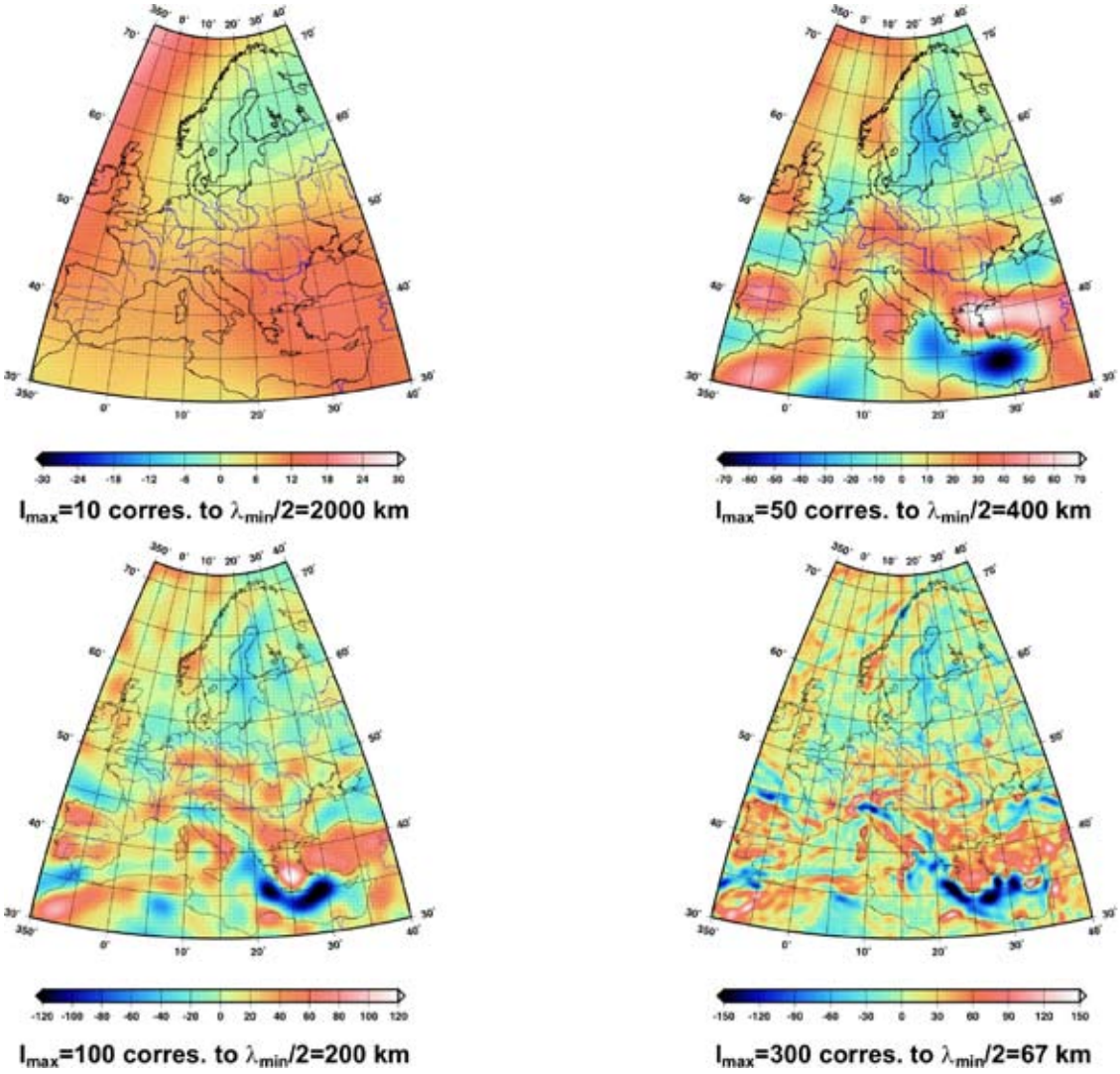

Figure A1.2.4: *Geographical distribution of gravity anomalies [mGal] over Europe with different spectral (l_{max}) and spatial resolution pixel size ($\lambda_{min}/2$).*

$$(2l+1)\ \bar{C}_{lm} = \frac{1}{MR^l} \iiint_{Earth} r^l\ \ \bar{P}_{lm}(\sin\varphi)\ \ \cos m\lambda\, dM \qquad \text{(A1.2.7a)}$$

$$(2l+1)\ \bar{S}_{lm} = \frac{1}{MR^l} \iiint_{Earth} r^l\ \ \bar{P}_{lm}(\sin\varphi)\ \ \sin m\lambda\, dM \qquad \text{(A1.2.7b)}$$

with the mass element $dM=dM\ (r,\varphi,\lambda)$.

Figure A1.2.4 depicts the geopotential distribution of gravity anomalies over Europe derived from spherical harmonic coefficients complete to l_{max} equal to 10, 50, 100, 300, respectively, in order to demonstrate the relation between spectral and spatial resolution according to Equation (A1.1.1).

A1.3 The power spectrum of the Earth's gravity field

Given the fully normalized Stokes' coefficients $\bar{C}_{lm}, \bar{S}_{lm}$ of a specific degree l over orders m $(m=0...l)$, the signal degree amplitudes σ_l (or square root of power per degree l) of functions of the disturbing potential $T\ (R,\varphi,\lambda)$ at the Earth's surface are readily computed by

$$\sigma_l = \sqrt{\sum_{m=0}^{l} (\bar{C}'^2_{lm} + \bar{S}^2_{lm})} \qquad \text{in terms of unitless coefficients} \qquad \text{(A1.3.1a)}$$

$$\sigma_l(T) = \frac{GM}{R} \cdot \sigma_l \qquad \text{in terms of disturbing potential values } (m^2/s^2) \qquad \text{(A1.3.1b)}$$

$$\sigma_l(N) = R \cdot \sigma_l \qquad \text{in terms of geoid heights (m)} \qquad \text{(A1.3.1c)}$$

$$\sigma_l(\delta g) = \frac{GM}{R^2}\,(l+1) \cdot \sigma_l \qquad \text{in terms of gravity disturbances } (m/s^2) \qquad \text{(A1.3.1d)}$$

$$\sigma_l(\Delta g) = \frac{GM}{R^2}\,(l-1) \cdot \sigma_l \qquad \text{in terms of gravity anomalies } (m/s^2) \qquad \text{(A1.3.1e)}$$

$$\sigma_l(g_r) = \frac{GM}{R^3}\,(l+1)\,(l+2) \cdot \sigma_l \qquad \text{in terms of vertical gravity gradients } (1/s^2) \qquad \text{(A1.3.1f)}$$

where the $\bar{C}_{lm}, \bar{S}_{lm}$ are related to the 'normal' potential. The SI units of the physical gravitational quantities are given in parenthesis. Following Kaula's 'rule of thumb' (Kaula, 1966) the power law follows approximately

$$\sigma_l \approx \sqrt{(2l+1) \cdot \frac{10^{-10}}{l^4}} \quad . \qquad \text{(A1.3.2)}$$

Examples for signal degree amplitudes are given in Figure A1.3.1.

If the estimation errors of the Stokes' coefficients in a global gravity field model are known, the **error degree amplitudes** (error spectrum) are computed accordingly replacing the coefficients in Equation (A1.3.1) by their standard deviations. **Difference degree amplitudes**, representing the agreement of two different gravity field models per degree, are readily computed replacing the coefficients in Equation (A1.3.1) by the coefficients' differences between the two models. Examples for difference degree amplitudes are given in Figure A1.3.2.

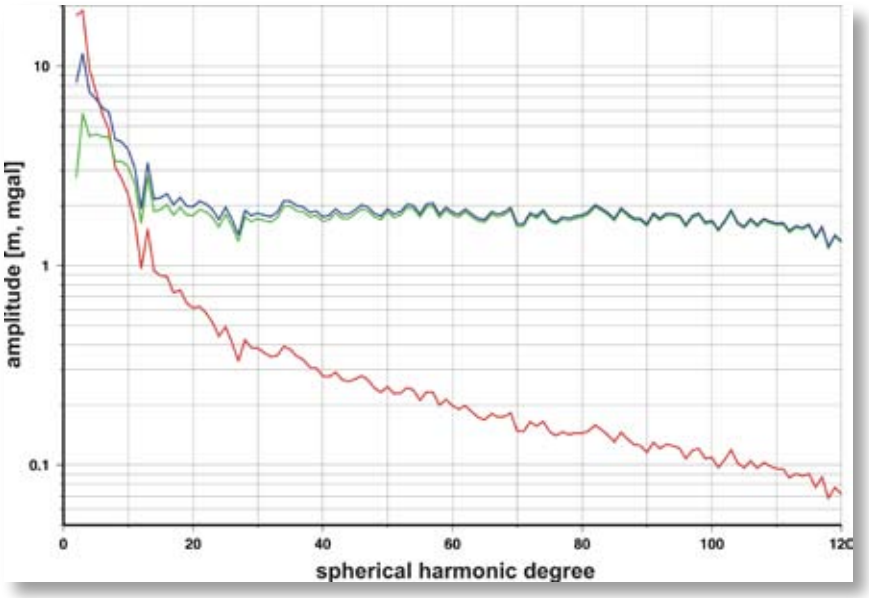

Figure A1.3.1: *Signal degree amplitudes for geoid undulations (red), gravity disturbances (blue) and gravity anomalies (green) in meter and mGal, respectively.*

The **degree amplitudes as a function of minimum and maximum degree** l displays the power (signal, error, difference) spectrum accumulated over a spectral band from l_1 to l_2:

$$\sigma_{l_1,l_2} \ (accumulated) = \sqrt{\sum_{l_1}^{l_2} \sigma_l^2} \qquad \text{(A1.3.3)}$$

Usually l_1=0 or 2 is taken to display the increase in overall power with increasing degree l_2. Recall that the spectral degree l is related to the spatial extension or wavelength of features in the gravity field according to Equation (A1.1.3). Examples for difference amplitudes as a function of maximum degree l (successive accumulation of the curves in Figure A1.3.1) are given in Figure A1.3.2.

Equations (A1.3.1) again demonstrate that the higher degree terms, i.e. the shorter wavelengths in the signal spectra, are enhanced by factors proportional to degree l for gravity anomalies and disturbances and proportional to l^2 for gravity gradients compared to the signals in the geoid and gravitational potential.

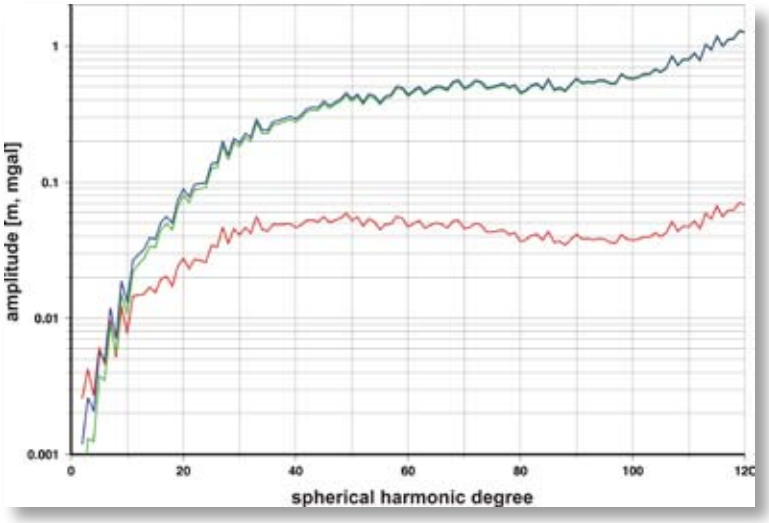

Figure A1.3.2: *Difference degree amplitudes (GRACE-01S vs. EGM96) in terms of geoid undulations (red), gravity disturbances (blue) and gravity anomalies (green) in meter and mGal, respectively*

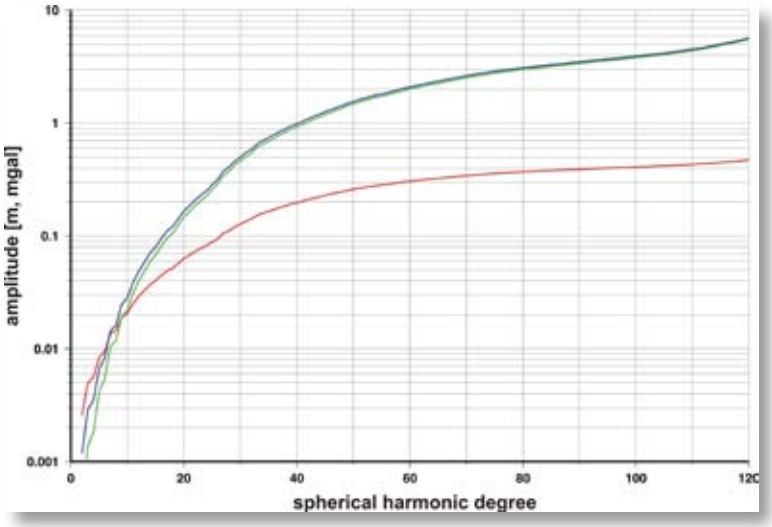

Figure A1.3.3: *Difference degree amplitudes (GRACE-01S vs. EGM96) as a function of maximum degree in terms of geoid undulations (red), gravity disturbances (blue) and gravity anomalies (green) in meter and mGal, respectively*

A1.4 Non-tidal temporal gravity field variations

The Earth and ocean tide induced time-varying part of the gravitational potential due to solid Earth deformation, water mass redistribution and loading is accounted for when solving for a global gravity field model. Variations of the spherical harmonic coefficients $\bar{C}_{lm}, \bar{S}_{lm}$ with time therefore can be attributed to environmental and climate related processes at the Earth surface causing mass redistributions within and among the atmosphere, cryosphere and hydrosphere. Solid Earth processes, like core/mantle coupling, post-glacial adjustment and subduction, add low amplitude secular variations (linear trend) of the spherical harmonic coefficients to the overall spectrum of temporal gravitational variations.

The formulae and derivations within this and the following chapter are based on Wahr et al. (1998).

When solving for a time series of spherical harmonic coefficients (e.g. monthly values from CHAMP/GRACE data), the gravitational potential and the Stokes' coefficients, Equation (A1.1.1), at the Earth surface (r=R) become time-dependent (t-time):

$$U(t,R,\varphi,\lambda) = \frac{GM}{R}\left[C_{00} + \sum_{l=1}^{l_{max}}\sum_{m=0}^{l}\bar{P}_{lm}(\sin\varphi)\left(\bar{C}(t)_{lm}\cos m\lambda + \bar{S}_{lm}(t)\sin m\lambda\right)\right]. \qquad \text{(A1.4.1)}$$

If we concentrate here on the surface processes (atmosphere, cryosphere, oceans, continental hydrology) with seasonal, interannual and long-term variations, the variation in surface density (i.e., mass/area) can be expanded into (fully normalized) spherical harmonics (thin layer approximation):

$$\sigma(t,\varphi,\lambda) = R\ \rho_w\left[\breve{C}_{00} + \sum_{l=1}^{l_{max}}\sum_{m=0}^{l}\bar{P}_{lm}(\sin\varphi)\left(\breve{C}(t)_{lm}\cos m\lambda + \breve{S}(t)_{lm}\sin m\lambda\right)\right] \qquad \text{(A1.4.2)}$$

with ρ_w - being the density of water to make the coefficients $\breve{C}(t)_{lm}, \breve{S}(t)_{lm}$ dimensionless.

The ratio $\sigma(t)/\rho_w$ means the variation in equivalent water thickness (1 mbar/g $\hat{=}$ 1 cm equivalent water thickness with g being the mean gravitational acceleration at the Earth's surface).

Then, the relation between the gravitational spherical harmonic coefficients in Equation (A1.4.1) and the surface density coefficients in Equation (A1.4.2) is given by:

$$\begin{Bmatrix}\bar{C}(t)_{lm}\\ \bar{S}(t)_{lm}\end{Bmatrix} = \frac{3\rho_w}{\rho_{ave}}\ \frac{1+k_l'}{2l+1}\ \begin{Bmatrix}\breve{C}(t)_{lm}\\ \breve{S}(t)_{lm}\end{Bmatrix} \qquad \text{(A1.4.3)}$$

with ρ_{ave} being the average density of the Earth (5517 kg/m^3) and k_l' being the degree dependent load Love numbers (e.g. Farrell, 1972). The factor (1+k_l') in Equation (A1.4.3) accounts for both the direct mass potential and the solid Earth loading deformation potential.

Equations (A1.4.2) and (A1.4.3) may be used for forward computations (potential, geoid, gravity, gradients) when a surface mass distribution with time is given from geophysical models and measurements.

Vice versa, inverting Equation (A1.4.3),

$$\begin{Bmatrix}\breve{C}(t)_{lm}\\ \breve{S}(t)_{lm}\end{Bmatrix} = \frac{\rho_{ave}}{3\rho_w}\ \frac{2l+1}{1+k_l'}\ \begin{Bmatrix}\bar{C}(t)_{lm}\\ \bar{S}(t)_{lm}\end{Bmatrix} \qquad \text{(A1.4.4)}$$

and inserting $\breve{C}(t)_{lm}, \breve{S}(t)_{lm}$ into Equation (A1.4.2), the CHAMP/GRACE satellite observed surface density variations can be estimated from the solved-for $\bar{C}(t)_{lm}, \bar{S}(t)_{lm}$ time series.

Equations (A1.4.2) to (A1.4.4) are for indicative purposes only. Refinements, e.g. taking into account the density variations over depths (oceans) or with altitude (atmosphere), are required for highest accuracy.

Filtering in the spectral and/or spatial domain (Wahr et al., 1998) also may be required for the localization of effects, for source separation and for reducing the impact of less well determined higher frequency parts of the gravitational spectrum.

A1.5 Spatial/temporal power spectra of temporal field variations

The spatial/temporal power spectra (degree amplitudes) of the time varying fields represented by the spherical harmonic coefficients $\bar{C}(t)_{lm}, \bar{S}(t)_{lm}$ (or $\Delta\breve{C}(t)_{lm}, \Delta\breve{S}(t)_{lm}$) are again computed following Equation (A1.3.1a) but replacing the coefficients by their root mean square (rms) about mean over the time of consideration ($\bar{C}'(t) = \bar{C}(t) - \bar{C}_{mean}$, $\bar{S}'(t) = \bar{S}(t) - \bar{S}_{mean}$:

$$\sigma_l = \sqrt{\sum_{m=0}^{l} \left[\left(rms\ \ \bar{C}'(t)_{lm} \right)^2 + \left(rms\ \ \bar{S}'(t)_{lm} \right)^2 \right]} \ . \qquad \text{(A1.5.1)}$$

Appropriate scaling of the coefficients like in Equations (A1.3.1b to f) or as being obvious from Equation (A1.4.2) allows the expression of the degree amplitudes in terms of functionals of the disturbing gravitational potential or in terms of surface density and equivalent water thickness, respectively (cf. Figure A1.5.1).

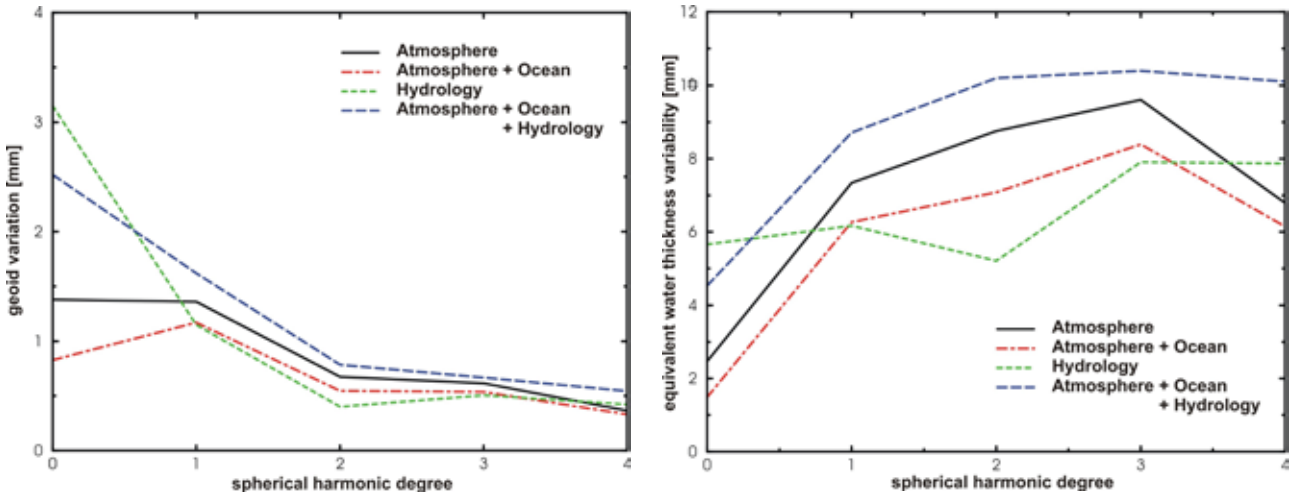

Figure A1.5.1: *Degree amplitudes of longest wavelength mass redistributions in terms of (left) geoid and (right) equivalent water thickness variations from monthly averages.*

The spherical harmonic coefficients in Equations (A1.4.3) and (A1.4.4) may be subject to a temporal spectral analysis to extract amplitudes $\bar{A}_c(f)_{lm}, \bar{A}_s(f)_{lm}$ and phases $\varphi_c(f)_{lm}, \varphi_s(f)_{lm}$ or, being equivalent, the sine $\bar{C}(f)^s_{lm}, \bar{S}(f)^s_{lm}$ and cosine terms $\bar{C}(f)^c_{lm}, \bar{S}(f)^c_{lm}$ at a given frequency f (e.g. annual as shown in Figure A1.5.2) for the time series of each individual coefficient $\bar{C}(t)_{lm}, \bar{S}(t)_{lm}$. The power spectrum expressed in degree amplitudes of the fields varying at a given frequency (cf. Figure A1.5.3) then may be computed starting from:

$$\sigma_l(f) = \frac{1}{\sqrt{2}} \sqrt{\sum_{m=0}^{l} \left[\left(\bar{C}(f)^s_{lm}\right)^2 + \left(\bar{C}(f)^c_{lm}\right)^2 + \left(\bar{S}(f)^s_{lm}\right)^2 + \left(\bar{S}(f)^c_{lm}\right)^2 \right]} \qquad \text{(A1.5.2a)}$$

being equivalent to

$$\sigma_l(f) = \frac{1}{\sqrt{2}} \sqrt{\sum_{m=0}^{l} \left[\left(\bar{A}_c(f)_{lm}\right)^2 + \left(\bar{A}_s(f)_{lm}\right)^2 \right]} \; . \qquad \text{(A1.5.2b)}$$

Inserting the frequency-dependent coefficients $\bar{C}(f)^s_{lm}, \bar{S}(f)^s_{lm}$, and $\bar{C}(f)^c_{lm}, \bar{S}(f)^c_{lm}$, respectively into one of the spherical harmonic expansions in Chapter A1.2, one gets the geographical distribution of the since and cosine component, respectively, of the corresponding functional (geoid, gravity, gravity gradient) or, applying Equations (A1.4.4) and (A1.4.2), of the surface density at a given frequency.

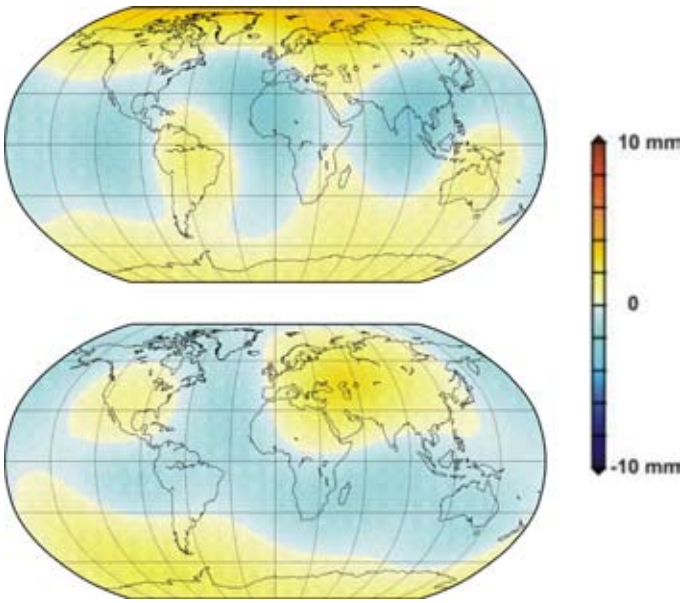

Figure A1.5.2: *Atmospheric, oceanic and hydrological contribution (spherical harmonic degrees 2 through 4) to the annually varying geoid component. (top) Sine component and (bottom) Cosine component (with t = 0 on January 1). Root mean square (weighted by cosine of latitude) is 1.2 mm.*

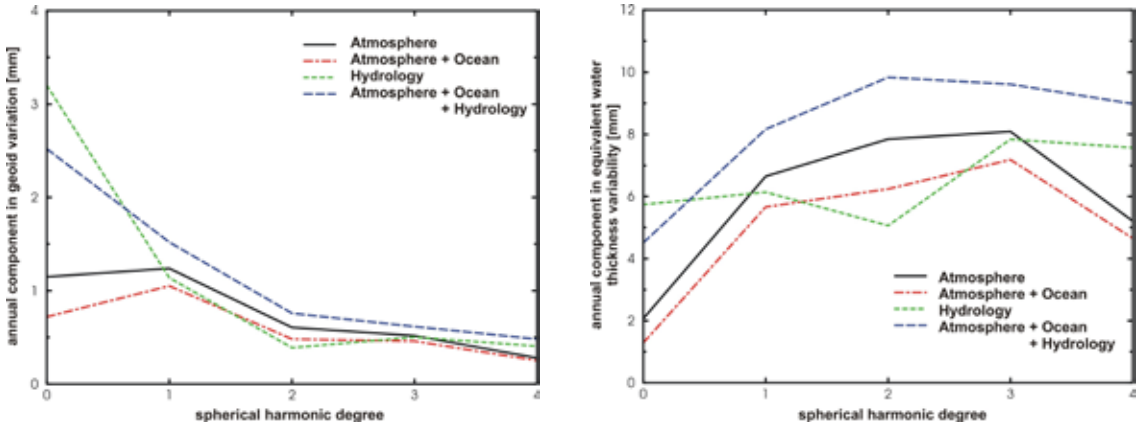

Figure A1.5.3: *Degree amplitudes of annual component in longest wavelengths mass redistributions in terms of (left) geoid and (right) equivalent water thickness variations.*

References

Heiskanen, W.A. and H. Moritz, 1967. Physical Geodesy, W.H. Freeman and Co., San Francisco.

Kaula, W.M., 1966. Theory of Satellite Geodesy, Blaisdell Publ. Company, Waltham, Mass.

Lambeck, K., 1990. Aristoteles – An ESA Mission to Study the Earth's Gravity Field, ESA Journal 14:1-21.

Wahr, J., M. Molenaar and F. Bryan, 1998. Time Variability of the Earth's Gravity Field – Hydrological and Oceanic Effects and their Possible Detection Using GRACE, Journal of Geophysical Research 103(B12):30 205-30 229.

A2 Physical oceanography

Basic equations

Ocean dynamics are based on physical first principles such as Newton's law of motion. A general description is given by the Navier-Stokes equations. However, these equations are far too complex to be solved for general circulation problems concerning the global ocean. A number of simplifications and approximations can be made to make the system of equations tractable which results in a set of coupled partial differential equations. The ocean is considered as a thin shell around the globe which is taken as a sphere with radius a. The surface $z=0$ is assumed to be the geoid, i.e. horizontal movement is defined as along the geoid. The earth rotates with constant angular velocity Ω. The flow field can then be described by

$$\frac{du}{dt} - \frac{uv\tan\varphi}{a} + \frac{uw}{a} - fv = -\frac{1}{a\cos\varphi\,\rho\partial\lambda}\frac{\partial p}{} + F_u + D_u \tag{A2.1}$$

$$\frac{dv}{dt} - \frac{u^2\tan\varphi}{a} + \frac{vw}{a} + fu = -\frac{1}{a}\frac{\partial p}{\rho\partial\varphi} + F_v + D_v \tag{A2.2}$$

$$\frac{dw}{dt} - \frac{u^2+v^2}{a} = -\frac{\partial p}{\rho\partial z} - g \tag{A2.3}$$

$$\frac{1}{a\cos\varphi}\left(\frac{\partial u}{\partial\lambda} + \frac{\partial(v\cos\varphi)}{\partial\varphi}\right) + \frac{\partial w}{\partial z} = 0 \tag{A2.4}$$

with the definition of the derivative

$$\frac{d}{dt} \equiv \frac{\partial}{\partial t} + \frac{u}{a\cos\varphi}\frac{\partial}{\partial\lambda} + \frac{v\partial}{a\partial\varphi} + \frac{w\partial}{\partial z} \tag{A.2.5}$$

Latitude is denoted by φ and longitude (east) by λ. Velocities in the zonal, meridional and upward (z) direction are u, v and w, respectively. The density of water is ρ, p is pressure and g is the acceleration of gravity (a negative quantity when z is defined as upward). f is commonly known as Coriolis parameter and is defined as $f=2\Omega\sin\varphi$. F_u and F_v are external forces such as action of wind or tides. D_u and D_v represent frictional and diffusive forces. These are largely unknown and depending on choice and application they are approximated by linear or quadratic bottom friction or viscosities of the type proportional to $\nabla^2 u, \nabla^2 v$, or $-\nabla^4 u, -\nabla^4 v$ called harmonic and biharmonic viscosity, respectively.

It turns out that the terms in (A2.1 – A2.3) proportional to squared velocity divided by the radius of the earth can be neglected compared to other terms. For large scale motion the horizontal scale is much longer than the vertical, which results in small vertical accelerations. A common choice is to set dw/dt to zero in (A2.3) leading to the *hydrostatic approximation* (A2.8). Another very good choice is to replace ρ with a constant ρ_0 in equations (A2.1-A2.2), which is part of the *Boussinesq approximation.* Both approximations are excellent for large-scale motion.

For many applications Cartesian coordinates are used with x, y and z pointing east, north and upward, respectively. Hydrostatic and Boussinesq equations of motion then read

$$\frac{du}{dt} - fv = -\frac{\partial p}{\rho_0 \partial x} + F_u + D_u \tag{A2.6}$$

$$\frac{dv}{dt} + fu = -\frac{\partial p}{\rho_0 \partial y} + F_v + D_v \tag{A2.7}$$

$$0 = -\frac{\partial p}{\partial z} - \rho g \tag{A2.8}$$

$$\frac{\partial u}{\partial x} + \frac{\partial v}{\partial y} + \frac{\partial w}{\partial z} = 0 \tag{A2.9}$$

The momentum equations are augmented by the conservation of temperature T and salinity S

$$\frac{dT}{dt} = F_T + D_T \tag{A2.10}$$

$$\frac{dS}{dt} = F_S + D_S \tag{A2.11}$$

and the equation of state that describes the nonlinear dependence of density on temperature, salinity and pressure

$$\rho = \rho(T, S, p) \tag{A2.12}$$

$F_{T,S}$ are external forcing by sources and sinks of temperature and salinity, respectively, which are non-zero only at the ocean-atmosphere boundary. The term $D_{T,S}$ describes internal mixing due to turbulent motion, frequently denoted as diffusivity and assumed proportional to $\nabla^2 T, \nabla^2 S$. Finally, the derivative is now defined as

$$\frac{d}{dt} \equiv \frac{\partial}{\partial t} + u\frac{\partial}{\partial x} + v\frac{\partial}{\partial y} + w\frac{\partial}{\partial z} \tag{A2.13}$$

Equations (A2.6-A2.12) are known as the *hydrostatic primitive equations*. They form the basis of practically all modern ocean general circulation models.

Conservation of trace substances like oxygen, carbon dioxide, freons, nutrients, trace metals and so on are in analogy to the equations for temperature and salinity (A2.10-A2.11). As temperature and salinity take an active part in the primitive equations, they are usually denoted active tracers while all other tracers are denoted passive.

Geostrophic balance and thermal wind

On time scales of days and longer and on spatial scales of longer than 10 km the momentum equations can be approximated very accurately by the balance between Coriolis force and that due to the pressure gradient known as the *geostrophic balance*

$$-fv = -\frac{\partial p}{\rho \partial x} \tag{A2.14}$$

$$fu = -\frac{\partial p}{\rho \partial y} \tag{A2.15}$$

where the Boussinesq approximation has been removed. Geostrophy holds in the open ocean away from boundaries and the Equator even on quite short time scales.

Pressure relative to the geoid cannot be measured from ships in an easy manner. However, by using the hydrostatic equation (A2.8) pressure may be eliminated in the geostrophic equations in favour of density, which can be measured accurately

$$f\frac{\partial v}{\partial z} = -\frac{g}{\rho}\left(\frac{\partial \rho}{\partial x}\right)_p \tag{A2.16}$$

$$f\frac{\partial u}{\partial z} = \frac{g}{\rho}\left(\frac{\partial \rho}{\partial y}\right)_p \tag{A2.17}$$

Here the index *p* denotes derivatives within surfaces of constant pressure, i.e. the p-system. These equations, which are very useful in both meteorology and oceanography, are called *thermal wind relation*. Vertical integration yields the form more familiar to oceanographers

$$\rho u(z) = (\rho u)_0 + \frac{g}{f}\int_{z_0}^{z}\frac{\partial \rho}{\partial y}dz \tag{A2.18}$$

$$\rho v(z) = (\rho v)_0 - \frac{g}{f}\int_{z_0}^{z}\frac{\partial \rho}{\partial x}dz \tag{A2.19}$$

The thermal wind equations allow the diagnosis of the geostrophic velocity at any depth *z* relative to a reference velocity u_0 or v_0. Up to this point, there is a similarity between atmosphere and ocean. The same equations can be applied to both fluids. Differences become visible when we consider boundaries. As reference velocities in the atmosphere bottom velocities can used and easily be measured. In oceanography, this is more difficult. A common choice for reference velocity is some deep level where the ocean is stagnant or the current direction reverses. Here a *level of no motion* is assumed with reference velocities u_0 and v_0 of zero.

The free sea surface

One of the most apparent differences between atmosphere and ocean is the ocean surface topography η. The governing equation for η describes the motion at the sea surface

$$\frac{\partial \eta}{\partial t} + u\frac{\partial \eta}{\partial x} + v\frac{\partial \eta}{\partial y} = w \quad z = \eta(x,y,t) \tag{A2.20}$$

The vertical velocity *w* can be derived by integration of the continuity equation (A.2.9) from the bottom *H* to the level *z*

$$w(z) = w(H) - \int_{H}^{z}\left(\frac{\partial u}{\partial x} + \frac{\partial v}{\partial y}\right)dz \tag{A2.21}$$

$$w(H) = -u\frac{\partial H}{\partial x} - v\frac{\partial H}{\partial y} \quad z = H(x,y) \tag{A2.22}$$

Equation (A2.22) is called kinematic boundary condition and ensures that there is no flow into the spatially varying bottom *H(x,y)*.

The free surface η and the density ρ vary on different time and space scales. It is useful to split the pressure *p* in the hydrostatic primitive equations (A2.6-A2.12) into a part that is due to the free surface and one due to density variations

$$p(z) = -g\int_{z}^{z=0}\rho dz - g\int_{z=0}^{\eta}\rho dz = -g\int_{z}^{z=0}\rho dz - g\rho_0\eta \tag{A2.23}$$

where the surface density is set to ρ_0 for simplicity. If we denote the first term of the right hand side of (A2.23) with p' we can rewrite the equations for horizontal momentum (A2.6-A2.7)

$$\frac{du}{dt} - fv = g\frac{\partial\eta}{\partial x} - \frac{\partial p'}{\rho_0\partial x} + F_u + D_u \tag{A2.24}$$

$$\frac{dv}{dt} + fu = g\frac{\partial\eta}{\partial y} - \frac{\partial p'}{\rho_0\partial y} + F_v + D_v \tag{A2.25}$$

Finally we arrive at an expression for the geostrophic surface flow u_s and v_s

$$fu_s = g\frac{\partial\eta}{\partial y} \tag{A2.26}$$

$$fv_s = -g\frac{\partial\eta}{\partial x} \tag{A2.27}$$

which concludes the oceanography tutorial. Please remember that g is negative and η is positive upward. If the free sea surface η (dynamic sea surface) is measured from space, the relations (A2.26-A2.27) can be used to calculate surface geostrophic velocities away from the equator. This surface velocity now serves as reference velocity in the thermal wind equations (A2.18-A2.19) and using measured density the full 3-dimensional geostrophic velocity field is available. Together with the wind driven surface currents estimated from the wind field total absolute currents can then be estimated.

A note of caution must be added. The total flow field derived this way may not be mass conserving and small additional corrections will be necessary before the velocities can be used for the calculation of transports.

A3 Gravity effect of ice mass changes and the sea level equation

Mass changes of ice caps (Antarctica, Greenland) and glaciers can be expressed as a function L of position φ,λ and time t:

$$L = L(\varphi, \lambda, t)\,. \tag{A3.1}$$

It is convenient to express the changing load in equivalent of water thickness. An expansion of this load function into (fully normalized) spherical harmonics leads directly to Equation (A1.4.2) with the relation (A1.4.3) between spherical harmonic coefficients and the surface density.

The resulting time variable parts of the geoid and gravity disturbance can be easily computed using Equations (A1.2.2b) and (A1.2.3), respectively. In addition, the viscoelastic response of the Earth's crust and mantle have to be taken into account (see A5).

The exchange of water between the global ocean and the continental ice causes global changes of the gravity field. Therefore the ocean surface will not change by a uniform water layer thickness, but following the new shape of the equipotential surfaces. This is expressed by the so-called sea level equation (Peltier 1998):

$$\delta S(\varphi,\lambda,t) = C(\varphi,\lambda,t)\cdot\left\{\delta G(\varphi,\lambda,t) - \delta R(\varphi,\lambda,t)\right\} \tag{A3.2}$$

with δS relative sea level change (with respect to the solid Earth)
C ocean function (1 for ocean, 0 for land)
δG geoid change
δR vertical deformation of the solid Earth

and

$$\delta S(\varphi,\lambda,t) = C(\varphi,\lambda,t)\cdot \cdot\left\{\int_{-\infty}^{t}\left[\iint_{\sigma}\left(\frac{1}{g}\Phi(\psi,t-t') - \Gamma(\psi,t-t')\right)\cdot L(\varphi',\lambda',t')\,d\sigma\right]dt' + \frac{1}{g}\Delta\Phi(t)\right\} \tag{A3.3}$$

with Φ, Γ Green's functions
$\Delta\Phi$ Mass conservation term.

Since the changing sea level on the left hand side of Equation (A3.3) is also part of the changing load term L on the right hand side, Equation (A3.3) has to be solved iteratively. It is easy to conclude that the effect of individual ice masses will not only be different in the gravity field, but also in relative sea level change ("fingerprints").

References

W.R. Peltier, Postglacial Variations in the Level of the Sea: Implications for Climate Dynamics and Solid-Earth Geophysics, Rev. Geophys. 36(4) p. 603-689,1998

A4 Mantle flow and gravity potential

Density anomalies within the Earth's mantle affect the long term gravity potential in several ways: they produce a signal due to Newton's law of attraction, and they lead to viscous flow stresses which deflect internal interfaces between regions of different density (such as the core mantle boundary) or the Earth's surface (dynamic topography). Deflected boundaries represent mass anomalies and produce an additional gravitational signal. The density anomalies within the Earth $\delta\rho(r,\varphi,\lambda)$ can be expanded into spherical harmonics, where r,φ,λ are the spherical coordinates

$$\delta\rho(r,\varphi,\lambda) = \rho_0 \left(\sum_{l=1}^{l_{\max}} \sum_{m=0}^{l} \bar{P}_{lm}(\sin\varphi)(C_{lm}^{\rho}(r)\cos m\lambda + S_{lm}^{\rho}(r)\sin m\lambda) \right) \tag{A4.1}$$

Here ρ_0 is the reference density, l and m are the degree and order of the spherical harmonic representation and $\bar{P}_{lm}, C_{lm}^{\rho}, S_{lm}^{\rho}$ are the fully normalized Legendre polynomials, and the spherical harmonic coefficients of the density anomaly distribution, respectively. The coefficient $C_{00}^{\rho}(r)$ is not considered, as its integrated effect is zero.

If the i-th interface at the radial distance r_i (or the Earth´s surface at $r = R$, R being the Earth´s radius) is associated with the density contrast $\Delta\rho_i$, any deflection of this interface may be described by the dynamic topography $h_i(\varphi,\lambda)$. The associated mass anomaly may be represented by a spherical shell with variable surface density (mass/area, thin layer approximation), which can be expanded into spherical harmonics

$$\sigma_i(r_i,\varphi,\lambda) = \Delta\rho_i R \left(\sum_{l=1}^{l_{\max}} \sum_{m=0}^{l} \bar{P}_{lm}(\sin\varphi)(C_{lm}^{i}\cos m\lambda + S_{lm}^{i}\sin m\lambda) \right) \tag{A4.2}$$

where C_{lm}^{i}, S_{lm}^{i} are the spherical harmonic coefficients of the dynamic topography of interface i, scaled by the Earth's radius R.

The density anomalies given in Equation (A4.1) produce a disturbing potential $T(R,\varphi,\lambda)$ (see Equation A1.1.2) at the Earth's surface, whose Stokes coefficients are given by

$$\begin{Bmatrix} \bar{C}_{lm} \\ \bar{S}_{lm} \end{Bmatrix} = \frac{3\rho_0}{\rho_{ave}} \frac{1}{2l+1} \frac{1}{R} \int_0^R \left(\frac{r}{R} \right)^{l+2} \begin{Bmatrix} C_{lm}^{\rho}(r) \\ S_{lm}^{\rho}(r) \end{Bmatrix} dr \tag{A4.3}$$

where ρ_{ave} is the average density of the Earth.

In a similar way, the disturbing potential due to all n deflected interfaces is given by

$$\begin{Bmatrix} \bar{C}_{lm} \\ \bar{S}_{lm} \end{Bmatrix} = \frac{3}{\rho_{ave}} \frac{1}{2l+1} \sum_{i=1}^{n} \left(\frac{r_i}{R} \right)^{l+2} \Delta\rho_i \begin{Bmatrix} C_{lm}^{i} \\ S_{lm}^{i} \end{Bmatrix} \tag{A4.4}$$

Internal density anomalies and dynamic topography (of the surface or an internal boundary) are coupled by the equations describing mantle flow. These are the equations of conservation of mass and momentum

$$\frac{\partial\rho}{\partial t} + \vec{\nabla}(\rho\vec{v}) = 0 \tag{A4.5}$$

$$0 = -\vec{\nabla}P + \frac{\partial}{\partial x_j}\eta\left(\frac{\partial v_i}{\partial x_j} + \frac{\partial v_j}{\partial x_i} \right) + \rho g\vec{e}_z \tag{A4.6}$$

where t is the time and $\vec{v}$ is the flow velocity of mantle flow, P is the pressure, x_i is the Cartesian coordinate, η is the viscosity, g is the gravity acceleration and $\vec{e}_z$ is the unit vector in z-direction.

It should be noted that in the equation of momentum inertial terms have been neglected. The driving force for mantle flow is represented by the last term in Equation (A4.6), which contains the internal density anomalies.

The internal density anomalies may be due to temperature and compositional variations within the Earth, and may be written as a linearized equation of state

$$\rho = \rho_0(r) + \left.\frac{\partial \rho}{\partial T}\right|_{P,C} \delta T + \left.\frac{\partial \rho}{\partial C}\right|_{P,T} \delta C \tag{A4.7}$$

where ρ_0 is a reference density, T is the temperature, δT is the deviation from a reference temperature, C is a parameter quantifying the composition. It should be noted that the pressure dependence of the density is not accounted for explicitly, since it may be included in the depth dependent reference state. Since temperature and composition is not known in the Earth's mantle, the density may also be related to observed quantities such as seismic velocities V_P or V_S

$$\rho = \rho_0(r) + \frac{\partial \rho}{\partial V_{P,S}} \delta V_{P,S} \quad . \tag{A4.8}$$

The partial derivative has to be determined in the laboratory or by inversion methods.

Once the internal density anomalies are known or assumed using Equations (A4.7) or (A4.8), Equation (A4.5) and (A4.6) may be solved giving the mantle flow field and the pressure distribution. From this the stress tensor

$$\sigma_{ij} = -P\delta_{ij} + \eta\left(\frac{\partial v_i}{\partial x_j} + \frac{\partial v_j}{\partial x_i}\right) \tag{A4.9}$$

can be derived (δ_{ij} is the Kronecker-δ). Usually the Earth's surface at $r = R$ (or internal interface i at r_i) is kept fixed in such calculations. This results in non-vanishing normal stresses at the surface $r = R$ or r_i. If the surface were allowed to move vertically (i.e. assuming a free boundary condition), the resulting dynamic topography will produce a lithostatic stress, which equilibrates the normal stress from the flow field at R or r_i to first order. Thus, the dynamic topography of the interface i (or of the surface) is given by

$$h_i = \frac{\sigma_{zz}(r_i)}{\Delta \rho g} \quad . \tag{A4.10}$$

Equations (A4.5), (A4.6), (A4.9) and (A4.10) describe a coupled fluid dynamical system of the Earth's mantle, which produce gravity perturbations given by Equations (A4.1), (A4.2), (A4.3) and (A4.4). It should be noted that this formulation also includes the effect of isostatic topography, as long as it is kept in place by a highly viscous lithosphere or crust.

In the case of only radial viscosity variations Equations (A4.5), (A4.6), (A4.9) and (A4.10) may also be decomposed into spherical harmonics, and the relation between a density anomaly at a given depth and the associated gravity potential at the surface may be represented by kernels. For example, the geoid anomaly δN_{lm} caused by an assumed density distribution in the mantle is obtained by a convolution of these kernels $G_l(r)$ with the density field:

$$\delta N_{lm} = \frac{4\pi GR}{(2l+1)g} \int_{r_{CMB}}^{R} G_l(r)\delta\rho_{lm} dr \tag{A4.11}$$

where G is the gravitational constant. The determination of $G_l(r)$ requires the full solution of the fluid dynamical problem for a given viscosity depth distribution and it includes the effect of dynamic topography.

A5 Glacial-isostatic adjustment

Glacial isostasy is concerned with the gravitational viscoelastic response of the Earth to surface loads. To derive the governing incremental field equations and interface conditions, infinitesimal perturbations of a compositionally and entropically stratified, compressible Earth initially in hydrostatic equilibrium are considered, where the perturbations are assumed to be isocompositional and isentropic. In the following, the Lagrangian representation of arbitrary tensor fields, $f_{ij\ldots}(\mathbf{X},t)$, will be used, which refers the field values to the current position, $r_i(\mathbf{X},t)$, of a particle whose initial position, X_i, at the time $t = 0$ is taken as the spatial argument. The total field, $f_{ij\ldots}(\mathbf{X},t)$, is then decomposed according to $f_{ij\ldots}(\mathbf{X},t) = f^{(0)}_{ij\ldots}(\mathbf{X}) + f^{(\delta)}_{ij\ldots}(\mathbf{X},t)$, where $f^{(0)}_{ij\ldots}(\mathbf{X})$ is the initial field and $f^{(\delta)}_{ij\ldots}(\mathbf{X},t)$ is the material incremental field, i.e. the increment with respect to the particle. Sometimes, it is more convenient to consider the spatial incremental field, i.e. the increment with respect to a fixed location, given by $f^{(\Delta)}_{ij\ldots}(\mathbf{X},t) = f^{(\delta)}_{ij\ldots}(\mathbf{X},t) - f^{(0)}_{ij\ldots,k}(\mathbf{X},t)u_i(\mathbf{X},t)$, where $u_i(\mathbf{X},t)$ is the particle displacement. For the material gradient of a field, we use $f_{ij\ldots,k}(\mathbf{X},t) = \partial f_{ij\ldots}(\mathbf{X},t)/\partial X_k$. Henceforth, the arguments X and t will be suppressed.

A5.1 Equations for the total fields

For a gravitating Earth undergoing perturbations of some initial state, the momentum equation is

$$\tau_{ij,j} + \rho^{(0)} g_i = \rho^{(0)} d_t^2 r_i, \tag{A5.1.1}$$

where τ_{ij} are the non-symmetric Piola-Kirchhoff stress, $\rho^{(0)}$ the initial volume mass density and g_i the gravitational force per unit mass. The symbols d_t and d_t^2, respectively, denote the first- and second-order material time derivative operators. The field g_i is given by

$$g_i = \phi_{,j}\, r^{-1}_{j,i}, \tag{A5.1.2}$$

with ϕ the gravitational potential and $r^{-1}_{i,j}$ the inverse of $r_{i,j}$. The gravitational potential equation can be written as

$$j\left(\phi_{,ij}\, r^{-1}_{i,k} r^{-1}_{j,k} + \phi_{,i} r^{-1}_{i,jj} \right) = -4\pi G \rho^{(0)}, \tag{A5.1.3}$$

where $j := \det r_{i,j}$ is the Jacobian determinant and G Newton's gravitational constant. The constitutive equation is of the form

$$t_{ij} = t^{(0)}_{ij} + M_{ij}\left[r_{m,k}\left(t - t'\right) r_{m,l}\left(t - t'\right) - \delta_{kl} \right], \tag{A5.1.4}$$

where $t_{ij} = j r^{-1}_{j,k} \tau_{ik}$ is the Cauchy stress, M_{ij} the anisotropic relaxation functional transforming the strain history given by the term in brackets into the material incremental Cauchy stress and t' the excitation time. With $M_{ij}, t^{(0)}_{ij}$ and $\rho^{(0)}$ prescribed, Equations (A5.1.1) to (A.5.1.4) constitute the system of total field equations for $g_i, j, r_i, t_{ij}, \tau_{ij}$ and ϕ.

In order to incorporate ice or water loads, the gravitating Earth is assumed to possess (internal or surficial) interfaces of discontinuity occupied by material sheets whose interface mass density, σ, is prescribed. Then, the following interface conditions result from Equations (A5.1.1) to (A5.1.4):

$$\left[r_i \right]^{+}_{-} = 0, \tag{A5.1.5}$$

$$\left[\phi\right]_{-}^{+} = 0\,, \tag{A5.1.6}$$

$$\left[n_i \phi_{,j} r_{j,i}^{-1}\right]_{-}^{+} = -4\pi G\sigma\,, \tag{A5.1.7}$$

$$\left[n_j t_{ij}\right]_{-}^{+} = -g_i\sigma\ . \tag{A5.1.8}$$

A5.2 Equations for the initial fields

Commonly, the Earth is assumed to be initially in hydrostatic equilibrium. With the mechanical pressure defined by $p := -t_{ii}/3$, then $t_{ij}^{(0)} = -\delta_{ij} p^{(0)}$ applies and Equations (A5.1.1) to (A5.1.4) reduce to

$$-p_{,i}^{(0)} + \rho^{(0)} g_i^{(0)} = 0\ , \tag{A5.2.1}$$

$$g_i^{(0)} = \phi_{,i}^{(0)}\,, \tag{A5.2.2}$$

$$\phi_{,ii}^{(0)} = -4\pi G\rho^{(0)}\ , \tag{A5.2.3}$$

$$p^{(0)} = \xi\left(\rho^{(0)}, \lambda^{(0)}, \varphi^{(0)}\right)\ . \tag{A5.2.4}$$

The last expression is the state equation, ξ the state function, $\lambda^{(0)}$ a field representing the initial composition and $\varphi^{(0)}$ the initial entropy density. With ξ, $\lambda^{(0)}$ and $\varphi^{(0)}$ prescribed, Equations (A5.2.1) to (A5.2.4) constitute the system of initial hydrostatic field equations for $g_i^{(0)}$, $p^{(0)}$, $\rho^{(0)}$ and $\phi^{(0)}$.

Supposing $\sigma^{(0)} = 0$, the following initial interface conditions are obtained from Equations (A5.1.5) to (A5.1.8):

$$\left[r_i^{(0)}\right]_{-}^{+} = 0\,, \tag{A5.2.5}$$

$$\left[\phi^{(0)}\right]_{-}^{+} = 0\,, \tag{A5.2.6}$$

$$\left[n_i^{(0)} \phi_{,i}^{(0)}\right]_{-}^{+} = 0\,, \tag{A5.2.7}$$

$$\left[p^{(0)}\right]_{-}^{+} = 0\,. \tag{A5.2.8}$$

A5.3 Equations for the incremental fields

After decomposition of the total fields in Equations (A5.1.1) to (A5.1.4) into initial and incremental parts followed by linearization, we obtain for isotropy

$$t_{ij,j}^{(\delta)} + \left(p_{,j}^{(0)} u_j\right)_{,i} - g_i^{(0)}\left(\rho^{(0)} u_j\right)_{,j} + \rho^{(0)} g_i^{(\Delta)} = \rho^{(0)} d_t^2 u_i\,, \tag{A5.3.1}$$

$$g_i^{(\Delta)} = \phi_{,i}^{(\Delta)}\,, \tag{A5.3.2}$$

$$\phi_{,ii}^{(\Delta)} = 4\pi G\left(\rho^{(0)} u_i\right)_{,i}\ , \tag{A5.3.3}$$

$$t_{ij}^{(\delta)} = \delta_{ij}\int_0^t \left[m_1(t-t') - \tfrac{2}{3}m_2(t-t') \right] d_{t'}\left[u_{k,k}(t') \right] dt' + \int_0^t m_2\,(t-t')\, d_{t'}\left[u_{i,j}(t') + u_{j,i}(t') \right] dt' , \tag{A5.3.4}$$

where m_1 and m_2 are the bulk and shear relaxation functions, respectively. With m_1 and m_2 prescribed and the initial fields given as the special solution to the initial field equations and interface conditions, Equations (A5.3.1) to (A5.3.4) constitute the material-local form of the incremental gravitational viscoelastic field equations for $g_i^{(\Delta)}, t_{ij}^{(\delta)}, u_i$ and $\phi^{(\Delta)}$.

Decomposing the total fields in Equations (A5.1.5) to (A5.1.8) into their initial and incremental parts followed by linearization gives

$$\left[u_i \right]_-^+ = 0 , \tag{A5.3.5}$$

$$\left[\phi^{(\Delta)} \right]_-^+ = 0 , \tag{A5.3.6}$$

$$\left[n_i^{(0)} \left(\phi_{,i}^{(\Delta)} - 4\pi G \rho^{(0)} u_i \right) \right]_-^+ = -4\pi G \sigma , \tag{A5.3.7}$$

$$\left[n_j^{(0)} t_{ij}^{(\delta)} \right]_-^+ = -g_i^{(0)} \sigma . \tag{A5.3.8}$$

Before solving the incremental field Equations (A5.3.1) to (A5.3.4) subject to the interface conditions (A5.3.5) to (A5.3.8), the relaxation functions must be specified. Usually, the bulk properties are taken as elastic and the shear properties as Maxwell viscoelastic. Then, the shear relaxation function, m_2, takes a simple form in terms of two parameters: the elastic shear modulus, μ, and the shear viscosity, η. The explicit form of m_2 and the basic response characteristics of the Maxwell analogue model are shown in Figure A5.1.

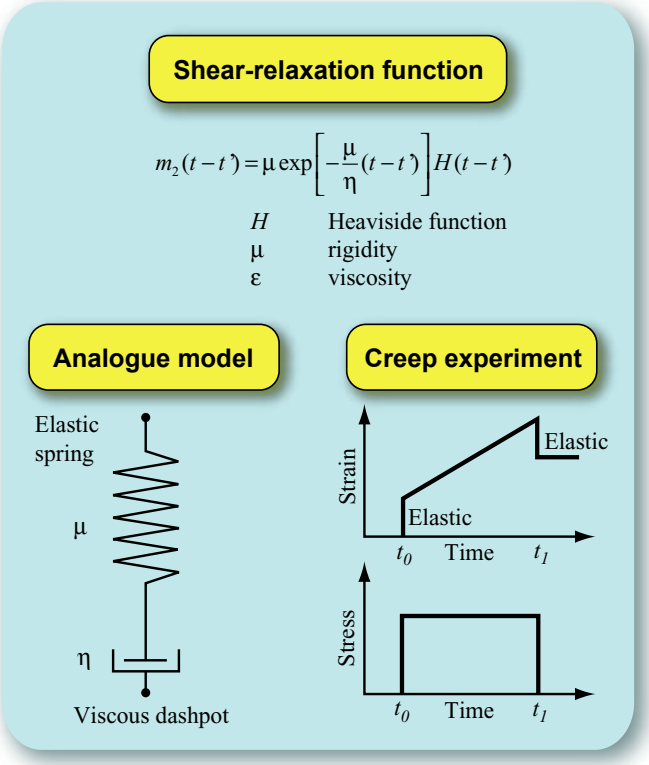

Figure A5.1: *Maxwell viscoelasticity*

A5.4 Solution methods, forward and inverse modelling

The standard method of solving the field equations for radially symmetric Earth models is illustrated in Figure A5.2. It involves Laplace transformation with respect to the time, t, followed by spherical harmonic expansion of the incremental field equations and interface conditions, where the ice model adopted determines the interface conditions on the boundary of the Earth model. This leads to a (6×6) system of linear first order differential equations representing the Earth's response and a load spectrum, representing the ice model. Matrix methods return transfer functions as the general solution to the differential system, which, upon multiplication with the load spectrum leads to the spectral solution. Inverse Laplace transformation followed by expansion of the spherical harmonic series finally results in the space-time solution. With the stratification of the Earth model given and the ice model specified, this procedure allows the calculation of arbitrary field quantities characterizing glacial isostatic adjustment. For Earth models involving lateral viscosity variations, finite difference or finite element methods must be employed to compute the Earth's response.

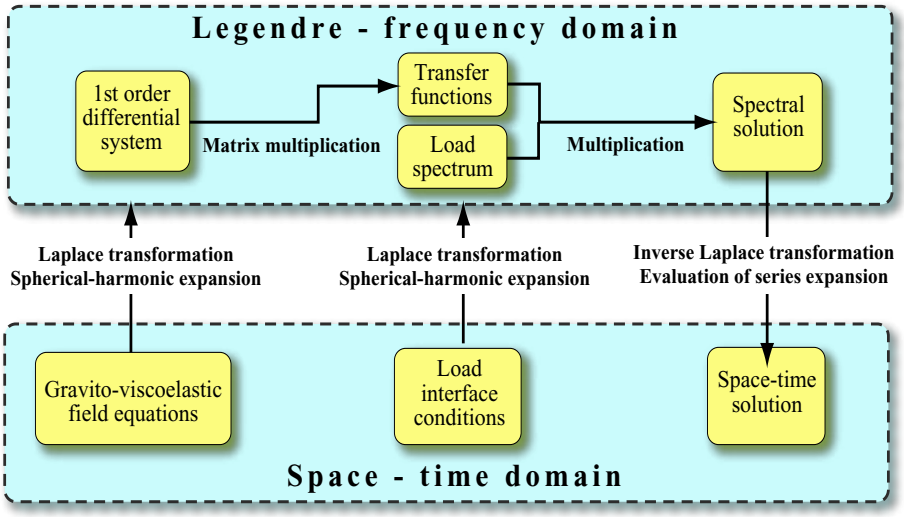

Figure A5.2: *Solution method*

Figure A5.3 illustrates the types of field quantity of interest in glacial isostasy and the terrestrial and satellite methods available to measure them. In the first instance, forward modelling of the time changes of these field quantities on the basis of standard Earth and ice models and the confirmation of this temporal variability by the observational data is of interest. At a later stage, time series of the individual types of data may be jointly inverted in terms of improved estimates of the Earth's viscosity, of the Pleistocene ice distribution or of the present day mass imbalances of the polar ice sheets.

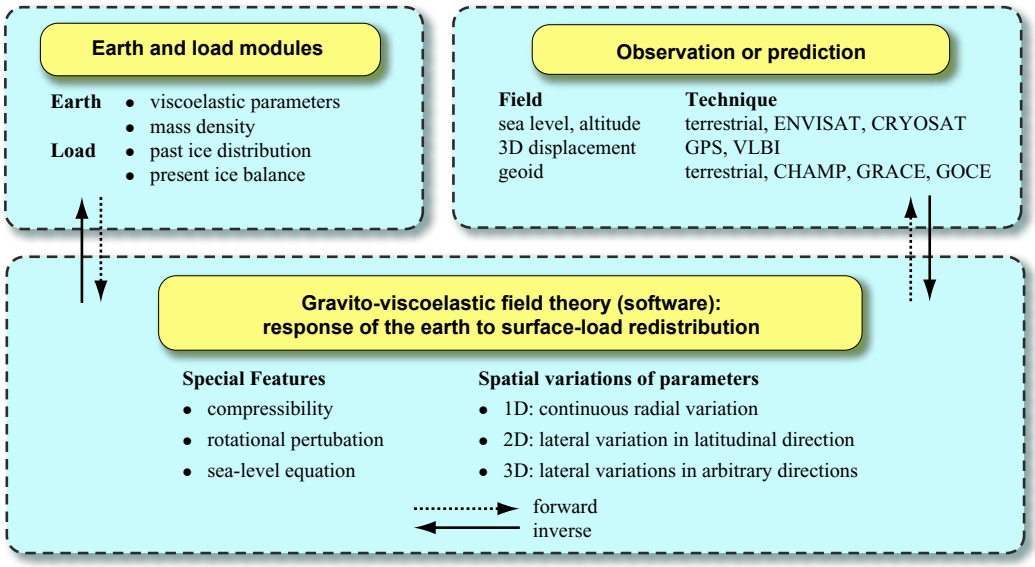

Figure A5.3: *Forward and inverse modelling of glacial isostatic adjustment*

A6 Hydrological processes and related mass transport

Mass changes due to changes in terrestrial water storage are conveniently expressed in hydrology in terms of changes in equivalent water thickness Δh, i.e., water mass changes per surface area (with 1mm water column corresponding to ~1 l/m² or ~1 kg/m²). The change of mass due to changes in water storage in a thin layer at the Earth's surface can be written in terms of changes in the geoid shape when expanded as a sum of spherical harmonics according to Equations (A1.4.2) and (A1.4.4):

$$\Delta h = \frac{\Delta\sigma(\varphi,\lambda)}{\rho_w} = R\sum_{l=0}^{\infty}\sum_{m=0}^{l}\bar{P}_{lm}(\sin\varphi)\left(\Delta\check{C}_{lm}\cos(m\lambda)+\Delta\check{S}_{lm}\sin(m\lambda)\right) \tag{A6.1}$$

with

$$\begin{Bmatrix}\Delta\check{C}_{lm}\\ \Delta\check{S}_{lm}\end{Bmatrix} = \frac{\rho_{ave}}{3\rho_w}\frac{2l+1}{1+k_l'}\begin{Bmatrix}\Delta\bar{C}_{lm}\\ \Delta\bar{S}_{lm}\end{Bmatrix} \tag{A6.2}$$

φ and λ are latitude and east longitude, $\Delta\sigma$ is the change in surface density (i.e. mass/area), ρ_w is the density of water, R is the radius of the Earth, ρ_{ave} is the average density of the Earth, $\bar{P}_{lm}$ are the normalized associated Legendre functions of degree l and order m, $\check{C}_{lm}, \check{S}_{lm}$, $\bar{C}_{lm}$ and $\bar{S}_{lm}$ are dimensionless coefficients with $\bar{C}_{lm}$ and $\bar{S}_{lm}$ defining the geoid model derived from GRACE satellite observations, and k_l' is the load Love number of degree l.

Changes of the water storage Δh per time interval are described for any spatial unit of the land surface, e.g. a river basin, by the water balance equation:

$$\Delta h = P - ET - Q \tag{A6.3}$$

where P is precipitation, ET is evapotranspiration and Q is runoff (all in mm). Spatial units for which Equation3 is valid range from the plot scale of a single soil profile to the catchment area of a river basin being the basic spatial unit of hydrological analysis and water management issues, and up to the continental scale. Precipitation as rain or snow is the main input to the terrestrial water storage. It is measured by point samplers, ground-based radar or remote sensing and subsequently interpolated to a spatial mean for the area of interest.

Evapotranspiration includes evaporation defined as the transformation of liquid water to vapour from open water surfaces (lakes, rivers), from bare soils and from water stored on plant surfaces (interception). Evapotranspiration also includes the transfer of water from the soil to the atmosphere by transpiration of plants. On scales with variations in soil and land use it cannot be measured directly like precipitation or discharge. Neither it can be calculated from the water balance equation (Equation A6.3) as the variations in storage cannot be determined with sufficient accuracy. Thus there is need for a description of evapotranspiration by climatic, soil and land use data .

There are a number of physical approaches as the evapotranspiration rate is controlled by the availability of energy and water at the evaporating surface, and by the ease with which water vapour can diffuse into the atmosphere, i.e., as a function of plant resistances and atmospheric turbulence. Basically, evapotranspiration, expressed as latent heat flux λE, is part of to the energy budget of land surfaces:

$$A = R_n - G = \lambda E + H \tag{A6.4}$$

where A is the available energy at the surface, R_n is incoming net radiant energy (i.e., the difference between incoming and reflected solar radiation plus the difference between incoming and

outgoing long-wave radiation), G is the energy transfer into the soil, H is the outgoing sensible heat flux and λ is a proportionality factor (latent heat of vaporization of water) to convert from energy units into equivalent water thickness. Practical models to describe evapotranspiration in hydrology often apply a resistance approach to represent, in addition to the energy balance, the impact of atmospheric turbulence and vegetation characteristics on evapotranspiration. One widely used model of this type is the Penman-Monteith approach. It includes the aerodynamic resistance r_a as a function of wind speed and surface roughness due to varying height of the vegetation, and the canopy resistance r_c to represent plant stomata control on the transpiration process as a function of vegetation type, leaf cover, soil water status and micro-meteorological conditions:

$$E = \frac{1}{\lambda}\left[\frac{\Lambda A + \rho_a c_p D / r_a}{\Lambda + \gamma\left(1 + r_c / r_a\right)}\right] \tag{A6.5}$$

D is the water vapour pressure deficit of the air,ρ_a is the density of air, Λ is the gradient of the saturated vapour pressure curve, c_p is the specific heat of moist air and γ is the psychometric constant. Being simplifications of Equation A6.5, a number of empirical formulations exist to assess evapotranspiration for large areas where data availability does not allow to account for each influencing factor explicitly.

Total runoff Q as another component of the water balance equation (Equation3) is composed of a surface runoff component, a fast interflow component in the shallow soil zone and a slow groundwater flow component of water percolating to deeper subsurface zones. In a general form, subsurface water flow Q_{sub} (in mm per time unit) through any cross section in the saturated or unsaturated soil zone can be described by Darcy's equation for a porous medium:

$$Q_{sub} = -K(\theta)\frac{\partial \psi}{\partial x} \tag{A6.6}$$

In Equation (A6.6), written in the one-dimensional form for simplicity, $K(\theta)$ is the hydraulic conductivity of the soil which is a highly non-linear function of the actual soil moisture θ, reaching its maximum value for a water-saturated soil. $\partial\psi$ in Equation (A6.6) is the gradient of the hydraulic head (or potential) over a distance ∂x, being the sum of primarily (1) the capillary-pressure head due to capillary forces acting on water in the soil matrix and (2) of the elevation head due to gravitational forces. It should be noted that the capillary-pressure head is again a non-linear function of soil moisture θ, with its form varying considerably with soil characteristics such as porosity and grain size distribution. When written for the vertical direction, Equation (A6.6) is the basis to describe infiltration of rain into the soil. Additional precipitation volumes which exceed the infiltrability of the soil are transformed into surface runoff Q_{surf}. The applicability of Equation6 for the description of subsurface runoff over large spatial scales such as river basins is limited, however. One reason is the deviation of natural soils from the idealized assumption of being a homogeneous porous medium. Macropores, for instance, may allow a very fast water transport, bypassing the soil matrix. Additionally, in view of the large natural heterogeneity, the available information in particular on soil characteristics is usually not sufficient for large areas to parameterize Equation (A6.6) appropriately. Thus, simplified formulations are often used to describe subsurface storage and water transport by representing the soil zone or the groundwater by one conceptual storage for an entire river basin or a part of it with similar hydrological characteristics. Subsurface runoff per time unit from such a storage, expressed in equivalent water thickness for the catchment area A (m^2), is represented as being proportional to the actual storage volume V (m^3):

$$Q_{sub} = \frac{V}{A \cdot \tau} \tag{A6.7}$$

The proportionality constant τ (with units of time) in Equation (A6.7) is a storage coefficient which is related to the average residence time of water in the groundwater or soil storage. τ depends on geological, topographic and soil characteristics and usually is a calibration parameter in hydrological models.

The flow of surface runoff, whether generated directly as infiltration-excess from precipitation or as return flow to the land surface or into river channels after the passage of the soil and groundwater zone, can basically be described by hydrodynamical equations based on mass and energy balancing such as the Saint-Venant equations. In order to describe flow routing in the river network of river basins, simplified schemes are often used which essentially introduce a time delay of the downstream movement of water masses as function of flow distance, flow volume and topographic gradient. The retention of river runoff in natural and man-made reservoirs or in wetlands causes an additional delay in flow routing. It influences the water balance and related changes in water storage (Equation A6.3) when considered at the basin scale.

A7 Satellite mission fact sheets

A7.1 Gravity missions

The satellite mission CHAMP (CHAllenging Minisatellite Payload)

Objectives:

(1) global mapping of the Earth's gravity field and
(2) the Earth's magnetic field and of temporal field variations, and
(3) sounding of the neutral atmosphere and ionosphere by GPS radio occultation technique

Satellite:

trapezoid body (4 m length, 1 m height, 1.7 m width) with 4 m long boom to carry the magnetometers, 500 kg mass
attitude: three-axes stabilized, Earth-oriented, boom in flight direction
attitude control: cold-gas thruster system, magneto-torquers
attitude sensors: four star cameras, GPS navigation, fluxgate magnetometers
manufacturing: Jena-Optronic/Astrium

Instrumentation and Sensors:

BlackJack GPS receiver (JPL/NASA, USA) with antennas for orbit determination (top side) and radio occultation (rear side), STAR three-axes accelerometer (CNES, France),
Overhauser scalar magnetometer, 2 Fluxgate vector magnetometers,
Digital Ion Drift Meter (USAF USA), Laser Retro-reflective Assembly,
two star cameras on both, body and boom for attitude knowledge

Mission and Orbit Profile:

launch on July 15, 2000 with Russian COSMOS-3M rocket from Plesetsk cosmodrome into an almost polar (inclination 87°) and circular (eccentricity < 0.01) orbit with an initial altitude of 454 km, decaying to 300 km around mid 2008 (predicted end of life time)

Responsibilities:

GeoForschungsZentrum Potsdam (GFZ): overall project management, instrument control, management of science ground segment, product dissemination
Deutsches Zentrum für Luft- und Raumfahrt (DLR): mission operation and satellite control

Funding:

Bundesministerium für Bildung und Forschung (BMBF), DLR, GFZ;
Exploitation phase funded within BMBF's GEOTECHNOLOGIEN geoscientific R + D programme

The dual-satellite mission GRACE (Gravity Recovery And Climate Experiment)

Objectives:

global mapping of the Earth's mean and time variable gravity field with enhanced resolution (primary objective), and sounding of the neutral atmosphere and ionosphere by GPS radio occultation technique (secondary objective)

Satellites:

two identical satellites (CHAMP heritage), each one with trapezoid bodies (3.1 m length, 0.7 m height, 1.9 m width) and 490 kg mass
attitude: three-axes stabilized, Earth-oriented
attitude control: cold-gas thruster system, magneto-torquers
attitude sensors: two star cameras, GPS navigation
manufacturing: Astrium

Instrumentation and Sensors per Satellite:

BlackJack GPS receiver with antennas for precise orbit determination (top side) and radio occultation (rear side and front side, resp.), SuperStar three-axes accelerometer, K-band Intersatellite Ranging System, Laser Retro Reflective Assembly, Center of Mass Trim Assembly to center the accelerometer, two star cameras for attitude knowledge

Mission and Orbit Profile:

launch on March 17, 2002 with a Russian ROCKET launch vehicle from Plesetsk cosmodrome into an almost polar (inclination 89°) and circular (eccentricity < 0.01) orbit with an initial altitude of 500 km (470 km in autumn 2004), design life is five years, both satellites are co-orbiting, separated along track by nominally 220 km

Responsibilities:

Jet Propulsion Laboratories (JPL), USA:	project management
Deutsches Zentrum für Luft- und Raumfahrt (DLR) :	mission operation
Centre for Space Research (CSR), USA:	management (PI) of science ground segment, product generation and dissemination
GeoForschungsZentrum Potsdam (GFZ):	management (Co-PI) of European science ground segment, product generation and dissemination

Funding:

National Aeronautics and Space Administration (NASA), USA,
Deutsches Zentrum für Luft- und Raumfahrt (DLR),
Funding of German science ground segment within BMBF's GEOTECHNOLOGIEN geoscientific R + D programme

The gravity gradiometry mission GOCE (Gravity field and steady-state Ocean Circulation Explorer)

Objectives:

global mapping of the Earth's static gravity field with very high resolution
(1 cm geoid accuracy and 1 mGal gravity accuracy for scales down to 100 km)
based on GPS satellite-to-satellite-tracking and gravity gradiometry

Satellite:

octagonal body (5 m length, 1 m diameter) and 1000 kg mass
structure: carbon fibre, several compartments with extreme mechanical and thermal stability, high stability thermal control
attitude: three-axes stabilized, Earth-oriented
drag free orbit and attitude control system: continuous ion thrusters, cold-gas thruster system, magneto-torquers
attitude sensors: star cameras, gradiometer, GPS navigation
manufacturing: Astrium

Instrumentation and Sensors:

Laben GPS receiver with antenna for precise orbit determination, three-axes gravity gradiometer consisting of 6 electrostatic three-axes accelerometers in asymmetric diamond configuration, mounted on an extremely stable gradiometer structure, Laser Retro Reflector, star cameras for attitude knowledge

Mission and Orbit Profile:

launch in 2006 with a Russian ROCKOT or similar launch vehicle into a near polar (inclination 96.5°), sun synchronous and circular orbit with very low constant altitude of 250 km, design mission duration is 2 years

Responsibilities:

European Space Agency (ESA): project management. mission operation, and level 1 mission data generation
Alenia Spazio (Italy): prime industrial contractor
science management and science product generation (PI): tbd

Funding:

European Space Agency (ESA)
Funding of German science ground segment (preparation) within BMBF's GEOTECHNOLOGIEN geoscientific R + D programme

A7.2 Altimetry missions

Table A7.2: *Main Characteristic of past, present and future satellite altimeter missions*

Mission	Pulsewidth-limited altimeter systems							New technologies	
	Geosat [1]	ERS-1	TOPEX/Poseidon [2]	ERS-2	GFO [3]	Jason-1 [4]	ENVISAT [5]	ICESat	CryoSat
Operated by …	NOAA	ESA	CNES/NASA	ESA	US-NAVY	CNES/NASA	ESA	NASA	ESA
Launch (month/year)	03/85	07/91	09/92	04/95	02/98	01/02	03/02	01/03	05/05
Acquisition until (month/year)	09/89	03/96	degraded but ongoing	degraded but ongoing	ongoing	ongoing	ongoing	ongoing	-
Mean height (km)	785.5	785.0	1336.0	781.4	784.5	1336.0	799.8	600	717
Inclination (°)	108.0	98.5	66.0	98.54	108.04	66.0	98.54	94.	92.
Latitude coverage (°)	±72.0	±81.5	±66.0	±81.46	±72.0	±66.0	±81,45	±86.0	±88.0
Repeat cycle (days)	17.05 [1]	3/35/168	9.9156	35	17	9.9156	35	183	369
Track separation (km)	165 [1]	933/80/16	316	80	165	316	80	15	7.5
Frequencies (GHz) /wavelengths	13.5	13.5	5.3 + 13.6	13.5	13.5	5.3 + 13.575	3.2 + 13.575	Laser 1064+532nm	SIRAL [6] 13.8
Altimeter noise (cm)	7	5	2	3	3.5	1.5	2	10 (ice)	0.7 [7]
Radiometer/Frequencies	no	yes/2	yes/2	yes/3	yes/2	yes/3	yes/2	no	no

1) Geosat had two different mission phases, a 'geodetic mission' (GM) with a non-repeat, drifting orbit, and an 'exact repeat mission' (ERM) with the orbit characteristics given in the table
2) After the tandem configuration with Jason-1 (up to 08/2002) the TOPEX/Poseidon orbit was shifted by half the track separation to double the spatial resolution of both missions.
3) GFO continues to observe the same ground tracks as monitored by Geosat ERM (exact repeat mission)
4) Jason-1 continues to observe the same ground tracks as monitored by TOPEX/Poseidon until 08/2002
5) ENVISAT continues to observes the same ground tracks as ERS-2
6) SIRAL = Synthetic Aperture Interferometric Radar Altimeter
7) Accuracy of ice sheet elevation trend. Due to SAR processing, single CryoSat altimeter measurements are subject to radar speckle.